HETEROCYCLIC OLIGOAMIDES AS NEW PEPTIDE MIMETICS

Dissertation

zur Erlangung des Grades

Doktor der Naturwissenschaften (Dr. rer. nat.)

der Naturwissenschaftlichen Fakultät IV
Chemie und Pharmazie
der Universität Regensburg

vorgelegt von
Stefan Miltschitzky
aus Burghausen

2005

Heterocyclic Oligoamides as New Peptide Mimetics

Dissertation

zur Erlangung des Doktorgrades der Naturwissenschaften

(Dr. rer. nat.)

an der Fakultät für Chemie und Pharmazie

der Universität Regensburg

vorgelegt von

Stefan Miltschitzky

aus Burghausen

2005

The experimental part of this work was carried out between November 2001 and June 2005 at the Institute for Organic Chemistry at the University of Regensburg under the supervision of *Prof. Dr. B. König*.

The PhD thesis was submitted on:		11.07.2005
The colloquium took place on:		29.07.2005
Board of Examiners:	Prof. Dr. G. Schmeer	(Chairman)
	Prof. Dr. B. König	(1st Referee)
	Prof. Dr. O. Reiser	(2nd Referee)
	Fr. Prof. Dr. C. Steinem	(Examiner)

Meinen Eltern

und meiner Familie

Table of Contents

A. Introduction 1

1. Introduction 1
2. Stabilized α-Peptides with a β-Hairpin Structure and their Biological Application 4
3. Turn Mimics for Peptide Hairpin Structures 13
4. Peptide Hairpin Structure Mimetics 24
5. Conclusions 34
6. References 35

B. Main Part 43

1. Synthesis of Substituted Pyrimidine Hydrazine Acids (PHA) and their Use in Peptide Recognition 43

1.1. Introduction 43
1.2. Results and Discussion 45
1.3. Conclusions 60
1.4. Experimental Part 61
1.5. References and Notes 87

2. Substituted Pyrimidine Hydrazine Acid (PHA) Oligoamides and their Binding Affinity to Peptides and Proteins 89

2.1. Introduction 89
2.2. Synthesis of Highly Water Soluble PHA Receptors 91
2.3. Spectroscopic Investigations of the Substituted PHA Receptors 94
2.4. Binding Affinities of PHA Receptors to Tetradecapeptide Somatostatin (SRIF) in Different Solvents 98
2.5. Binding Affinities of PHA Receptors to Concanavalin A under Physiological Conditions 103

2.6. Conclusions 110
2.7. Experimental Part 111
2.8. References 120

3. Molecular Recognition of His with NTA Ligands 123
3.1. Introduction 123
3.2. Results and Discussion 125
3.3. Conclusions 130
3.4. Experimental Part 131
3.5. References and Notes 136

4. Synthesis of an Amino Acid with Protected Cyclen Side Chain Functionality 139
4.1. Introduction 139
4.2. Results and Discussion 140
4.3. Conclusions 141
4.4. Experimental Part 143
4.5. References and Notes 147

C. Summary 149

D. Abbreviations 151

E. Appendix 153

F. Acknowledgements 157

A. Introduction

Small Peptides with a β-Hairpin Structure*

1. Introduction

In recent years, β-hairpin peptides have been studied in detail. β-turns are the most common element of non-repetitive structure recognised in proteins.[1] They consist of supersecondary structural elements in which two antiparallel adjacent peptide β-sheets are linked by a short loop. The loop size can vary; the majority of β-hairpins have loops of two to six residues,[2] whereby the most common loop size is two. Their dihedral angels (Table 1) classify them.[3]

Turn Type	Φ (i+1)	Ψ (i+1)	Φ (i+2)	Ψ (i+2)
Type I β	-60	-30	-90	0
Type I´β	60	30	90	0
Type I´ β	60	30	90	0
Type II´ β	60	-120	-90	0

Table 1: Most common hydrogen bonded β-turns in β-hairpins and their dihedral angels

* The results of this chapter have been published: S. Miltschitzky and B. Koenig, *OPPI* **2005**, in press.

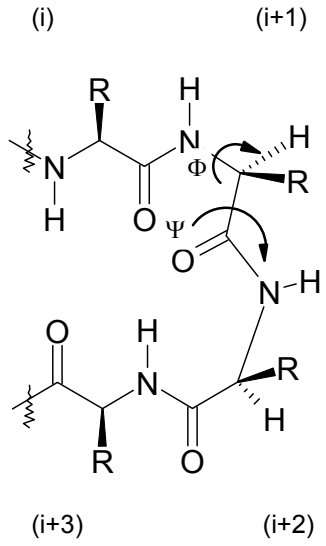

Figure 1: Illustration of the four residues in a β-turn demonstrating the Φ and Ψ angels of the (i+1) residue

The two number nomenclature was introduced by *Sibanda & Thornton* using symbols of the form X:Y.[4] X is defined as the number of residues in the connecting segment if strand residues have at least one of their NH or CO main chain groups involved in the hydrogen bonding pattern. Y is defined as the number of residues in the connecting segment, when the strand residues have both their NH and CO main chain group involved. If both hydrogen bonds are formed, then X=Y. If only a single hydrogen bond is formed between the terminal NH of the first strand and the CO of the second strand, then Y = X+2. In protein structures, 2:2 β-hairpins are most abundant, followed by 3:5 β-hairpins and 4:4 β-hairpins.[5]

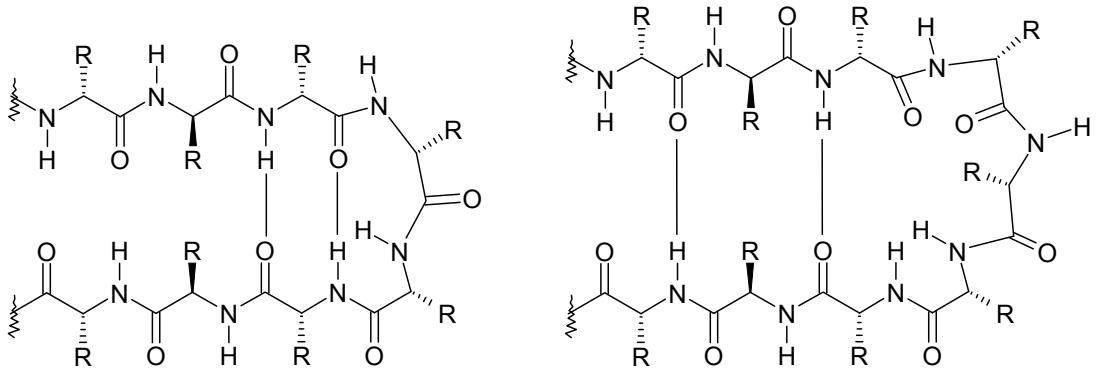

Figure 2: Schematic representation of a 2:2 and a 3:5 β-hairpin structure in proteins. R = amino acid side chain

To understand the formation of β-hairpins, it is necessary to analyze the energy contribution of the intrinsic secondary structure propensities of the different amino acids. In addition, interstrand side-chain side-chain interactions, in two structurally different regions of this secondary structure, the β-strand and the turn region, have to be considered. This review will recapitulate the genesis of linear and cyclic, non-aggregating peptides and peptidomimetics that display β-sheet folding within this decade.[6] The following sections will focus on studies that have investigated the effect of turn-sequences, interstrand hydrogen bonding, side-chain interactions, and cyclization of the β-hairpin structure and its stability.

2. Stabilized α-Peptides with a β-Hairpin Structure and their Biological Application

Autonomously folding β-hairpins have emerged recently as vehicles for probing local interactions in β-sheet folding and assembly,[7] and as building blocks in protein design.[8] This section will focus on electrostatic and hydrophobic side-chain-side-chain interactions stabilizing the β-hairpin structure and leading to autonomously folding. It is generally believed, that salt bridges contribute significantly to the stability of the native state of the protein. An elongated version of the *de novo* designed β-hairpin peptide, BH8, has allowed *Ramirez-Alvarado et al*. to gain insight into the role of electrostatic interactions in β-hairpin stability.[9] A Lys-Glu electrostatic pair has been introduced by adding a residue at the beginning and at the *N*-terminal and *C*-terminal strands of the β-hairpin structure, in both orientations. The two resulting peptides and controls having Ala residues at theses positions and different combinations of Ala with Lys, or Glu residues, were analyzed under different pH and ionic strength conditions. The investigated peptides had the following amino acid sequences:

BH8 (**1a**):	Arg-Gly-Ile-Thr-Val-Asn-Gly-Lys-Thr-Tyr-Gly-Arg
BHKE (**1b**):	Arg-Gly-**Lys**-Ile-Thr-Val-Asn-Gly-Lys-Thr-Tyr-**Glu**-Gly-Arg
BHEK (**1c**):	Arg-Gly-**Glu**-Ile-Thr-Val-Asn-Gly-Lys-Thr-Tyr-**Lys**-Gly-Arg
BHKA (**1d**):	Arg-Gly-**Lys**-Ile Thr-Val-Asn-Gly-Lys-Thr-Tyr-**Ala**-Gly-Arg
BHAE (**1e**):	Arg-Gly-**Ala**-Ile-Thr-Val-Asn-Gly-Lys-Thr-Tyr-**Glu**-Gly-Arg
BHAA (**1f**):	Arg-Gly-**Ala**-Ile-Thr-Val-Asn-Gly-Lys-Thr-Tyr-**Ala**-Gly-Arg.

The NMR analysis confirms that all of the peptides adopt a β-hairpin structure in equilibrium with random-coil conformations in aqueous solution. The population ranking is BHKE > BHAE > BHEK > BHKA ≈ BHAA. In previous work, the authors have shown that a plateau of β-hairpin population was found at 40 % TFE for the BH8.[10] The conformational shifts of the Cα protons in 40 % TFE are larger than in aqueous solution indicating an increase of the structured population. As in aqueous solution, peptide BHKE

is the one with the highest population, close to 100 %. All of the peptides are more structured at higher pH values as shown by the downfield shift of the CαH of the two Thr residues.

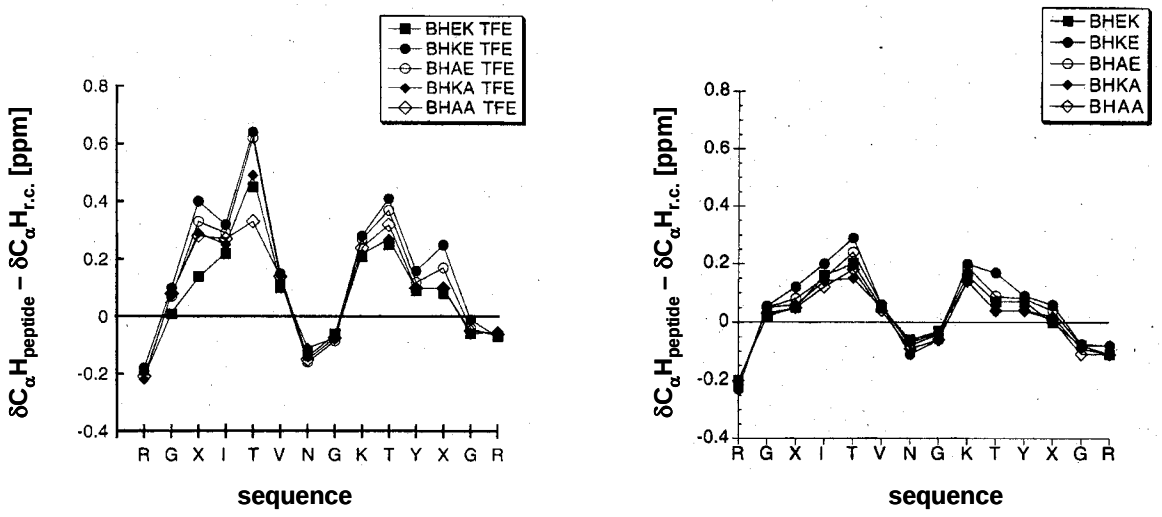

Figure 3: CαH conformational shifts of the different BH-peptides. The conformational shifts of the CαH protons are obtained by subtracting the random-coil values.[11] A: aqueous solution; B: 40 % TFE

Searle and co-workers, using a model β-hairpin system of 16 residues, investigated energetic contributions to the stability of Glu-Lys salt bridges.[12] The authors mutated two Ser-Lys interstrand pairs in **2a** to Glu-Lys salt bridges (**2b** and **2c**) and examined the energetic effects of introducing two salt bridges simultaneously at these two positions (**2d**).

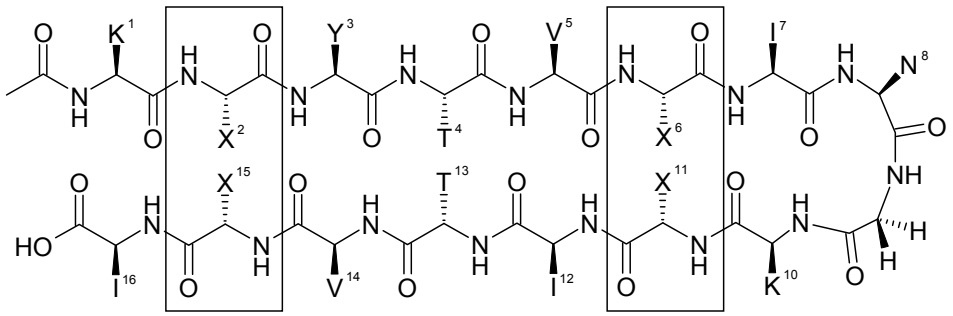

2a: X_2 = Lys, X_6 = Ser, X_{11} = Lys, X_{15} = Ser
2b: X_2 = Lys, X_6 = Glu, X_{11} = Lys, X_{15} = Ser
2b: X_2 = Lys, X_6 = Ser, X_{11} = Lys, X_{15} = Glu
2d: X_2 = Lys, X_6 = Glu, X_{11} = Lys, X_{15} = Glu

Figure 4: Schematic representation of the b-hairpin peptides β1-β4. "X" indicates the sites of the mutated residues with boxes representing the position of the salt bridge

The analytical data show clearly that the selective introduction of an ion-pairing interaction at either position enhances the stability of the folded state by increasing the magnitude of $\Delta\delta_{H\alpha}$ values. Individually, each interaction contributes 1.2-1.3 kJ/mol to stability; however, when introduced simultaneously, the contribution (-3.6 kJ/mol) is greater than the sum of the individual contributions.

In addition to electrostatic interactions, hydrophobic interactions have been investigated. *Cochran* and co-workers used the stabilization of the β-hairpin conformation in short peptides by a tryptophan zipper (trpzip).[13] These trpzips are minimal units of β tertiary structure and have the thermodynamic properties of typical folded proteins.

3a	trpzip1	Ser-Trp-Thr-Trp-Glu-Gly-Asn-Lys-Trp-Thr-Trp-Lys	Type II´turn
3b	trpzip2	Ser-Trp-Thr-Trp-Glu-Asn-Gly-Lys-Trp-Thr-Trp-Lys	Type I´turn
3c	trpzip3	Ser-Trp-Thr-Trp-Glu-^{D}Pro-Asn-Lys-Trp-Thr-Trp-Lys	Type II´turn

Table 2: Amino acid sequences of the trpzip peptides

High-resolution NMR structures show the two cross-strand Trp pair`s interdigitating in a zipper-like motif on the surface of the folded peptide. In each case, the peptides are highly water-soluble, well structured, and monomeric. Trpzip2 (**3b**) appears to be the most stable peptide due to the stronger promoting turn sequence Asn-Gly, despite previous conclusions that the D-Pro-Asn turn is more stabilizing than Asn-Gly.[14]

Based on the results of *Cochran´s* trpzip, a β-hairpin peptide, which functions as a molecular receptor for nucleotides in water, was synthesized by *Butterfield* and co-workers.[15] The diagonal Trp-Trp pair in the non-hydrogen-bonding sites of the β-hairpin peptide WKWK (**4**) provides a binding cleft for aromatic intercalation.

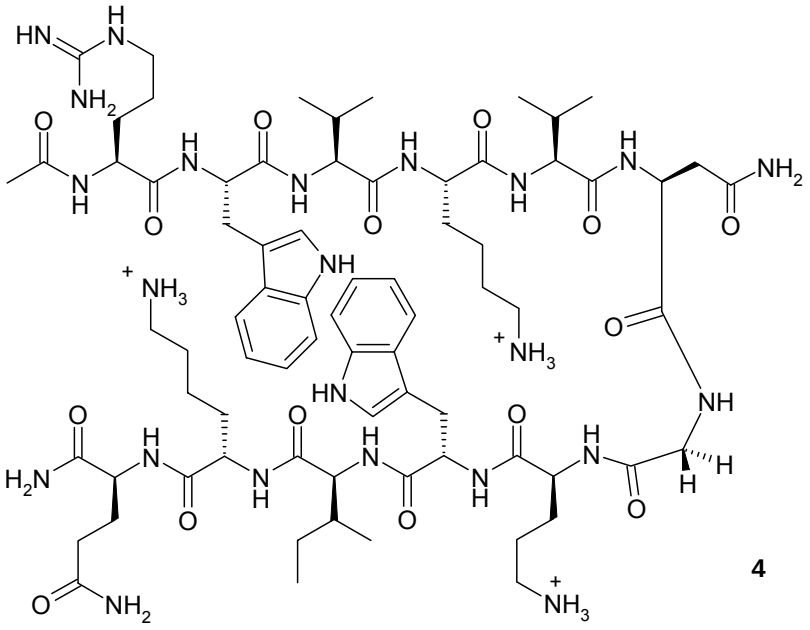

WKWK (**4**): Ac-Arg-Trp-Val-Lys-Val-Asn-Gly-Orn-Trp-Ile-Lys-Gln-NH_2

Figure 5: Structure of the peptide WKWK (**4**)

The ability of WKWK (**4**) to bind ATP in aqueous solution was investigated by fluorescence titration. A remarkable association constant for ATP in aqueous solvent of 5800 M^{-1} was determined from tryptophan emission quenching. Titration of ATP into peptide WKWK (**4**) produced significant upfield shifting of aromatic protons on both Trp

residues as well as the adenine protons of ATP, indicating that the adenine base is interacting with both Trp residues of WKWK (**4**). The selectivity of nucleotide recognition by WKWK (**4**)[16] was investigated by proton NMR titrations and the affinity constants for WKWK binding to ATP, guanosine 5´-triphosphate (GTP), cytidine 5´-triphosphate (CTP), and thymidine 5´-triphosphate (dTTP) are summarized in table 3.

nucleotide	K_{assoc}, M^{-1}	K_d, mM	ΔG (error*), kcal/mol	Δ_0, ppm
ATP	700	1.4	- 3.9 (0.1)	- 0.12
GTP	2200	0.45	- 4.6 (0.1)	- 0.06
dTTP	3700	0.27	- 4.9 (0.1)	- 0.05
CTP	270	3.7	- 3.3 (0.1)	- 0.03

Table 3: Affinity constants for WKWK (**4**) binding to nucleotide triphosphates (in 10 mM d_3-acetate buffer, 10 mM NaCl, pH 5.0 (uncorrected) at 298 K. * Errors determined from the average deviation between 2 and 4 separate titration experiments

Peptide WKWK (**4**) demonstrates measurable selectivity of dTTP and GTP binding. The order of binding affinity follows dTTP>GTP>ATP>CTP, with differences in binding energies spanning as much as 1.6 kcal/mol.

The two Lys residues of WKWK (**4**) on the same face of the hairpin allow a favorable electrostatic interaction with flavin mononucleotide (FMN).[17] Several analytical methods demonstrate that the flavin ring intercalates between the two Trp residues. The difference in binding affinities between FMN (K_{assoc} = 2200 M^{-1}) and riboflavin (K_{assoc} = 310 M^{-1}) indicates that electrostatic interactions of the FMN phosphate group contribute approximately - 1 kcal/mol to the overall FMN binding. This value is in agreement with electrostatic contributions to ATP recognition by WKWK (**4**).

The interaction between proteins and single-stranded DNA (ssDNA) plays an important role in the regulation of critical biological processes such as the DNA replication and repair.[18] Due to the remarkable association constants of WKWK (**4**) to nucleotides, the authors expected the dimer $(WKWK)_2$ (**5**) as a potential receptor for ssDNA. A disulfide bond between *N*-terminal Cys side chains dimerizes WKWK.

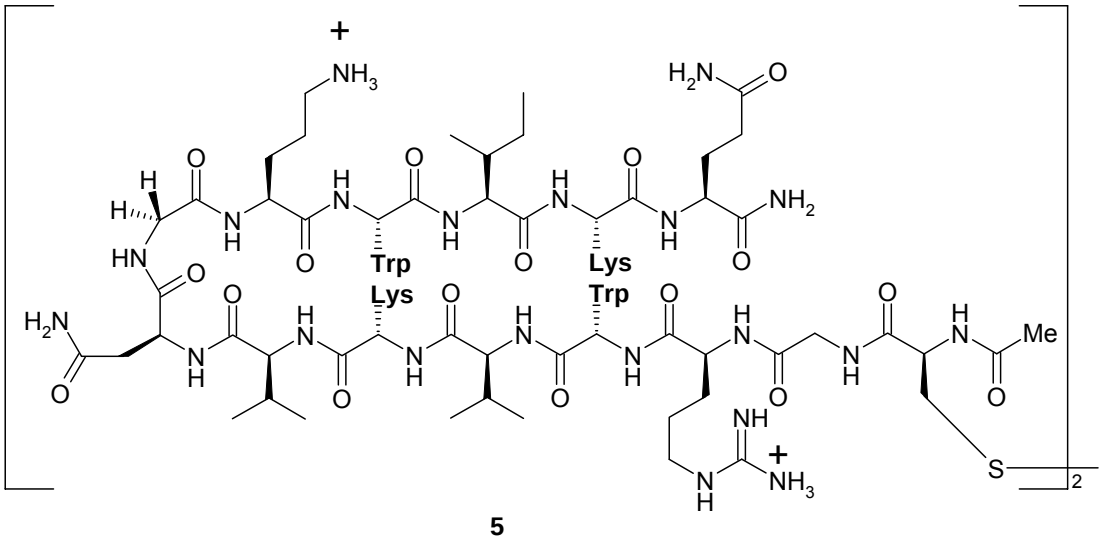

Figure 6: Structure of peptide (WKWK)$_2$ (**5**). The residues in bold create the nucleic acid binding site

The structure of the (WKWK)$_2$ dimer (**5**) creates two nucleotide binding sites which are expected to be well-structured due to the highly populated β-hairpin conformation of WKWK. The recognition of a single-stranded pentanucleotide sequence 5´-d(AAAAA)-3´ (dA$_5$) was investigated, followed by the determination of sequence selectivity between dA$_5$, dT$_5$, and dC$_5$. Finally, the binding of (WKWK)$_2$ (**5**) to an 11-residue single-stranded oligonucleotide and its corresponding duplex was investigated.

Entry	sequence	[NaCl], mM	K_a, M^{-1}	K_d, μM	ΔG (error*), kcal/mol
1	5´-AAAAA-3´	0	8 x 10^4	12	- 6.7 (0.1)
2	5´-TTTTT-3´	0	3 x 10^4	30	-6.1 (0.1)
3	5´-CCCCC-3´	0	5 x 10^4	20	- 6.4 (0.1)
4	5´-CCATCGCTACC-3´	100	3 x 10^5	3	- 7.5 (0.1)
	5´-CCATCGCTACC-3´				
5	3´-GGTAGCGATGG-5´	100	2 x 10^5	5	- 7.2 (0.1)

Table 4: affinity constants for (WKWK)$_2$ (**5**) with DNA sequences in a 10 mM sodium phosphate buffer, pH 7.0, at 298 K. * Errors determined from the average deviation between 2 and 4 separate titration experiments

The modest selectivity for dA_5 is not surprising given the ssDNA-binding proteins interacting with their nucleotide target in a largely independent manner.[19] The stronger interaction with the 11-mer relative to the pentanucleotides can be attributed to an increased number of favorable contacts that are possible with the longer oligonucleotide.

The growing problem of resistance to established antibiotics has stimulated intense interest in the development of novel antimicrobial agents with new modes of action. One emerging class of antibiotics is based on naturally occurring cationic peptides.[20] These include the disulfide-bridged β-hairpin and β-sheet peptides protegrins,[21] tachyplesins,[22] and defensins, which adopt a β-hairpin-like structure.[23]

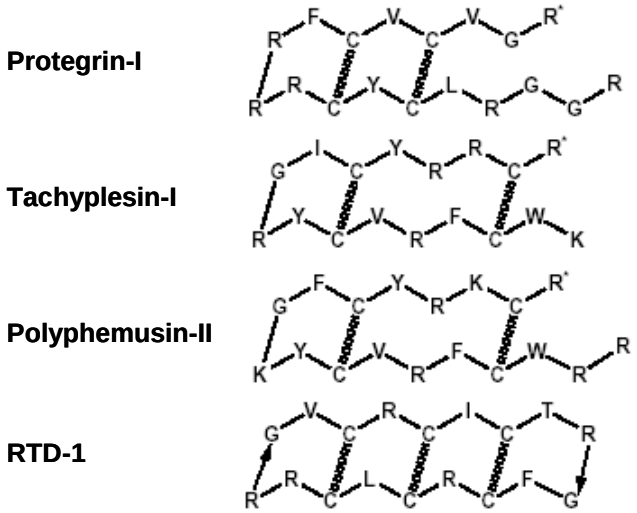

Figure 7: Naturally occurring β-hairpin antimicrobial peptides. R^* = C-terminal arginine amide.

The naturally occurring protegrins and tachyplesins exert a significant haemolytic activity against human red blood cells, a key indicator of toxicity. Based on the natural peptides (Figure 3), *Robinson et al.* synthesized new antimicrobial peptidomimetics that show potent and selective activity.[24]

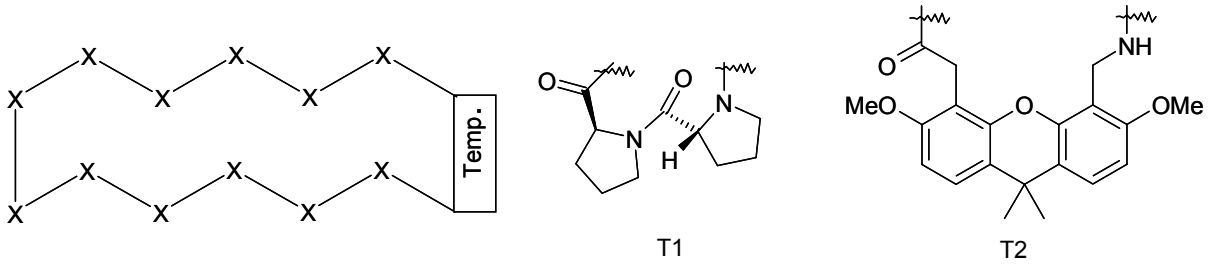

Figure 8: β-hairpin mimetics. X = cationic and/or hydrophobic/aromatic amino acid residue, Temp. = template T1 or T2.

Screening of a library of 12-amino acid residue mimetics (Figure 4), which contain a D-Pro-L-Pro template (T1) or a xanthene template (T2), gave several members with activity against Gram-positive and Gram-negative bacteria, as well as the yeast *Candida albicans* (Table 5).

Mimetic	Amino acid sequence*	MIC [μg ml^{-1}]				% Hemolysis
		S. aureus	*E. coli*	*P. aerug*	*C. albic*	
6a	LRLKYRRFKYRV-T1	25	12	25	12	27
6b	LRLQYRRFQYRV-T1	12	6	12	6	27
6c	LRLEYRRFEYRV-T1	100	100	> 100	50	14
6d	LRLKKRRWKYRV-T1	12	12	6	12	1
6e	LRLKKRRWKYRV-T2	6	25	25	6	13
6f	LCLKKRRWKYCV-T1	25	6	25	12	3
6g	LRCKKRRWKCRV-T1	25	25	50	50	1
	Protegrin I	6	3	3	6	37
	Tachyplesin I	2	1	2	2	34

Table 5: Assay of antibiotic and hemolytic activity. *: Amino acids in the single letter code

The structure of the mimetics is different to the naturally occurring peptides that adopt a β-hairpin-like structure. While mimetic compound **6d** is largely unstructured in water, despite the effect of the D-Pro-L-Pro template, it clearly adopts a β-hairpin conformation in the

presence of DPC micelles. A regular β-hairpin geometry is not present in compound **6g**, although a short stretch of 3_{10} helix is seen.

3. Turn Mimics for Peptide Hairpin Structures

Peptides showing a turn conformation are of high relevance since, in many cases, the turn region is responsible for biological activity. Well known examples are somatostatin[25] and oxytocin.[26] Consequently, β-turns and β-turn mimetic adopting discrete conformations ("foldamers") have become target structures in medicinal research. This section will focus on turn mimetics and their ability to promote a turn structure. *Lubell* pursued two strategies for generating peptide mimics: the first employs the use of biciclics to constrain a dipeptide unit. The second uses the steric interactions of bulky ring substituents to influence the geometry.[27] *Golebiowski* and co-workers using the Ugi reaction as a key step describe the synthesis of a bicyclic diketopiperazine.[28] This compound overlaps well with a type II β-turn.

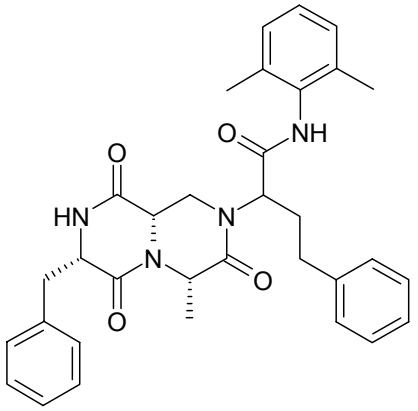

7

Figure 9: A bicyclic diketopiperazine β-turn mimetic

Next to their ability to induce β-turns, diketopiperazines are rigid backbones of peptide receptors.[29] Several receptors with two identical arms were prepared in order to examine their binding properties against a peptide library of 24,389 peptides.

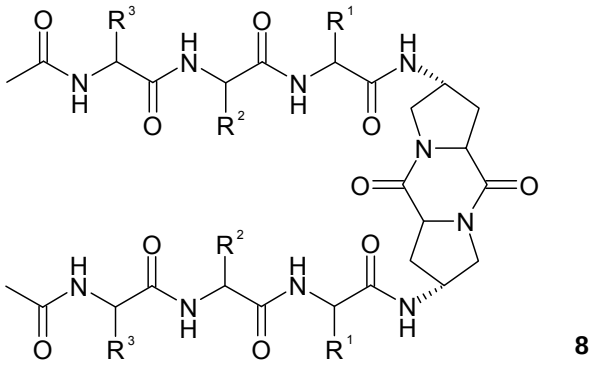

8

Figure 10: Two-armed diketopiperazine receptors.

The receptors were marked with the red azo dye Disperse Red 1 (DR1) which allows the monitoring of the peptide bonding. The following receptors were used:

DR mimetic 1 (**8a**)	Phe-Asn(Trt)-Tyr
DR mimetic 2 (**8b**)	Phe-Asn(Trt)-D-Tyr
DR mimetic 3 (**8c**)	Asn(Trt)-Phe-D-Tyr
DR mimetic 4 (**8d**)	Phe-Gln(Trt)-Tyr
DR mimetic 5 (**8e**)	Gln(Trt)-Phe-Tyr

The assays of DR mimetic 1 (**8a**) and DR mimetic 5 (**8e**) indicated a particularly high level of binding specificity since only 25 beads from all tested members of the library showed the red color of the receptor. This corresponds to a selectivity of one selected bead out of 5000. While **8a** exclusively selects peptides containing a D-His following two hydrophobic D-amino acids, **8e** solely chooses peptides with an Asn following both a hydrophobic L- and D-amino acid. Affinity constants up to $K_a = 1420 \pm 200\ M^{-1}$ were observed.

Most of the synthetic foldamers have homogeneous backbones, i.e. they are built from a single type of monomer. Oligomers of heterogeneous backbones are also important in conformational design. *Gellman* and co-workers reported an oligomer that adopts a β-hairpin shape. The loop is composed of β-amino acids while the strands consist of α-amino

acids.[30] The loop segments made from dinipecotic acid (Nip) adopts a loop conformation in β-hairpins as shown in previous studies.[31]

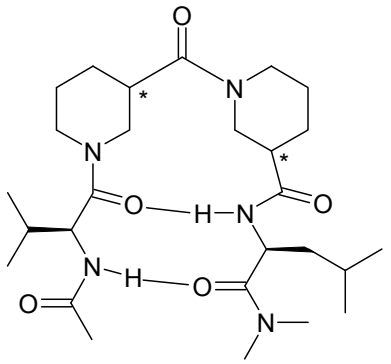

9a: *R*-NIP-*S*-NIP
9b: *S*-NIP-*R*-NIP
9c: *R*-NIP-*R*-NIP
9d: *S*-NIP-*S*-NIP

Figure 11: β-Turn hairpins bearing a nipecotic acid loop segment

The data of IR and NMR analysis indicate that the heterochiral loops (**9a**, **9b**) support hairpin formation while the homochiral loops (**9c**, **9d**) do not. A homochiral dinipecotic acid β-peptide does not allow the formation of a 12-membered ring hydrogen bond that is necessary for the hairpin folding.[32]

To help understand the folding and stability of peptides, a negatively charged dibenzofuran-based β-turn mimic was incorporated into the loop 1 of the PIN1 WW domain.[33] These three-stranded β-sheet domains are found in more than 200 multidomain proteins where loop 1 of PIN1 plays a critical role in binding of the phosphoserine (pS) residue in the YSPTpSPS peptide substrate.[34] The formation of the loop 1 is rate limiting for the folding of the PIN1 WW domain.[35]

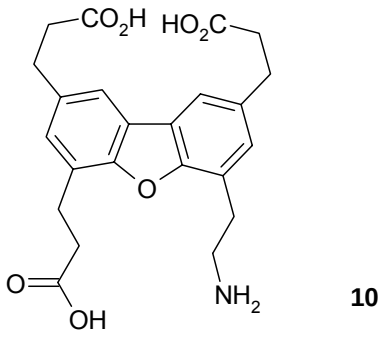

Figure 12: 4-(2-aminoethyl)-6-dibenzofuran propionic acid (**10**)

The incorporation of the bis-anionic version of 4-(2-aminoethyl)-6-dibenzofuran propionic acid (**10**) as turn mimetic in lieu of the uncharged analogue resulted in enhanced solubility. The thermodynamic stability of the PIN WW domain is not perturbed significantly.

Dipeptide isosters derived from Leu and *meso*-tartraic acid derivatives (6-*endo*-BTL (**11a**) and 6-*endo*-BtL (**11b**)) were inserted in a small peptide.[36] The chair conformation of the six-membered ring locked in the biciclic structure, in conjunction with the *endo* configuration at C6 gives the right shape for imposing a reverse β-turn.

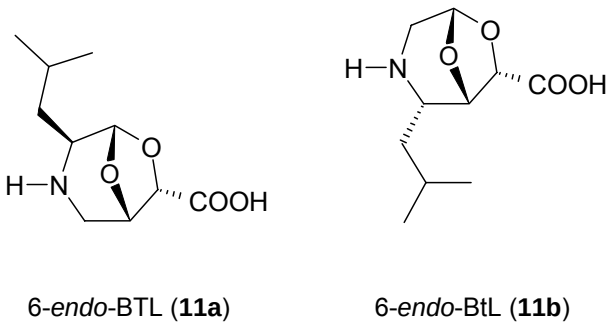

Figure 13: 6-*endo*-BTL (**11a**) and 6-*endo*-BtL (**11b**)

Both turn structures were incorporated into a tetrapeptide, giving Ac-Val-Ala-6-*endo*-BT(t)L-Val-Gly-OMe. The 6-*endo*-BTL peptide shows the turn structure as a minor conformer in a 1:3 ratio to an open reverse turn conformation, while the corresponding

peptide shows a unique turn conformation. However, the 6-*endo*-BTL peptide, having the Leu side chain in axial position, is a better turn inducer since it can promote a tighter turn.

A turn mimic derived from PLG (prolyl-glycine amide) containing a β-lactam in the turn area was prepared by *Podlech et al.*[37] The substrate has a turn configuration even though no stabilizing central hydrogen bond is present. The so-called "open turn conformation"[38] is in fact stabilized by a hydrogen bond between the β-lactam carbonyl group and the neighboring NH moiety.

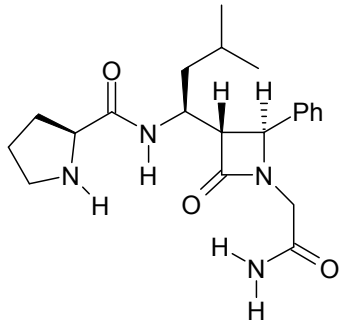

12

Figure 14: Targeted peptidomimetic (**12**) bearing a β-lactam moiety.

The resulting six-membered twist-boat-like ring is not only present in the solid state but also in solution in $CDCl_3$. The stabilization is only possible because of the additional alkylidene group between incoming and leaving peptide strands.

Proline substitution has been widely used to search for turns[39] because Pro is frequently found at the i+1 position of a β-turn.[40] *Ishiguro et al.* have synthesized (2*S*,4*S*)- and (2*S*,4*R*)-4-(2´-guanidinoethyl) proline as a conformational restricted arginine.[41] These analogues were incorporated into mini atrial natruretic polypeptide (miniANP), which has an important turnlike conformation at Gly^6-Arg^7-Met^8-Asp^9.[42] The backbones of the arginine analogues fit the turn because of the bent backbone of proline. Although NMR could not determine the overall conformation of the analogues, in each case the distance constraints were consistent with and converged well into a type I β-turn. MiniANP is the smallest analogues of ANP-related peptides.[43] It contains 15 natural amino acids and binds selectively to natriuretic peptide receptor A (NPR-A). In biological activity measurements,

the production of cGMP in Chinese hamster ovary cells expressing NPR-A in response to peptides **13a-e** was measured.

Peptide		Biological avtivity EC_{50} (nmol)	Relative biological activity EC_{50} (analogue)/ EC_{50} (miniANP)
miniANP	**13a**	3.1 ± 0.5	1.0
[4*S*-GEPro^7]miniANP	**13b**	4.6 ± 0.4	1.5
[4*R*-GEPro^7]miniANP	**13c**	1.3 ± 0.6	0.4
[Pro^7]miniANP	**13d**	58.1 ± 17.2	18.7
[Ala^7]miniANP	**13e**	137.3 ± 11.3	44.3

Tabelle 1: Biological activity of miniANP (**13a**) and analogues (**13b-e**)

The table shows that [4*S*-GEPro^7]miniANP (**13b**) and [4*R*-GEPro^7]miniANP (**13c**) are as potent as miniANP (**13a**) but of 19 times lower activity than [Pro^7]miniANP (**13d**).

To develop a definitive approach towards the design of an I´ turn nucleated β-hairpin, *Shamala & Balaram* have investigated α-aminoisobutyric (Aib) Aib-D-Xxx nucleating segments.[44] The incorporation of a D-residue intends to favor a formation of a type I´ β-turn, as in the analogue D-Pro-Gly segments.[45] The Aib-D-Ala segment was incorporated into a hexapeptide, giving Boc-Leu-Phe-Val-Aib-D-Ala-Leu-Phe-Val-OMe. This peptide adopts a β-hairpin structure with a type I´ β-turn at the Aib-D-Ala segment.

Tomasini and co-workers described the synthesis and the conformational analysis of a small library of fully protected tetramers containing pseudoprolines.[46] The general structure of the tetramers and the pseudoprolines is shown in figure 14.

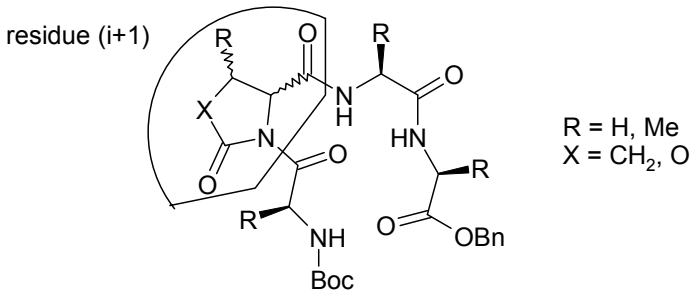

Figure 15: General structure of the fully protected tetramers

L-Pyroglutamic acid (L-pGlu), (4*S*,5*R*)-4-methyl-5-carboxybenzyloxazolidin-2-one (L-Oxd), or (4*R*,5*S*)-4-methyl-5-carboxybenzyloxazolidin-2-one (D-Oxd) are used in place of pseudoproline. Table 6 summarizes the amino acid sequences of the investigated tetrapeptides.

Entry	Amino acid sequence
14a	Boc-Ala-L-pGlu-Gly-Ala-OBzl
14b	Boc-Val-L-pGlu-Gly-Ala-OBzl
14c	Boc-Val-L-pGlu-Aib-Ala-OBzl
14d	Boc-Val-L-Oxd-Gly-Ala-OBzl
14e	Boc-Val-D-Oxd-Gly-Ala-OBzl
14f	Boc-Val-D-Oxd-Aib-Ala-OBzl

Table 6: Amino acid sequences of the investigated tetrapeptides (**14a-f**)

Gly is widely found in natural reverse-turn structures while Aib tends to form helical structures (helycogenic).[47] The molecules containing D-Oxd showed a good propensity to form a β-hairpin conformation. Among them, Boc-Val-D-Oxd-Gly-Ala-OBzl (**14e**) had a preferential β-turn conformation in chloroform and a preferential γ-turn conformation in DMSO. Its epimer, Boc-Val-L-Oxd-Gly-Ala-OBzl (**14d**) is less able to assume ordered forms in solution.

Metzler-Nolte and co-workers prepared Di- and tertapeptides bearing a metallocene backbone.[48] The metal was altered between Fe^{2+} and Co^{+} to change the overall charge of the constructs.

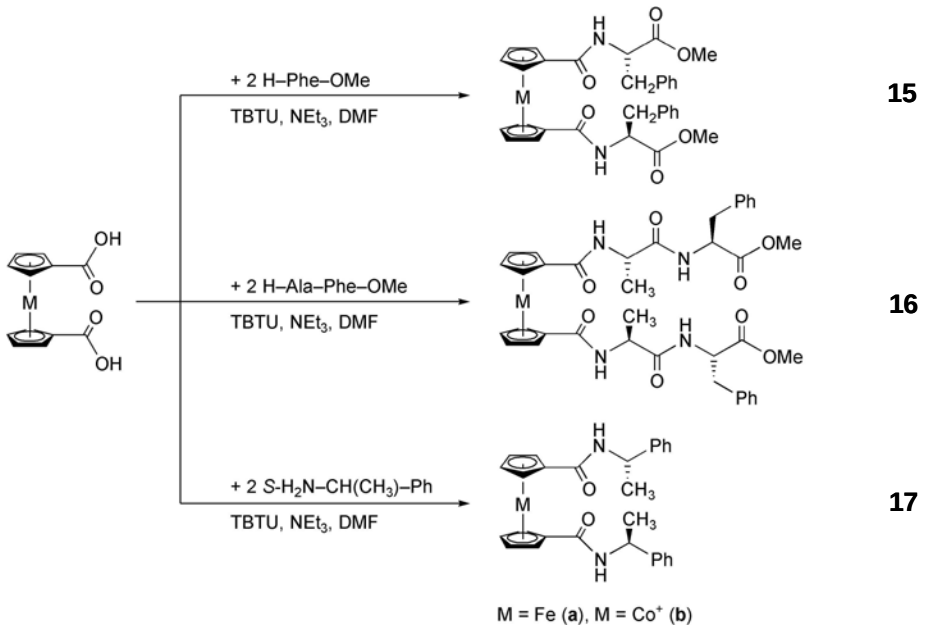

Figure 16: Synthesis of the di- and tetrapeptides with a metallocene backbone

Evidence of strong interaction was found in **15** and **16**, while **17a** shows no intramolecular hydrogen bond. In the solid state, an intramolecular hydrogen bond is formed between the amide NH and the ferrocene CO in **15a**. If connecting atoms are counted, an 8-membered ring is formed. The situation for **16a** is different. Two intramolecular hydrogen bonds N1···O6 and N3···O2 are formed. Both define 11-membered rings between O (i) and N (i+3). This describes **15a** as a γ-turn-like and **16a** as a β-turn-like structure. Similar results are found in chloroform solution for **16a** but **15a** shows now a NH···CO (ester) hydrogen bond. A comparison between uncharged ferrocene derivatives **15a** and 16**a** and positively charged cobaltocenium derivatives **15b** and **16b** shows that both pairs do presumably form very similar structures.

Photochromic compounds, which undergo large conformational changes when exposed to light, are also interesting in the field of turn mimetics. Azobenzenes are potentially well

suited for this application. *Hilvert* and co-workers incorporated substituted azobenzenes in a 12-residue peptide, derived from GB1.[49] GB1 has been shown to adopt a hairpin structure in aqueous solution.[50]

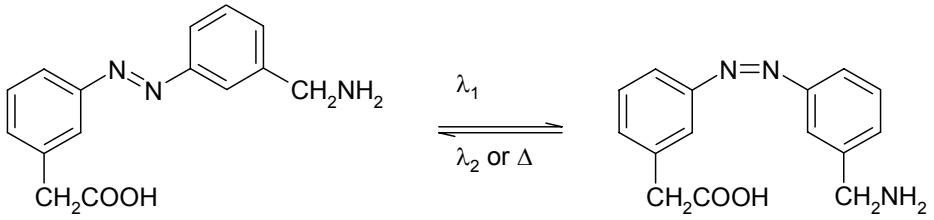

18a **18b**

Arg-Trp-Gln-Tyr-Val-X-Lys-Phe-Thr-Val-Gln-NH_2

GB1: X = D-Pro-Gly
mimetic: X = azobenzene

Figure 17: *Cis-trans* isomerization of azobenzene and the amino acid sequence of the peptides

Irradiation at the wavelength of the $\pi \rightarrow \pi^*$ transition converts the *trans* (**18a**) into the *cis* (**18b**) isomer. The reverse process can be induced either thermally or by the irradiation at the wavelength of the $n \rightarrow \pi^*$ transition. In its *cis* configuration, the meta-substituted azoebenzene mimics the dipeptide D-Pro-Gly in nucleating a stable and monomeric hairpin structure. In contrast, the *trans* configurated peptide did not adopt a unique structure.

Short linear peptides are inherent flexible molecules, especially in aqueous solution, and so are often poor mimetics of the secondary structures. To circumvent this folding-problem, much attention has been paid to the design of templates that constrain peptide chains into biologically relevant secondary structures such as cyclic peptides.[51] Linear synthetic peptides containing tandemly repeated NPNA motifs were evaluated in the late 1980s as potential malaria vaccine candidates.[52] Such linear peptides are flexible in water, but presumably adopt a folded conformation in the intact protein.[53] A bicyclic template, containing a diketopiperazine derived from Asp and (2*S*,3*R*,*4R*)-diaminoproline was incorporated in an acyclic peptide bearing the NPNA-motif.[54]

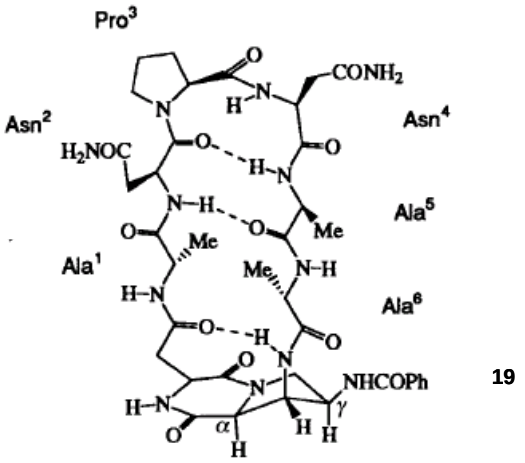

Figure 18: Structure of the NPNA-motif containing mimetic

NMR spectra indicate a well-defined β-hairpin conformation for (**19**) in DMSO solution. NOEs and H/D-exchange rates show a well-populated 2:2 conformation with a type I β-turn in the Asn^2-Pro^3-Asn^4-Ala^5 (NPNA) motif in the tip of the hairpin loop.

Amino acid 7/5 bicyclic lactams are dipeptide surrogates in angiotensin-converting enzyme (ACE) inhibitors.[55] The 7/5 bicyclic lactam was used as external constraints for the GLDV motif by *Young* and co-workers.[56]

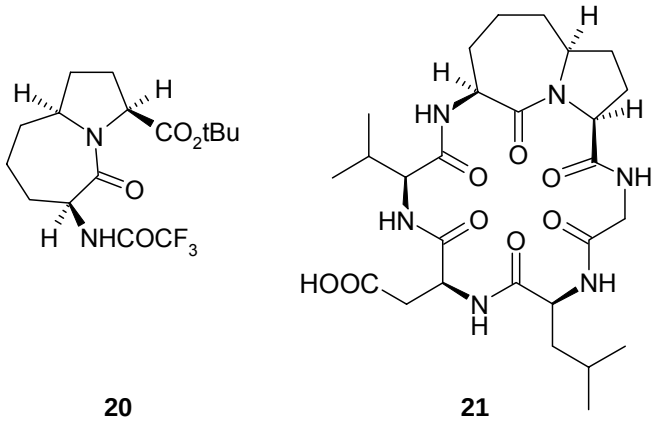

Figure 19: The structure of the 7/5 bicyclic lactam (**20**) and of the synthesized peptide (**21**)

In agreement with X-ray crystal structure analysis and calculations, the 7/5 bicyclic lactam (**20**) was not a β-turn mimetic on its own. However, the high-resolution NMR spectroscopic data for the cyclic peptide (**21**) was consistent with a single backbone conformation, either type VI or type II´ β-turn properties.

The effects of chirality and side-chain interactions on the formation of a type II´ β-turn were studied by *Wishart et al.*[57] The appealing β-hairpin model is based on gramicidin S (GS). GS is a cyclic, amphiphatic decapeptide composed of two evenly spaced type II´ β-turn connected by an antiparallel β-sheet.[58] For this study, a 14-residue cyclic analogue of GS was selected bearing different amino acids in the i+1 and i+2 positions in both turns.

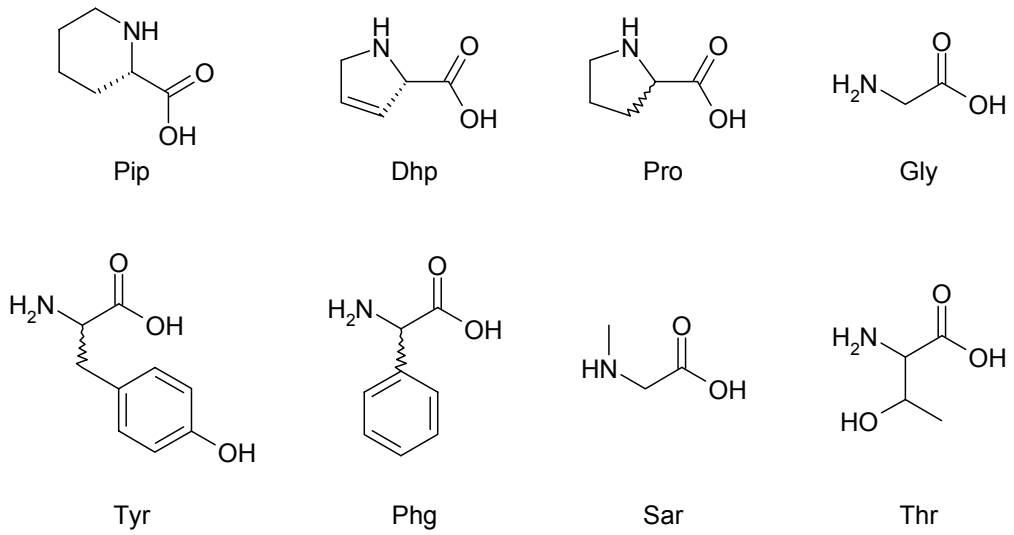

Figure 20: Amino acids at position i+1 and i+2 in both turn 1 and turn 2.

Heterochirality is an essential requirement for type II´ β-turn conformation supporting Rose´s "equatorial-axial rule".[59] Gly-Gly and Sar-Sar analogues are not able to adopt or stabilize a type II´ β-turn. The content of β-sheet formation and proper side-chain interactions accounts for ≈ 10 % type II´ β-turn stabilization. Analogues with L-Pro at position i+2 and/or D-Pro at position i+1 have a predisposition to form a β-turn. Furthermore, D-Pro (i+1), pipecolic acid (Pip), and 3,4-dehydroproline (Dhp) act as excellent type II´ β-turn promoters and lead to 20 % type II´ β-turn stability.

4. Peptide Hairpin Structure Mimetics

β-Strands are usually found hydrogen bonded at least in pairs, forming β-sheet structures in proteins. Isolated β-strands are not common. In the former sections, we focused on natural amino acids as (anti-)parallel strands connected by a β-turn. This chapter describes peptide mimetics incorporated into a hairpin structure.[60]

In immune defense, the major histocompatability complex (MHC) proteins selectively bind the extended β-strand conformation of peptides. The peptides derive from intracellular process of viral, bacterial, and endogenous proteins.[61] This type of recognition has implications in leukaemia, inflammatory, and neurological diseases.[62] A series of pathological processes is associated with the formation of a β-sheet structure and protein aggregation in the form of β-amyloid deposition. Alzheimer´s disease as well as Creutzfeld-Jakob disease and BSE are connected with β-sheet aggregation.[63] For these reasons alone, small molecules that mimic β-strands are of great interest in medicinal applications.

Over the past decade, *Nowick* and co-wokers investigated the β-sheet structure and developed useful peptidomimetic blocks that mimic protein β-proteins. The core is 5-amino-2-methoxybenzoic acid. This aromatic system contains an intramolecular hydrogen bond between the oxygen atom of the methoxy group to the lone pair of the nitrogen atom of an amide bond making the receptor more rigid.

An artificial β-sheet with either β-strand mimics either along the upper or the lower edge forming a double stranded turn was described in the last decade.[64] In further studies, a triply templated artificial β-sheet is reported.

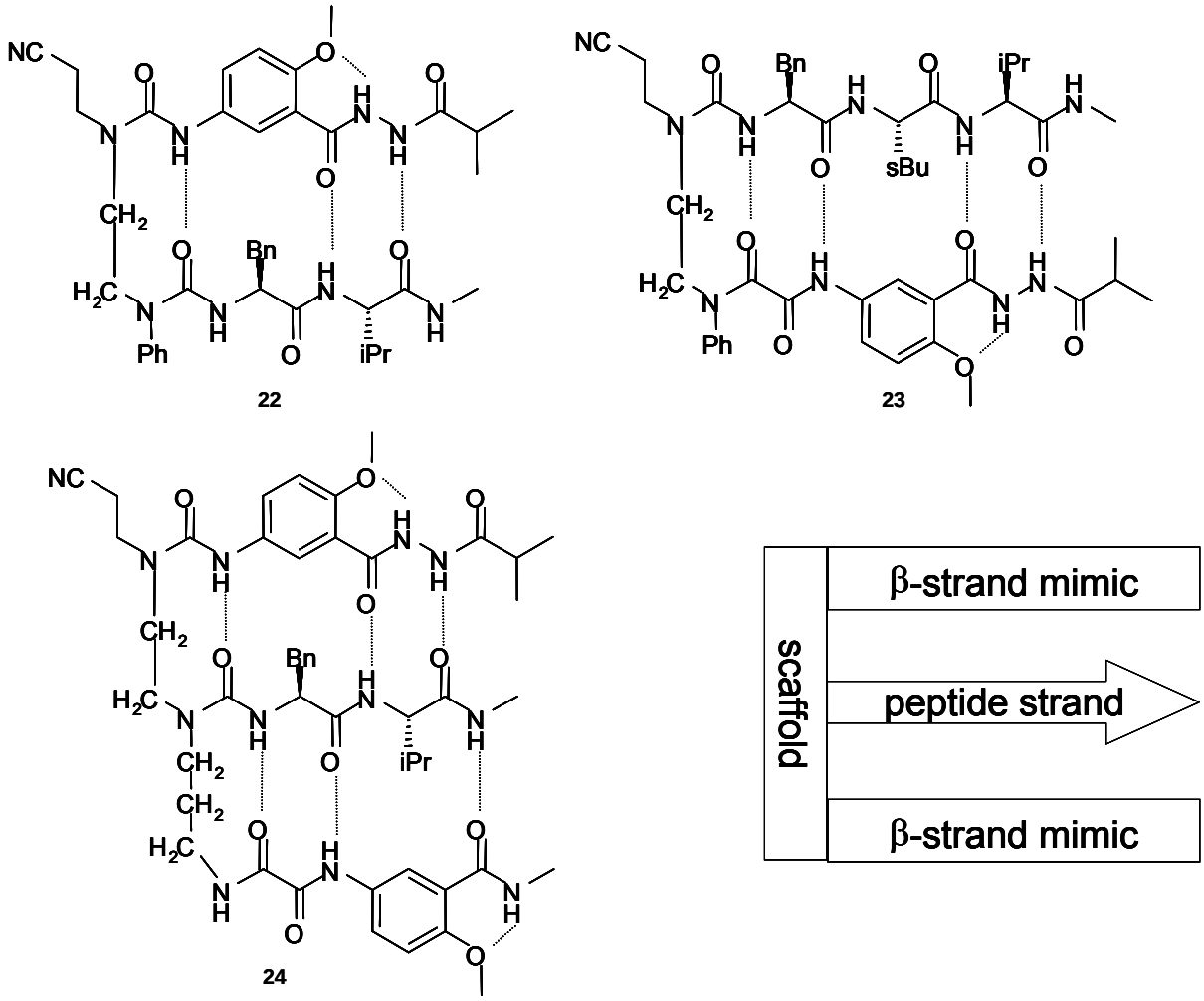

Figure 21: *Nowick´s* double (**22**, **23**) and triple stranded (**24**) artificial β-sheet structures

The NOE and coupling constant data of (**24**) indicate that the component peptide and the strand mimics adopt a β-sheet tlike conformation in chloroform. The folded structure is only observed in a non-compeptitive solvent such as chloroform. It is lost in methanol, a competitive solvent. The upper and lower strand mimics induces a β-sheet structure on an attached peptide strand.[65] The new amino acid, Orn(^{i}PrCO-Hao) (**25**), was introduced, consisting of an ornithine residue (Orn) with the β-strand-mimicking amino acid Hao.[66]

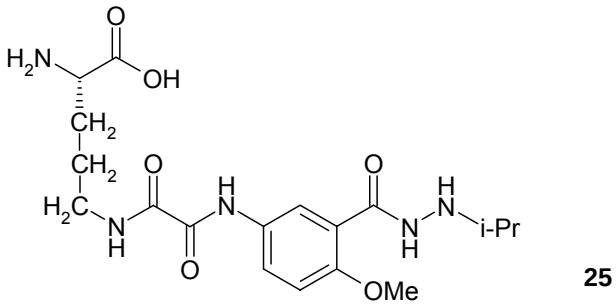

Figure 22: Structure of Orn(^{i}PrCO-Hao) (**25**)

The Orn side chain allows the Hao oxalamide carbonyl group to form a 10-membered ring with the amino group of a connected peptide, forming a β-turn in a β-hairpin. The Orn(^{i}PrCO-Hao) amino acid (**25**) works as a splint that helps to enforce a β-sheet like structure. The triple stranded artificial β-sheet (**24**) depicted in figure 21 shows both the upper and the lower sheet in an antiparallel binding motif. Replacing the lower artificial sheet by a α-peptide strand (Phe-Ile) leads to a combined parallel and anti- β-sheet (**26**).[67]

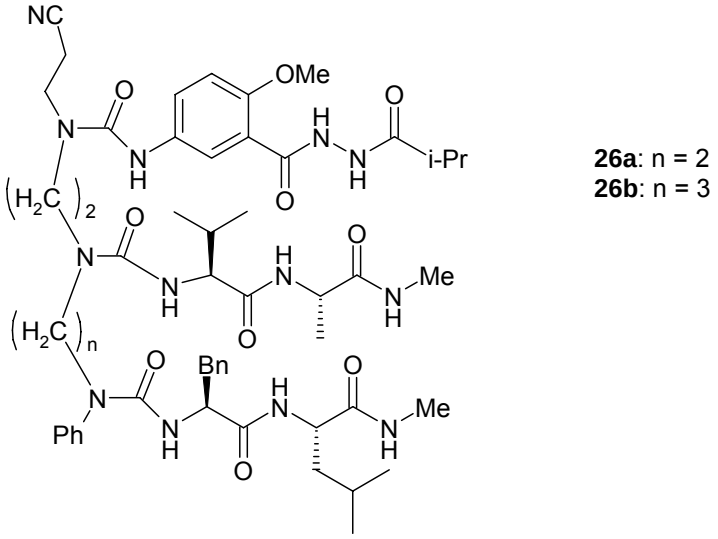

Figure 23: A triple stranded β-sheet with mixed parallel and antiparallel β-sheets

The Hao template forms a pattern of hydrogen bonds similar to that of an antiparallel β-sheet with the middle peptide strand while the middle peptide strand forms a pattern of hydrogen bonds similar to that of a parallel β-sheet with the bottom peptide. The β-strand mimic may be viewed as acting in conjunction with the triurea template to form a "corner bracket". This leads to a stabilized β-sheet structure (**26**) in both of the attached peptide strands. *Nowick´s* artificial β-strand mimetic was also used for the investigation of sequence-selective recognition of peptide strands across non-hydrogen-bonded rings.[68] Therefore, Orn(^{i}PrCO-Hao) (**25**) was attached to a peptide. Two residues, Thr and Val, were replaced in all possible orders at position R_1 and R_4. The residues R_2 (Phe) and R_3 (Ile) were not changed.

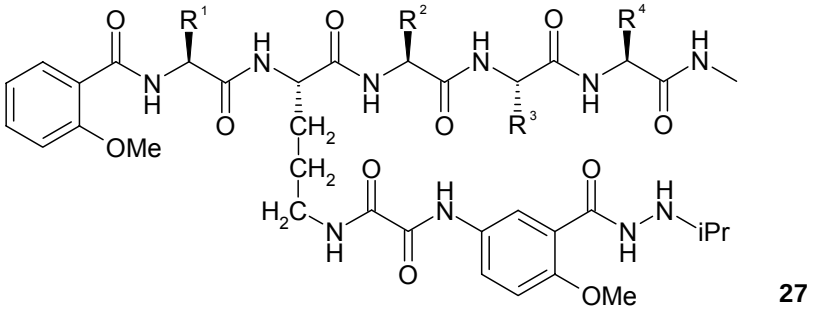

Figure 24: Structure of the investigated molecules (**27a-d**)

Entry	R^1	R^2	R^3	R^4
27a	Thr	Phe	Ile	Val
27b	Val	Phe	Ile	Thr
27c	Thr	Phe	Ile	Thr
27d	Val	Phe	Ile	Val

Table 7: Sequence of the investigated molecules (**27a-d**)

It was expected that Thr would preferentially pair with Thr and Val with Val, through self-complementary non-covalent interactions that occur frequently in the non-hydrogen-bonded rings of antiparallel β-sheets.[69] The investigation was carried out by ^{1}H-NMR spectroscopic

studies. The analysis revealed a strong preference for Thr-Val (**27a**) and Val-Thr (**27b**) to form a heterodimer, while Thr-Thr (**27c**) and Val-Val (**27d**) remain as homodimers. These results confirm the hypothesis that pairing of like residues is preferred.

Koenig and co-workers used structurally similar compounds. First, methoxypyrrole amino acids (MOPAS) and a peptide strand were connected by the D-Pro-Gly turn fragment.[70]

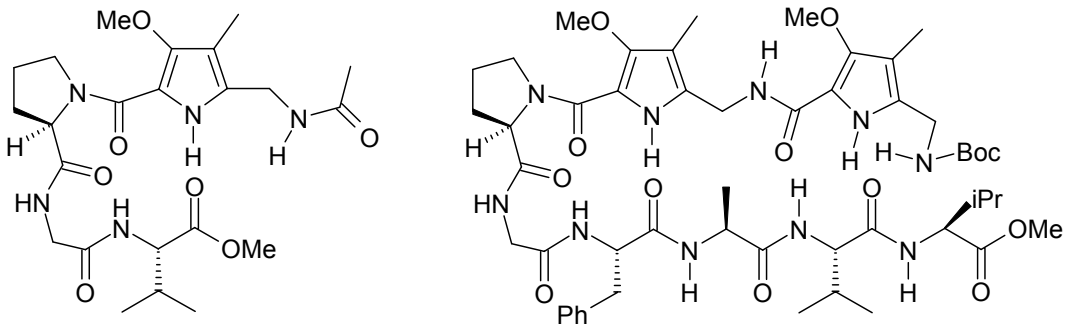

28 **29**

Figure 25: Monomer (**28**) and dimer MOPAS receptors (**29**) connected to peptide strands

It was reported earlier that 5-(aminomethyl)pyrrole-2-carboxylic acid can be considered as a constrained surrogate of Gly-ΔAla.[71] The replacement of the methyl group by a methoxy substituent allows the oxygen atom to form an intramolecular hydrogen bond to the amide proton of a second MOPAS unit. This should keep the pyrrole rings in one plane making the receptor more rigid. The turn structure was proven by 1H-NMR investigation and by X-ray structure analysis of the monomer MOPAS turn (**28**). In further studies, a pyrimidine ring substitutes the pyrrole.[72] As shown by the systems of *Nowick*, a hydrazine unit is necessary for the right pattern of geometry of the pyrimidine hydrazine acids (PHA) to build up extended artificial β-strands. It also allows the formation of an intramolecular hydrogen bond to the lone pair of the nitrogen atom of the pyrimidine ring. This was confirmed by the analysis of temperature dependent ^{1}H-NMR spectra.

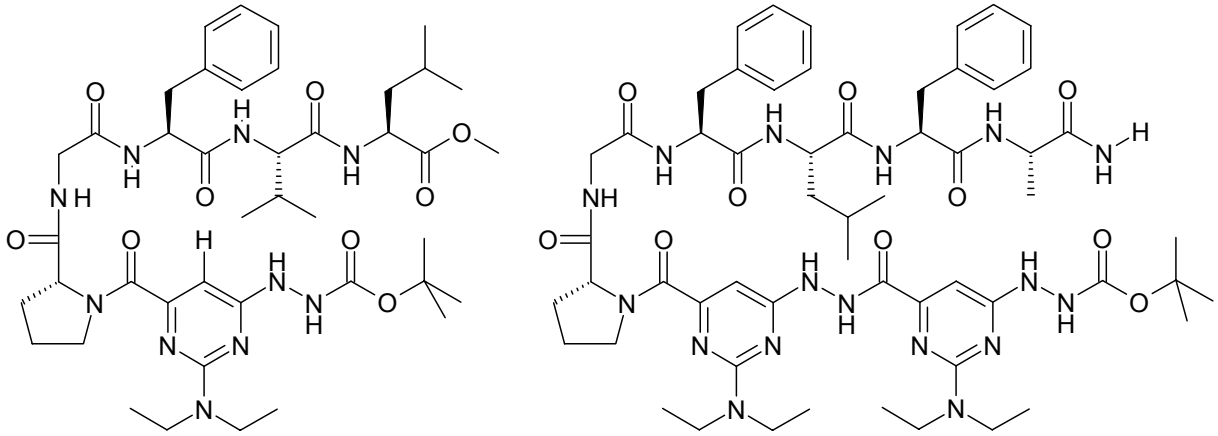

30 **31**

Figure 26: Monomer (**30**) and dimer PHA receptors (**31**) connected to peptide strands

The PHA receptors are not only UV active but show also emission around 420 nm in non-protic solvents after irradiation at 380 nm. The emission intensity decreased upon peptide binding and signaled the binding event.

In this connection with heteroaromatic peptide mimetics, the intensive studies of sequence-selective DNA recognition are to be mentioned. Based on the natural dDNA binding peptides of distamycin[73] and netropsin,[74] *Dervan* and co-workers developed the art of polyamide technology, using *N*-methylpyrazole (Py) and *N*-methylimidazole (Im) covalently linked side-by-side and in a specific manner.[75] We cannot discuss the work in detail here, but is covered in recent reviews.[76]

Fluorescence labeling has become also a general technique for studying the intermolecular accumulation and localization of exogenously administered materials.[77] Phosphotyrosyl (pTyr) mimetic-containing Grb2 SH2 domain binding antagonists are known as anticancer therapeutics typified by naphthylpropylamide analogues (**32**).[78] *Burke Jr.* and co-workers have used these results and modified a potential anticancer drug (**33**) to monitor cellular distribution studies of this class of inhibitors.[79] The environmentally sensitive nitrobenzoxadiazole (NBD) serves as fluorophore by replacing the naphthyl function.

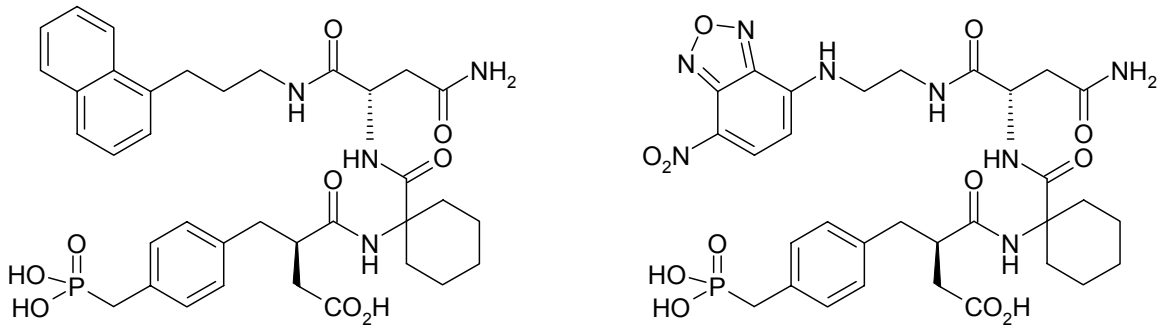

32 **33**

Figure 27: Structures of the parent compounds with a naphthylpropylamide ligand (left) and a nitrobenzoxadiazole ligand (NBD) (right)

The binding affinities of the two compounds were determined using an ELISA-based competition assay. Although modeling studies suggest that the level of bonding interactions afforded by the NBD ring system may not be as great as those provided by the naphthyl ring, the binding affinities are similar.

Cyclic peptides and peptide mimetics are of great interest in medicinal applications because of their rigid shape. Starting from a combinatorial approach, *Burgess* and co-workers discovered a lead structure of a small macrocyclic molecule that potentates the effect of nerve growth factor (NGF) via interactions with its high affinity transmembrane tyrosine kinase receptor (TrkA).[80]

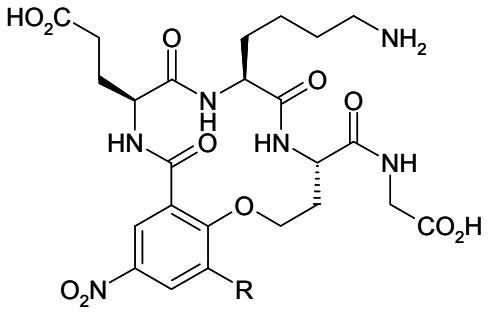

34a R = H (lead structure)
34b R = I
34c R = C≡CPh
34d R = C_6H_4-4-OMe

Figure 28: Structure of the synthesized macrocycles (**34a-d**)

All compounds consist of three natural amino acids (Glu-Lys-Ser) connected by 2-hydroxy-5-nitro-benzoic acid derivatives. However, there are conformational differences among (**34a-d**), NMR experiments and molecular simulations indicate that all compounds can access a turn conformation, close to type I.

The type VI β-turn involving a *cis* imide bond N-terminal to a L-Pro residue situated at the i+2 position plays a significant role in protein folding. It has a profound influence on the recognition process involving protein-ligand interaction.[81] Derived from the tetrapeptide *N*-cinnamoyl-Val-Pro-Phe-Leu-methyl ester (**35**), *Iqbal* and co-workers synthesized a novel *cis*-Pro cyclic peptide (**36**) via ring closing metathesis adopting a type VI β-turn.[82]

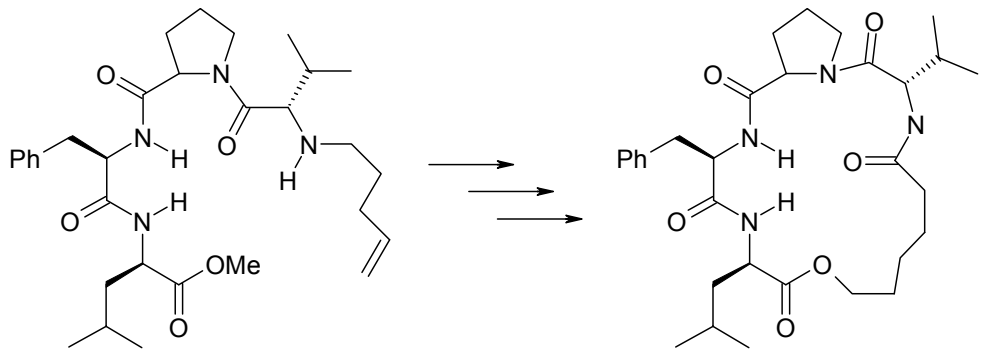

Figure 29: Synthesis of the desired cyclic peptide (**36**).

The open peptide (**35**) exists in a 3_{10} helical structure.[83] The conformation of the cyclic peptide (**36**) depends on the solvent. The solution NMR studies indicate that the major conformer adopts a type VIa β-turn in chloroform, but a type VIb β-turn in DMSO.

β-Peptide foldamers stabilize helical conformation in organic solvents.[84] Hairpin designs have been used to stabilize antiparallel β-peptide sheets.[85] *Gellman* and co-workers report examples of these two concepts.[86] Two β-tetrapeptides were connected by (*R*)-nipecotic-acid-(3*S*,4*R*)-4-aminopiperidine-3-carboxylic acid (Nip-APiC) and both enentiomeric forms of β^2-valine-β^3-lysine.

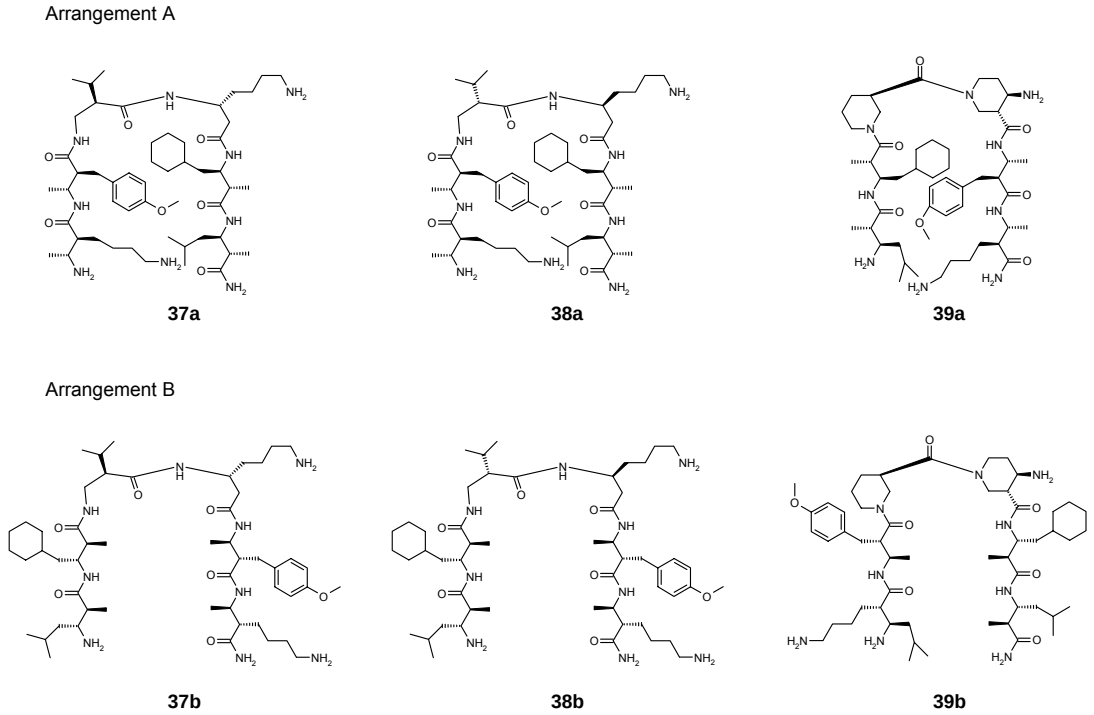

Figure 30: Six antiparallel hairpins with different reverse turn side chain arrangements

The compounds differ in the arrangement of the side chains. All of the large side chain groups are either oriented above (arrangement A) or below (arrangement B) the plane of the amide group. While each pair in of the arrangements differs from the turn segment, the two peptides differ from one another in the juxtaposition of the side chains. In methanol solution, (**37**) and (**38**) adopt at least a partial population of an expected hairpin conformation. The change from *S*- to *R*-configuration (**37a**↔**37b**, **38a**↔**38b**) has no influence on the hairpin population. The arrangements A and B are both tolerated in antiparallel β-peptide sheets. Finally, pairing of large side chains on neighboring strands does not sterically disallow the hairpin formation. No distinct conformations were observed for (**39a**) and (**39b**).

Non-peptidic β-strand complements could also provide a basis for disrupting protein-protein interactions that depend on the recognition of peptide segments in an extended conformation.[87] *Gellman* and co-workers introduced hydrogen bonding complementarity between a secondary sulfonamide and a α-amino acid residue.[88]

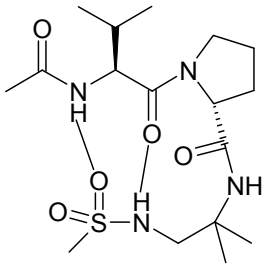

40

Figure 31: The two point hydrogen-bonded interaction between a secondary sulfonamide group and the C=O and N-H of a single peptide residue

Compound (**40**) is the first molecule for which a double hydrogen-bonding pattern of the shown type has been characterized. Both, IR and NMR data confirm the turn structure.

5. Conclusions

In summary, we report herein the recent publications in the field of small peptides adopting a hairpin conformation. These peptides are of great interest due to their biological activity and medicinal applications. Peptide mimetics based on β-turns are important, as many peptides are required to adopt such a conformation while effecting biological response. The article describes the different factors leading to stabilization or destabilization of the peptides´ conformation and activity. Nearby natural peptides, we focus on mimetics incorporated either in the turn region, the peptide strand, or both of them. These pseudo amino acids consist mainly of (heteroaromatic) cycles, metallogenic centers, and inorganic units. The combination of naturally active peptides adopting one conformation as a lead structure and combinatorial chemistry as a tool is supposed to be a promising method resulting in new peptide mimetics. In the ongoing research of biological and medicinal active compounds mediating Alzheimer, AIDS, and cancer, these compounds might help understanding and treating the diseases.

6. References

[1] W. Kabsch and C. Sander, *Biopolymers* **1983**, *19*, 1183.

[2] B. L. Sibanda and J. M. Thornton, *Nature* **1986**, *316*, 170.

[3] G. D. Rose, L. M. Gierosch, and J. A. Smith, *Adv. Protein Chem.* **1985**, *34*, 167.

[4] B. L. Sibanda, and J. M. Thornton, *Nature* **1985**, *316*, 170.

[5] B. L. Sibanda, T. L. Blundell, and J. M. Thornton, *J. Mol. Biol.* **1989**, *206*, 759.

[6] M. Kahn and M. Eguchi, *"Synthesis of Peptides Incorporating β-Turn Inducers and Mimetics"*, Chapter 12.1, Vol. E22c, p. 695, M. Goodman, A. M. Felix, L. Moroder, and C. Toniolo, *"Synthesis of Peptides and Peptidomimetics"*, Houben-Weyl, Stuttgart, Germany, **2003**.

[7] S. H. Gellman, *Curr. Opin. Biol.* **1998**, *2*, 717.

[8] J. J. Ottesen, and B. Imperiali, *Nat. Struct. Biol.* **2001**, *8*, 535; M. D. Struthers, R. P. Cheng, and B. Imperiali, *Science* **1996**, ***271***, 342.

[9] M. Ramirez-Alvarado, F. J. Blanco, and L. Serrano, *Protein Science* **2001**, *10*, 1381.

[10] M. Ramirez-Alvarado, F. J. Blanco, H. Niemann, and L. Serrano, *J. Mol. Biol.* **1997**, *273*, 898.

[11] G. Merutka, H. J. Dyson, and P. E. Wright, *J. Biol. Mol.* **1995**, *5*, 14.

[12] B. Ciani, M. Jourdan, and M. S. Searle, *J. Am. Chem. Soc.* **2003**, *125*, 9038.

[13] A. G. Cochran, N. J. Skelton, and M. A. Starovasnik, *Proc. Nat. Acad. Sci.* **2001**, *98*, 5578.

[14] A. G. Cochran, R. T. Tong, M. A. Starovasnik, E. J. Park, R. S. McDowell, J. E. Theaker, and N. J. Skelton, *J. Am. Chem. Soc.* **2001**, ***123***, 625; F. A. Suyd, J. F. Espinosa, and S. H. Gellman, *J. Am. Chem. Soc.* **1999**, *121*, 11577.

[15] S. M. Butterfield, and M. L. Waters, *J. Am. Chem. Soc.* **2003**, *125*, 9580.

[16] S. M. Butterfield, M. M. Sweeney, and M. L. Waters, *J. Org. Chem.* **2005**, *70*, 2205.

[17] S. M. Butterfield, C. M. Goodman, V. M. Rotello, and M. L. Waters, *Angew. Chem. Int. Ed.* **2004**, *43*, 724.

[18] A. Bocharev, R. A. Pfuetzner, A. M. Edwards, and L. Frappier, *Nature* **1997**, *385*, 176; C. P. A. Kloks, C. A. E. M. Spronk, E. Lasonder, A. Hoffman, G. W. Vuister, S. Grzesiak, and C. W. Hilbers, *J. Mol. Biol.* **2002**, *16*, 317.

[19] E. M. Anderso, W. A. Halsey, and D. S. Wuttke, *Biochemistry* **2003**, *42*, 3751.

[20] M. G. Scott, and R. E. W: Hancock, *Crit. Rev. Immunol.* **2000**, *20*, 407; W. van´t Hof, E. C. I. Veerman, E. J. Helmerhorst, and A. V. N. Amerongen, *Biol. Chem.* **2001**, *382*, 597.

[21] V. N. Kokryakov, S. S: L. Harwig, E. A. Panyutich, A. A. Shevchenko, G. M. Aleshina, O. V. Shamova, H. A. Korneva, and R. I. Lehrer, *FEBS Lett.* **1993**, *327*, 231.

[22] T. Nakamura, H. Furunaka, T. Miayata, F. Tokunaga, T. Muta, S. Iwanga, M. Niwa, T. Takao, and Y. Shimonishi, *J. Biol. Chem.* **1988**, *263*, 16709.

[23] R. I. Lehrer, A. K. Lichtenstein, and T. Ganz, *Annu. Rev. Immunol.* **1993**, *11*, 105.

[24] S. C. Shankaramma, Z. Athanassiou, O. Zerbe, K. Moehle, C. Mouton, F. Bernardini, J. W. Vrijbloed, D. Obrecht, and J. A. Robinson, *Chem. Bio. Chem.* **2002**, *3*, 1126.

[25] K. Hallenga, G. van Binst, A. Scarso, A. Michel, M. Knappenberg, C. Dremier, J. Brison, and J. Driks, *FEBS Lett.* **1980**, *119*, 47; D. F. Veber, R. M. Freidinger, D. S. Perlow, W. J. Paleveda Jr., F. W. Holly, R. G. Strachan, R. F. Nutt, B. H. Aryson, C. Homnick, W. C. Randall, M. S. Glitzer, R. Saperstein, and R. Hirschmann, *Nature* **1981**, *292*, 55; J. Rivier, M. Spiess, W. Thorner, and W. Vale, *Nature* **1982**, *300*, 276.

[26] D. W. Urry and R. Walter, *Proc. Natl. Acad. Sci. U.S.A.* **1971**, *68*, 956.

[27] L. Halab, F. Gosselin, and W. D. Lubell, *Biopolymers (Peptide Sci.)* **2000**, *55*, 101; F. Polyak and W. D. Lubell, *J. Org. Chem.* **2001**, *66*, 1171; F. Gosselin and W. D. Lubell, *J. Org. Chem.* **2000**, *65*, 2163; L. Halab and W. D. Lubell, *J. Am. Chem. Soc.* **2002**, *124*, 2474.

[28] A. Golebiowski, S. R. Klopfenstein, X. Shao, J. J. Chen, A.-O. Colson, A. L. Grieb, and A. F. Russel, *Org. Lett.* **2000**, *2*, 2615.

[29] H. Wennemers, M. Conza, M. Nold, and P. Krattiger, *Chem. Eur. J.* **2001**, *7*, 3342.

[30] B. R. Huck, J. F. Fisk, and S. H. Gellman, *Org. Lett.* **2000**, *2*, 2607.

[31] T. S. Haque, J. C. Little, and S. H. Gellman, *J. Am. Chem. Soc.* **1996**, *118*, 6975.

[32] Y. J. Chung, L. A. Christianson, H. E. Stanger, D. R. Powell, and S. H. Gellman, *J. Am. Chem. Soc.* **1998**, *120*, 10555.

[33] R. Kaul, S. Deechongkit, and J. W. Kelly, *J. Am. Chem. Soc.***2002**, *124*, 11900.

[34] M. J. Macias, V. Gervias, C. Civera, and H. Oschkinat, *Nat. Struct. Biol.* **2000**, *7*, 375; M. Sudol, *Prog. Biophys. Mol. Biol.* **1996**, *65*, 113; K. P. Lu, S. D. Hanes, and T. Hunter, *Nature* **1996**, *380*, 544; P. J. Lu, X. Z. Zhou, M. Shen, and K. P. Lu, *Science* **1999**, *283*, 1325.

[35] M. Jaeger, H. Nguyen, J. C. Crane, J. W. Kelly, and M. Gruebele, *J. Mol. Biol.* **2001**, *311*, 373.

[36] A. Trabocchini, E. G. Occhiato, D. Potenza, and A. Guarna, *J. Org. Chem.* **2002**, **67**, 7483.

[37] T. C. Maier, W. U. Frey, and J. Podlech, *Eur. J. Org. Chem.* **2002**, 1686.

[38] J. L. Crawford, W. N. Lipscomb, and C. G. Schellman, *Proc. Natl. Acad. Sci. U.S.A.* **1973**, *70*, 538.

[39] A. Morimoto, K. Irie, K. Murakami, H. Ohigashi, M. Shingo, M. Nagao, T. Shimizu, and T. Shirasawa, *Biochem. Biophys. Res. Commun.* **2002**, *295*, 306; H. Situ, S. V. Balasubramanian, and L. A. Bobek, *Biochim. Biophys. Acta* **2000**, *1475*, 377.

[40] K. Guruprasad and S. Rajkumar, *J. Biosci.* **2000**, *25*, 143.

[41] K. Sugase, M. Horikawa, M. Sugiyama, and M. Ishiguro, *J. Med. Chem.* **2004**, *47*, 489.

[42] K. Sugase, Y. Oyama, K. Kitano, H. Akutsu, and M. Ishiguro, *Bioorg. Med. Chem. Lett.* **2002**, *12*, 1245.

[43] L. Bing, Y. K. T. Jeff, O. David, Y. Randy, J. F. Wayne, and C. C. Brian, *Science* **1995**, *270*, 1657.

[44] S. Aravinda, N. Shamala, R. Rajkishore, H. N. Gopi, and P. Balaram, *Angew. Chem. Int. Ed.* **2002**, *41*, 3868.

[45] I. L. Karle, S. K. Awasthi, and P. Balaram, *Proc. Natl. Acad. Sci. U.S.A.* **1996**, *93*, 8189; J. F. Espinosa, and S. H. Gellman, *Angew. Chem. Int. Ed.* **2000**, *39*, 2330; I. L. Karle, H. N. Gopi, and P. Balaram, *Proc. Natl. Acad. Sci. U.S.A.* **2001**, *98*, 3716.

[46] G.Luppi, D. Lanci, V. Trigari, M. Garavelli, A. Garelli, and C. Tomasini, *J. Org. Chem.* **2003**, *68*, 1982.

[47] C. Toniolo, and C. Benedetti, *Macromolecules* **1991**, *24*, 4004; C. Toniolo, A. Aubry, J. Kamphuis, *Biopolymers* **1993**, *33*, 1061.

[48] D. R. van Staveren, T. Weyhermueller, and N. Metzler-Nolte, *Dalton Trans.* **2003**, 210.

[49] A. Aemissegger, V. Kraeutler, W. F. van Gunsteren, and D. Hilvert, *J. Am. Chem. Soc.* **2005**, *117*, 2929 (2005).

[50] J. F. Espinosa, and S. H. Gellman, *Angew. Chem. Int. Ed.* **2000**, *39*, 2330.

[51] D. Obrecht, M. Altorfer, and J. A. Robinson, *Adv. Med. Chem.* **1999**, *4*, 1.

[52] D. A. Herrington, D. F. Clyde, G. Losonsky, M. Cortesia, J. R. Murphy, J. Davis, S. Baqar, A. M. Felix, E. P. Heimer, D. Gillesen, E. Nardin, R. S. Nussenzweig, V. Nussenzweig, M. R. Hollingdale, and M. M. Levine, *Nature* **1987**, *328*, 257.

[53] H. J. Dyson, A. C. Satterthwait, R. A. Lerner, and P. E. Wright, *Biochemistry* **1990**, *29*, 7828.

[54] M. E. Pfeifer, K. Moehle, A. Linden, and J. A. Robinson, *Helv. Chim. Acta* **2000**, *83*, 444.

[55] J. A. Robl, M. P. Cimarusti, L. M. Simpkins, B. Brown, D. E. Ryono, and J. E. Bird, *J. Med. Chem.* **1996**, *39*, 494.

[56] D. E. Davies, P. M. Doyle, R. D. Hill, and D. W. Young, *Tetrahedron* **2005**, *61*, 301.

[57] A. C. Gibbs, T. C. Bjorndahl, R. S. Hodges, and D. S. Wishart, *J. Am. Chem. Soc.* **2002**, *124*, 1203.

[58] R. Schwyzer, *Chimia* **1958**, *12*, 53; R. Schwyzer, J. P. Garrion, B. Gorup, H. Nolting, and A. Tun-Kyi, *Helv. Chim. Acta* **1964**, *47*, 441.

[59] G. D. Rose, L. M. Gierasch, and L. M. Smith, *Adv. Protein Chem.* **1985**, *37*, 1.

[60] For reviews see: M. W. Reczuh and A. D: Hamilton, *Chem. Rev.* **2000**, *100*, 2479; W. A. Loughlin, J. D. A. Tyndall, M. P. Glenn, and D. P. Frairlie, *Chem. Rev.* **2004**, *104*, 6085.

[61] J. S. Richardson, *Adv. Protein Chem.* **1981**, *34*, 167.

[62] D. R. Madden, J. C. Gorga, J. L. Strombringer, and D. C: Wiley, *Cell* **1992**, *70*, 1035.

[63] T. Wisniewski, P. Aucouturier, C. Soto, and B. Frangione, *Amyloid: Int. J. Exp., Clin. Invest.* **1998**, *5*, 212; R. W. Carell and D. A. Lomas, *Lancet* **1997**, *350*, 134.

[64] E. M. Smith, D. L. Holmes, A. J. Shaka, and J. S. Nowick, *J. Org. Chem.* **1997**, *62*, 7906; J. S. Nowick, J. H. Tsai, Q.-C. D. Bui, S. Maitra, *J. Am. Chem. Soc.* **1999**, *121*, 8409.

[65] J. S. Nowick, K. S. Lam, T. V. Khasanova, W. E. Kemnitzer, S. Maitra, H. T. Mee, and R. Liu, *J. Am. Chem. Soc.* **2002**, *124*, 4972.

[66] J. S. Nowick, D. M. Chung, K. Maitra, S. Maitra, K. D. Stigers, and Y. Sun, *J. Am. Chem. Soc.* **1999**, *121*, 8409.

[67] J. S. Nowick, E. M. Smith, J. W. Ziller, and A. J. Shaka, *Tetrahedron* **2002**, *58*, 727.

[68] J. S. Nowick and D. M. Chung, *Angew. Chem. Int. Ed.* **2003**, *42*, 1765.

[69] S. Lifson and C. Sander, *J. Mol. Biol.* **1980**, *139*, 627; M. A. Wouters and P. M. G: Curmi, *Proteins Struct. Funct. Genet.* **1995**, *22*, 119; E. G. Hutchinson, R. B: Sessions, J. M: Thornton, and D. N: Woolfson, *Protein Sci.* **1998**, *7*, 2287; Y. Mandel-Gutfreund, S. M. Zaremba, and L. M. Gregoret, *J. Mol. Biol.* **2001**, *305*, 1145.

[70] C. Bonauer, M. Zabel, and B. Koenig, *Org. Lett.* **2004**, *6*, 1349.

[71] T. K. Chakraborty, B. K. Mohan, K. S. Kumar, and A. C. Kunwar, *Tetrahedron Lett.* **2003**, *44*, 471.

[72] S. Miltschitzky, V. Michlova, S. Stadlbauer, and B. Koenig, *Heterocycles* **2005**, in press.

[73] F. Arcamone, S. Penco, P. Orezzi, V. Nicolella, and A. Pirelli, *Nature* **1964**, *203*, 1064.

[74] A. C. Finlay, F. A. Hochstein, B. A. Sobin, and F. X. Murphy, *J. Am. Chem. Soc.* **1951**, *73*, 341.

[75] For example: S. White, J. W. Szewczyk, J. M. Turner, E. E: Baird, and P. B. Dervan, *Nature* **1998**, *391*, 468; C. L. Kielkopf, S. White, J. W. Szewczyk, J. M. Turner, E. E. Baird, P. B. Dervan, and D. C. Rees, *Science* **1998**, *282*, 111; J. M. Gottesfeld, J. M: turner, and P. B. Dervan, *Gene Expression* **2000**, *9*, 77; P. B. Dervan, *Bioorg. Med. Chem.* **2001**, *9*, 2215; P. B. Dervan and B. S. Edelson, Curr. *Opin. Stru. Biol.* **2003**, *13*, 284.

[76] For reviews see: H.-C. Gallmeier and B. Koenig, *Eur. J. Org. Chem.* **2003**, 3473; M. Murty an H. Sugiyama, *Biol. Pharm. Bull.* **2004**, *27*, 468.

[77] I. Berque-Bestel, J.-L. Soulier, M. Giner, L. Rivail, M. Langlois, and S. Sicsic, *J. Med. Chem.* **2003**, *46*, 2606; P. Ettmayer, A. Billich, T. Baumruker, D. Mechtcheriakova, H. Schmid, and P. Nussbaumer, *Bioorg. Med. Chem. Lett.* **2004**, *14*, 1555.

[78] P. Furet, B. Gay, G. Caravatti, C. Garcia-Echeverria, J. Rahuel, J. Schoepfer, and H. Fretz, *J. Med. Chem.* **1998**, *41*, 3442; Z. J. Yao, C. R. King, T. Cao, J. Kelley, G. W. A. Milne, J. H. Voigt, and T. R. Burke, *J. Med. Chem.* **1999**, ***42***, 25; C.-Q. Wei, B. Li, R. Guo, D. Yang, and T. R. Burke Jr., *Bioorg. Med. Chem. Lett.* **2002**, *12*, 2781.

[79] Z.-D. Shi, R. G. Karki, S. Oishi, K. M. Worthy, L. K. Bindu, P. G. Dharmawardana, M. C. Nicklaus, D. P. Bottaro, R. J. Fisher, and T. R. Burke Jr., *Bioorg. Med. Chem. Lett.* **2005**, *15*, 1385.

[80] C. Park and K. Burgess, *J. Comb. Chem.* **2001**, *3*, 257.

[81] G. Muller, M. Gurrath, M. Kurz, and H. Kessler, *Proteins. Struct. Funct. Genet.* **1993**, *14*, 235; C. M. Wilmot and J. M. Thornton, *J. Mol. Biol.* **1988**, *203*, 221; G. Fischer, *Angew. Chem. Int. Ed.* **1994**, *33*, 1415; J. Liu, C. M. Chen, and C. T. Walsh, *Biochemistry* **1991**, *30*, 2306.

[82] A. Boruah, I. N. Rao, J. P. Nandy, S. K. Kumar, A. C: Kunwar, and J. Iqbal, *J. Org. Chem.* **2003**, *68*, 5006.

[83] H. C. Patel, T. P. Singh, V. S. Cauchan, and P. Kaur, *Biopolymer* **1990**, *29*, 509; M. R. Ciajolo, A. Tuzi, C. R. Pratesi, A. Fissi, and O. Pieroni, *Biopolymer* **1992**, *32*, 727; K. R. Rajashankar, S. Ramakumar, and V. S. Cauchan, *J. Am. Chem. Soc.* **1992**, *114*, 9225; O. Pieroni, A. Fissi, C. Pratesi, P. A. Temussi, and F. Ciardelli, *Biopolymer* **1994**, ***33***, 1.

[84] R. P. Cheng, S. H. Gellman, and W. F. DeGrado, *Chem. Rev.* **2001**, ***101***, 3219; D. Seebach and J. L. Matthews, *Chem. Commun.* **1997**, *21*, 2015.

[85] For example: S. Krauthauser, L. A: Christianson, D. R. Powell, and S. H. Gellman, *J. Am. Chem. Soc.* **1997**, *119*, 11719; Y. J. Chung, B. R. Huck, L. A. Christianson, H. E. Stanger, D. R. Powell, and S. H. Gellman, *J. Am. Chem. Soc.* **2000**, *122*, 3995; D. Seebach, S. Abele, K. Gademann, and B. Jaun, *Angew. Chem. Int. Ed.* **1999**, *38*, 1595; X. Daura, K. Gademann, H. Schafer, B. Jaun, D. Seebach, and W. F. van Gunsteren, *J. Am. Chem. Soc.* **2001**, *123*, 2393.

[86] J. M. Langenhan and S. H. Gellman, *Org. Lett.* **2004**, *6*, 937.

[87] S. Harrison, *Cell* **1996**, *86*, 341; D. Doyle, A. Lee, J. Lewis, E. Kim, M. Sheng, and R. MacKinnon, *Cell* **1996**, *86*, 1067; J. Cabral, C. Petosa, M. Sutcliffe, S. Raza, O. Byron, F. Poy, S. Marfatia, A. Chishti, and R. Liddington, *Nature* **1996**, *382*, 649.

[88] J. M. Langenhan, J. D. Fisk, and S. H. Gellman, *Org. Lett.* **2001**, *3*, 2559.

B. Main Part

1. Synthesis of Substituted Pyrimidine Hydrazine Acids (PHA) and their Use in Peptide Recognition*

1.1 Introduction

Interactions between peptide β-sheets are of importance for protein quaternary structure formation, protein-protein interaction, and protein aggregation. They are involved in important biological processes and the development of diseases - ranging from cancer and AIDS, to anthrax and Alzheimer´s.[1,2] Small synthetic molecules that mimic surface epitopes on proteins are a potential source of novel ligands for use in drug and vaccine design.[3] Over the last years peptidomimetics have attracted interest from both organic and medicinal chemists. In the biological, chemical, and pharmaceutical areas, they offer advantages over physiologically active peptides, which as active substances are crucial for the organism and may lead to severe side effects.[4] There is much current interest in the preparation of peptides and peptidomimetics with a well-defined conformation.[5] These conformationally constrained peptides are useful to probe protein folding and to mimic peptide structures.

Since 1992, Nowick *et al.* have reported the development of peptidomimetic templates, which have been termed molecular scaffolds.[6] These templates have oligourea structure and reassemble, in some ways, β-turns. Early in 1996, Nowick described an artificial antiparallel β-sheet **(1)**, in which a 5-amino-2-methoxybenzamide β-strand mimic **(2)** and a diurea molecular scaffold stabilize a β-sheet structure in an attached peptide strand (Scheme 1).[7]

* The results of this chapter have been published: S. Miltschitzky, V. Michlova, S. Stadlbauer, and B. Koenig, *Heterocycles* **2005**, in press.

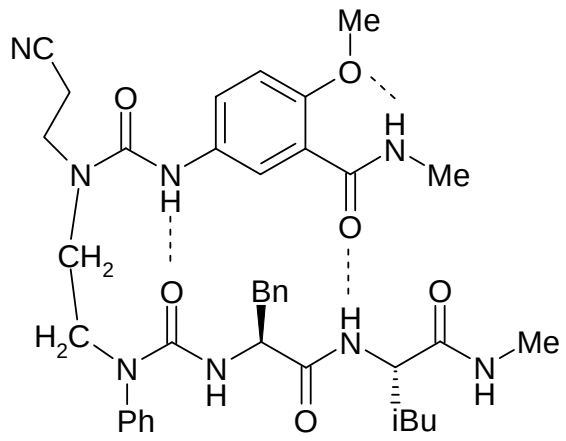

artificial sheet **1**

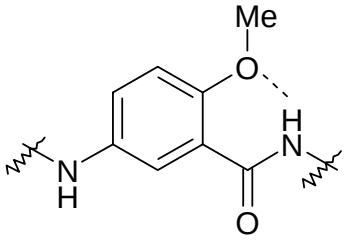

β-strand mimic **2**

Scheme 1: Nowick´s artificial antiparallel β-sheet (**1**) and β-strand mimic (**2**)

1.2 Results and Discussions

We report in this paper the synthesis of substituted pyrimidine-hydrazine-acids (PHA), and their inter- and intramolecular peptide binding properties as determined by NMR spectra and emission changes.

We envisioned 6-hydrazinopyrimidine-4-carboxylic acids as a building block for extended β-strand mimics. Molecular modelling calculations on force field level (MMFF, program package Spartan)[8] were carried out to explore the conformational preferences of PHA. The calculations show that oligomers of PHA adopt a linear conformation required to be complementary to peptide β-sheets.

The hydrazine provides the right pattern of hydrogen bond donor and acceptor geometry complementary to extended peptide β-sheets and allows the formation of an intramolecular hydrogen bond. This should keep the pyrimidine ring of PHA oligoamides in a planar arrangement.

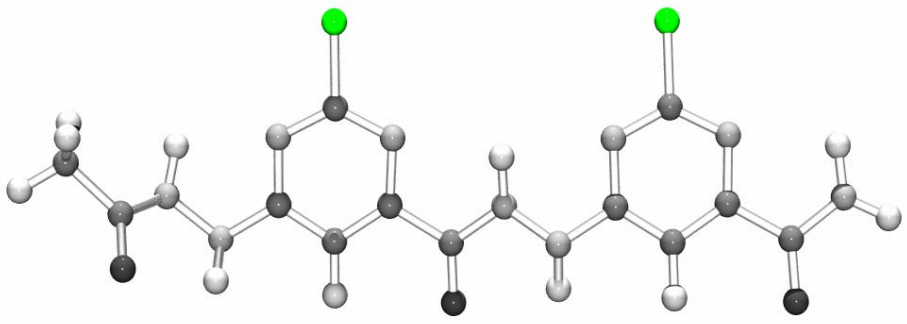

Scheme 2: Low energy conformation of a PHA dimmer as calculated by force field method

Starting material for PHA derivatives is the commercial available orotic acid **(3)**. The acid is converted into the ester with methanol according to a literature procedure,[9] followed by a halogenation with $POCl_3$[9] or $POBr_3$, respectively. The substitution of a halogen atom by Boc- or Cbz-monoprotected hydrazine takes place selectively in 6-position. The yields of the substitution reaction are typically between 60 and 95 %.

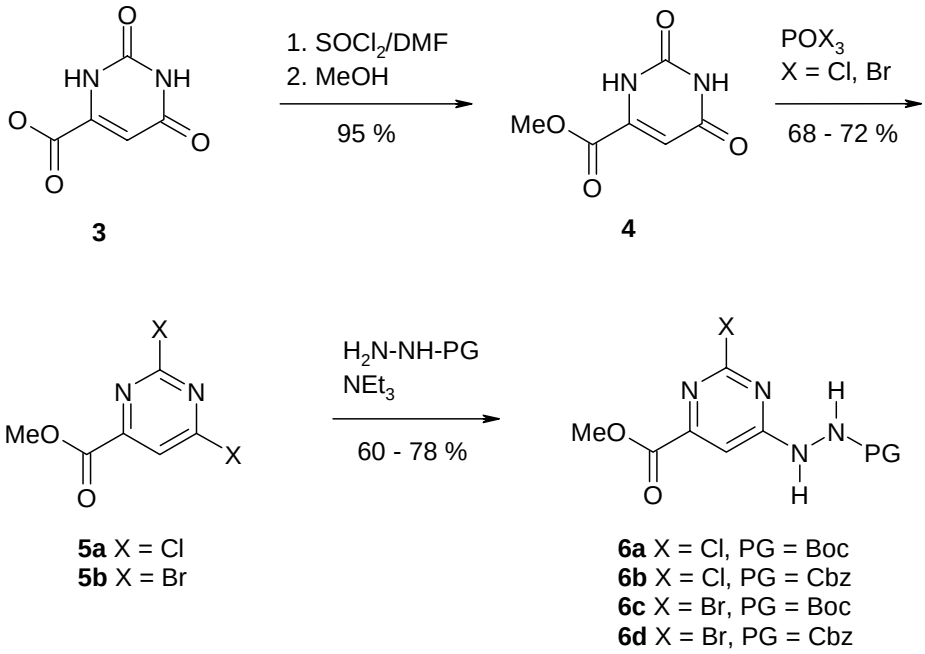

Scheme 3: Synthesis of the PHA parent structure

The selective substitution of the chlorine and bromine was investigated by Yamanaka *et al* in detail.[10] Computational and experimental studies both showed a dependency on the substituent in 4-position. Acceptors, such as the methyl ester guide substitution in 6-position, while a methoxy groups yields selective substitution in 2-position. The X-Ray structure analysis of **6a** and **6b** and the HMBC spectrum of **6a** confirm the expected substitution pattern.

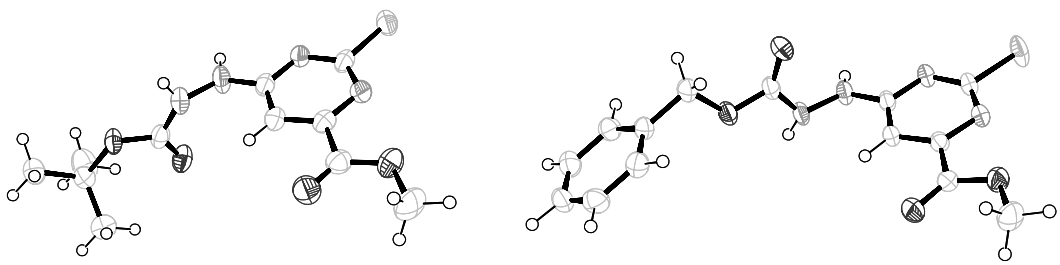

Scheme 4: Structures of **6a** (left) and **6b** (right) in the crystal

The HMBC spectra of an 8 mM solution in deuterated DMSO at room temperature of **6a** shows a sharp cross peak between the protons on hydrazine nitrogen NH^2 and on

carbon CH^1, supporting the structure of the expected compound. The double set of signals arises from the *cis*- and *trans*-isomers of the Boc protecting group.[11]

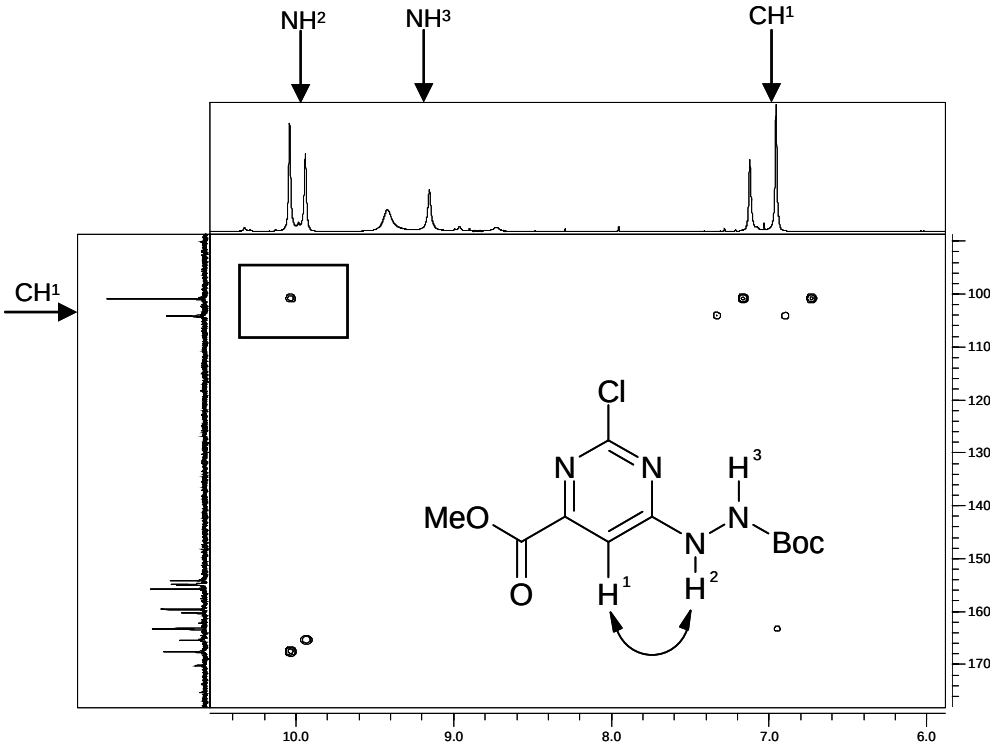

Scheme 5: HMBC-spectrum of **6a** in deuterated DMSO.

However, the X-ray structure of **6a** does not show the assumed intramolecular hydrogen bond of the proton on hydrazine nitrogen and the pyrimidin nitrogen. The temperature dependence of the ^1H NMR chemical shift of the NH^2 proton (-5.15 ppb/K) in 10 mmol solution $CDCl_3$ reflects its state of hydrogen bonding.

The course of the subsequent substitution in 2-position with *N*-nucleophiles depends on the halogen atom. Chlorine substitution occurs only when activated with DMAP *in situ*.

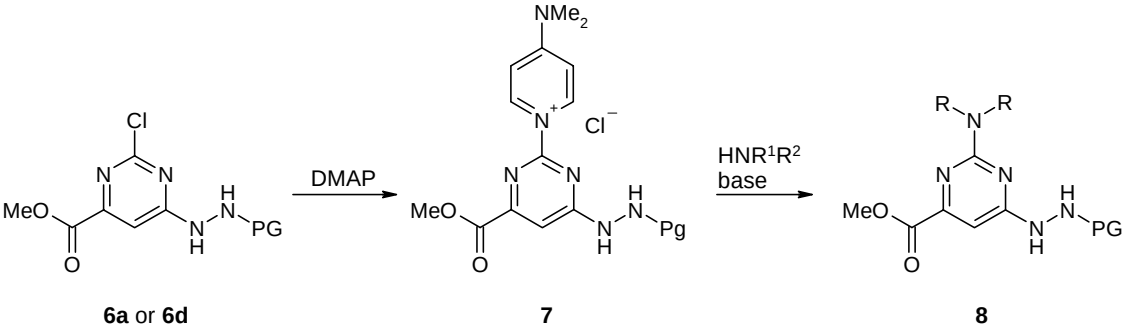

Scheme 6: Proposed mechanism of the substitution of 2-chlorine atoms by *N*-nucleophiles

The DMAP displaces the chlorine atom as a nucleophile forming the charged intermediate **7**. The amine attacks in the subsequent step the more electrophilic carbon C2 under basic conditions. The amine is nucleophile and base, but an excess of 10 equivalents is used. In case of NEt_3 as an auxiliary base, still 5 equivalents of the nucleophile are required. Although the second step of the reaction releases the DMAP, stoichiometric amounts are required to achieve good yields. The highest yields were obtained in the presence of 1.2 equivalents of DMAP, 2 equivalents of NEt_3 and 8 equivalents of amine (see Experimental). The bromine derivative is, as expected, more reactive than the chlorine substituted compound. No activation or addition of base is required for the substitution. In the presence of DMAP and NEt_3 however, complete conversion requires a 5-fold excess of amine. Best yields were obtained by using 2 equivalents of NEt_3 and a 10-fold excess of amine (see Experimental). Table 1 summarizes the different compounds either derived from **6a** (method A) or **6c** (method B). In general, the more nucleophilic secondary amines give higher yields than primary amines. The hydrazine protecting group (PG) does not influence the yield of the substitution reaction.

PHA	**Amine**	**PG**	**Method**	**Yield** (corrected*) **[%]**
8a	$HNEt_2$	Boc	A	42
8a	$HNEt_2$	Boc	B	74
8b	$HNEt_2$	Cbz	B	80
8c	H_2NBu	Boc	B	13 (26)

* Yield of the reaction adjust to conversion in brackets

Table 1: Synthesized derivatives (**8**)

To avoid a side reaction by aminolysis of the ester, **4** was converted into the butylamide (**9**) according to a literature procedure[12] followed by bromination and subsequent substitution in 6- and 2-position with Boc-protected hydrazine and amines. The amidic hydrogen atom allows the formation of another intramolecular hydrogen bond to the pyrimidine nitrogen. Table 2 summarizes the results of the Br-substitution in 2-position of compound (**11**) with several amines.

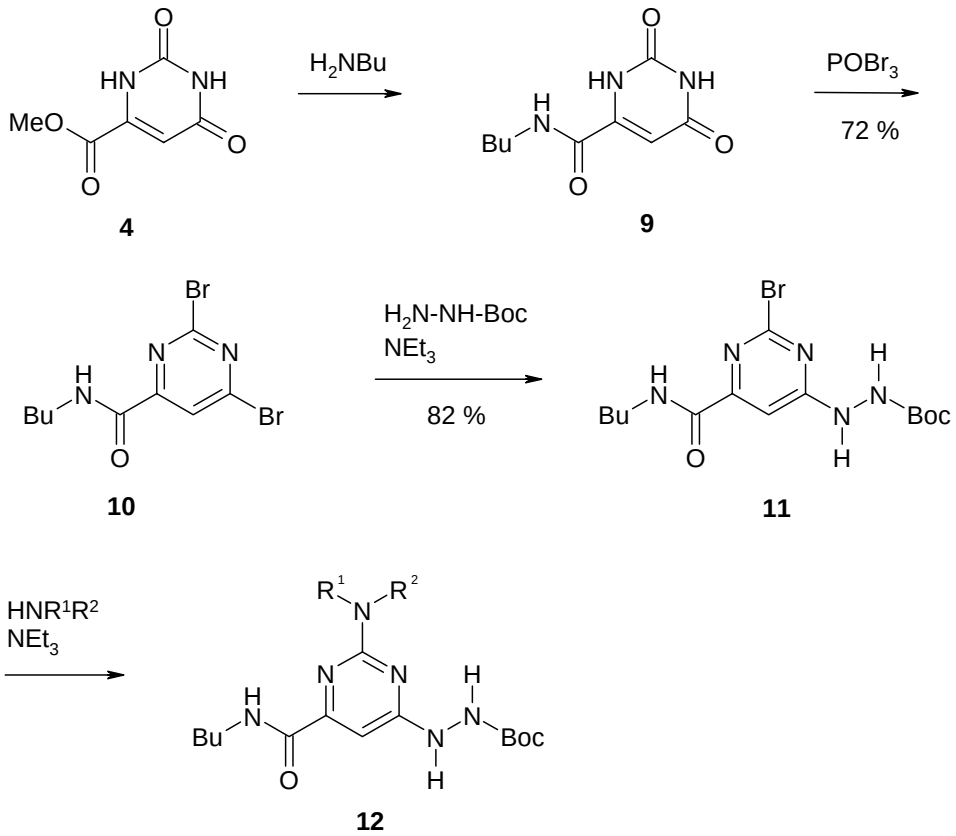

Scheme 7: Synthesis of compounds **(12)**

Entry	Amine	Yield (corrected*) [%]
12a	H_2NBu	68
12b	$HNEt_2$	82
12c	Morpholine	67
12d	18-aza-crown-6	56
12e	2-(2-Methoxy-ethoxy)-ethylamine	33 (68)

* Reaction yield adjust to conversion given in brackets

Table 2: Synthesized derivatives **(12)**

A more extended peptide **(15)** was prepared to show the complementary structure and binding affinity of PHA oligomers to peptide β-sheet structures. Cleaving off the ester and the Boc-group of **8a** under basic and acidic conditions gives the acid (**13**) and amine (**14**), respectively. A coupling of (**13**) and (**14**) under standard peptide coupling conditions yields dipeptide (**15**) in moderate yield.[13]

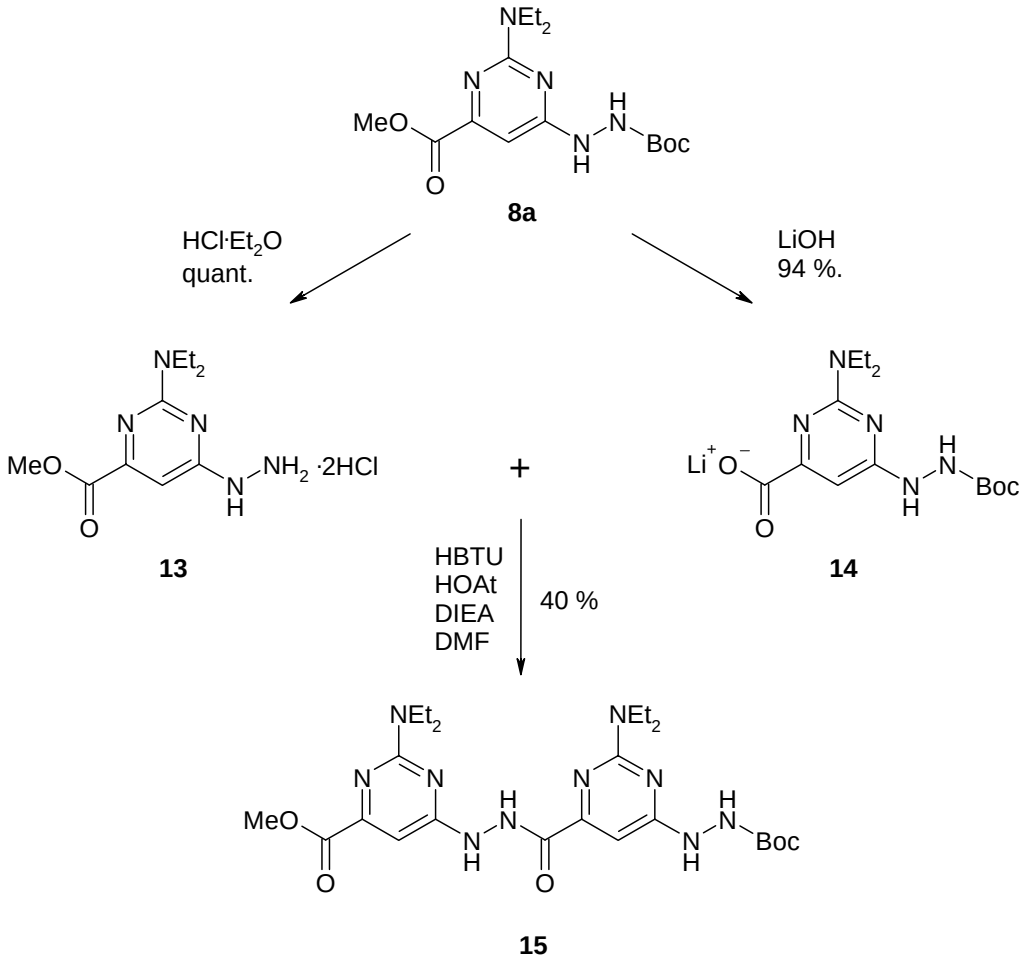

Scheme 8: Synthesis of dipeptide (**15**)

All synthesized PHA derivatives appear as mixtures of *cis*- and *trans*-isomers of the carbamate protecting groups in the ^{1}H NMR spectra. The pyrimidine ring and the hydrazine protons do not show tautomerisation. Compounds (**8**, **12** and **15**) emit around 420 nm when irradiated at 330 nm. The halogenated compounds (**5**, **6**, **10**, and **11**) have no luminescence. The emission intensity of solutions of the compounds decreases from less polar (e.g. $CHCl_3$) to polar aprotic solvents (e.g. MeCN). Polar protic solvents, such as H_2O, quench the emission completely. The intensity of emission changes with hydrogen bonds to PHA. Therefore, fluorescence titration is a tool to monitor the binding process between PHA and β-sheet peptides in aprotic solvents.

The mono PHA (**8a**) provides three binding sites as acceptor-donor-acceptor (ADA) motif, while bis PHA **(15)** can form up to five (ADADA) intermolecular hydrogen

bonds with a complementary binding partner. Top and bottom face of an *N*- and *C*-terminal protected tripeptide differ in their hydrogen bond donor and acceptor pattern. While the top face can form four hydrogen bonds (DADA), the bottom face has only three (ADA). An *N*- and *C*-terminally protected tetrapeptide offers five hydrogen binding sites (ADADA) at the top face and four (DADA) on the bottom face.

The binding affinities of the PHA derivatives (**8a**) and (**15**) to small peptides of natural amino acids were determined by ^{1}H NMR spectra and fluorescence titrations in $CDCl_3$ and $CHCl_3$. Binding constants were determined by non-linear fitting of chemical induced shifts (CIS) of several protons[14] in the NMR spectrum and of the decrease of emission intensity. Self-associations of the peptides and the PHA (**8a** K_{11} = 17 L/mol, **15** K_{11} = 28 L/mol) were determined independently and were taken into account. Emission intensities corrected for dilution during the titration are used. The stoichiometry of the complexes was determined according to Job´s method of continuous variations.[15] Table 3 summarizes the results of our binding studies.

Entry	PHA	Peptide	Stoichiometry	K_a [L/mol][a]
1	**8a**	Ac-Phe-Val-Leu-OMe	1:1	101
2	**15**	Boc-Phe-Ala-Val-Leu-OMe	1:1	78
3	**15**	Boc-Phe-Gly-Val-Leu-OMe	2:1	2742 15381

[a]All binding constants have errors of approx. ± 10 %.

Table 3: K_a values determined from NMR and fluorescence titrations in $CDCl_3$ and $CHCl_3$

The affinity of **8a** to the tripeptide is 101 L/mol. Figure 3 shows the CIS of the acetyl singlet during titration. By formation of three cooperative hydrogen bonds with PHA **8a** the binding of the peptide´s top face should be favoured (see Figure 1).

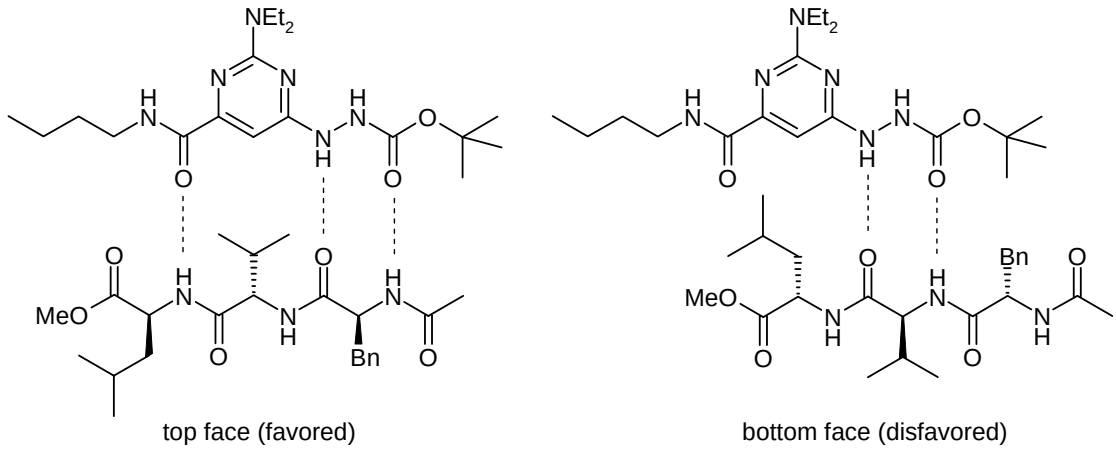

Figure 1: A 1:1 complex between **8a** and Ac-Phe-Val-Leu-OMe

The binding affinity determined for (**15**) to the tetrapeptide Boc-Phe-Ala-Val-Leu-OMe is in the same order of magnitude as the binding of (**8a**) to a tripeptide, although an additional hydrogen bond formation should be possible between (**15**) and the tetrapeptide. Figure 2 summarizes the possible 1:1 binding motifs between (**15**) and Boc-Phe-Ala-Val-Leu-OMe.

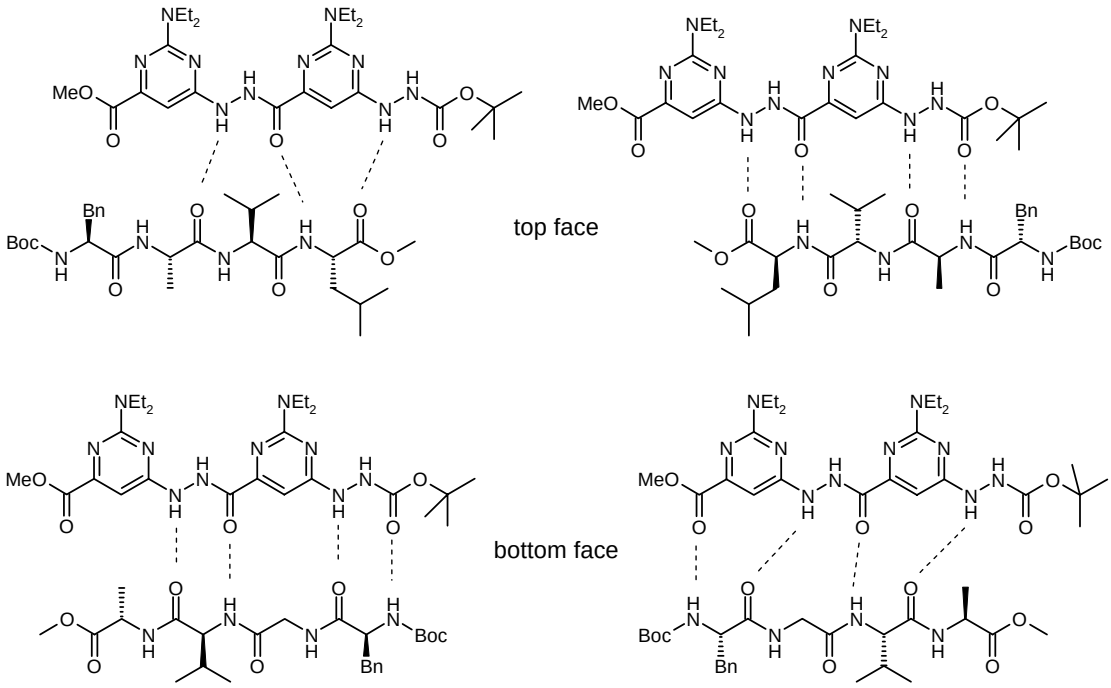

Figure 2: Possible 1:1 complexes between **15** and Boc-Phe-Ala-Val-Leu-OMe

For steric reasons, the binding motifs containing Boc protecting group on different ends might be favoured. The observed CIS and the calculated binding affinity result from an average value of the experiment. The different aggregates are presumably in a fast dynamic equilibrium and NMR cannot distinguish between them. All efforts to co-crystallize (**8a**) and (**15**) with a peptide giving a picture of the binding motif failed so far.

Figures 3 and 5 illustrate that a plateau in CIS or a minimum of emission is reached after the addition of 1 equivalent of the peptide to a solution of PHA. The ^{1}H NMR Job´s plot of **8a** and Ac-Phe-Val-Leu-OMe (Figure 4) shows a maximum at x = 0.5, confirming a 1:1 binding motif.

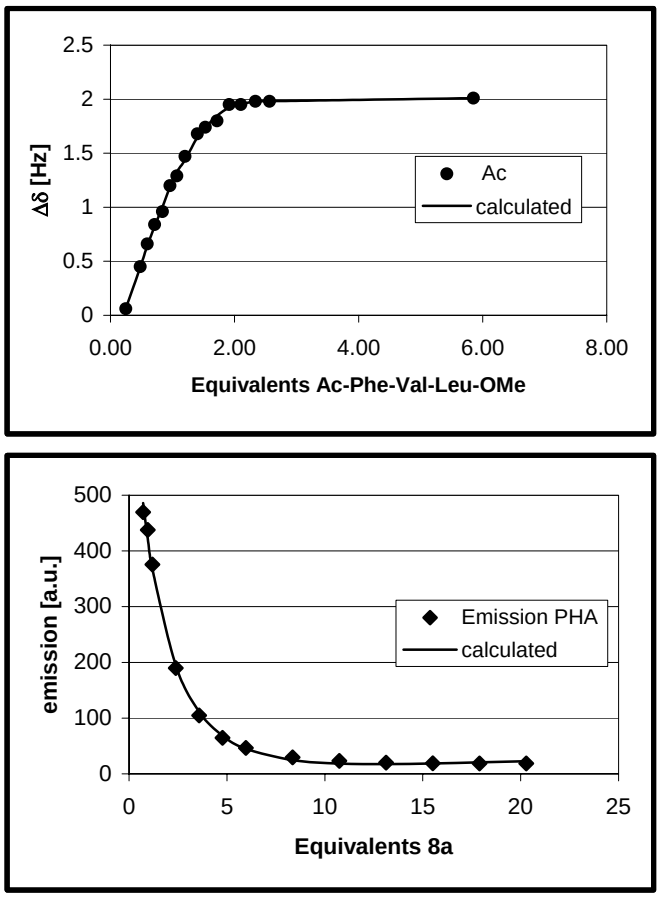

Figure 3: NMR titration curve (up) and fluorescence titration curve (below) of Ac-Phe-Val-Leu-OMe with compound (**8a**) in $CDCl_3$, c_0 = 10 mmol/L, observing CIS of the acetyl hydrogen resonance and the emission intensity at 423 nm (excitation at 330 nm)

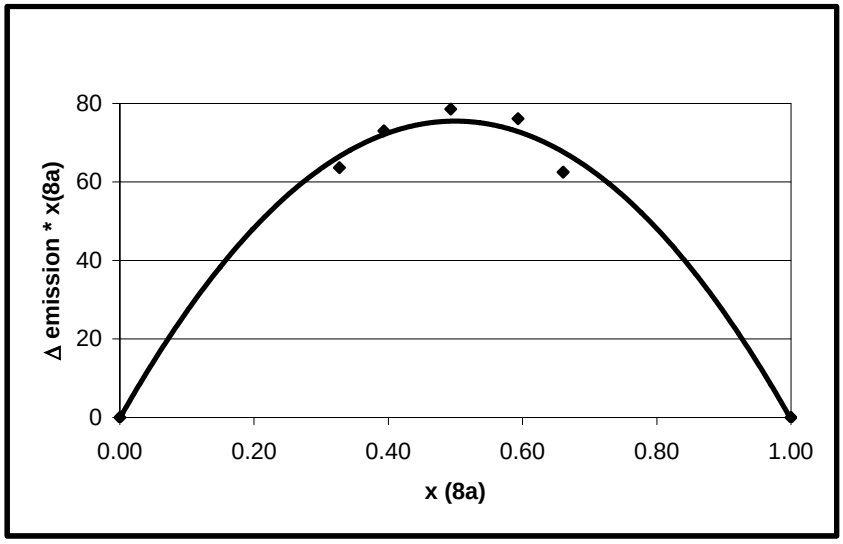

Figure 4: ^{1}H NMR job-plot of **8a** and Ac-Phe-Val-Leu-OMe

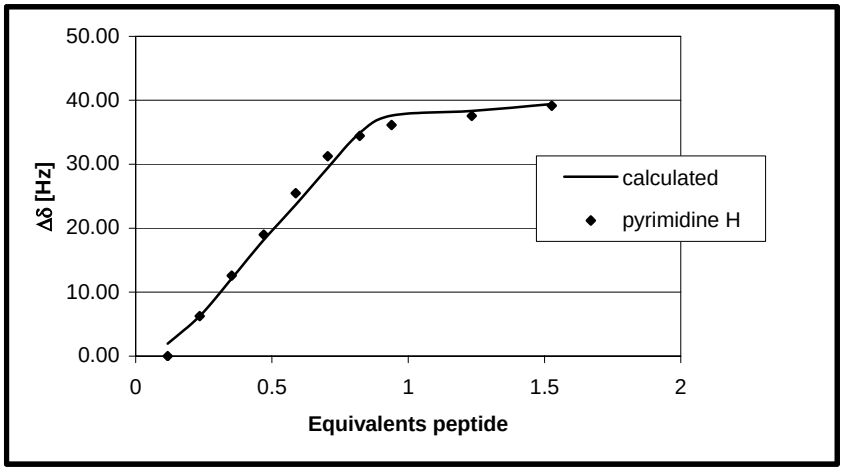

Figure 5: NMR titration curve of Boc-Phe-Ala-Val-Leu-OMe with compound **15** in $CDCl_3$, c_0 = 6.0 mmol/L, monitoring CIS of the pyrimidine hydrogen resonance.

The titration of (**15**) with Boc-Phe-Gly-Val-Leu-OMe gives a different picture. A slight chance in the peptide sequence from Ala to Gly in position 2 leads to a significant increase of the binding affinity and change of the aggregate stoichiometry. The NMR spectra titration curve indicates two subsequent binding processes.

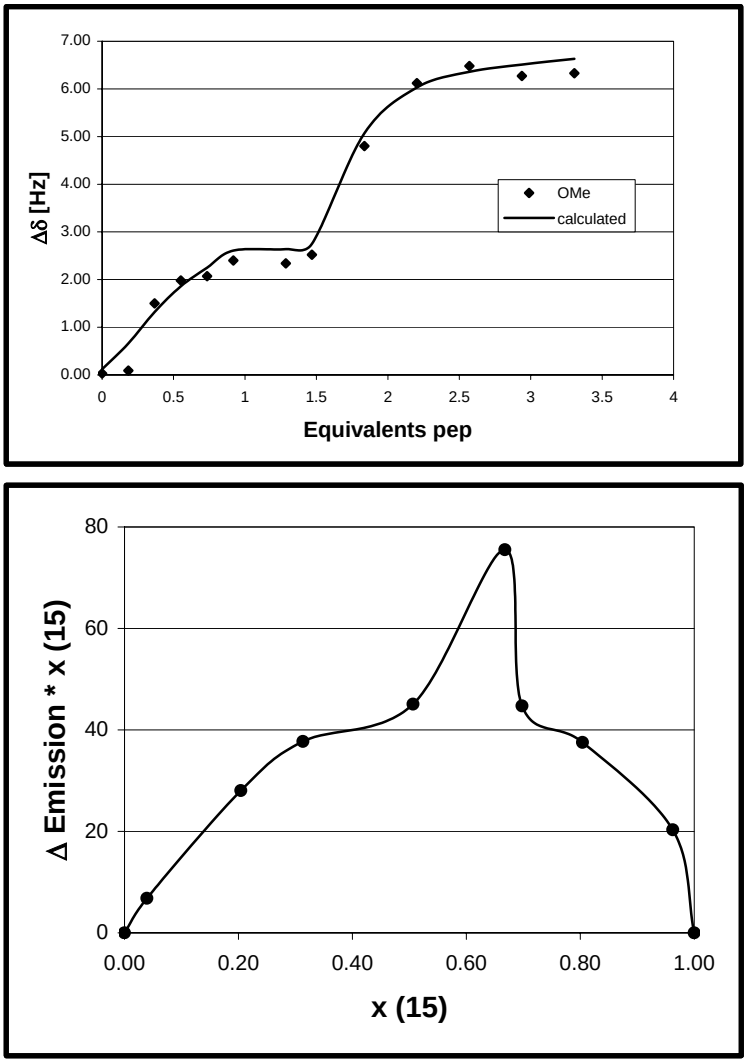

Figure 6: NMR spectra titration curve (above; CIS of the methyl ester group) and emission Job´s plot analysis (below; emission intensity at 423 nm,excitation at 330 nm)) of Ac-Phe-Val-Leu-OMe with compound (**15**) in $CDCl_3$, c_0 = 9.5 mmol/L.

The first part of the NMR titration curve is identical in shape to the titrations of (**8a**) with the tripeptide Boc-Phe-Val-Leu-OMe or (**15**) with the tetrapeptide Boc-Phe-Ala-Val-Leu-OMe, respectively. Addition of one equivalent **15** to Boc-Phe-Gly-Val-Leu-OMe saturates the CIS. Addition of a second equivalent of **15** leads to a further CIS of the methoxy resonance signal. For the first binding process an affinity constant of K_{11} = 2742 L/mol is derived, while the subsequent binding with K_{12} of 15381 L/mol indicates a highly cooperative assembly process. We cannot provide a structure for the complex assembly, but the exchange of alanine for glycine in the tripeptide sequence allows almost free rotation around the C-C and the C-N bond in the glycine residue.[16]

To avoid higher aggregates and arrive at a more defined PHA – peptide interaction a short β-turn fragment incorporating PHA was prepared. Scheme 9 shows the synthesis. Extension of Gellman´s β-turn fragment Gly-D-Pro[17] by H-Phe-Leu-Val-OMe required 1.1 equivalents of EDC and HOBt and 2 equivalents of Huenig´s Base. The product precipitates from DMF solution after the addition of water. Lithium salt (**14**) and the deprotected pentapeptide couple to (**16**) in moderate yields.

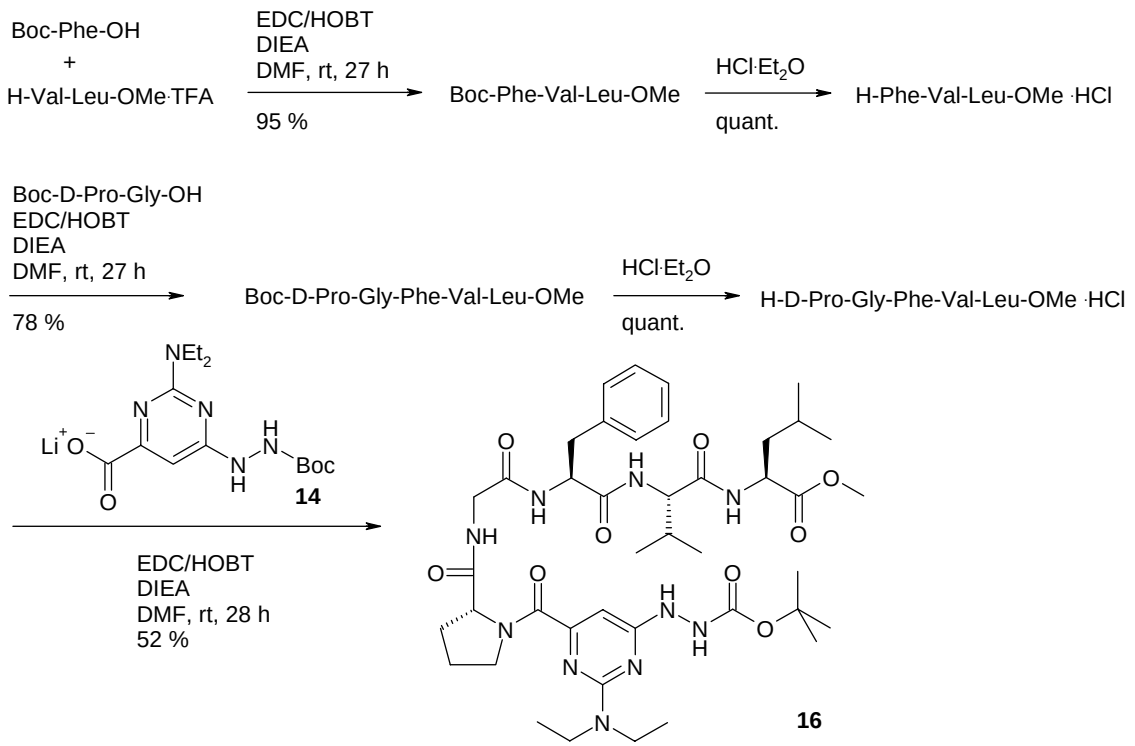

Scheme 9: Synthesis of the β-turn fragment (**16**)

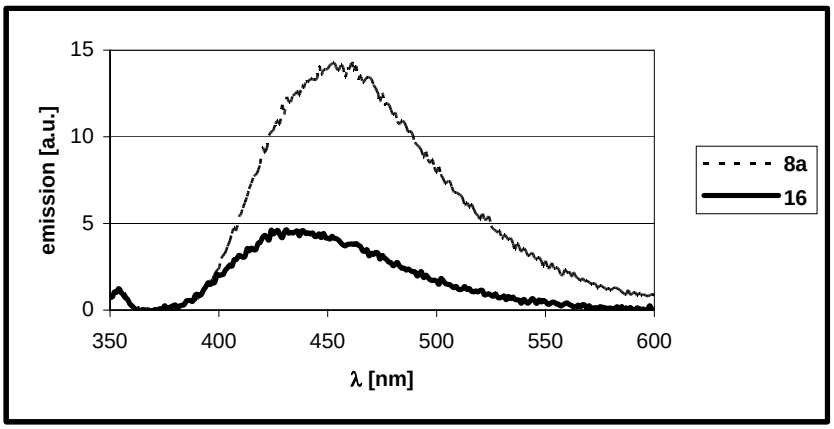

Figure 7: Emission spectra of (**8a**) and (**16**) in a 8 mM solution in acetonitrile

Figure 7 shows the emission intensity of equally concentrated solutions of (**8a**) and (**16**) (8 mM) in acetonitrile. The significant decreased emission intensity of (**16**) in comparison to (**8a**) indicates an intramolecular binding process of PHA and peptide.

NMR spectra in 10 mM deuterated DMSO solution show only one conformer for (**16**) in solution. Analysis of the observed intramolecular NOE contacts in deuterated DMSO clearly confirm a β-turn structure as depicted in figure 8.

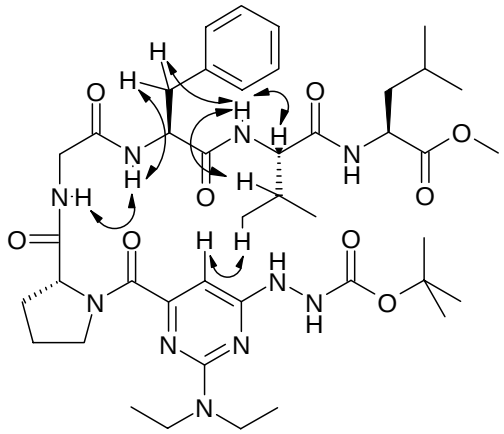

Figure 8: NOE contacts found in the analysis of compound (**16**)

ROESY experiments revealed numerous short-range and long-range NOEs. The NOE contact between the pyrimidine proton and the Val-*i*-Pr-residue indicates a folded conformation. Due to signal overlap and broad NH signals no further NOE contacts of PHA and peptide are observable.[18]

A more extended β-turn fragment was prepared incorporating dipeptide (**15**). The β-turn fragment Gly-D-Pro was extended by H-Phe-Leu-Phe-Ala-NH_2 and coupling of the deprotected hexapeptide with the lithium carboxylate (**17**) gave (**18**) in good yield.

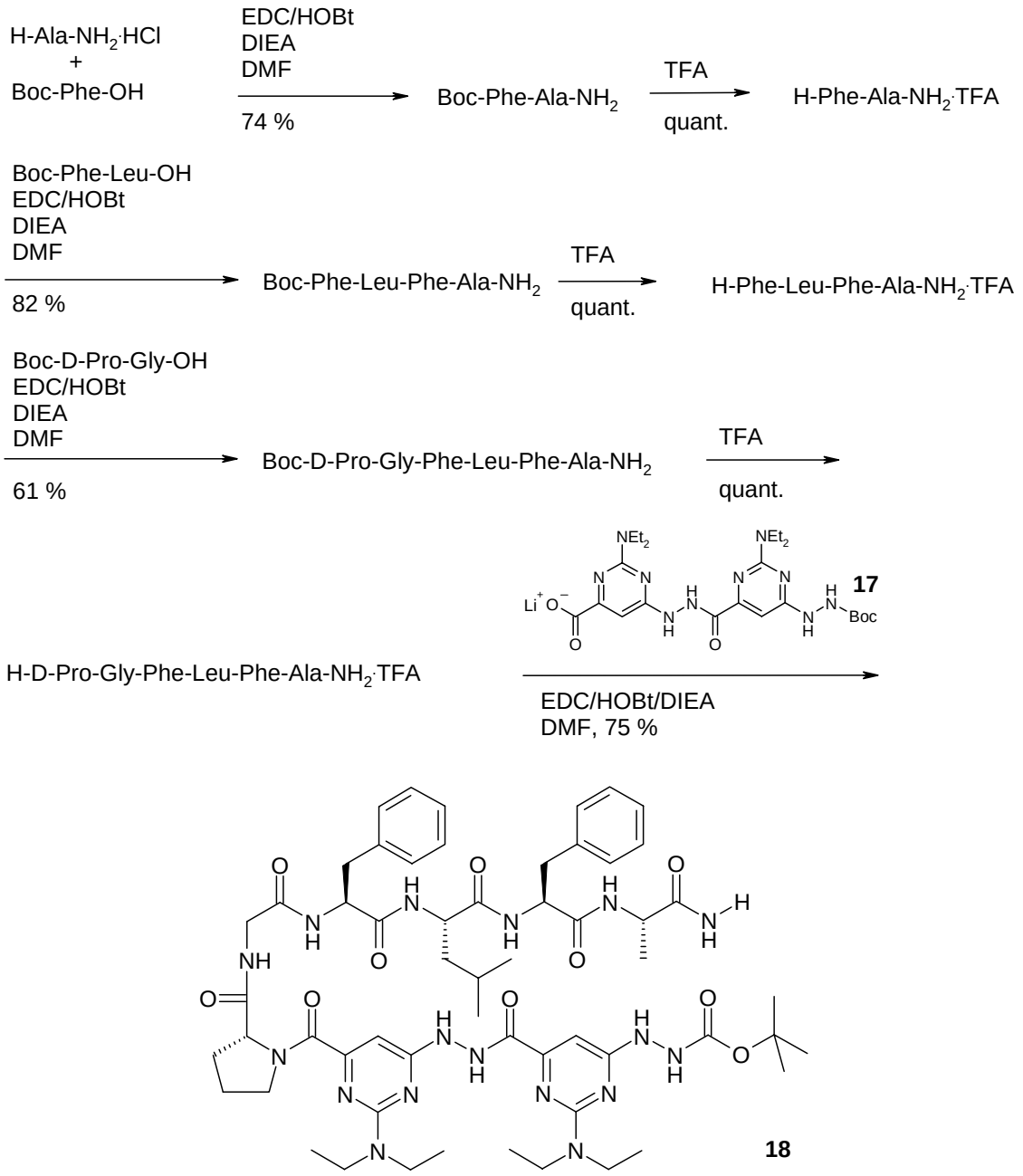

Scheme 10: Synthesis of the β-turn fragment (**18**)

Figure 9 shows the analysis of the intramolecular NOE contacts of compound (**18**) in deuterated DMSO solution. The NOE contacts between the *N*-terminal PHA unit and the *C*-terminal amino acid residue indicate that the interaction of heterocycles and peptide chain propagates the turn. The proton on the hydrazine of the terminal PHA unit shows a contact to the methyl group and the C_α proton of alanine to the CH_2 group of the phenylalanine. In both cases, signal overlap prohibits distinction of the diasterotopic

protons of the CH_2 group in the phenylalanine and leucine side chain. The NOE contact of a PHA proton and the glycine amide proton confirms the turn structure. Overall, eight NOE contacts support a solution structure of **18** as shown in Figure 9.

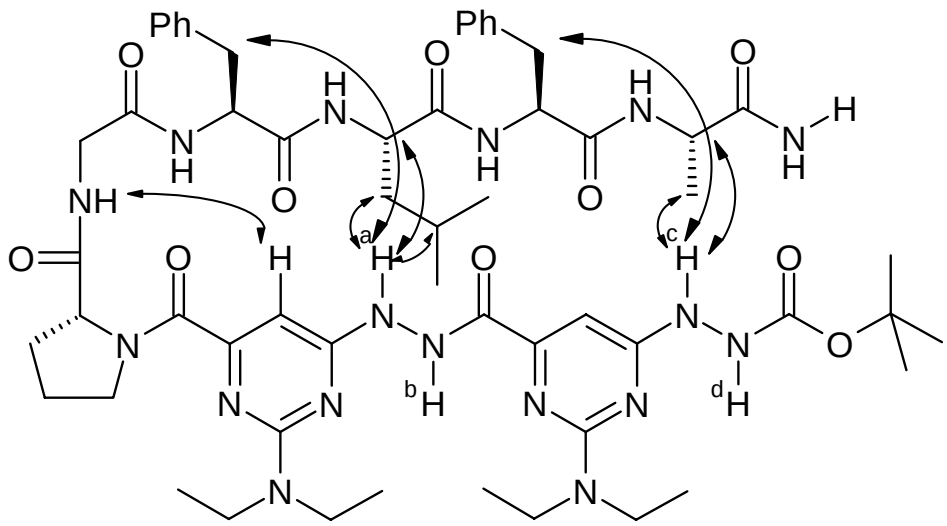

Figure 9: NOE contacts found in the analysis of compound (**18**)

1.3 Conclusions

We have reported the synthesis of substituted pyrimidine-hydrazine-acids (PHA) from orotic acid. Standard peptide coupling procedures couple or incorporate the heterocyclic hydrazine acids into peptides of natural amino acids. Their geometry of hydrogen bond acceptor and donor sites make them suitable for complementary interaction with peptide β-sheets. An interesting feature is their luminescence in non-polar solvents, which changes upon peptide binding. PHA´s are simple dipeptide mimics, with a build in luminescence chemosensor monitoring the local polarity of the environment and interaction with adjacent peptide chains.

1.4 Experimental

General Methods: Melting points were determined on a Tottoli micromelting point apparatus and are uncorrected. ^{1}H-NMR spectra were recorded on a Bruker Avance 300 NMR spectrometer at 300 K. Chemical shifts (δ) are reported in ppm downfield from internal TMS. Emission spectra were recorded on a Cary Eclipse spectrophotometer. Thin layer chromatographic (TLC) analyses were performed on silica gel 60 F-254 with a 0.2 mm layer thickness. Preparative chromatography columns were packed with silica gel Geduran SI 60. Mass spectra were recorded on a Finnigan MAT TSQ 7000 (ESI) and on a Finnigan MAT 95 (HRMS).

X-Ray Structures: Crystallographic data for the structures (**6a**) and (**6b**) have been deposited with the Cambridge Crystallographic Data Centre as supplementary publication numbers CCDC 267816 & 267817. Copies of the data can be obtained, free of charge, on application to CDC, 12 Union Road, Cambridge CB2 1EZ, UK [fax: +44(0)1223-336033 or e-mail: deposit@ccdc.cam.ac.uk].

^{1}H-NMR and Emission Titrations: A solution of the PHA molecule (c = 15 mmol/L) was added in portions via a microsyringe to a solution of a peptide (c = 1 mmol/L). Volume and concentration changes were taken into account for the analysis of the binding event.[14]

Job´s Plot: Equimolar solutions (0.1 mM) of PHA molecule and peptide were prepared and mixed in various amounts. Emission spectra of the mixtures were recorded, and the emission intensities were analyzed by Job´s method modified for emission results.[15]

General procedure for the substitution of a halogen atom by a protected hydrazine (GP1): To a solution of the halogenated pyrimidine (1 mmol) in DMF (1 mL/mmol) was added triethylamine (1.1 mmol), followed by a solution of the protected hydrazine (1.1 mmol) in DMF (2 mL/mmol). The solution was stirred at 60 °C until complete conversion of the pyrimidine (12-24 h). The reaction mixture was allowed to cool to rt, diluted with water, and extracted with ethyl acetate. The organic phases were dried over

Na_2SO_4, evaporated, and then concentrated under reduced pressure. If necessary, the residue was purified by column chromatography (mixtures of hexanes and ethyl acetate) to afford the products.

General procedure for the substitution of a halogen atom by an amine (GP2): To a solution of the brominated pyrimidine (1 mmol) in DMF (2 mL/mmol) was added the amine (10 mmol). The solution was stirred at 60 °C until complete conversion of the pyrimidine was observed (18-36 h). The reaction mixture was allowed to cool to rt, diluted with ethyl acetate, and washed with brine. The organic phases were dried over Na_2SO_4, evaporated, concentrated under reduced pressure and purified by column chromatography (mixtures of hexanes and ethyl acetate) to afford the products.

General procedure for the peptide synthesis (GP3): A solution of Boc-AA-OH (1.0 mmol), H-AA-R·X (R = OMe, NH_2, X = TFA, HCl) (1.0 mmol), EDC (1.1 mmol), HOBt (1.1 mmol) and Huenig´s base (2.5 mmol) in DMF (1 mL/mmol) was stirred at rt until complete conversion was observed (10-24 h). The reaction mixture was allowed to cool to 0 °C and treated with water. The precipitate was filtered off and washed with water affording the desired peptide. The crude product was used without further purification.

General procedure for cleavage of the Boc-protecting group by Et_2O·HCl (GP4): The Boc-protected amino acid (1 mmol) was dissolved in Et_2O·HCl (2 mL/mmol) at 0 °C. The reaction mixture was allowed to warm to rt and stirred for 30 min. The precipitate was filtered off and washed with Et_2O affording the deprotected amino acid. The crude product was used without further purification.

General procedure for cleavage of the Boc-protecting group by TFA (GP5): The Boc-protected amino acid (1 mmol) was dissolved in a 20 % solution of TFA in CH_2Cl_2 (2 mL/mmol). The reaction mixture was stirred at rt for 2 h. The solvent was removed under reduced pressure. The crude product was used without further purification.

X-Ray appendix:

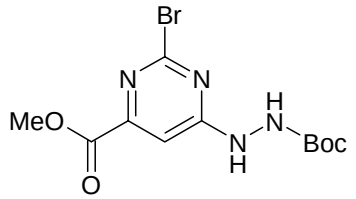

6a

Crystal data and structure refinement for compound **6a**:

Identification code	B132	
Empirical formula	$C_{11}H_{15}ClN_4O_4$	
Formula weight	302.72	
Temperature	173(1) K	
Wavelength	0.71073	
Crystal system, space group	Monoclinic, P2(1)c	
Unit cell dimensions	a = 10.5874(8) Å	α = 90°
	b = 25.3603(19) Å	β = 94.871(9)°
	c = 10.9279(8) Å	γ = 90°
Volume	2923.5(4) $Å^3$	
Z, calculated density	8, 1.376 Mg/m^3	
Absorption coefficient	0.280 mm^{-1}	
F(000)	1264	
Crystal size	0.24·0.20·0.03 mm	
θ-range for data collection	2.04 to 25.20°	
Index ranges	-12<=h<=12, -30<=k<=30, -13<=l<=13	
Reflection collected/unique	20704 / 4750 [R_{int} = 0.0822]	
Refinement method	Full-matrix least-squares on F^2	
Data/restraints/parameters	4750 / 0 / 373	
Goodness-of-fit on F^2	0.764	
Final R indices [I>2σ(I)]	R_1 = 0.0398, wR_2 = 0.0694	
R indices (all data)	R_1 = 0.1054, wR_2 = 0.0809	
Largest diff. peak and hole	0.181 and -0.149 e. $Å^{-3}$	

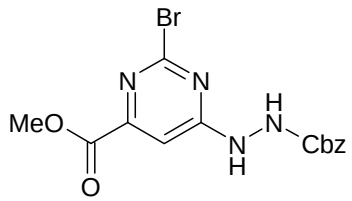

6b

Crystal data and structure refinement for compound **6a**:

Identification code	C123	
Empirical formula	$C_{14}H_{13}ClN_4O_4$	
Formula weight	336.73	
Temperature	173(1) K	
Wavelength	0.71073	
Crystal system, space group	Trclinic, P -1	
Unit cell dimensions	*a* = 7.5068(6) Å	α = 86.402(11)°
	b = 8.0366(7) Å	β = 89.652(10)°
	c = 13.7126(12) Å	γ = 68.834(10)°
Volume	769.82(13) $Å^3$	
Z, calculated density	2, 1.453 Mg/m^3	
Absorption coefficient	0.274 mm^{-1}	
F(000)	348	
Crystal size	0.28·0.20·0.06 mm	
θ-range for data collection	2.72 to 25.81°	
Index ranges	-9<=h<=9, -9<=k<=9, -16<=l<=16	
Reflection collected/unique	10185 / 2758 [R_{int} = 0.0500]	
Refinement method	Full-matrix least-squares on F^2	
Data/restraints/parameters	2758 / 0 / 239	
Goodness-of-fit on F^2	1.055	
Final R indices [I>2σ(I)]	R_1 = 0.0535, wR_2 = 0.1261	
R indices (all data)	R_1 = 0.0696, wR_2 = 0.1311	
Largest diff. peak and hole	0.375 and -0.190 e. $Å^{-3}$	

Synthesis of the peptides:

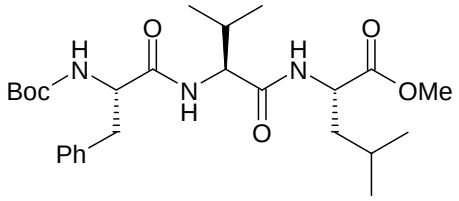

Boc-Phe-Val-Leu-OMe: H-Val-Leu-OMe·TFA (200 mg, 0.56 mmol) was allowed to react with Boc-Phe-OH (70 mg, 0.56 mmol), EDC (109 µL, 96 mg, 0.62 mmol), HOBt (83 mg, 0.62 mmol) and Huenig´s Base (240 µL, 181 mg, 1.40 mmol) following **GP3** to yield Boc-Phe-Val-Leu-OMe (258 mg, 0.53 mmol, 94 %) as a colorless powder.
mp.: 151 °C, ^{1}H-NMR ($CDCl_3$, 600 MHz): δ = 0.87-0.94 ppm (m, 12 H; HSQC: CH_3 Leu, CH_3 Val), 1.40 (s, 9 H; HSQC: Boc-CH_3), 1.54-1.59 (m, 1 H; HMBC: CH_s Leu), 1.61-1.69 (m, 2 H; HMBC: CH_2 Leu), 2.10-2.19 (m, 1 H; COSY: CH_s Val), 3.05 (dd, ^{3}J = 7.2 Hz, ^{3}J = 13.7 Hz, 1 H; HMBC: CH_2 Phe), 3.11 (dd, ^{3}J = 6.2 Hz, ^{3}J = 14.0 Hz, 1 H; HMBC: CH_2 Phe), 3.72 (s, 3 H; HSQC: OCH_3), 4.27 (t, ^{3}J = 7.2 Hz, 1 H; COSY: CH Val), 4.39 (bs, 1 H; COSY: CH Phe), 4.55-4.59 (m, 1 H; HMBC: CH Leu), 5.05 (bs, 1 H; COSY: NH Phe), 6.48 (bs, 1 H; COSY: NH Leu), 6.63 (d, ^{3}J = 8.6 Hz, 1 H; COSY: NH Val), 7.19-7.29 (m, 5 H; HSQC: Ar-H). ^{13}C-NMR ($CDCl_3$, 150 MHz): δ = 17.8 ppm (+; HSQC: CH_3 Leu, CH_3 Val), 19.0 (+; HSQC: CH_3 Leu, CH_3 Val), 21.8 (+; HSQC: CH_3 Leu, CH_3 Val), 22.8 (+; HSQC: CH_3 Leu, CH_3 Val), 24.8 (+; HSQC: CH_s Leu), 28.2 (+; HSQC: Boc-CH_3), 30.8 (+; HSQC: CH_s Val), 37.8 (-; HMBC: CH_2 Phe), 41.2 (-; HSQC. CH_2 Leu), 50.8 (+; HSQC: CH Leu), 52.2 (+; HSQC: OCH_3), 55.9 (+; HSQC: CH Phe), 58.5 (+; HSQC: CH Val), 80.3 (C_{quat}; HMBC: Boc), 127.0 (+; HSQC: Ar-H), 128.7 (+; HSQC: Ar-H), 129.3 (+; HSQC: Ar-H), 136.5 (C_{quat}; HMBC: Ar), 155.5 (C_{quat}; HMBC: C=O Boc), 170.5 (C_{quat}; HMBC: C=O Val), 171.4 (C_{quat}; HMBC: C=O Phe), 173.0 (C_{quat}; HMBC: C=O Leu). MS (ESI, MeOH): *m/z* (%) = 1005.7 [2M+Na^+] (8), 1000.7 [2M+NH_4^+] (4), 983.7 [2M+H^+] (2), 509.3 [M+NH_4^+] (30), 492.3 [MH^+] (100), 436.1 [MH^+-C_4H_8] (18).

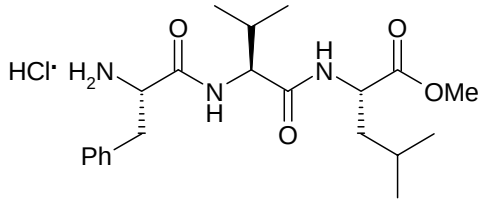

H-Phe-Val-Leu-OMe·HCl: Boc-Phe-Val-Leu-OMe (80 mg, 0.16 mmol) was allowed to react with Et_2O·HCl following **GP4** to afford H-Phe-Val-Leu-OMe·HCl (68 mg, 0.16 mmol, 98 %) as a colorless powder.

mp.: 188 °C. IR (KBr disk): 3319cm^{-1}, 3031, 2959, 1743, 1646, 1545, 1458, 1374, 1212, 1159, 1077. ^{1}H-NMR (DMSO-[D6], 300 MHz): δ = 0.85-0.93 ppm (m, 12 H, CH_3 Leu, CH_3 Val), 1.45-1.68 (m, 3 H, CH_2 Leu, CH_s Leu), 1.91-2.03 (m, 1 H, CH_s Val), .2.95 (dd, ^{3}J = 7.0 Hz, ^{3}J = 14.0 Hz, 1 H, CH_2 Phe), 3.10 (dd, ^{3}J = 5.5 Hz, ^{3}J = 14.0 Hz, 1 H, CH_2 Phe), 3.60 (s, 3 H, OCH_3), 4.21-4.32 (m, 3 H, CH Phe, CH Val, CH Leu), 7.22-7.31 (m, 5 H, Ar-H), 8.22 (bs, 2 H, NH), 8.49 (d, ^{3}J = 7.4 Hz, 1 H, NH), 8.68 (d, 8.9 Hz, 1 H, NH). ^{13}C-NMR (DMSO-[D6], 75 MHz): δ = 18.3 ppm (+, CH_3 Val), 18.9 (+, CH_3 Val), 21.1 (+, CH_3 Leu), 22.7 (+, CH_3 Leu), 24.1 (+, CH_s Leu), 30.0 (+, CH_s Val), 30.6 (-, CH_2 Phe), 39.3 (-, CH_2 Leu), 50.1 (+, CH Phe), 51.7 (+, CH Leu), 52.8 (+, OCH_3), 57.6 (+, CH Val), 126.9 (+, Ar-H), 128.2 (+, Ar-H), 129.5 (+, Ar-H), 134.7 (C_{quat}, Ar), 167.6 (C_{quat}), 170.5 (C_{quat}), 172.6 (C_{quat}). MS (ESI, MeOH + 10 mmol/l NH_4Ac): *m/z* (%) = 783.6 [2M+H$^+$] (14), 392.1 [MH$^+$] (100).

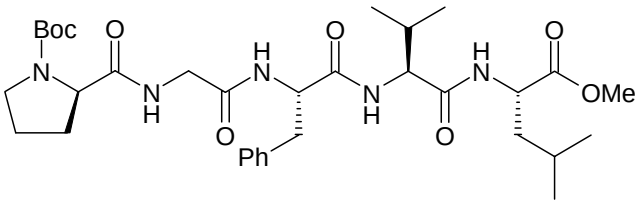

Boc-D-Pro-Gly-Phe-Val-Leu-OMe: H-Phe-Val-Leu-OMe·HCl (471 mg, 1.10 mmol) was allowed to react with Boc-D-Pro-Gly-OH (299 mg, 1.10 mmol), EDC (214 µL, 188 mg, 1.21 mmol), HOBt (164 mg, 1.21 mmol) and Huenig´s Base (471 µL, 355 mg, 2.75 mmol) following **GP3** to yield Boc-D-Pro-Gly-Phe-Val-Leu-OMe (612 mg, 0.95 mmol, 86 %) as a colorless powder.

mp.: > 210 °C (decomp). IR (KBr disk): 3292cm^{-1}, 3069, 2963, 1743, 1641, 1532, 1394, 1207, 1162, 744, 691. ^{1}H-NMR ($CDCl_3$, 600 MHz): δ = 0.88-0.96 ppm (m, 12 H: HSQC: CH_3 Leu, CH_3 Val), 1.45-1.48 (m, 9 H; HSQC: Boc-CH_3), 1.52-1.63 (m, 3 H;

COSY: CH_s Leu, CH_2 Leu), 1.67-1.70 (m, 1 H; COSY: CH_s Val), 1.96-1.99 (m, 2 H; COSY: CH_2 Pro), 2.12-2.15 (m, 2 H; COSY: CH_2 Pro), 2.96-3.01 (m, 2 H; HSQC: CH_2 Phe), 3.98-4.03 (m, 2 H; HSQC: CH_2 Gly), 3.36-3.42 (m, 2 H; COSY: $C_\delta H_2$ Pro), 3.70 (s, 3 H; HSQC: OCH_3), 4.21-4.27 (m, 1 H; COSY: CH Pro), 4.55-4.58 (m, 1 H; COSY: CH Leu), 4.62-4.67 (m, 1 H; COSY: CH Val), 5.04-5.06 (m, 1 H; COSY: CH Phe), 7.09-7.27 (m, 5 H; HSQC: Ar-H), 7.35-7.40 (m, 1 H, NH), 7.55-7.60 (m, 1 H, NH), 7.75 (bs, 1 H, NH), 8.08 (bs, 1 H, NH). ^{13}C-NMR ($CDCl_3$, 150 MHz): δ = 18.1 ppm (+; HSQC: CH_3 Val), 18.6 (+; HSQC: CH_3 Val), 21.9 (+; HSQC: CH_3 Leu), 22.8 (+; HSQC: CH_3 Leu), 23.8 (+; HSQC: CH_s Leu), 28.5 (+; HSQC: Boc-CH_3), 29.7 (+; HSQC: CH_s Val), 31.1 (-; HSQC: CH_2 Pro), 32.1 (-; HSQC: CH_2 Pro), 39.8 (-; HSQC: CH_2 Phe), 40.5 (-; HSQC: CH_2 Leu), 43.2 (-; HSQC: CH_2 Gly), 47.3 (-; HSQC: $C_\delta H_2$ Pro), 50.7 (+; HSQC: CH Leu), 52.1 (+; HSQC: OCH_3), 55.2 (+; HSQC: CH Phe), 58.3 (+; HSQC: CH Val), 60.3 (+; HSQC: CH Pro), 80.1 (C_{quat}, Boc), 126.8 (+; HSQC: Ar-H), 128.4 (+; HSQC: Ar-H), 129.3 (+; HSQC: Ar-H), 137.0 (C_{quat}, Ar), 155.3 (C_{quat}, C=O Boc), 162.5 (C_{quat}), 169.0 (C_{quat}), 170.5 (C_{quat}), 170.8 (C_{quat}), 173.1 (C_{quat}). UV (CH_3OH): λ_{max} (lg ε) = 258 nm (3.503), 281 (3.397), 310 (3.501). MS (ESI, MeOH + 10 mmol/l NH_4Ac): *m/z* (%) = 1313.9 [2M+Na^+] (3), 668.4 [M+Na^+] (42), 663.5 [M+NH_4^+] (63), 646.5 [MH^+] (100). Anal. Calcd. for $C_{33}H_{51}N_5O_8$: C: 61.4; H: 8.0; N: 10.8; O: 19.8; Found: C: 61.5; H: 7.5; N: 11.2.

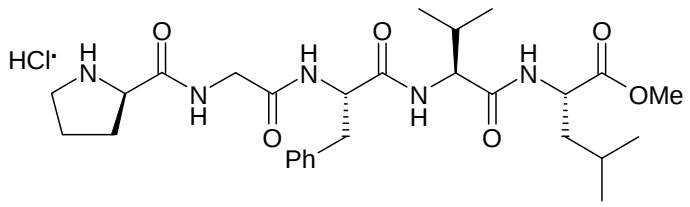

H-D-Pro-Gly-Phe-Val-Leu-OMe·HCl: Boc-D-Pro-Gly-Phe-Val-Leu-OMe (250 mg, 0.39 mmol) was allowed to react with Et_2O·HCl following **GP4** to afford H-D-Pro-Gly-Phe-Val-Leu-OMe·HCl (225 mg, 0.39 mmol, 99 %) as a colorless powder.

mp.: > 210 °C (decomp). IR (KBr disk): 3332cm^{-1}, 3281, 3054, 2955, 1744, 1640, 1531, 1439, 1374, 1238. ^{1}H-NMR (DMSO-[D6], 300 MHz): δ = 0.83-0.91 ppm (m, 12 H, CH_3 Leu, CH_3 Val), 1.41-1.64 (m, 3 H, CH_s Leu, CH_2 Leu), 1.72-1.88 (m, 3 H, CH_s Val, CH_2 Pro), 1.92-2.03 (m, 1 H, CH_2 Pro), 2.19-2.28 (m, 1 H, CH_2 Pro), 2.70-2.79 (m, 1 H, CH_2 Phe), 2.89-3.04 (m, 1 H, CH_2 Phe), 3.59 (s, 3 H, OCH_3), 3.65 (dd, ^3J = 5.6 Hz,

^3J = 16.9 Hz, 1 H, CH_2 Gly), 3.83 (dd, ^3J = 5.9 Hz, ^3J = 16.9 Hz, 1 H, CH_2 Gly), 4.15-4.31 (m, 3 H), 4.57-4.67 (m, 3 H), 7.13-7.24 (m, 5 H, Ar-H), 8.16 (d, ^3J = 8.8 Hz, 1 H, NH), 8.23 (d, ^3J = 8.2 Hz, 1 H, NH), 8.41 (d, ^3J = 7.1 Hz, 1 H, NH), 8.46-8.54 (m, 1 H, NH) 8.77 (d, ^3J = 5.6 Hz, 1 H, NH Gly), 10.01-10.10 (m, 1 H, NH). ^{13}C-NMR (DMSO-[D6], 75 MHz): δ = 18.2 ppm (+, CH_3 Val), 19.0 (+, CH_3 Val), 21.1 (+, CH_3 Leu), 22.7 (+, CH_3 Leu), 23.4 (-, CH_2 Leu), 24.1 (+, CH_s Leu) 29.5 (-, CH_2 Pro), 30.6 (+, CH_s Val), 37.4 (-, CH_2 Pro), 39.4 (-, CH_2 Phe), 39.9 (-, $C_\delta H_2$ Pro), 45.4 (-, CH_2 Gly), 50.1 (+, CH Leu), 51.6 (+, OCH_3), 53.6 (+, CH Phe), 57.4 (+, CH Val), 58.5 (+, CH Pro), 126.1 (+, Ar-H), 127.8 (+, Ar-H), 129.2 (+, Ar-H), 137.6 (C_{quat}, Ar), 167.7 (C_{quat}), 168.3 (C_{quat}), 170.6 (C_{quat}), 171.0 (C_{quat}), 172.6 (C_{quat}). UV (CH_3OH): λ_{max} (lg ε) = 259 nm (3.733), 286 (3.453). MS (ESI, H_2O/MeOH/AcN): *m/z* (%) = 1091.8 [2M+H$^+$] (22), 546.3 [MH$^+$] (100).

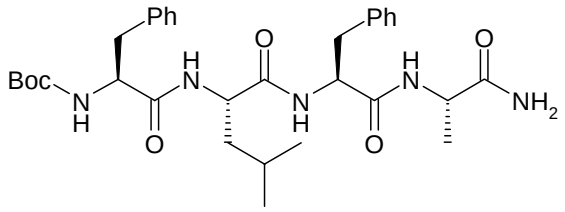

Boc-Phe-Leu-Phe-Ala-NH$_2$: H-Phe-Ala-NH$_2$·HCl (176 mg, 0.50 mmol) was allowed to react with Boc-Phe-Leu-OH (189 mg, 0.50 mmol), EDC (97 µL, 85 mg, 0.55 mmol), HOBt (74 mg, 0.55 mmol) and Huenig´s Base (214 µL, 162 mg, 1.25 mmol) following **GP3** to yield Boc-Phe-Leu-Phe-Ala-NH$_2$ (239 mg 0.40 mmol, 82 %) as a colorless powder.

mp.: 223 °C. IR (KBr disk): 3292 cm^{-1}, 3064, 2962, 2373, 2168, 1644, 1525, 1455, 1367, 1251, 1169, 1026, 856, 741. ^{1}H-NMR (DMSO-[D6], 400 MHz): δ = 0.82 ppm (d, ^3J = 6.5 Hz, 3 H; HSQC: CH_3 Leu), 0.86 (d, ^3J = 6.6 Hz, 3 H; HSQC: CH_3 Leu), 1.20 (d, ^3J = 7.1 Hz, 3 H; HSQC: CH_3 Ala), 1.29 (s, 9 H; HSQC: Boc-CH_3), 1.38-1.45 (m, 2 H; COSY:, CH_2 Leu), 1.53-1.61 (m, 1 H: COSY: CH_s Leu), 2.67-2.73 (m, 1 H; HMBC: CH_2 Phe), 2.80-2.92 (m, 2 H: HMBC: CH_2 Phe), 3.05 (dd, ^3J = 4.8 Hz, ^3J = 14.0 Hz, 1 H: HMBC: CH_2 Phe), 4.12-4.23 (m, 2 H: COSY: CH Ala, CH Phe), 4.30 (q, ^3J = 7.6 Hz, 1 H; COSY: CH Leu), 4.50-4.55 (m, 1 H; HMBC: CH Phe), 6.91 (d, ^3J = 8.7 Hz, 1 H; COSY: NH Ala), 7.00 (bs, 1 H; HSQC: NH_2), 7.15-7.20 (m, 1 H; HSQC: NH_2), 7.23-7.27 (m, 10 H; HSQC: Ar-H), 7.89 (d, ^3J = 8.3 Hz, 1 H; COSY: NH

Phe), 7.94 (d, ^3J = 7.5 Hz, 1 H; COSY: NH Leu), 8.00 (d, ^3J = 8.0 Hz, 1 H; COSY: NH Phe). ^{13}C-NMR (DMSO-[D6], 100 MHz): δ = 18.3 ppm (+; HSQC: CH_3 Ala), 21.6 (+; HSQC: CH_3 Leu), 23.0 (+; HSQC: CH_3 Leu), 23.8 (+, HSQC: CH_s Leu), 28.0 (+; HSQC: Boc-CH_3), 37.1 (-; HSQC: 2 CH_2 Phe), 41.0 (-; HMBC: CH_2 Leu), 47.9 (+; HMBC: CH Ala), 50.9 (+; HSQC: CH Leu), 53.5 (+; HSQC: CH Phe), 55.5 (+; HSQC: CH Phe), 77.9 (C_{quat}; HMBC: Boc), 126.1 (+; HSQC: Ar-H), 126.2 (+; HSQC: Ar-H), 127.8 (+; HSQC: Ar-H), 127.9 (+; HSQC: Ar-H), 129.1 (+; HSQC: Ar-H), 137.5 (C_{quart}; HMBC: Ar), 138.2 (C_{quat}; HMBC: Ar), 155.1 (C_{quat}; HMBC: C=O Boc), 170.2 (C_{quat}; HMBC: C=O Leu), 171.4 (C_{quat}; HMBC: C=O Phe), 171.7 (C_{quat}; HMBC: C=O Phe), 173.8 (C_{quat}; HMBC: C=O Ala). UV (CH_3OH): λ_{max} (lg ε) = 253 nm (3.825), 258 (3.862), 264 (3.768). MS (ESI, DCM/MeOH + 10 % NH_4Ac): *m/z* (%) = 613.4 [M+NH_4^+] (47), 596.3 [MH^+] (100).

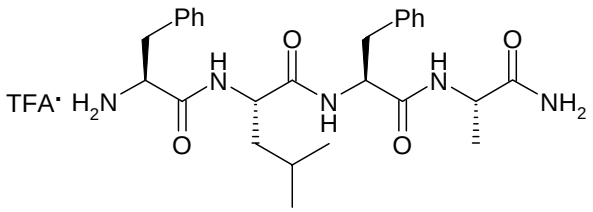

H-Phe-Leu-Phe-Ala-NH_2·TFA: Boc-Phe-Leu-Phe-Ala-NH_2 (250 mg, 0.39 mmol) was allowed to react with 20 % TFA in CH_2Cl_2 following **GP5** to afford H-Phe-Leu-Phe-Ala-NH_2·TFA (203 mg, 0.33 mmol, 99 %) as a colorless powder.

mp.: 225 °C. IR (KBr disk): 3269cm^{-1}, 3082, 2955, 1636, 1544, 1456, 1180, 1032, 800. ^{1}H-NMR (DMSO-[D6], 300 MHz): δ = 0.82-0.91 ppm (m, 6 H, CH_3 Leu), 1.20 (d, ^3J = 7.0 Hz, 3 H, CH_3 Ala), 1.34-1.47 (m, 2 H, CH_2 Leu), 1.51-1.65 (m, 1 H, CH_s Leu), 2.75-2.88 (m, 2 H, CH_2 Phe), 2.92-3.11 (m, 2 H, CH_2 Phe), 3.96-4.07 (m, 1 H CH Phe), 4.12-4.23 (m, 1 H, CH Ala), 4.32-4.42 (m, 1 H, CH Leu), 4.50-4.60 (m, 1 H, CH Phe), 7.04 (bs, 1 H, NH), 7.11-7.36 (m, 10 H, Ar-H), 7.98-8.21 (m, 4 H, NH), 8.26 (d, ^3J = 8.0 Hz, 1 H, NH), 8.60 (d, ^3J = 8.3 Hz, 1 H, NH). ^{13}C-NMR (DMSO-[D6], 75 MHz): δ = 18.3 ppm (+, CH_3 Ala), 21.6 (+, CH_3 Leu), 22.9 (+, CH_3 Leu), 23.9 (+, CH_s Leu), 36.9 (-, CH_2 Phe), 37.0 (-, CH_2 Phe), 41.1 (-, CH_2 Leu), 47.9 (+, Ala), 50.9 (+, CH Leu), 53.0 (+, CH Phe), 53.6 (+, CH Phe), 126.1 (+, Ar-H), 127.0 (+, Ar-H), 127.9 (+, Ar-H), 128.4 (+, Ar-H), 129.0 (+, Ar-H), 129.4 (+, Ar-H), 134.7 (C_{quat}, Ar), 137.7 (C_{quat}, Ar), 167.5 (C_{quat}), 170.2 (C_{quat}), 171.2 (C_{quat}), 173.8 (C_{quat}). UV (CH_3OH):

λ_{max} (lg ε) = 252 nm (3.698), 258 (3.738), 264 (3.649). MS (ESI, H_2O/AcN): *m/z* (%) = 596.3 [MH^+] (100).

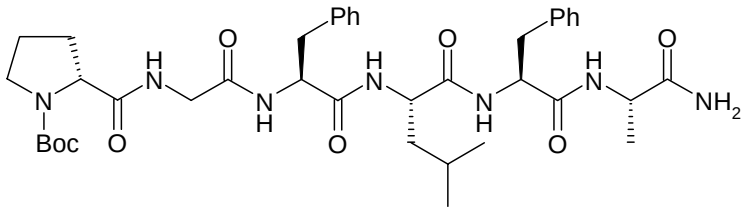

Boc-D-Pro-Gly-Phe-Leu-Phe-Ala-NH_2: H-Phe-Leu-Phe-Ala-NH_2·HCl (179 mg, 0.29 mmol) was allowed to react with Boc-D-Pro-Gly-OH (215 mg, 0.29 mmol), EDC (56 µL, 50 mg, 0.32 mmol), HOBt (43 mg, 0.32 mmol) and Huenig´s Base (124 µL, 94 mg, 0.73 mmol) following **GP3** to yield Boc-D-Pro-Gly-Phe-Leu-Phe-Ala-NH_2 (138 mg 0.18 mmol, 61 %) as a colorless powder.

mp.: 228 °C. IR (KBr disk): 3269cm^{-1}, 3084, 2953, 1635, 1544, 1459, 1184, 1030. ^{1}H-NMR (DMSO-[D6], 300 MHz): δ = 0.80 ppm (d, ^3J = 6.2 Hz, 3 H; HSQC: CH_3 Leu), 0.85 (d, ^3J = 6.4 Hz, 3 H; HSQC: CH_3 Leu), 1.20 (d, ^3J = 7.0 Hz, 3 H; HSQC: CH_3 Ala), 1.24-1.44 (m, 11 H; HSQC: Boc-CH_3; COSY: CH_2 Leu), 1.45-1.59 (m, 1 H, COSY: CH_s Leu), 1.61-2.13 (m, 4 H; COSY: CH_2 Pro), 2.63-3.13 (m, 4 H; HMBC: CH_2 Phe), 3.16-3.29 (m, 2 H; HSQC: CH_2 Pro), 3.42-3.61 (m, 1 H; HMBC. CH Phe), 3.64-3.86 (m, 1 H; HMBC: CH Phe), 4.00-4.29 (m, 3 H; HMBC: CH Pro, CH Ala, CH Leu), 4.39-4.62 (m, 2 H; HMBC: CH_2 Gly), 7.03 (s, 1 H, NH), 7.08-7.30 (m, 11 H; HMBC: Ar-H; NH), 7.76-8.04 (m, 3 H, NH), 8.16 (d, ^3J = 8.2 Hz, 1 H, NH), 8.33-8.40 (m, 1 H, NH). ^{13}C-NMR (DMSO-[D6], 100 MHz): δ = 18.2 ppm (+; HSQC: CH_3 Ala), 21.6 (+; HSQC: CH_3 Leu), 22.8 (+; HSQC. CH_3 Leu), 23.4 (-; HSQC. CH_2 Pro), 24.0 (+; HSQC: CH_s Leu), 27.9 (+; HSQC: Boc-CH_3), 36.8 (-; HSQC. CH_2 Phe), 37.0 (-; HSQC: CH_2 Phe), 40.5 (-; HSQC: CH_2 Leu), 42.2 (-; HSQC: CH_2 Gly), 46.5 (-; HSQC: CH_2 Pro), 47.9 (+; HSQC: CH Ala), 51.2 (+; HMBC: CH Leu), 53.4 (+; HMBC: CH Phe), 53.6 (+; HMBC: CH Phe), 59.4 (+; HMBC: CH Pro), 78.6 (C_{quat}; HMBC: Boc), 126.1 (+; HSQC: Ar-H), 127.9 (+; HSQC: Ar-H), 128.0 (+; HSQC: Ar-H), 128.9 (+; HSQC: Ar-H), 129.1 (+; HSQC: Ar-H), 137.6 (C_{quat}; HMBC: Ar), 137.8 (C_{quat}; HMBC: Ar), 153.5 (C_{quat}; HMBC: C=O Boc), 168.5 (C_{quat}; HMBC: C=O Phe), 170.1 (C_{quat}; HMBC: C=O Gly), 170.7 (C_{quat}; HMBC: C=O Pro), 171.6 (C_{quat}; HMBC: C=O Leu), 172.8 (C_{quat}; HMBC: C=O Phe), 173.8 (C_{quat}; HMBC: C=O Ala). UV (CH_3OH):

λ_{max} (lg ε) = 257 nm (3.488), 281 (3.367), 310 (3.492). MS (ESI, MeOH + 10 mmol/l NH_4Ac): *m/z* (%) = 772.4 [M+Na$^+$] (37), 750.4 [MH$^+$] (100).

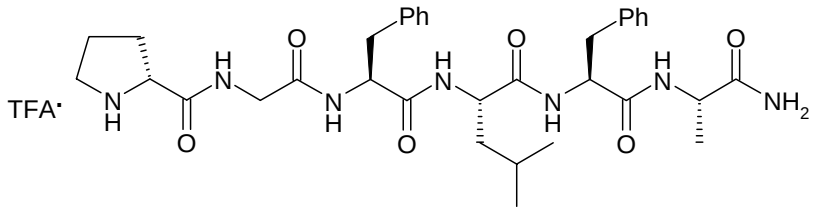

D-Pro-Gly-Phe-Leu-Phe-Ala-NH$_2$.TFA: Boc-D-Pro-GlyPhe-Leu-Phe-Ala-NH_2 (100 mg, 0.0.13 mmol) was allowed to react with 20 % TFA in CH_2Cl_2 following **GP5** to afford H—D-Pro-Gly-Phe-Leu-Phe-Ala-NH_2·TFA (98 mg, 0.13 mmol, 99 %) as a colorless powder.

mp.: 224 °C. IR (KBr disk): 3753cm^{-1}, 3423, 3067, 2955, 2376, 2249, 1656, 1528, 1447, 1178, 801. ^{1}H-NMR (DMSO-[D6], 300 MHz): δ = 0.76 ppm (d, ^{3}J = 6.3 Hz, CH_3 Leu), 0.81 (d, ^{3}J = 6.4 Hz, CH_3 Leu), 1.15 (d, ^{3}J = 7.0 Hz, CH_3 Ala), 1.29-1.39 (m, 2 H, CH_2 Leu), 1.40-1.54 (m, 1 H, CH_s Leu), 1.66-1.88 (m, 3 H, CH_2 Pro), 2.13-2.26 (m, 1 H, CH_2 Pro), 2.63 (dd, ^{3}J = 10.0 Hz, ^{3}J = 13.8 Hz, 1 H, CH_2 Phe), 2.76 (dd, ^{3}J = 9.1 Hz, ^{3}J = 13.9 Hz, 1 H, CH_2 Phe), 2.86-2.95 (m, 1 H, CH_2 Phe), 2.96-3.05 (m, 2 H, CH_2 Phe), 3.07-3.21 (m, 2 H, CH_2 Pro), 3.58 (dd, ^{3}J = 5.3 Hz, ^{3}J = 16.8 Hz, CH_2 Gly), 3.79 (dd, ^{3}J = 5.8 Hz, ^{3}J = 16.8 Hz, CH_2 Gly), 4.06-4.28 (m, 3 H, CH Ala, CH Leu, CH Pro), 4.42-4.55 (m, 2 H, CH Phe), 6.99 (bs, 1 H, NH), 7.17-7.28 (m, 11 H, Ar-H, NH), 7.90-8.01 (m, 2 H, NH), 8.14 (d, ^{3}J = 8.2 Hz, 1 H, NH), 8.47 (bs, 1 H, NH), 8.58-8.67 (m, 1 H, NH), 9.31 (bs, 1 H, NH). ^{13}C-NMR (DMSO-[D6], 75 MHz): δ = 18.3 ppm (+, CH_3), 21.6 (+, CH_3), 22.9 (+; CH_3), 23.4 (-), 24.0 (+, CH), 29.4 (-), 37.1 (-), 37.5 (-), 40.7 (-), 41.6 (-), 45.6 (-), 47.9 (+, CH), 51.0 (+, CH), 53.3 (+), 53.4 (+), 58.7 (+, CH), 126.1 (+, Ar-H), 127.9 (+, Ar-H), 129.1 (+, Ar-H), 137.5 (C_{quat}, Ar), 137.6 (C_{quat}, Ar), 167.6 (C_{quat}), 168.2 (C_{quat}), 170.2 (C_{quat}), 170.6 (C_{quat}), 171.6 (C_{quat}), 173.8 (C_{quat}). UV (CH_3OH): λ_{max} (lg ε) = 253 nm (3.858), 258 (3.878), 264 (3.828). MS (ESI, H_2O/AcN): *m/z* (%) = 672.5 [M+Na$^+$] (54), 650.5 [MH$^+$] (100).

Synthesis of new compounds:

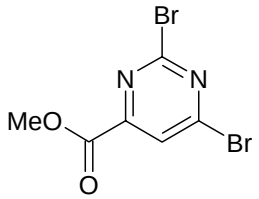

2,6-Dibromopyrimidine-4-carboxylic acid methyl ester (5b): Orotic acid methyl ester (**4**) (0.4 g, 2.35 mmol) was dissolved in acetonitrile (5 mL) and $POBr_3$ (3.37 g, 11.8 mmol) was added. The reaction mixture was stirred for 3 h under reflux. The resulting yellow solution was allowed to cool to rt, poured into 20 ml of crushed ice water, and extracted with ethyl acetate. The combined extracts were dried over Mg_2SO_4, and evaporated off. The residue was recrystallized from ethyl acetate/hexanes (3:1) to give **5b** as brown crystalline needles (541 mg, 78 %).

mp: > 185 °C (decomp). IR (KBr disk): 3116 cm^{-1}, 3069, 1729, 1549, 1517, 1439, 1314, 1233, 1103, 957, 784, 730. ^{1}H-NMR (DMSO-d_6): δ = 3.94 ppm (s, 3 H, OCH_3), 8.33 (s, 1 H, PHA-H). ^{13}C-NMR (DMSO-d_6): δ = 53.4 ppm (+; HMBC: OCH_3), 124.8 (+; HMBC: PHA-H), 150.8 (C_{quat}), 155.0 (C_{quat}), 157.0 (C_{quat}), 161.8 (C_{quat}; HMBC: -CO-OCH_3). UV (MeCN): λ_{max} (log ε) = 283 nm (4.664). MS *m/z* (%): 313.9 [M+NH_4^+] (100), 296.9 [MH^+] (15).

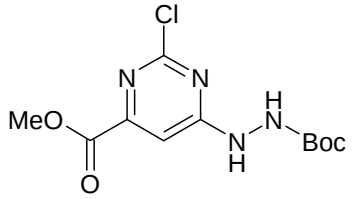

Methyl 6-(*N'*-*tert*-butoxycarbonylhydrazino)-2-chloro-pyrimidine-4-carboxylate (6a): Compound (**5a**) (1.32 g, 6.38 mmol) was allowed to react with triethylamine (1.06 mL, 0.78 g, 7.73 mmol) and Boc-hydrazine (1.02 g, 7.73 mmol) following **GP1** (hexanes/ethyl acetate 2:1, R_f = 0.30) to yield **6a** (1.17 g, 60 %) as a colorless powder.

mp: 151-152 °C. IR (KBr disk): 3264 cm^{-1}, 3230, 3109, 2982, 1735, 1609, 1446, 1263, 1159, 993, 754. ^{1}H-NMR ($CDCl_3$): δ = 1.39-1.41 ppm (m, 9 H, Boc-CH_3), 3.85 (s, 3 H, O-CH_3), 6.61 (s, 1 H, NH), 7.33 (s, 1 H, PHA-H), 7.77 (br, 1 H, NH). ^{13}C-NMR ($CDCl_3$): δ = 28.1 ppm (+; HMQC: Boc-CH_3), 53.4 (+; HMQC: OCH_3), 82.8 (C_{quat};

HMBC: Boc), 102.1 (+; HMQC: PHA-H); 155.1 (C_{quat}), 156.6 (C_{quat}), 160.5 (C_{quat}), 163.8 (C_{quat}; HMBC: C=O ester), 168.0 (C_{quat}). UV/VIS (MeCN): λ_{max} (log ε) = 244 nm (4.860), 301 (4.517). MS *m/z* (%): 622.1 [$2M+NH_4^+$] (1), 605.2 [$2M+H^+$] (2), 303.2 [MH^+] (100), 247.1 [MH^+-C_4H_8] (8), 203.1 [MH^+-Boc] (2). Anal. Calcd for $C_{11}H_{15}N_4O_4Cl$: C: 43.6; H: 5.0; N: 18.5; Found: C: 43.9; H: 5.0; N: 17.9.

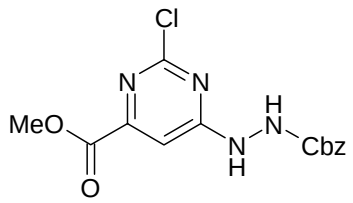

Methyl 6-(*N*'-benzyloxycarbonylhydrazino)-2-chloro-pyrimidine-4-carboxylate (6b): Compound (**5a**) (228 mg, 1.10 mmol) was allowed to react with triethylamine (128 µL, 122 mg, 1.21 mmol) and Cbz-hydrazine (201 mg, 1.21 mmol) following **GP1** (hexanes/ethyl acetate 3:2, R_f = 0.25) to yield **6a** (280 mg, 75 %) as a colorless powder. mp: 94-96 °C. IR (KBr disk): 3264 cm^{-1}, 3116, 2956, 1729, 1597, 1561, 1443, 1267, 1203, 978, 754. ^{1}H-NMR ($CDCl_3$): δ = 3.98 ppm (s, 3 H, O-CH_3), 5.21 (s, 2 H, CH_2-Ar), 6.78 (br s, 1 H, N-H), 7.31-7.60 (m, 7 H, 5 Ar-H + PHA-H + N-H). ^{13}C-NMR ($CDCl_3$): δ = 53.3 ppm(+; HMQC: OCH_3), 68.4 (-; HMQC: CH_2 Bzl), 102.2 (+; HMQC: PHA-H), 128.3 (+; HMQC: Ar-H), 128.7 (+; HMQC: Ar-H), 135.0 (C_{quat}, Ar), 156.1 (C_{quat}), 156.7 (C_{quat}), 160.6 (C_{quat}), 163.6 (C_{quat}; HMBC: C=O ester), 168.2 (C_{quat}). UV/VIS (MeCN): λ_{max} (log ε) = 234 nm (4.689), 300 (4.360). MS *m/z* (%): 337.1 [MH^+] (100), 228.9 [MH^+-$PhCH_2OH$] (7), 202.9 [MH^+-Cbz] (22), 188.1 [MH^+-Cbz-NH] (29). Anal. Calcd for $C_{14}H_{13}N_4O_4Cl$: C: 49.9; H: 3.9; N: 16.6; Found: C: 49.8; H: 4.2; N: 16.5.

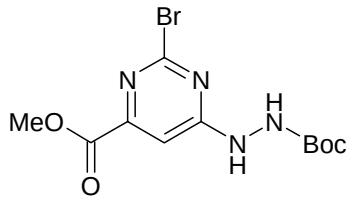

Methyl 2-bromo-6-(*N*'-*tert*-butoxycarbonylhydrazino)pyrimidine-4-carboxylate (6c): Compound (**5b**) (164 mg, 0.55 mmol) was allowed to react with triethylamine

(91 µL, 87 mg, 0.66 mmol) and Boc-hydrazine (87 mg, 0.66 mmol) following **GP1** (hexanes/ethyl acetate 1:1, R_f = 0.54) to yield **6a** (123 mg, 64 %) as a colorless powder. mp: 227-228 °C. IR (KBr disk): 3228 cm^{-1}, 3105, 2981, 1734, 1603, 1445, 1259, 1159, 752. ^{1}H-NMR (DMSO-d_6, 363 K): δ = 1.44 ppm (s, 9 H, Boc-CH_3), 3.89 (s, 3 H, OCH_3), 7.36 (s, 1 H), 8.92 (bs, 1 H), 9.71 (s, 1 H). ^{13}C-NMR (DMSO-d_6): δ = 28.2 ppm (+; HMQC: Boc-CH_3), 53.5 (+; HMQC: OCH_3), 83.0 (C_{quat}; HMBC: Boc), 102.7 (+; HMQC: PHA-H), 152.1 (C_{quat}), 155.0 (C_{quat}; HMBC: C=O Boc), 156.3 (C_{quat}), 163.7 (C_{quat}; HMBC: C=O ester), 167.1 (C_{quat}). UV (MeCN): λ_{max} (log ε) = 235 nm (4.973), 303 (4.654). MS *m/z* (%): 340.0 [MH^+] (100). HRMS Calcd for $C_{11}H_{15}BrN_4O_4$: 346.0277; Found: 346.0275±0.0002.

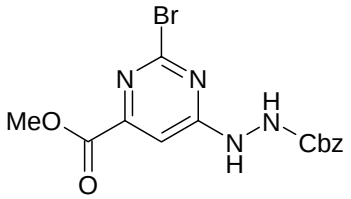

Methyl 6-(*N*'-benzyloxycarbonylhydrazino)-2-bromo-pyrimidine-4-carboxylate (6d): Compound (**5b**) (836 mg, 2.83 mmol) was allowed to react with triethylamine (470 µL, 343 mg, 3.39 mmol) and Cbz-hydrazine (563 mg, 3.39 mmol) following **GP1** (ethyl acetate/hexanes 2:3, R_f = 0.22) to yield **6a** (839 mg, 78 %) as a colorless powder. mp: 94-95 °C. IR (KBr disk): 3354 cm^{-1}, 3270, 2958, 2930, 1721, 1691, 1591, 1512, 1376, 1287, 1211, 1121, 995, 968, 773, 743, 695. ^{1}H-NMR ($CDCl_3$): δ = 3.92 ppm (s, 3 H, OCH_3), 5.16 (s, 2 H, CH_2), 7.05-7.58 (m, 7 H, Ar-H, PHA-H, NH), 8.60 (br s, 1 H, NH). ^{13}C-NMR ($CDCl_3$): δ = 53.5 ppm (+, OCH_3), 68.4 (-, CH_2), 102.4 (+, PHA-H), 127.3 (+, Ar-H), 127.7 (+, Ar-H), 134.1 (C_{quat}, Ar), 150.8 (C_{quat}), 155.2 (C_{quat}, C=O Cbz), 162.5 (C_{quat}), 162.6 (C_{quat}), 165.8 (C_{quat}). UV (MeCN): λ_{max} (log ε) = 301 nm (4.644). MS *m/z* (%): 380.9 [MH^+] (100). Anal. Calcd for $C_{14}H_{13}BrN_4O_4$: C: 44.1; H: 3.4; Br: 21.0; N: 14.7; O: 16.8; Found: C: 44.6; H: 3.4; N: 14.9.

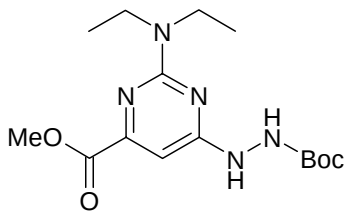

Methyl 6-(N'-tert-butoxycarbonylhydrazino)-2-diethylaminopyrimidine-4-carboxylate (8a): Method A: A solution of (**6a**) (117 mg, 0.39 mmol), DMAP (59 mg, 0.48 mmol) and diethylamine (80 µL, 57 mg, 0.78 mmol) in DMF (6 mL) is stirred for 1 d at 40 °C. The red solution is diluted with ethyl acetate (8 mL) and washed with brine (2x15 mL). The organic extract is dried over $MgSO_4$, evaporated under reduced pressure and the residue purified by column chromatography (hexanes/ethyl acetate 3:1, R_f = 0.22) to afford **8a** (55 mg, 42 %) as a colorless powder.

Method B: A solution of **6c** (200 mg, 0.58 mmol) and diethylamine (299 µL, 212 mg, 2.90 mmol) in DMF (4 mL) is stirred for 8 h at 80 °C. The solvent is evaporated and the crude product purified by column chromatography (hexanes/ethyl acetate 3:1, R_f = 0.22) to afford **8a** (146 mg, 74 %).

mp: 176-177 °C. IR (KBr disk): 3237 cm^{-1}, 2967, 2933, 1732, 1668, 1601, 1531, 1368, 1253, 1161. ^{1}H-NMR (DMSO-d_6): δ = 1.09 ppm (t, ^3J = 6.9 Hz, 6 H, CH_3), 1.25-152 (m, 9 H, Boc-CH_3), 3.54 (q, ^3J = 6.9 Hz, 4 H, CH_2), 3.81 (s, 3 H, OCH_3), 6.32 (s, 1 H, PHA-H), 8.48-9.17 (m, 2 H, N-H). ^{13}C-NMR (DMSO-d_6): δ = 13.1 ppm (+, CH_3), 27.9 (+, Boc-CH_3), 40.7 (-, CH_2), 52.2 (+, OCH_3), 78.8 (C_{quat}, Boc), 93.5 (+, PHA-H), 155.2 (C_{quat}), 155.6 (C_{quat}), 160.6 (C_{quat}), 164.3 (C_{quat}), 165.5 (C_{quat}). UV (MeCN): λ_{max} (log ε): 243 (5.316) nm, 329 (4.660). MS *m/z* (%): 701.5 [$2MNa^+$] (6), 340.0 [MH^+] (100)

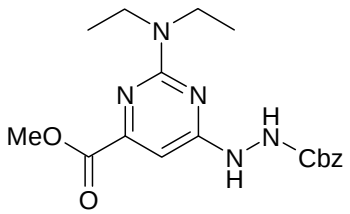

Methyl 6-(*N*'-benzyloxycarbonylhydrazino)-2-diethylaminopyrimidine-4-carboxylate (8b): To a solution of **6d** (270 mg, 0.71 mmol) in DMF (5 mL) was added diethylamine (366 µL, 260 mg, 3.55 mmol). The reaction mixture was stirred for 16 h at 70 °C. The solution was diluted with ethyl acetate (7 mL) and washed with brine (2x10 mL). The organic phase washed dried over $MgSO_4$, evaporated under reduced pressure and purified by column chromatography (hexanes/ethyl acetate 3:2, R_f = 0.40) affording **8b** (212 mg, 80 %).

mp: 174-177 °C. IR (KBr disk): 3262 cm^{-1}, 2955, 1783, 1596, 1499, 1443, 1263, 1196, 976, 748. ^{1}H-NMR ($CDCl_3$): δ = 1.12 ppm (t, ^3J = 7.0 Hz, 6 H, NCH_2CH_3), 3.58 (q,

^3J = 6.6 Hz, 4 H, N*CH*$_2$CH$_3$), 3.89 (s, 3 H, OCH$_3$), 5.18 (s, 2 H, CH$_2$ Cbz), 6.51-6.72 (m, 3 H, PHA-H, NH), 7.22-7.38 (m, 5 H, Ar-H). ^{13}C-NMR (CDCl$_3$): δ = 13.1 ppm (+, NCH$_2$*CH$_3$*), 41.6 (-, N*CH$_2$*CH$_3$), 52.7 (+, OCH$_3$), 67.9 (-, CH$_2$ Cbz), 92.1 (+, PHA-H), 128.3 (+, Ar-H), 128.5 (+, Ar-H), 128.6 (+, Ar-H), 135.5 (C_{quat}, Ar), 156.0 (C_{quat}, C=O Cbz), 156.8 (C_{quat}), 161.1 (C_{quat}), 165.6 (C_{quat}), 166.0 (C_{quat}). UV (MeCN): λ_{max} (log ε) = 246 nm (5.289), 341 (4.579). MS *m/z* (%): 374.0 [MH$^+$] (100).

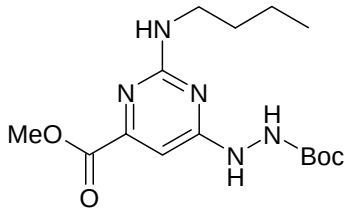

Methyl 6-(*N'*-*tert*-butoxycarbonylhydrazino)-2-butylaminopyrimidine-4-carboxylate (8c): To a stirred solution of (**6c**) (100 mg, 0.29 mmol) in DMF (3 mL) was added butyl amine (71 µL, 53 mg, 0.72 mmol) and the reaction mixture was stirred for 18 h at 65 °C. The solution was diluted with ethyl acetate (5 mL) and washed with brine (3x8 mL). The organic extract was dried over Na$_2$SO$_4$, evaporated off and purified by column chromatography (hexanes/ethyl acetate 3:2, R_f = 0.14) to afford **8c** (13 mg, 13 %) as colorless powder and unreacted **6c** (49 mg, 0.14 mmol).

mp: 110-112 °C. IR (KBr disk): 3337 cm^{-1}, 2959, 2873, 1735, 1591, 1542, 1439, 1368, 1249, 1160, 1102, 778. ^{1}H-NMR (CDCl$_3$): δ = 0.92 ppm (t, ^3J = 7.2 Hz, CH$_3$), 1.24-1.58 (13 H, Boc-CH$_3$, CH$_3$*CH$_2$*, CH$_3$CH$_2$*CH$_2$*), 3.36 (q, ^3J = 6.4 Hz, 2 H, *CH$_2$*NH), 3.93 (s, 3 H, OCH$_3$), 5.34 (br s, 1 H, NH), 6.55 (s, 1 H, NH), 6.65 (s, 1 H, PHA-H), 6.76 (br s, 1 H, NH). ^{13}C-NMR (DMSO-d$_6$): δ = 13.8 ppm (+, CH$_3$), 20.1 (-, CH$_3$*CH$_2$*), 28.2 (+, Boc-CH$_3$), 31.6 (-, CH$_3$*CH$_2$*), 36.9 (-, CH$_3$CH$_2$*CH$_2$*), 53.0 (+, OCH$_3$), 82.0 (C_{quat}, Boc), 93.2 (+, PHA-H), 155.6 (C_{quat}, 2 C), 162.4 (C_{quat}), 165.5 (C_{quat}), 166.7 (C_{quat}). UV (MeCN): λ_{max} (log ε) = 244 (5.213) nm, 323 (4.552). MS *m/z* (%): 340.1 [MH$^+$] (100).

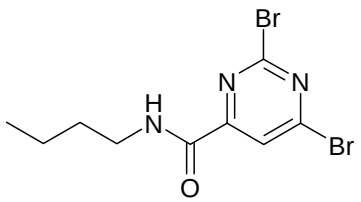

2,6-Dibromopyrimidine-4-carboxylic acid butylamide (10): Orotic acid butylamide (**9**) (1.65 g, 5.76 mmol) and $POBr_3$ (7.74 g, 28.8 mmol) were suspended in acetonitrile (15 mL). The reaction mixture was stirred for 3.5 h at 65 °C. The clear solution was allowed to cool to rt and poured on crushed ice (20 mL) and water (10 mL) and extracted with ethyl acetate (3x45 mL). The organic extract was washed with sat. $NaHCO_3$ solution and dried over Na_2SO_4, evaporated off affording **10** (466 mg, 72 %) in analytical pure form.mp: > 175 °C (decomp). IR (KBr disk): 3010 cm^{-1}, 2987, 2979, 1650, 1636, 1225, 675. ^{1}H-NMR (DMSO-d_6): δ = 0.88 ppm (t, 3 H; ^3J = 7.4 Hz, CH_3), 1.18-1.36 (m, 2 H, CH_3-CH_2), 1.40-1.57 (m, 2 H, CH_2-CH_2-NH), 3.27 (q, 2 H, ^3J = 6.7 Hz, CH_2-NH), 8.21 (s, 1 H, PHA-H), 9.02 (t, 1 H, ^3J = 6.8 Hz, N-H). ^{13}C-NMR (DMSO-d_6): δ = 13.5 ppm (+, CH_3), 19.4 (-, CH_3-CH_2), 30.8 (-, CH_2-CH_2-NH), 38.8 (-, CH_2-NH), 122.4 (+, PHA-H), 146.6 (C_{quat}), 150.1 (C_{quat}), 154.7 (C_{quat}), 160.1 (C_{quat}). UV (MeCN): λ_{max} (log ε) = 276 nm (4.774). MS *m/z* (%): 333.7 [M+H$^+$] (100).

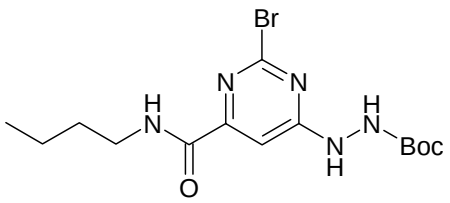

2-Bromo-6-[*N'*-(*tert*-butoxyhydroxymethyl)hydrazino]pyrimidine-4-carboxylic acid butylamide (11): (**10**) (350 mg, 1.04 mmol) was allowed to react with triethylamine (173 µL, 127 mg, 1.25 mmol) and Boc-hydrazine (165 mg, 1.25 mmol) following **GP1** (ethyl acetate/hexanes 3:5, R_f = 0.18) to yield **11** (331 mg, 82 %) as a colorless powder.

mp: 161-163 °C. IR (KBr disk): 3339 cm^{-1}, 3227, 2974, 2932, 1725, 1651, 1593, 1526, 1392, 1272, 1254, 1165. ^{1}H-NMR ($CDCl_3$): δ = 0.95 ppm (t, 3 H, ^3J = 7.3 Hz; HSQC: CH_3), 1.36-1.45 (m, 2 H; ROESY: CH_3CH_2), 1.47 (s, 9 3.43 (q, 2 H, ^3J = 6.7 Hz, CH_2-NH), 6.79 (s, 1 H; ROESY: ^{1}NH), 7.46 (s, 1 H; HSQC: PHA-H), 7.62 (bs, 1 H; ROESY: ^{2}NH), 7.77 (t, ^3J = 5.8 Hz, 1 H; HMBC: NHCO). ^{13}C-NMR (DMSO-d_6): δ: 13.7 ppm (+; HSQC: CH_3), 20.1 (-; HSQC: CH_3CH_2), 28.2 (+; HSQC: Boc-CH_3), 31.5 (-; HSQC: $CH_3CH_2CH_2$), 39.4 (-; HSQC: CH_2NH), 82.7 (C_{quat}; HMBC: Boc), 99.6 (+; HSQC: PHA-H), 150.8 (C_{quat}), 154.8 (C_{quat}; HMBC: C=O Boc), 161.7 (C_{quat}), 167.3 (C_{quat}). UV (MeCN): λ_{max} (log ε) = 240 nm (5.227), 295 (4.709). MS *m/z* (%): 388.0

[MH^+] (88), 331.9 [MH^+ - C_4H_8] (100). Anal. Calcd for $C_{14}H_{22}BrN_5O_3$: C. 43.3; H: 5.7; N: 18.0; O: 12.4; Br: 20.6; Found: C: 43.6; H: 5.6; N: 17.9.

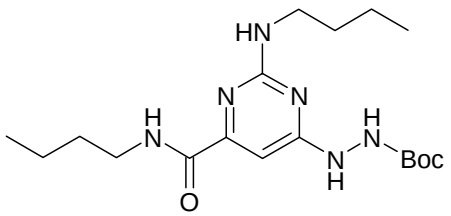

6-[*N'*-(*tert*-Butoxyhydroxymethyl)hydrazino]-2-butylaminopyrimidine-4-carboxylic acid butyl-amide (12a): (**11**) (142 mg, 0.36 mmol) was allowed to react with butylamine (357 µL, 263 mg, 3.60 mmol) following **GP2** (ethyl acetate/hexanes 1:1, R_f = 0.37) to give **12a** (93 mg, 68 %) as a yellow solid.

mp: 184-186 °C. IR (KBr disk): 3372 cm^{-1}, 3213, 2962, 1735, 1665, 1589, 1528, 1460, 1367, 1250, 1161, 1015, 771. ^{1}H-NMR ($CDCl_3$): δ = 0.73-0.97 ppm (m, 6 H, 2 CH_3), 1.32-1.66 (m, 17 H, Boc-CH_3, 4 CH_2), 3.32-3.45 (m, 4 H, 2 CH_2NH), 5.14 (br s, 1 H, NH), 6.73 (br s, 1 H, NH), 6.80 (s, 1 H, PHA-H), 7.09 (br s, 1 H, NH), 7.89 (br s, 1 H, NHCO). ^{13}C-NMR ($CDCl_3$): δ = 13.8 ppm (+, CH_3), 13.9 (+, CH_3), 20.0 (-), 20.1 (-) 28.2 (+, Boc-CH_3), 31.6 (-), 31.7 (-), 39.0 (-), 41.2 (-), 88.9 (C_{quat}, Boc), 91.0 (+, PHA-H), 155.7 (C_{quat}), 156.0 (C_{quat}), 161.3 (C_{quat}), 161.4 (C_{quat}), 163.8 (C_{quat}), 164.1 (C_{quat}). UV (MeOH): λ_{max} (log ε) = 236 nm (5.197), 328 (4.460). MS *m/z* (%): 381.1 [MH^+] (100).

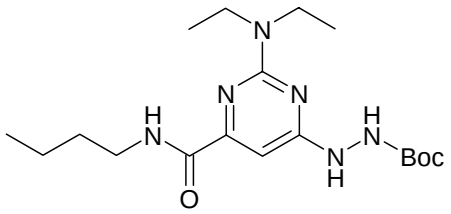

6-[N'-(tert-Butoxy-hydroxy-methyl)-hydrazino]-2-diethylamino-pyrimidine-4-carboxylic acid butylamide (12b): To a solution of (**11**) (242 mg, 0.62 mmol) in DMF (3 mL) was added diethylamine (312 µL, 228 mg, 3.12 mg) and the solution was stirred for 16 h at 70 °C. The solution was diluted with ethyl acetate (10 mL) and washed with brine (2x20 mL). The organic extract was dried over $MgSO_4$ and evaporated off. The

residue was purified by column chromatography (hexanes/ethyl acetate 1:2, $R_f = 0.33$) to afford **12b** (200 mg, 82 %).

mp: 165-167 °C. IR (KBr disk): 3226cm^{-1}, 2967, 2933, 1732, 1668, 1601, 1531, 1368, 1253, 1161. ^{1}H-NMR ($CDCl_3$): $\delta = 0.95$ ppm (t, $^3J = 7.3$ Hz, 3 H, CH_3 Bu), 1.17 (t, $^3J = 7.0$ Hz, 6 H, CH_3 Et), 1.30-1.73 (m, 13 H, Boc-CH_3, CH_3*CH_2*, CH_3CH_2*CH_2*), 3.41 (q, $^3J = 6.7$ Hz, *CH_2*NHCO), 3.57 (q, $^3J = 7.0$ Hz, CH_2 Et), 6.68-6.77 (m, 2 H, NH), 6.91 (s, 1 H, PHA-H), 7.88 (br s, 1 H, NHCO). ^{13}C-NMR ($CDCl_3$): $\delta = 13.5$ ppm (+, CH_3 Bu), 13.6 (+, CH_3 Et), 19.4 (-, CH_3*CH_2*), 27.9 (+, Boc-CH_3), 31.0 (-, CH_3CH_2*CH_2*), 38.2 (-, CH_2 Et), 38.5 (-, CH_2 Et), 40.7 (-, CH_2NHCO), 80.2 (C_{quat}, Boc), 98.3 (+, PHA-H), 155.6 (C_{quat}, C=O Boc), 158.6 (C_{quat}), 161.3 (C_{quat}), 163.5 (C_{quat}), 167.2 (C_{quat}). UV (MeCN): λ_{max} (log ε) = 243 nm (5.316), 330 (4.645). MS *m/z* (%): 783.6 [2M+Na$^+$] (4), 761.7 [2M+H$^+$], 381.0 [M+H$^+$] (100), 324.9 [MH$^+$-C_4H_8] (32), 280.8 [MH$^+$-Boc] (48).

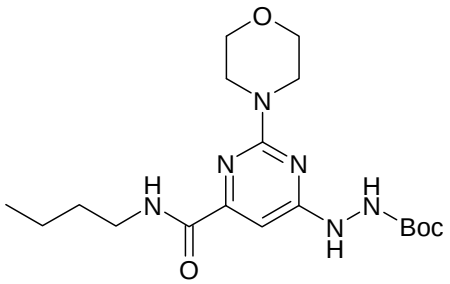

***tert*-Butyl *N*'-(6-butylcarbamoyl-2-morpholin-4-ylpyrimidin-4-yl)hydrazine carboxylate (12c):** Compound (**11**) (100 mg, 0.26 mmol) was allowed to react with 1,4,7,10,13-pentaoxa-16-aza-cyclo-octa-decane (225 µL, 225 mg, 2.58 mmol) following **GP2** (ethyl acetate/hexanes 1:1, $R_f = 0.24$) to give **12c** (68 mg, 0.17 mmol, 66 %) as a colourless, hygroscopic solid.

mp: 167-170 °C. IR (KBr disk): 3356 cm^{-1}, 3290, 3197, 2691, 1724, 1659, 1558, 1523, 1447, 1361, 1254, 1161, 1104, 1002, 875. ^{1}H-NMR ($CDCl_3$): $\delta = 0.95$ ppm (t, $^3J = 7.3$ Hz, 3 H, CH_3), 1.23-1.64 (m, 13 H, Boc-CH_3, CH_3*CH_2*, CH_3CH_2*CH_2*), 3.41 (dd, $^3J = 7.1$ Hz, $^3J = 13.4$ Hz, 2 H, *CH_2*NHCO), 3.75 (br s, 8 H, CH_2 morpholine), 6.61-6.82 (m, 3 H, PHA-H, 2 NH), 7.79 (t, $^3J = 5.6$ Hz). ^{13}C-NMR ($CDCl_3$): $\delta = 13.8$ ppm (+, CH_3), 20.2 (-, CH_3CH_2), 28.2 (+, Boc-CH_3), 31.7 (-, CH_3CH_2*CH_2*), 39.1 (-, CH_2NHCO), 44.3 (-, CH_2 morpholine), 66.8 (-, CH_2 morpholine), 81.8 (C_{quat}, Boc), 91.2 (+, PHA-H), 155.8 (C_{quat}, C=O Boc), 157.4 (C_{quat}), 160.7 (C_{quat}), 163.8 (C_{quat}), 166.7 (C_{quat}). UV

(MeOH): λ_{max} (log ε) = 242 nm (5.449), 328 (4.680). MS *m/z* (%): 395.1 [MH^+] (100), 296.8 [MH^+-Boc] (52). HRMS Calcd for $C_{18}H_{30}N_6O_4$: 394.2329; Found: 394.2330±0.0004. Anal. Calcd for $C_{18}H_{30}N_6O_4$: C: 54.8; H: 7.7; N: 21.3; O: 16.2; Found: C: 54.8; H: 7.5; N: 21.5.

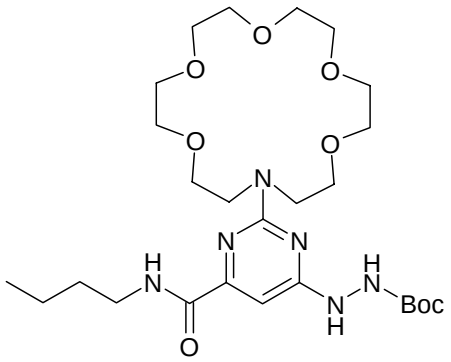

***tert*-Butyl *N'*-[6-butylcarbamoyl-2-(1,4,7,10,13-pentaoxa-16-azacyclooctadec-16-yl)pyrimidin-4-yl]hydrazine carboxylate (12d):** Compound (**11**) (145 mg, 0.37 mmol) and triethylamine (154 µL, 112 mg, 1.11 mmol) were dissolved in DMF (3 mL) and 1,4,7,10,13-pentaoxa-16-aza-cyclooctadecane (292 mg, 1.11 mmol) was added. The resulting solution was stirred for 36 h at 65 °C, diluted with ethyl acetate (5 mL) and washed with brine (2x10 mL). The organic extract was dried over $MgSO_4$, evaporated off and purified by column chromatography (ethyl acetate, R_f = 0.17) to afford **12d** (118 mg, 56 %).

mp: > 180 °C (decomp). IR (CH_2Cl_2): 3110 cm^{-1}, 2979, 1665, 1571, 1259, 902, 886. ^{1}H-NMR ($CDCl_3$): δ = 0.87 ppm (t, ^3J = 7.3 Hz, 3 H, CH_3), 1.21-1.72 (m, 13 H, Boc-CH_3, 2 CH_2), 3.32 (q, ^3J = 6.8 Hz, 2 H, *CH_2*NHCO), 3.41-3.94 (m, 24 H, CH_2 crown ether), 6.39-6.99 (m, 3 H, PHA-H, 2 NH), 7.84 (t, ^3J = 5.6 Hz, 1 H, NHCO). ^{13}C-NMR ($CDCl_3$): δ = 13.8 ppm (+, CH_3), 20.1 (-, CH_3CH_2), 28.2 (+, Boc-CH_3), 39.0 (-, CH_3CH_2*CH_2*), 48.8 (-, *CH_2*NHCO), 69.5 (-, CH_2 crown ether), 70.7 (-, CH_2 crown ether), 70.8 (-, CH_2 crown ether), 81.6 (C_{quat}, Boc), 90.1 (+, PHA-H), 155.8 (C_{quat}, Boc C=O), 157.4 (C_{quat}), 160.4 (C_{quat}), 164.1 (C_{quat}), 166.6 (C_{quat}). UV (MeCN): λ_{max} (log ε) = 244 nm (5.255), 331 (4.578). MS *m/z* (%): 609.3 [$M+K^+$] (12), 593.3 [$M+Na^+$] (10), 571.4 [MH^+] (100). HRMS Calcd for $C_{26}H_{46}N_6O_8$: 570.3377; Found: 570.3379±0.0004.

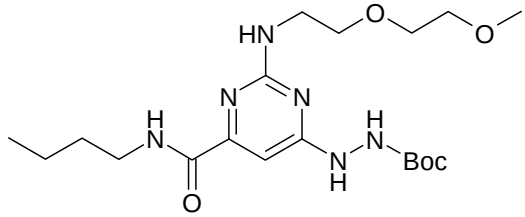

***tert*-Butyl N'-{6-butylcarbamoyl-2-[2-(2-methoxyethoxy)ethylamino]pyrimidin-4-yl}-hydrazine carboxylate (12e):** Compound (**11**) (110 mg, 0.28 mmol) was allowed to react with 2-(2-methoxy-ethoxy)ethylamine (361 µL, 334 mg, 2.80 mmol) following **GP2** (ethyl acetate, $R_f = 0.16$) to give **12e** (33 mg, 28 %) as a colourless powder and unreacted **11** (51 mg, 0.13 mmol).

mp: 88-89 °C. IR (KBr disk): 3436 cm^{-1}, 3376, 3242, 2963, 1730, 1670, 1590, 1569, 1522, 1440, 1257, 1149, 1091, 802. ^{1}H-NMR ($CDCl_3$): δ = 0.95 ppm (t, ^3J = 7.3 Hz, 3 H, CH_3), 1.36-1.46 (m, 11 H, Boc-CH_3, 2 CH_2), 1.53-1.63 (m, 2 H, CH_2), 3.36-3.43 (m, 5 H, OCH_3, CH_2), 3.55-3.65 (m, 8 H, 4 CH_2), 5.55 (br s, 1 H, NH), 6.74-6.81 (m, 2 H, PHA-H, NH), 7.00 (br s, 1 H, NH), 7.86 (br s, 1 H, NH). ^{13}C-NMR ($CDCl_3$): δ = 12.8 ppm (+, CH_3 Bu), 19.1 (-), 27.2 (+, Boc-CH_3), 30.6 (-), 38.1 (-), 40.1 (-), 58.0 (+, OCH_3), 69.0 (-), 69.3 (-), 70.9 (-), 80.8 (C_{quat}, Boc), 90.3 (+, PHA-H), 154.6 (C_{quat}, C=O Boc), 158.6 (C_{quat}), 160.2 (C_{quat}), 162.7 (C_{quat}), 166.1 (C_{quat}). UV (MeOH): λ_{max} (log ε) = 242 nm (4.758). MS *m/z* (%): 427.1 [MH^+] (100), 853.6 [$2M+H^+$] (8).

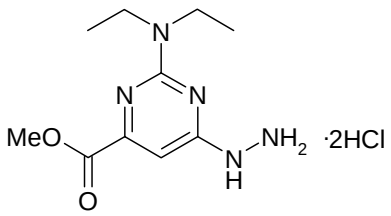

Methyl 2-diethylamino-6-hydrazinopyrimidin-4-carboxylate bishydrochloride (13): Compound (**8a**) (53 mg, 0.16 mmol) is dissolved in ether saturated with HCl (2 mL) at 0 °C and stirred for 15 min. Removal of the solvent under reduced pressure gives **13** in quantitative yield (50 mg). The product is used without further purification.

mp: > 185 °C (decomp). IR (KBr disk): 3446 cm^{-1}, 2887, 1744, 1643, 1591, 1521, 1449, 1337, 1254, 1182, 1058. ^{1}H-NMR (DMSO-d_6): δ = 1.14 ppm (t, ^3J = 6.9 Hz, 6 H, CH_3), 3.64 (q, ^3J = 6.9 Hz, 4 H, CH_2), 3.86 (s, 3 H, OCH_3), 6.56 (s, 1 H, PHAt-H), 10.55 (br s, 5 H, NH). MS *m/z* (%): 240.0 [MH^+] (100).

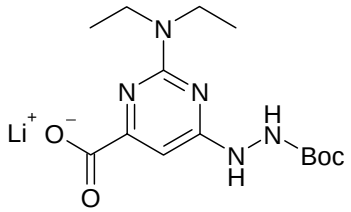

Lithium 6-(*N'*-*tert*-butoxycarbonylhydrazino)-2-diethylaminopyrimidine-4-carboxylate (14): To a solution of (**8a**) (108 mg, 0.32 mmol) in a 4:1 mixture of acetone/water (6 mL) was added $LiOH{\cdot}2H_2O$ (13.4 mg, 0.32 mmol). The reaction mixture was stirred for 6 h at rt. The solvents are removed under reduced pressure to afford **14** (100 mg, 94 %) in almost quantitative yield. The salt is used without further purification.

mp: > 185 °C (decomp). IR (KBr disk): 3298 cm^{-1}, 2974, 1725, 1589, 1520, 1420, 1362, 1247, 1164, 1077, 859, 784. ^{1}H-NMR (DMSO-d_6): δ = 1.06 ppm (t, ^3J = 6.9 Hz, 6 H, CH_3), 1.42 (s, 9 H, Boc-CH_3), 3.51 (q, ^3J = 6.9 Hz, 4 H, CH_2), 6.33 (s, 1 H, PHA-H), 8.68 (bs, 1 H, NH), 8.95 (bs, 1 H, NH). ^{13}C-NMR (DMSO-d_6): δ = 13.8 ppm (+, CH_3), 29.5 (+, Boc-CH_3), 40.6 (-, CH_2), 78.9 (C_{quat}, Boc), 90.4 (+, PHA-H), 155.7 (C_{quat}, C=O Boc), 160.4 (C_{quat}), 166.9 (C_{quat}), 167.7 (C_{quat}), 174.6 (C_{quat}, C=O carboxylate). MS *m/z* (%): 326.0 [M-H$^+$] (100).

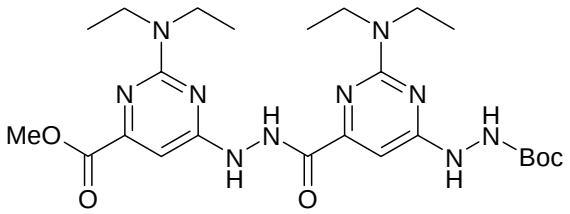

Methyl 6-{*N'*-[6-(*N'*-tert-butoxycarbonylhydrazino)-2-diethylaminopyrimidine-4-carbonyl]-hydrazino}-2-diethylamino-pyrimidine-4-carboxylate (15): Lithium salt (**14**) (198 mg, 0.35 mmol), hydrazine dihydrochloride (**13**) (109 mg, 0.35 mmol), HOAt (57 mg, 0.42 mmol), HATU (160 mg, 0.42 mmol), and Huenig´s Base (238 µL, 181 mg, 1.40 mmol) are dissolved in dichloromethane (5 mL). The solution is stirred for 30 h at rt. The solvent is removed under reduced pressure and the yellow residue purified by column chromatography (ethyl acetate/hexanes 3:1, R_f = 0.68) to afford **15** (78 mg, 40 %) as a colorless powder.

mp: 154-156 °C. IR (KBr disk): 3257 cm^{-1}, 3388, 2974, 1720, 1604, 1583, 1548, 1474, 1435, 1130, 1259, 1165, 1122. ^{1}H-NMR (DMSO-d_6): δ = 0.81-1.22 ppm (m, 12 H, 4 CH_3), 1.28-1.54 (m, 9 H, Boc-CH_3), 3.34-3.78 (m, 8 H, 4 CH_2), 3.80 (s, 3 H, OCH_3), 6.15-6.70 (m, 4 H, 2 N-H, 2 PHA-H), 8.50-10.2 (m, br s, 2 H, N-H). ^{13}C-NMR (DMSO-d_6): δ = 12.7 ppm (+, CH_3), 13.1 (+, CH_3), 28.0 (+, Boc-CH_3), 40.8 (-, CH_2), 52.2 (+, OCH_3), 85.8 (C_{quart}, Boc), 121.6 (+, PHA-H), 129.5 (+, PHA-H), 152.3 (C_{quat}, C=O Boc), 160.5 (C_{quat}, C=O), 165.4 (C_{quat}, C=O); further signals could not be labelled. UV (MeCN): λ_{max} (log ε) = 211 nm (5.483), 245 (5.519), 346 (4.933). MS *m/z* (%): 547.4 [MH^+] (100). HRMS Calcd for $C_{24}H_{38}N_{10}O_5$: 546.3027; Found: 546.3026±0.0004.

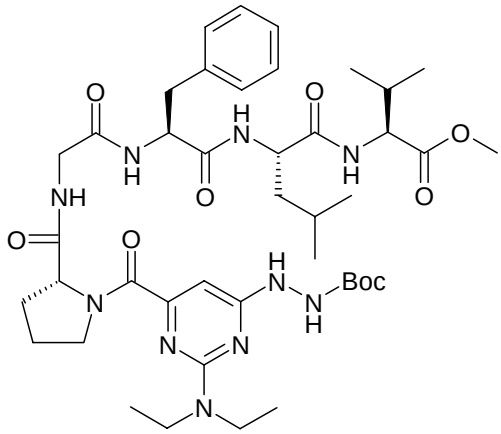

Methyl 2-(2-{2-[2-({1-[6-(*N'*-*tert*-butoxycarbonylhydrazino)-2-diethylaminopyrimidine-4-carbonyl]-pyrrolidine-2-carbonyl}amino)acetylamino]-3-phenylpropionylamino}-4-methylpentanoyl-amino)-3-methyl-butyrate (16): Compound (**14**) (75 mg, 0.23 mmol), H-D-Pro-Gly-Phe-Val-Leu-OMe (131 mg, 0.23 mmol), EDC (45 µL, 39 mg, 0.25 mmol), HOBt (34 mg, 0.25 mmol), and Huenig´s Base (75 µL, 57 mg, 0.46 mmol) were dissolved in DMF (3 mL). The reaction mixture was stirred for 18 h at rt. At 0 °C, water (5 mL) was added to precipitate **16** (99 mg, 52 %) in analytical pure form.

MP: 121 °C. IR (KBr disk): 3349cm^{-1}, 3024, 2995, 1754, 1670, 1591, 1364, 1275, 1161, 913, 898. ^{1}H-NMR (DMSO-d_6): δ = 0.74-0.95 ppm (m, 12 H; HSQC: CH_3 Leu, CH_3 Val), 1.04-1.18 (m, 6 H; HSQC: CH_3 PHA), 1.34-1.45 (m, 9 H; HSQC: Boc-CH_3), 1.46-1.53 (m, 1 H; COSY: CH_s Val), 1.54-1.70 (m, 2 H; COSY: CH_2 Pro), 1.75-1.85 (m, 2 H; COSY CH_2 Pro), 1.86-2.01 (m, 2 H; COSY: CH_2 Leu), 2.02-2.16 (m, 1 H; COSY: CH_s Leu), 2.70-2.89 (m, 1 H; HMBC: CH_2 Phe), 2.94-3.08 (m, 1 H; HMBC:

CH_2 Phe), 3.41-3.81 (m, 11 H; COSY: $C_\delta H_2$ Pro, CH_2 PHA; HSQC: OCH_3, CH_2 Gly), 4.12-4.22 (m, 1 H; COSY: CH Pro), 4.24-4.33 (m, 1 H; COSY: CH Val), 4.38-4.47 (m, 1 H; COSY: CH Leu), 4.51-4.71 (m, 1 H; COSY: CH Phe), 5.99-6.24 (m, 1 H; HSQC: PHA-H), 7.10-7.29 (m, 5 H; HSQC: Ar-H), 7.79-7.91 (m, 1 H, NH), 7.92-8.00 (m, 1 H; NH), 8.04-8.11 (m, 1 H; NH), 8.14-8.24 (m, 1 H; NH), 8.30-8.38 (m, 1 H; NH), 8.45-8.55 (m, 1 H; NH). ^{13}C-NMR (DMSO-d_6): δ = 13.5 ppm (+; HMQC: CH_3 PHA), 18.5 (+; HMQC: CH_3 Leu), 18.7 (+; HMQC: CH_3 Leu), 19.5 (+; HMQC: CH_3 Val), 21.7 (+; HMQC: CH_3 Val), 23.2 (-; HSQC: CH_2 Pro), 24.6 (+; HSQC: CH_s Leu), 28.5 (+; HMQC: Boc-CH_3), 28.6 (+; HMQC; Boc-CH_3), 29.6 (-; HSQC: CH_2Pro), 31.1 (+; HSQC: CH_s Val), 40.2 (-; HSQC: CH_2 PHA), 40.7 (-; HSQC: CH_2 Leu), 41.8 (-; HSQC: CH_2 Pro), 42.5 (-; HSQC: CH_2 Gly), 50.7 (-; HSQC: CH_2 Phe), 52.2 (+; HSQC: OCH_3), 54.4 (+; HSQC: CH Val), 58.2 (+; HMBC: CH Phe), 60.7 (+; HSQC: CH Pro), 62.5 (+; HSQC: CH Leu), 79.4 (C_{quart}; HMBC: Boc), 116.7 (+; HSQC: PHA-H), 126.7 (+; HSQC: Ar-H), 128.5 (+; HSQC: Ar-H), 129.7 (+; HSQC: Ar-H), 138.2 (C_{quart}; HMBC: Ar), 156.8 (C_{quart}; HMBC: C=O Boc), 167.5 (C_{quart}), 168.4 (C_{quart}; HMBC: C=O Gly), 168.5 (C_{quart}; HMBC: C_{Het}-NEt_2), 169.3 (C_{quart}), 170.6 (C_{quart}; HMBC: C=O Phe), 170.7 (C_{quart}; HMBC: C=O Pro), 172.5 (C_{quart}; HMBC: C=O Leu), 172.7 (C_{quart}; HMBC: C=O Val). UV (MeOH): λ_{max} (log ε): 330 nm (6.961). MS *m/z* (%): 853.6 [MH^+] (100). HRMS Calcd for $C_{42}H_{65}N_{10}O_9^+$: 853.4936; Found: 853.4926±0.0006.

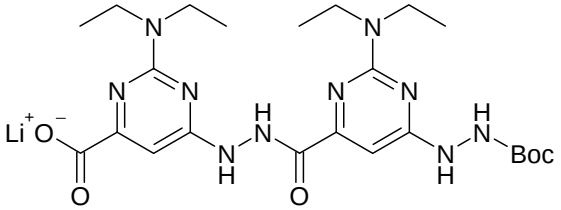

Lithium 6-{*N'*-[6-(*N'*-*tert*-butoxycarbonylhydrazino)-2-methylpyrimidine-4-carbonyl]-hydrazino}-2-methylpyrimidine-4-carboxylate (17): To a solution of (**15**) (216 mg, 0.50 mmol) in a 4:1 mixture of acetone/water (8 mL) was added LiOH·$2H_2O$ (20.6 mg, 0.50 mmol). The reaction mixture was stirred for 14 h under reflux. The solvents are removed under reduced pressure to afford **17** (202 mg, 95 %) in almost quantitative yield. The salt is used without further purification.

mp: 185 °C (decomp). IR (KBr disk): 3332 cm^{-1}, 2977, 1725, 1588, 1524, 1360, 1247, 1167. ^{1}H-NMR (DMSO-d_6): δ = 0.96-1.11 ppm (m, 12 H, CH_3), 1.44 (s, 9 H, Boc-CH_3),

3.38-3.55 (m, 8 H, CH_2), 6.39 (s, 1 H, PHA-H), 6.89 (s, 1 H, PHA-H), 8.24 (br s, 1 H, NH), 8.68 (br s, 1 H, NH), 8.87 (br s, 1 H, NH), 8.95 (br s, 1 H, NH). ^{13}C-NMR (DMSO-d_6): δ = 13.6 ppm (+, CH_3), 13.8 (+, CH_3), 29.5 (+, Boc-CH_3), 40.2 (-, CH_2), 40.6 (-, CH_2), 78.5 (C_{quat}, Boc), 90.4 (+, PHA-H), 98.7 (+, PHA-H), 155.7 (C_{quat}, C=O Boc), 160.4 (C_{quat}), 160.9 (C_{quat}), 164.7 (C_{quat}), 165.4 (C_{quat}), 166.9 (C_{quat}), 167.7 (C_{quat}), 169.6 (C_{quat}), 174.8 (C_{quat}, C=O carboxylate). MS *m/z* (%): 419.1 [M-H$^+$] (100).

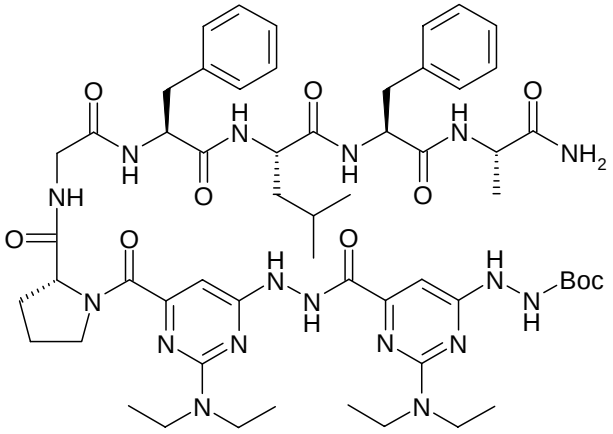

Turn structure (**18**): Compound (**17**) (43 mg, 0.10 mmol), D-Pro-Gly-Phe-Leu-Phe-Ala-NH_2.TFA (73 mg, 0.10 mmol), EDC (54 µL, 47 mg, 0.30 mmol), HOBt (41 mg, 0.30 mmol), and Huenig´s Base (65 µL, 50 mg, 0.40 mmol) were dissolved in DMF (4 mL). The reaction mixture was stirred for 15 h at rt. At 0 °C, water (5 mL) was added to precipitate **18** (87 mg, 75 %) in analytical pure form.

mp: 118 °C. IR (KBr disk): 3321 cm^{-1}, 2961, 2297, 1728, 1662, 1576, 1531, 1456, 1373, 1272, 1161, 1125, 1074, 779, 703. ^{1}H-NMR (DMSO-d_6, 290 K): δ = 0.61-0.64 ppm (m, 3 H; COSY: CH_3 Leu), 0.72-0.76 (m, 3 H; COSY: CH_3 Leu), 0.90-1.14 (m, 18 H; COSY: CH_3 PHA), 1.21 (d, ^{3}J = 7.05 Hz, 3 H; COSY: CH_3 Ala), 1.25-1.33 (m, 3 H; COSY: CH_2 Leu, CH_s Leu), 1.35-1.44 (m, 13 H; HMBC: Boc-CH_3; COSY: 2xCH_2 Pro), 1.76-1.87 (m, 1 H; COSY: CH_2 Pro), 2.06-2.13 (m, 1 H; COSY: CH_2 Pro), 2.75-2.85 (m, 1 H; NOESY: CH_2 Phe), 2.89-2.98 (m, 1 H; NOESY: CH_2 Phe), 3.02-3.10 (m, 2 H; NOESY: CH_2 Phe), 3.27-3.68 (m, 8 H; COSY: CH_2 PHA), 3.70-3.83 (m, 2 H; COSY: CH_2 Gly), 4.06-4.20 (m, 2 H; COSY: CH Leu, CH Ala), 4.35-4.55 (m, 3 H; COSY: CH Pro; NOESY: CH Phe, CH Phe), 6.29 (s, 1 H: HMBC: PHA-H), 6.99-7.37 (m, 13 H; HMBC: Ar-H, PHA-NH, Ala-NH_2), 7.70 (d, ^{3}J = 7.8 Hz, 1 H; COSY: NH Phe), 7.74-7.82 (m, 1 H; COSY: NH Ala), 7.85 (d, ^{3}J = 7.4 Hz, 1 H; NOESY: PHA-

NH), 7.88-7.96 (m, 1 H; COSY: NH Phe), 7.97-8.00 (m, 1 H; COSY: NH Leu), 8.14-8.17 (m, 1 H; NOESY: PHA-NH), 8.93 (bs, 1 H; NOESY: PHA-NHN*H*), 10.09 (s, 1 H; NOESY: PHA-NHN*H*). ^{13}C-NMR (DMSO-d_6): δ = 15.7 ppm (+; HMQC: CH_3 Ala) 17.4 (+; HMQC: CH_3 Leu), 18.9 (+; HMQC: CH_3 Leu), 22.0 (+; HMQC: CH_3 PHA), 24.0 (-; HMQC: CH_2 Pro), 27.8 (-; HMQC: CH_2 Pro), 29.8 (+; HMBC: CH_s Leu), 31.2 (+; HMQC: Boc-CH_3), 33.7 (-; HMQC: CH_2 Pro), 36.7 (-; HMQC: CH_2 Phe), 37.4 (-; HMQC: CH_2 Phe), 39.4 (-; HMBC: CH_2 Leu), 47.4 (-; HMQC: CH_2 Gly), 50.1 (+; HMQC: CH Pro), 51.3 (-; HMQC: CH_2 PHA) 53.5 (+; HMQC: CH Phe), 57.4 (+; HMBC: CH Leu), 57.7 (+; HMQC: CH Ala), 60.3 (+; HMQC: CH Phe), 79.7 (C_{quat}; HMBC: Boc), 126.0 (+; HMBC: Ar-H), 127.7 (+; HMBC: Ar-H), 128.1 (+; HMBC: Ar-H), 129.1 (+; HMBC: Ar-H), 130.7 (+; HMBC: Ar-H), 137.3 (C_{quat}; HMBC: Ar), 137.5 (C_{quat}; HMBC: Ar). Further signals are not detectable. UV (MeOH): λ_{max} (log ε) = 245 nm (3.275), 346 (1.730). UV (MeOH): λ_{max} (lg ε): 245 nm (3.275), 346 nm (1.730). MS *m/z* (%): 1186.8 [M+Na$^+$] (30), 1164.7 [MH$^+$] (80), 583.1 [M+2H$^+$] (100). HRMS Calcd for $C_{57}H_{82}N_{17}O_{10}^+$: 1164.6431; Found: 1164.6436±0.0005.

1.5. References and Notes

[1] S. Maitra and J. S. Nowick, *"The Amide Linkage: Structural Significance in Chemistry, Biochemistry and Material Science"* ed. by A. Greenberg, C. M. Brenemann, and J. F. Liebman, John Wiley & Sons, New York, **2000**, Chapter 15.

[2] C. Petosa, R. J. Collier, K. R. Klimpel, S. H. Leppla, and R. C. Liddington, *Nature* **1997**, *385*, 833.

[3] D. P. Fairlie, M. L. West, and A. K., Wong, *Curr. Med. Chem.* **1998**, *5*, 29.

[4] For reviews, see: A. Gianni and T. Kolter, *Angew. Chem.* **1993**, *105*, 1303; *Angew. Chem. Int. Ed. Engl.* **1993**, *32*, 1244; R. A. Wiley, and D. H. Rich, *Med. Res. Rev.* **1993**, *13*, 327.

[5] L. Regan and W. F. DeGrado, *Science* **1988**, *241*, 976; J. J. Osterhout, T. Handel Jr., G. Na, A. Toumadje, R. C. Long, P. J. Connolly, J. C. Hoch, W. C. Johnson, D. Live Jr., and W. F. DeGrado, *J. Am. Chem. Soc.* **1992**, *114*, 331.

[6] J. S. Nowick, N. A. Powell, E. J. Martinez, E. M. Smith, and G. J. Noronha, *J. Org. Chem.* **1992**, *57*, 3763; J. S. Nowick, M. Abdi, K. A. Bellamo, J. A. Love, E. J. Martinez, G. Noronha, E. M. Smith, and J. W. Ziller, *J. Am. Chem. Soc.* **1995**, *117*, 89; J. S. Nowick, S. Mahrus, E. M. Smith, and J. W. Ziller, *J. Am. Chem. Soc.* **1996**, *118*, 1066.

[7] J. S. Nowick, D. L. Holmes, G. Mackin, G. Noronha, A. J. Shaka, and E. M. Smith, *J. Am. Chem. Soc.* **1996**, *118*, 2764

[8] Wavefunction Inc., 18401 Von Karmann Ave., Suite 370, Irvine, CA 92612; J. J. P. Stewart, *J. Comput. Chem.* **1989**, *10*, 209.

[9] H. Gershon, *J. Org. Chem.* **1962**, *27*, 3507.

[10] M. Yukawa, T. Niiya, Y. Goto, T. Sakamoto, H. Yoshizawa, A. Watanabe, and H. Yamanaka, *Chem. Pharm. Bull.* **1989**, *37*, 2892.

[11] Temperature dependent spectra show characteristic coalescence for *cis-trans* isomerisation of carbamates.

[12] L. O. Ross, L. Goodman, and B. R. Baker, *J. Org. Chem.* **1960**, *25*, 1950.

[13] Several conditions to form the amide bond have been tried, but the yield of the coupling reaction could not be improved.

[14] H. J. Schneider, R. Kramer, S. Simova, and U. Schneider, *J. Am . chem. Soc.*, 1988, **110**, 6442; C. S. Wilcox, *"Frontiers in Suplramolecular Chemistry and Photochemistry"* ed. by H. J. Schneider and H. Duerr, VCH, Weinheim, **1991**.

[15] P. Job, *Comput. Rend.* **1925**, *180*, 928; M. T. Blanda, J. H. Horner, and M. Newcomb, *J. Org. Chem.* **1989**, 54, 4626.

[16] G. N. Ramachandran and V. Sasisekharan, *Adv. Protein Chem.* **1968**, *23*, 332.

[17] F. A. Syud, H. E. Stanger, and S. H. Gellman, *J. Am. Chem. Soc.* **2001**, *123*, 8667; J. D. Fisk, D. R. Powell, and S. H. Gellman, *J. Am. Chem. Soc.* **2000**, *122*, 5443; T. S. Haque, J. C. Little, and S. H. Gellman, *J. Am. Chem. Soc.* **1996**, *118*, 6975.

[18] Additional NOE contacts between the PHA unit and the peptide strand are expected, but not observed due to broad NH signals of the protons of the hydrazine. Resonances of NH protons of **16** appear shifted downfield of the analogous protons of the controls Boc-D-Pro-Gly-Phe-Val-Leu-OMe and **8a**. The analysis of the NH-$C_{\alpha}H$ coupling constants is not possible due to signal overlap.

2. Substituted Pyrimidine Hydrazine Acid (PHA) Oligoamides and their Binding Affinity to Peptides and Proteins

2.1. Introduction

Although peptides play an essential role in wide-ranging biological processes their use as biological probes and therapeutic agents has been complicated by poor receptor selectivity, poor water solubility, low binding affinities, or unfavorable absorption properties.[1] The design of high affinity and constrained peptidomimetics has therefore been studied intensively in the fields of medicinal chemistry and molecular recognition. The synthesis of small artificial receptors that mimic the interactions of ligands with binding sites in proteins has been an ongoing goal in recent research.[2] We recently reported the synthesis and properties of a luminescent benzo crown ether with a pendant copper imidodiacetic acid complex, which coordinates with high affinity to His.[3]

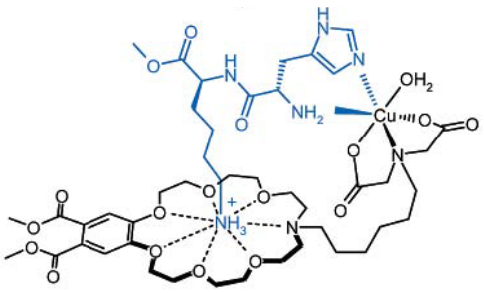

Figure 1: Proposed mode of binding of a luminescent crown ether and H-Lys-HisOMe

Sequence specific synthetic peptide receptors are model systems for biologically relevant peptide-protein interactions and may find applications in the area of biosensors, therapeutics, and catalysis.[4]

Substituted pyrimidine hydrazine acids (PHA) are peptidomimetics, which were recently reported.[5] Their geometry of hydrogen bond acceptor and donor sites make them suitable for complementary interaction with peptide β-sheets.[6]

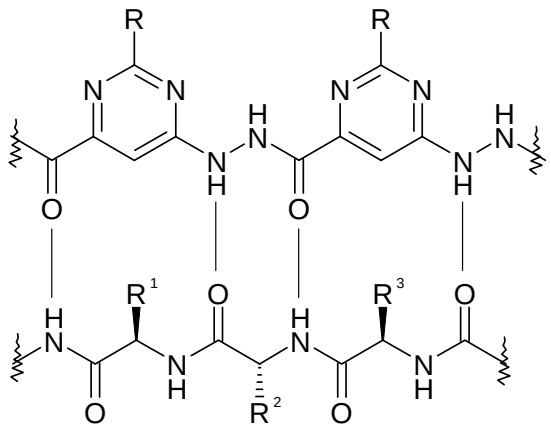

Figure 2: General binding motif of substituted PHA to peptides β-sheets

Binding affinities between oligoamides and small peptides were measured by ^{1}H-NMR and fluorescence titration in chloroform. Assuming a 1:1 stoichiometry affinity constants of 10^{3} M^{-1} were derived from the titration data. Unfortunately, no indicative data about the binding motif geometry could be obtained. The spectroscopic properties of the synthesized PHA receptors are interesting for analytical applications. After excitation at 330 nm emission around 420 nm occurs, depending on the polarity of the solvent. An important method used in biological applications to probe interactions is the Forster type fluorescence resonance energy transfer (FRET).[7] This approach implies that the investigated samples carry two fluorophores, one acting as an acceptor (A) and the other one as donor (D). When a long-range energy transfer occurs ($D^{*} \rightarrow A$), one can evaluate the energy transfer efficiency depending on the interprobe distance. This tool has been used previously to investigate the conformations of amyloid aggregations,[8] determining the structural features of ordered peptides in solution,[9] and visualizing the binding process of a metal-complex to a Trp residue.[10] The natural amino acids Phe, Tyr, and Trp show emission around 285 (excitation at 255 nm) 305 (270), and 350 nm (280). If the binding of PHA receptors occurs in proximity to a Trp residue, a FRET signal should be observed.

2.2. Synthesis of Highly Water Soluble PHA Receptors

The previously synthesized PHA receptors have poor water solubility and dimerisation using standard peptide coupling conditions gives low coupling yields prohibiting the preparation of extended structures. Therefore, a new generation of PHA was prepared bearing ethylene glycol chains to increase water solubility. According to a literature known procedure, bis-[2-(2-methoxy-ethoxy)-ethyl]-amine **4** was synthesized in three steps and 80 % overall yield.[11] 2-(2-Methoxy-ethoxy)-ethanol is tosylated first, treated with benzylamine, and finally deprotected with Pd/C and H_2 to give the desired amine **4**.

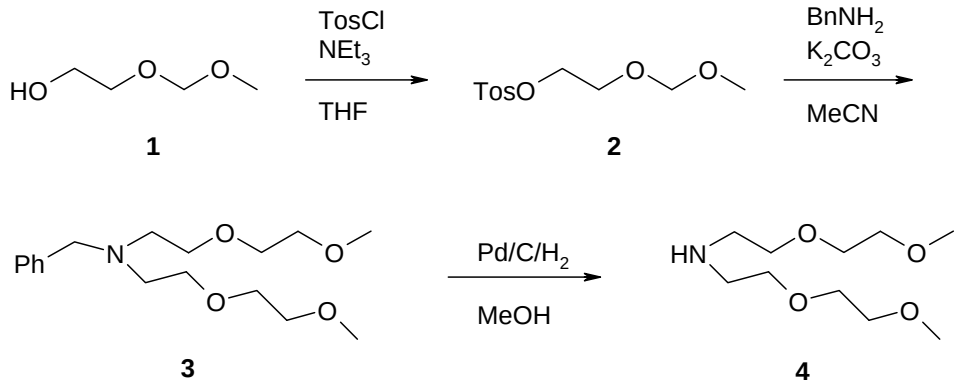

Figure 3: Synthesis of bis-[2-(2-methoxy-ethoxy)-ethyl]-amine **4**

Amine **4** was used for the substitution of the bromine atom of compound **5** to yield the water soluble compound **6** in high yields.

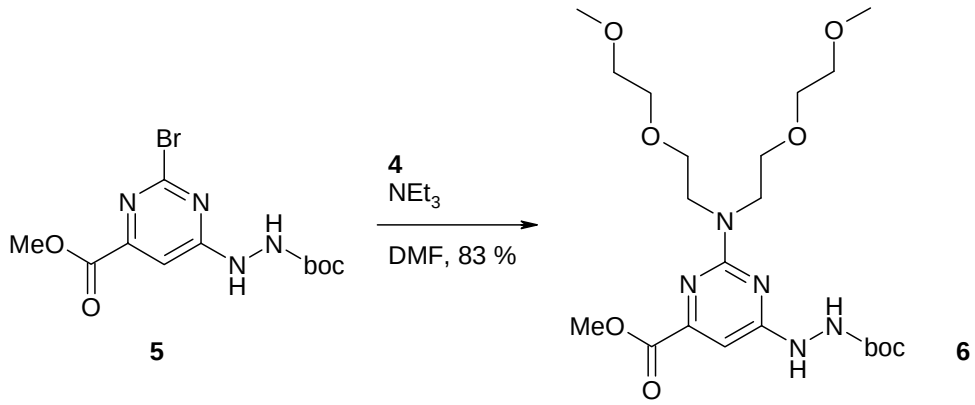

Figure 4: Synthesis of the hydrophilic PHA receptor **6**

The extension of water soluble PHA receptor strands was possible by regioselective bromine substitution reaction. PHA **6** was converted quantitatively into the corresponding hydrazide **7**. This hydrazide is used as a nucleophile substituting a bromine atome of **8** regioselective in 4-position. The subsequent substitution of the bromine in 2-position with amine **6** yields PHA receptor **10,** which is highly water soluble.

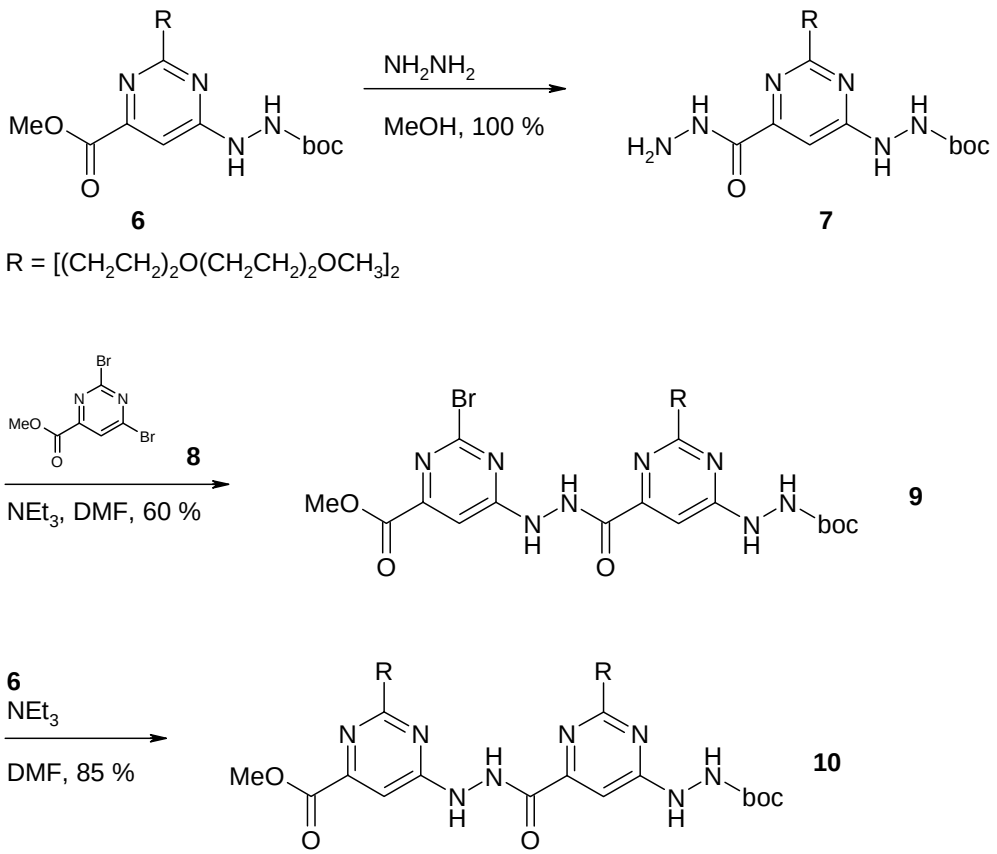

Figure 5: Synthesis of the PHA receptor **10**

Starting from **6**, compound **10** was synthesized in three steps and 51 % overall yield. This method can be used for the synthesis of the PHA trimer (**11**) and PHA tetramer (**12**). Compound **16** is converted in the corresponding hydrazide with hydrazine hydrate first, alkylated with heterocycle **8**, and finally treated with amine **6** yielding **11** in overall 44 %. Repeating these three steps starting from the trimer **11** leads to the tetramer **12** in 9 % overall yield.

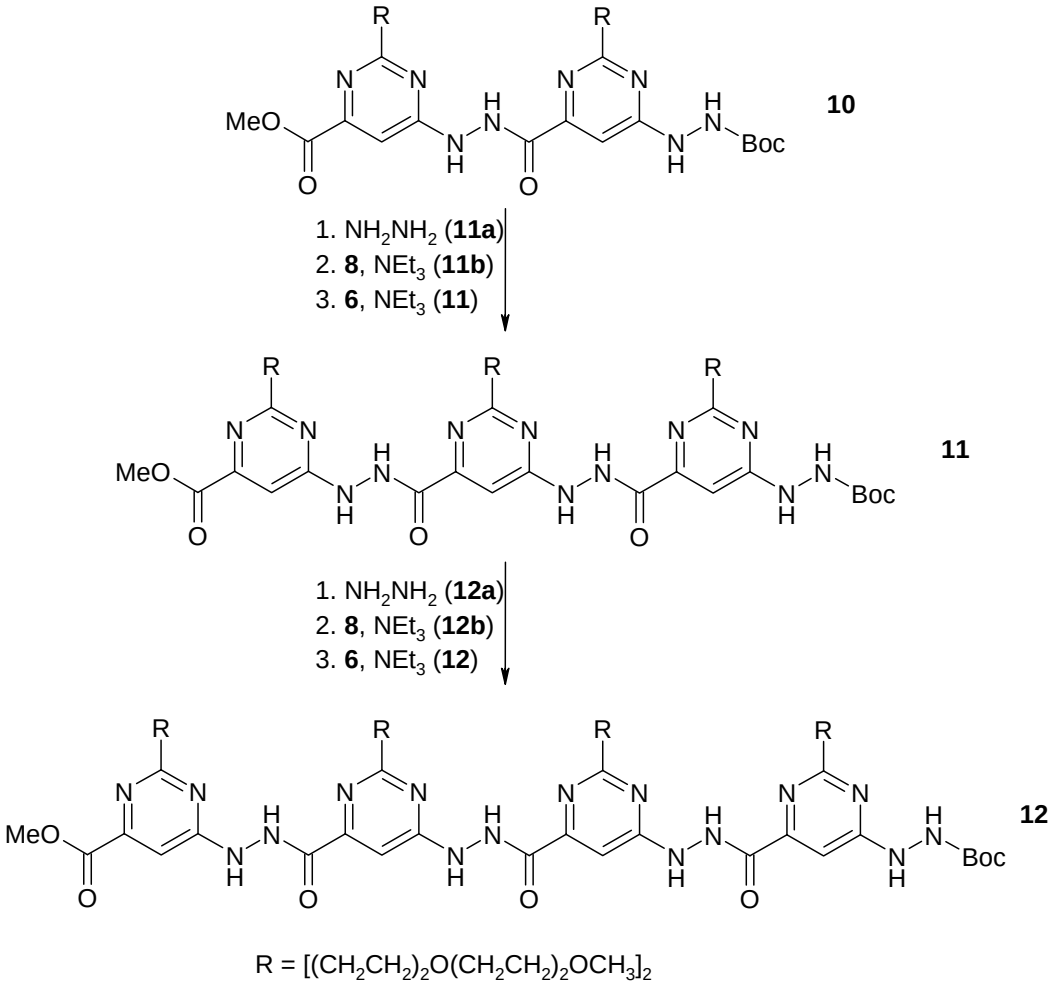

Figure 6: Synthesis of highly water soluble PHA receptors **11** and **12**

2.3. Spectroscopic Investigation of the Substituted PHA Receptors

The emission quantum yields of the PHAs were measured in different solvents with chinine bisulfate as reference. The effect of solvent on emission is similar for all compounds showing decreasing quantum yields with higher polarity. Electron donating groups in position 2, such as secondary (**17**) and tertiary amines (**13**, **15**, **19**) increase the emission quantum yield. Acceptors, such as chlorine (**18**) and bromine (**5**) decrease the emission quantum yield. Table 1 summarizes the results.

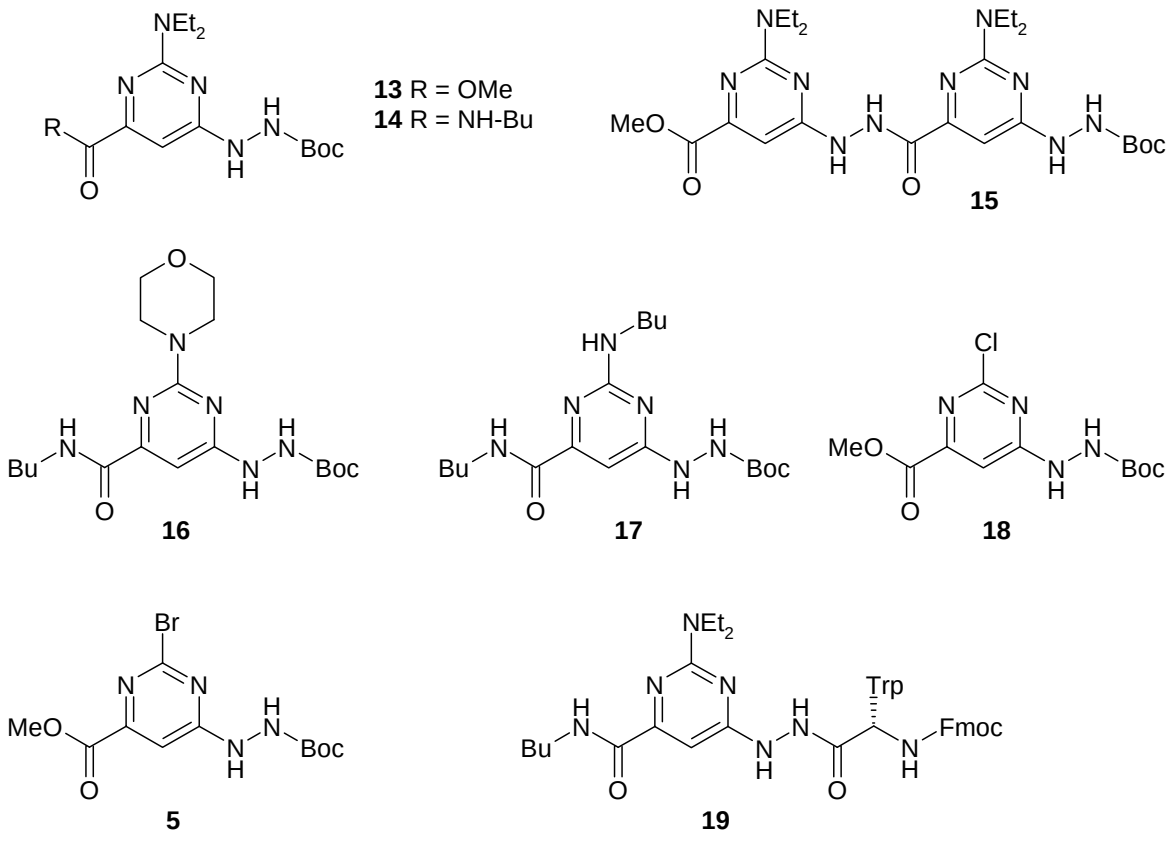

Figure 7: Investigated PHA compounds

Entry	$CHCl_3$	MeCN	MeOH
5	1.0		
13	10.0	2.1	
15	8.1	2.1	0.9
16	6.6	5.2	2.0
17	2.8	2.8	2.3
18	1.0		
19	20.7		

Table 1: Relative quantum yields of PHAs in %. Chinine bisulfate was used as standard; concentration: $4 \cdot 10^{-5}$ M

Compound **19** shows the highest quantum yield due to the aromatic Trp side chain, which acts as an antenna chromophore (*vide infra*). Additional PHA units do not increase the quantum yield of the system. The dimeric PHA receptor **15** shows a quantum yield of 8 % in $CHCl_3$, which is similar to the monomeric molecule **13** with 10 %.

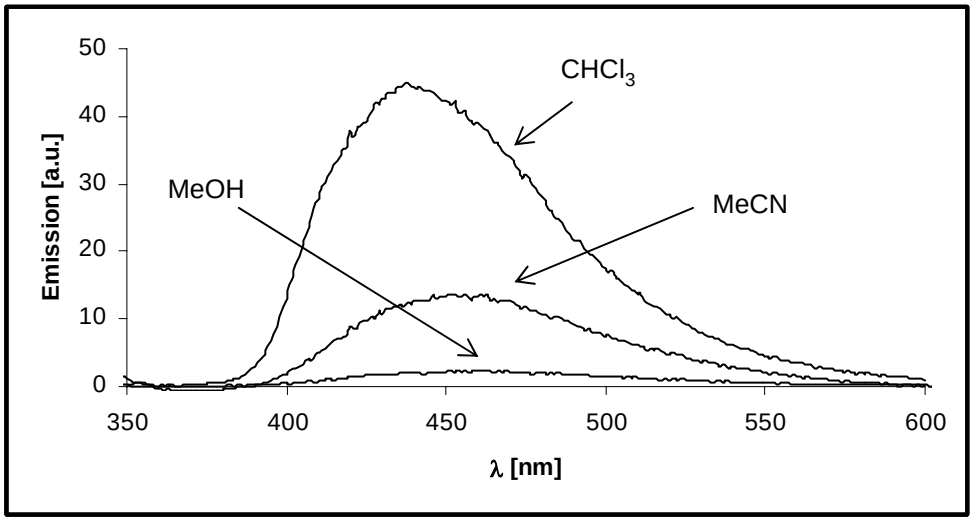

Figure 8: Emission spectra of substituted PHA **13** (R = NEt_2) in a 12 mM solution of different solvents (excitation at 330 nm)

Solvent polarity effects, beside emission intensity, effect the maximum emission wavelength. The substituted PHA **13** exhibits an emission maximum at 437±1 nm in $CHCl_3$, which gradually red-shifts with increasing solvent polarity. The emission

intensity decreases in the presence of water in MeCN solution. Similar results are obtained in the case of the water soluble PHA receptor **11**. The emission intensity is decreased with an increased polarity of the solvent and is red shifted.

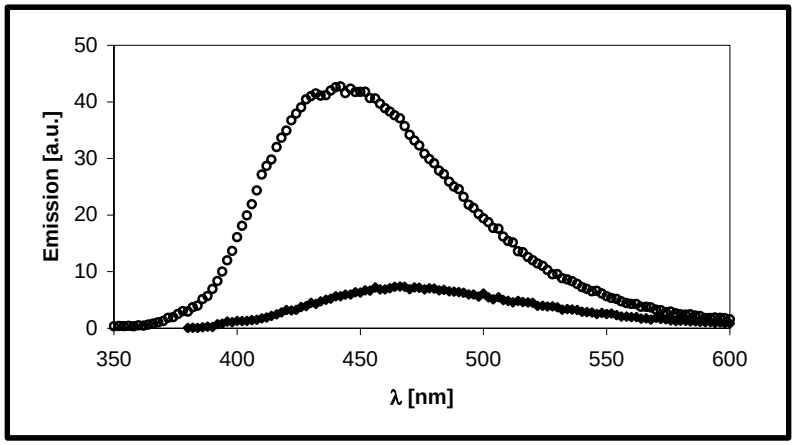

Figure 9: Emission spectra of substituted PHA **11** in a $1 \cdot 10^{-5}$ M solution of $CHCl_3$ (circle) and H_2O (dotted)

The PHA chromophore can be sensitized by Trp. Excitation of a mixture of Fmoc-Trp(Boc)-OH (1.21 mM) and **14** (1.54 mM, 0 to 0.15 equivalents) in MeCN at wavelengths of 280 nm results in a emission of the PHA around 320 nm. The emission of Fmoc-Trp(Boc)-OH at 320 nm is quenched in the presence of PHA receptor **81** resulting from a FRET process.

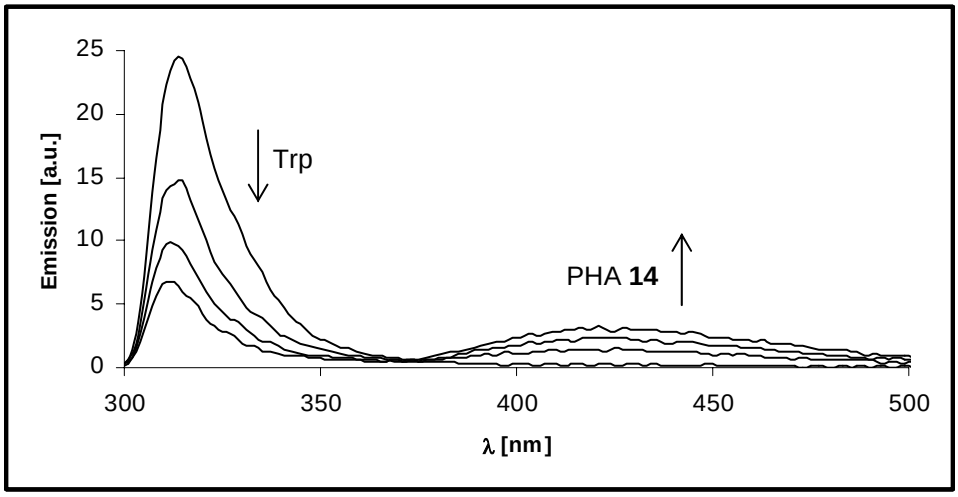

Figure 10: FRET experiment with a 1.21 mM solution of Fmoc-Trp(Boc)-OH and **14** (1.54 mM, 0 to 0.15 equivalents) in MeCN

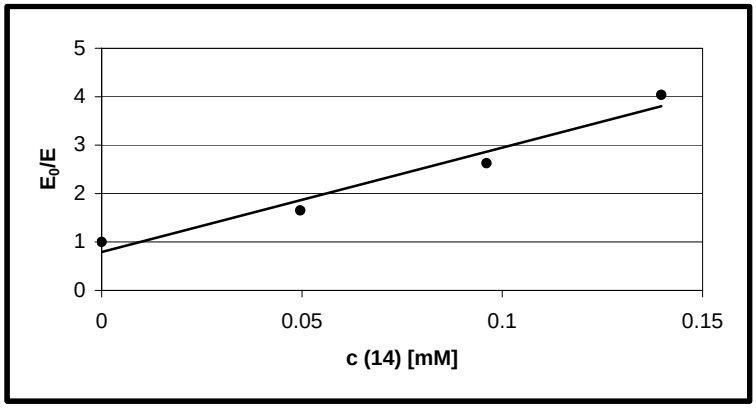

Figure 11: Stern-Volmer plot of a 1.21 mM solution of Fmoc-Trp(Boc)-OH and **14** (1.54 mM, 0 to 0.15 equivalents) in MeCN

PHA **14** reveals as a compound quenching the emission of Trp rather strong. A quenching constant of $21.5 \cdot 10^3$ L/mol can be determined from the slope of the corresponding Stern-Volmer plot of a mixture of Fmoc-Trp(Boc)-OH and **14** (1.54 mM, 0 to 0.15 equivalents) in MeCN (figure 11).

2.4. Binding Affinities of PHA Receptors to Tetradecapeptide Somatostatin in Different solvents

For medicinal and biological applications the binding effectiveness of artificial receptors on biological active compounds is of interest. Therefore, the binding of PHA receptors to the tetradecapeptide somatostatin (SRIF)[12] was investigated. The peptide is a potent regulator of multiple biological functions. In clinical studies this substance was shown to suppress the release of growth hormone (GH) secretion from the anterior pituitary.[13] It inhibits the secretion of glucagon and insulin[14] as well as gastrin.[15] For our experiments we used commercial available ampoules of Curamed® containing SRIF-x-acetate. The amino acid sequence and the secondary structure of SRIF are shown below.

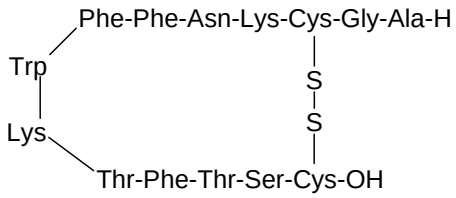

Figure 12: Secondary structure and amino acid sequence of SRIF

Structure-activity-relations have shown that amino acid residues Phe7, Trp8, Lys9, and Thr10, which compromise a β-turn, are necessary for biological activity, with residues Trp8 and Lys9 being crucial.[16] Selective interactions between the Trp8 and a synthetic receptor might influence its activity. The titration to determine the binding of **14** to SRIF was monitored spectroscopically. At different ratios of both compounds, the sample is excited at 281 nm and the quenching of the Trp emission is recorded. In addition at each titration point, the PHA moiety is excited at 320 nm to monitor its spectroscopic change upon peptide binding. Figure 3 summarizes the titration results.

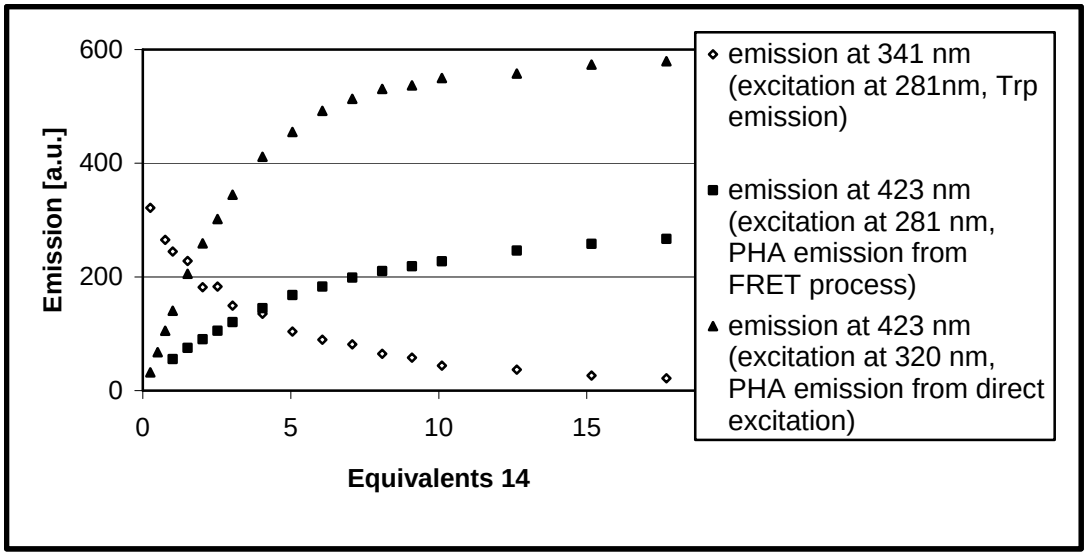

Figure 13: Fluorescence titration of a $7.4 \cdot 10^{-5}$ M solution of SRIF in MeCN with PHA receptor **14**

The fluorescence titration of SRIF with PHA receptor **14** in MeCN shows an increase of emission intensity of **14** with an increase of the receptor concentration if either excited at either 281 nm or 320 nm. Saturation is observed in the presence of approximately 7 equivalents. Simultaneously the emission (excitation at 281 nm) is quenched with increasing amounts of PHA added, reaching saturation after the addition of 8 equivalents. of PHA. This indicates clearly an intramolecular FRET process between the peptides Trp and the binding PHA compound.[17]

The calculation of a binding affinity constant requires the assumption of a specific stoichiometry. In the following, binding affinity constants were calculated by non-linear fitting of the emission intensity of Trp8 and **14**.[18] Assuming a 1:1 binding motif, an apparent affinity constant of $3.4 \cdot 10^3 \pm 0.2$ L/mol is derived from the Trp quenching curve. As SRIF contains only one Trp, the observed FRET requires donor and acceptor in close proximity (less than 10 Å),[19] and the affinity of the PHA is moderate, the 1:1 motif is likely and its assumption is justified. Job plot[20] contribute the expected 1:1 stoichiometry.

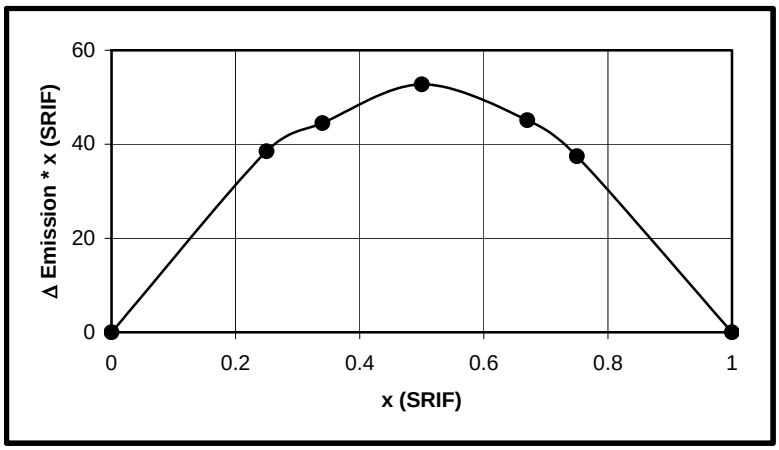

Figure 14: Job plot of SRIF and **14** (c = $1.5 \cdot 10^{-4}$ mol/L)

Next, the PHA-SRIF binding process was studied in buffered water using compounds **10** and **11**, which are soluble under physiological conditions. A 0.01 M phosphate buffer (PBS, pH 7.2) was used as solvent. The fluorescence titration of **10** and SRIF is shown in the next figure 15. Trp8 is selectively excited at 280 nm.

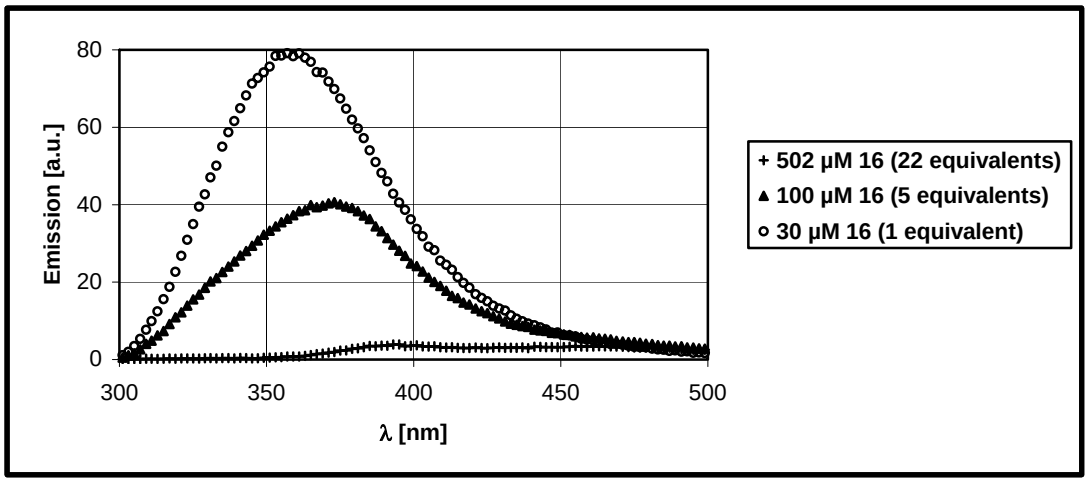

Figure 15: Fluorescence titration of a $2.3 \cdot 10^{-5}$ M solution of SRIF in 0.01 M PBS with PHA receptor **10** (excitation at 280 nm)

The wide range of emission maxima of Trp residues in proteins is attributed to differences in the microenvironment and its effect on the excited indole ring of Trp. For example, a fluorescence red shift occurs as the microenvironment surrounding Trp residues changes from nonpolar to polar.[21] At low concentrations of **10**, SRIF exhibits an emission maximum at 358 ± 1 nm. It gradually red shifts with increasing

concentration of **10**, and finally levels off at 393 ± 1 nm. This indicates the Trp8 exposure to the receptor and its hydrophilic ethylene glycol chains. The emission curve of Trp8 is overlapping with the PHA emission around 451 nm. The increase of the emission intensity of **10** at 452 nm is shown by the excitation at 392 nm.

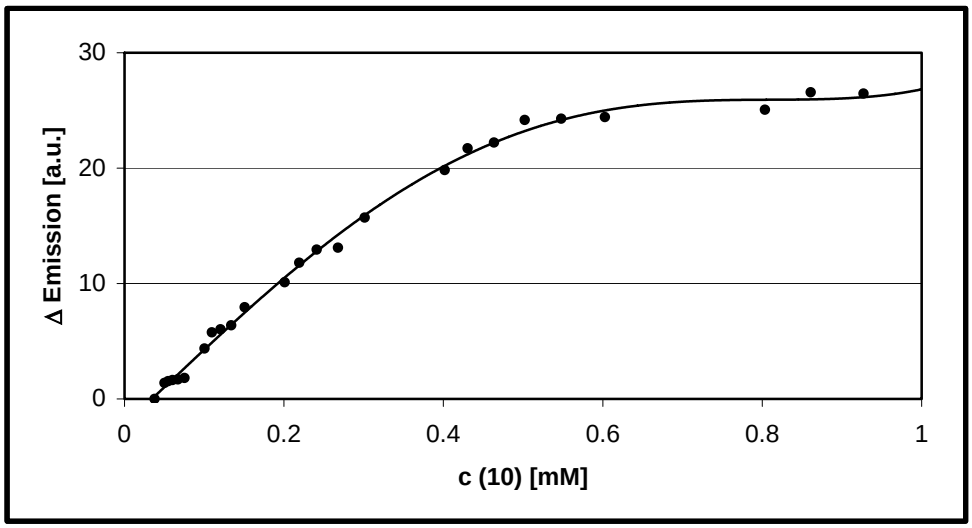

Figure 16: Fluorescence titration of a $2.3 \cdot 10^{-5}$ M solution of SRIF in 0.01 M PBS with PHA receptor **10** (excitation at 392 nm)

The relative enhancement of the emission intensity is lower than in the case of PHA receptor **14** and the binding experiment in MeCN. The phosphate buffer solution suppresses the emission due to a possible protonation of **10**.

Similar results are obtained for the binding affinity of the trimer **11** to SRIF under the same conditions. The emission maximum of SRIF is red-shifted with higher concentrations of **11** (358→395 nm, data not shown). The quenching of Trp8 with increasing amounts of PHA receptors **10** and **11** together with their initial slopes is shown in figure 15. The initial slope of **11** ($2.62 \cdot 10^6$ M^{-1}) is more than twice the one of **10** ($1.22 \cdot 10^6$ M^{-1}). This indicates a higher affinity constant due the more extended geometry and additional hydrogen bonds of **11**.[22]

The emission changes of PHA in the presence of the peptide are similar to the effects in MeCN, but less pronounced. Quenching of the Trp emission indicates an energy transfer to the PHA, but emission of this chromophore is not effective in the protic solvent (see above). Direct excitation of PHA (at 392 nm) leads to a small, but detectable emission in the presence of the peptide. Binding to the peptide may lead to

small polarity changes in the PHA environment becoming less polar and increasing the emission intensity.

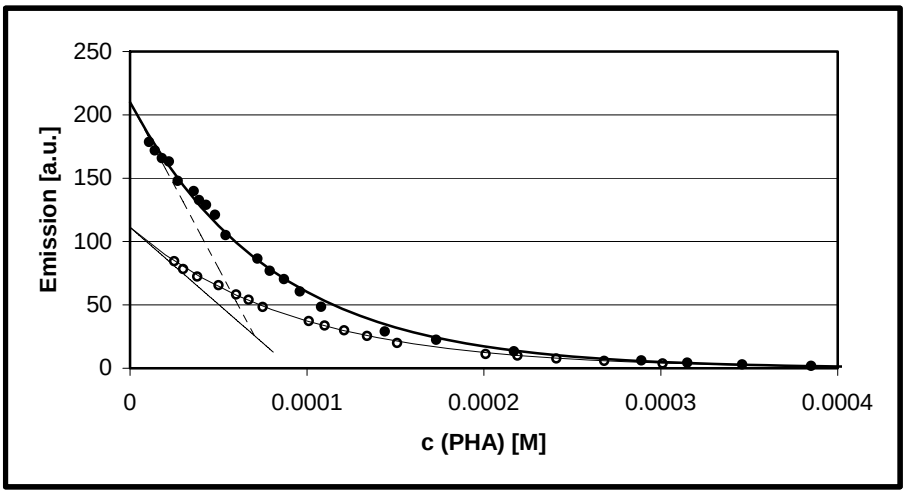

Figure 17: Fluorescence titration of a $2.3 \cdot 10^{-5}$ M solution of SRIF in 0.1 M PBS with PHA receptor **10** (circle) and **11** (dotted), initial slopes are dashed

2.5. Binding Affinities of Highly Water Soluble PHA Receptors to Concanavalin A under Physiological Conditions

Next, the investigation were extended to the interaction of PHA receptors **10** and **11** to a larger protein bearing several β-sheets and Trp. Concanavalin A (ConA) is a lectin isolated from jack beans.[23] It is the best known member of legume lectins because of its numerous biological applications as probing normal and tumor cell membrane structures and studying glycosylation mutants of transformed cells.[24]The three-dimensional structure of the lectin at 1.75 Å resolution has been determined by X-ray diffraction analysis,[25] and was further refined at 1.2 Å.[26] The lectin monomer (figure 18) features a 'jelly roll' fold architecture. It is made up largely of three antiparallel β-sheets: a six-stranded nearly flat 'back' sheet, a seven-stranded concave 'front' sheet and a five-stranded sheet forming a 'roof' over the two.

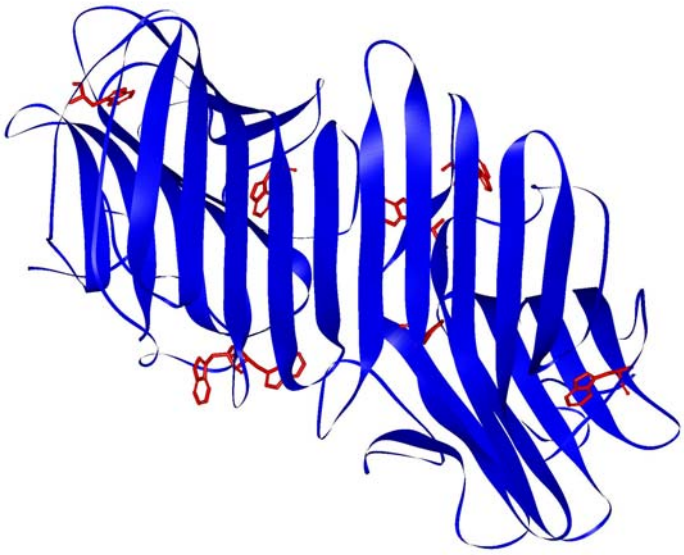

Figure 18: X-ray structure of ConA monomer displayed in flat ribbon style; sticks: Trp

The lectin dimer is termed the 'canonical dimer', which is characterized by a large 12-stranded β-sheet resulting from the antiparallel side-by-side alignment of the two six-stranded back sheets (figure 19). Two such canonical dimmers associate with the center parts of their back sheets in a perpendicular manner forming the tetramer.

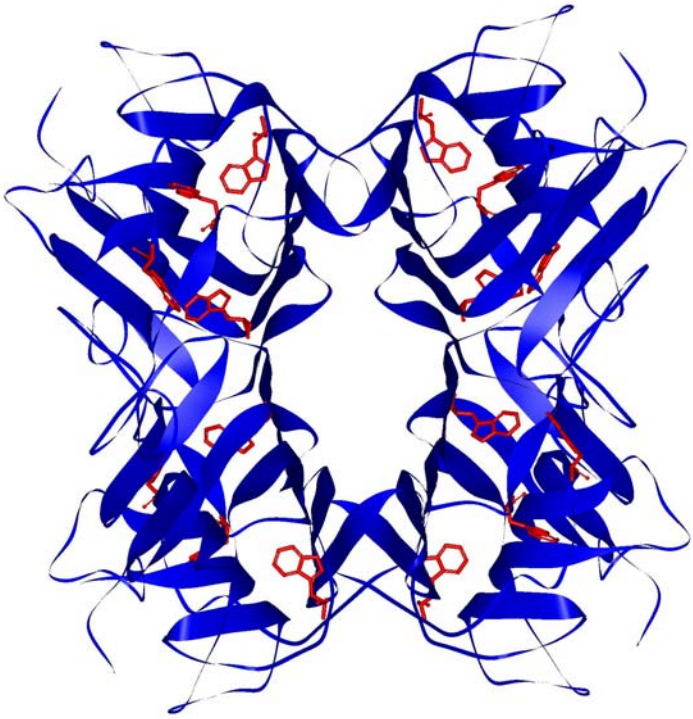

Figure 19: X-ray structure of ConA dimer displayed in flat ribbon style; sticks: Trp

Depending on the concentration of denaturating urea one can affect a specific structure of ConA.[27] The denaturation equilibrium displays a three-state mechanism involving a structured monomeric state (2.7 M urea) between native tetrameric and unfolded monomeric state (> 8 M urea). In addition, ConA was denaturated in the presence of Trypsin following a modified method of *Burger* and *Noonan*[28] to eliminate most structural elements of the peptide. Depending on the state, ConA has several extended β-sheets. With increasing concentration of urea or in the presence of Trypsin, the number of β-sheet regions is decreased leading to an unfolded peptide strand. When enzymatically digested, ConA remains with almost no distinct secondary and tertiary structure. The CD spectra indicate clearly the states of structure under different conditions.

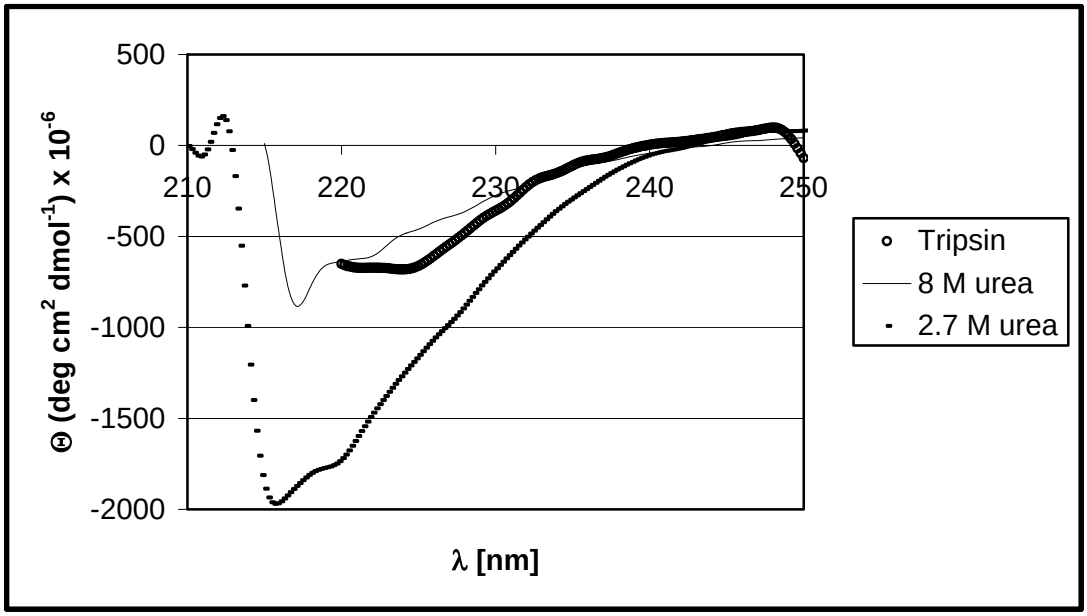

Figure 20: Far-UV CD spectra of ConA (2 µM) at 25 °C in PBS in the presence of 2.7 M urea (dotted), 8 M urea (line), and tripsin (circle)

The native tetramer (data not shown) and the dissociated monomer in 2.7 M urea show the characteristics of β-sheet structures. Both spectra are different from that in 8 M urea and from tripsinized ConA. ConA denaturated by 8 M urea may still have some extended β-sheet substructures, while these are clearly eliminated in the case of tripsinized ConA.

First, we investigated the affinity of the PHA dimer **10** to ConA in PBS. As shown in figures 19 and 20, ConA has eight Trp per monomer located both on the surface and in the core of the peptide. They can be excited at 280 nm and show emission around 340 nm in PBS. A series of titration experiments were carried out in the presence of different concentrations of urea and after tripsin digestion of ConA. Due to the extended β-sheet structures of ConA, which are potential binding sites for PHA, no clear evidence of the binding motif and the stoichiometry of PHA receptors to ConA can be derived from the titration data. Therefore, the Trp emission data were analyzed graphically and the initial slope of Trp emission quenching, which depends on the efficiency of energy transfer from Trp to PHA, correlates to the ability of the PHA compound to bind to the peptide.

The Trp emission maximum is only slightly red shifted from 332±1 to 340±1 nm. Even at high concentrations of **10** (100 µM, 50 equivalents), an emission of Trp is still

detectable. Some of the proteins Trp units are shielded inside by the peptide structure and are not accessible by PHA binding to the surface exposed β-sheet structures. Therefore, their emission is not quenched.

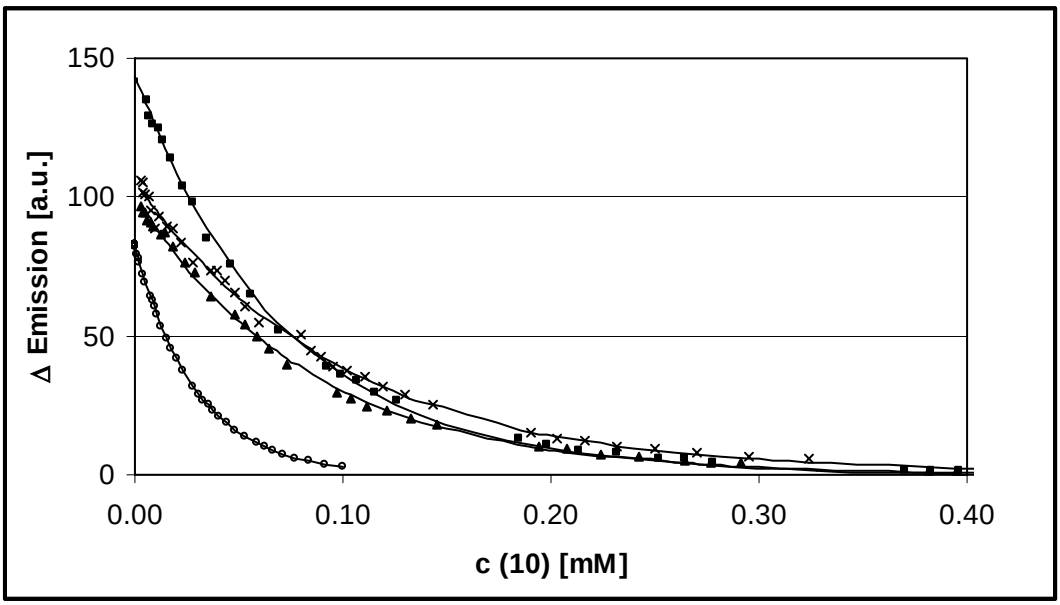

Figure 21: Fluorescence titration of a 2 µM solution of ConA in 0 M urea (circle), 2.7 M urea (square), 8 M urea (triangle), and tripsinized (cross) with **10**

Going from the native protein state to the monomeric structure and to the denaturated structures, leads to distinct differences in the PHAs efficiency to quench the Trp emission. Table 3 summarizes the initial slopes derived from the Trp titration curve and the shifts of the emission maximum.

	initial slope [$-M^{-1}/10^6$]	**shift emission max. [nm]**	**Δ shift emission max [nm]**
ConA (2 µM) native	2.81	332 → 340	8
ConA (2 µM) + 2.7 M urea	1.99	341 → 387	46
ConA (2 µM) + 8 M urea	1.16	349 → 383	34
ConA (2 µM) + tripsin	1.23	349 → 393	44
SRIF (22 µM)	1.22	359 → 403	44

Table 2: Initial slopes and red-shift of Trp emission maximum of a peptide solution in PBS with PHA receptor **10**

The ability of PHA **10** to quench the Trp emission and likewise its binding affinity to ConA depends on the secondary and tertiary structure of the peptide. ConA has extended β-sheets in its native state. In the presence of 2.7 M urea, the resulting monomeric protein offers a smaller number of suitable binding motifs which leads to a decreased binding affinity. When ConA is either denaturated with 8 M urea or treated with tripsin, the affinity is diminished by a factor of 3. Table 3 also contains the slope of the titration curve of **10** and SRIF. Similar values are obtained for the binding of **10** to SRIF and denaturated ConA. This indicates a diminished binding affinity due to unfolded or more unstructured peptide. The initial slope of Trp emission quenching in denatured and digested ConA is comparable to the value obtained with SRIF. This indicates that the higher Trp emission quenching and binding affinity of PHA for native and partly denatured ConA is an effect of the secondary and tertiary protein structure. In its unfolded and unstructured state, the affinity of PHA to the protein is comparable to a small peptide without distinct structure.

The emission maximum is red-shifted in all titrations. The shift is small for **10** and native ConA due to the shielded Trp inside the protein, which are not accessible by the PHA. A shift of 40 nm during the titration is observed for all the other experiments with small but significant differences. The emission levels off around 390 nm indicating a hydrophilic microenvironment of Trp. In contrast to native ConA, the fluorescence of Trp decreased gradually to almost negligible intensity at high concentrations of **10**.

Due to the extended binding motif of PHA trimer **11**, a higher binding affinity was expected. The Trp emission quenching was again analyzed graphically and the initial slope of the titration curves was determined as an indicator. Figure 22 shows the relative change of emission of Trp (excitation at 280 nm) as a function of PHA **11** concentration.

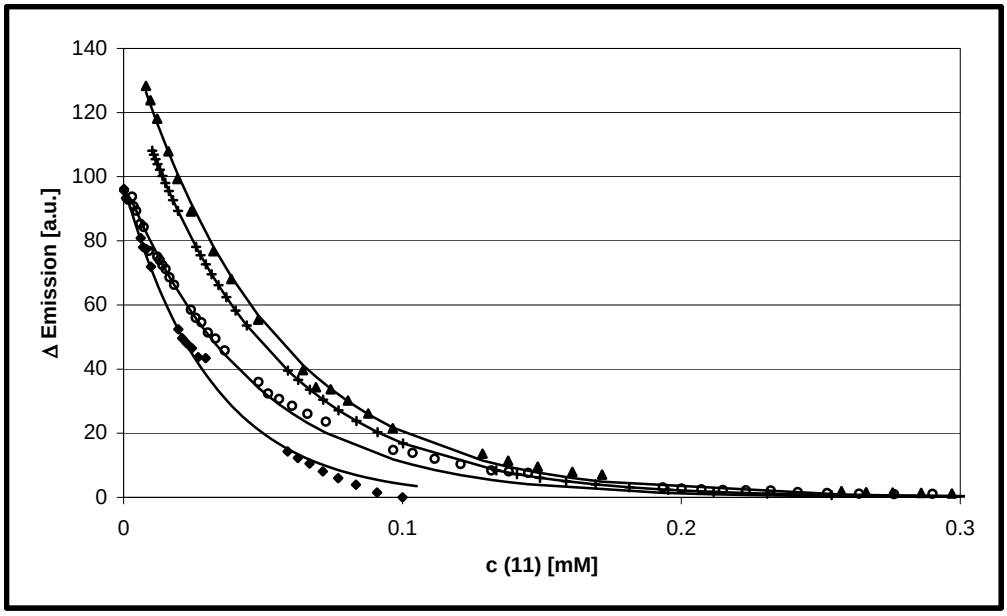

Figure 22: Fluorescence titration of a 2 µM solution of ConA in 0 M urea (diamond), 2.7 M urea (triangle), 8 M urea (circle), and tripsinized (+) with **11**

The binding affinity of **11** to ConA in the native state shows the steepest initial slope ($-3.09 \cdot 10^6$ M^{-1}) of all the binding experiments. Table 4 summarizes the results.

	initial slope [$-M^{-1}/10^6$]	**shift emission max. [nm]**	**Δ shift emission max [nm]**
ConA (2 µM) native	3.09	336 → 347	11
ConA (2 µM) + 2.7 M urea	2.95	339 → 383	44
ConA (2 µM) + 8 M urea	1.96	349 → 387	38
ConA (2 µM) + tripsin	2.76	346 → 391	45
SRIF (22 µM)	2.62	359 → 401	42

Table 3: Initial slopes and red-shift of Trp emission maximum of a peptide solution in PBS with PHA receptor **11**

The initial slope decreases with an increase of unfolded and unstructured peptide. ConA in the presence of 8 M urea shows the lowest binding affinity. The slopes for tripsinized ConA ($-2.76 \cdot 10^6$ M^{-1}) and SRIF ($-2.62 \cdot 10^6$ M^{-1}) are similar, but somewhat steeper than ConA denaturated by urea ($-1.96 \cdot 10^6$ M^{-1}), which is surprising because structural differences are expected to be small.

The red-shift of the Trp emission maxima is again small for **11** and the native ConA. A shift of 40 nm is observed in the titration in all the other experiments with small differences. The emission wavelength shift shows the increasing exposure of the Trp to the hydrophilic environment upon denaturation. While in the titration of **11** with native ConA the fluorescence of Trp is quenched only partly, an almost quantitative quenching with increasing concentration of **11** is observed with the denatured protein.

2.6. Conclusions

The emission intensity of PHA chromophores strongly depends on solvent polarity and PHA excitation is possibly by direct light absorption (at 382 nm) or a FRET process utilizing the Trp emission. PHA oligomers mimic a peptide structure in β-sheet conformation and therefore interaction with peptide β -sheet structures was expected. Previous investigations confirmed this for non polar solvents ($CDCl_3$) and small peptides. With a newly established synthetic route water-soluble PHAs became available, which were extended to di-, tri- and tetramers. Although the emission intensity of the water soluble PHAs is significantly diminished in polar solvents, they are suitable molecular sensors probing protein structure. In the presence of the Trp containing tetradecapeptide somatostatin a FRET from the peptides Trp to the bound PHA is observed. At the same time, binding to the peptide leads to an increase in PHA emission intensity if excited directly at 382 nm, most likely due to a less polar microenvironment in the proximity of the peptide. Using the protein ConA in different denaturated and even digested structural states, significant differences in the PHA receptor Trp quenching and likewise binding ability were observed. The native or only partially denaturated protein, possessing extended and surface exposed β-sheet structures, show higher PHA affinity than the completely denaturated or digested protein. The protein binding affinity of the PHA, indicated by its ability to quench the proteins Trp emission, changes with the proteins secondary and tertiary structure. Extended β-sheet structures, complementary to the PHA structure, lead to higher affinities. PHA receptors can therefore be envisaged as fluorescent molecular probes for the determination of the extent of protein β-sheet structures.

2.7. Experimental Part

General Methods:

Melting points were determined on a Tottoli micromelting point apparatus and are uncorrected. ^{1}H-NMR spectra were recorded on a Bruker Avance 300 NMR spectrometer at 300 K. Chemical shifts (δ) are reported in ppm downfield from internal TMS. Emission spectra were recorded on a Cary Eclipse spectrophotometer. Thin layer chromatographic (TLC) analyses were performed on silica gel 60 F-254 with a 0.2 mm layer thickness. Preparative chromatography columns were packed with silica gel Geduran SI 60. Mass spectra were recorded on a Finnigan MAT TSQ 7000 (ESI) and on a Finnigan MAT 95 (HRMS). Elemental analyses were carried out by the microanalytical laboratory University of Regensburg. Commercially available reagents were used as received. Organic extracts were dried over anhydrous Na_2SO_4 and concentrated *in vacuo*.

Emission Titrations:

A solution of the PHA molecule (c = 0.5 mmol/L) was added in portions by a microsyringe to a solution of a peptide (c = 2 µmol/L) and PHA (c = 0.1 mmol/L). Volume and concentration changes were taken into account for the analysis of the binding event.

Far-UV circular dichroism (CD):

Far-UV circular dichroism (CD) spectra were measured on a JASCO J-720 spectropolarimeter purged with N_2, and equipped with a constant temperature cell holder. The buffer used during measurement was PBS (pH 7.2). The spectra were measured at 25 °C in 1-mm-pathlength cell using a scan speed of 20 nm/min with a response time of 2 s, and averaged over ten scans to eliminate signal noise. The data are represented as the mean residue ellipticity [θ], which is defined as $[\theta] = 100 \cdot \theta_{obs}/(c \cdot l)$, where θ_{obs} is the observed ellipticity in degrees, l is the length of the light path in centimeters, and c is the concentration in moles of residue per liter.

Protein denaturation with urea:

The denaturation experiments in urea were carried out in 0.01 M PBS (pH 7.2) at 25 °C. For each denaturation experiment, a known amount of PBS was mixed with a fixed amount of the protein stock solution and varying amounts of the concentrated denaturant. The mixture was incubated at 25 °C for 18 h to ensure that the equilibrium was achieved.

Protein denaturation with trypsin:

11 mg ConA was dissolved in 1 ml 0.01 M PBS (pH 7.2). 40 µl of 2.5 % trypsin was added, and the solution was incubated at 37 °C for 12 h.

Synthesis of new cmpounds:

Compounds **5**, **13**, **16**, **17**, **18**, and **19** were synthesized following a literature procedure.[5] The following compounds were synthesized in a cooperation with Dr. Li during his post doc at the University of Regensburg based on preliminary studies.

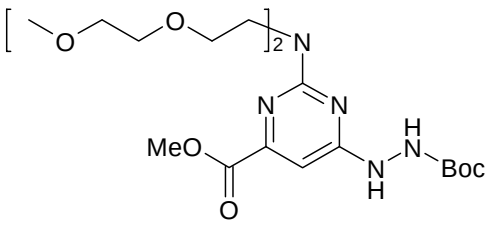

2-{Bis-[2-(2-methoxy-ethoxy)-ethyl]-amino}-6-(N'-tert-butoxycarbonyl-hydrazino)-pyrimidine-4-carboxylic acid methyl ester (6): A solution of **5** (1.4 g, 4.09 mmol), **4** (1.8 g, 8.20 mmol), and NEt_3 (621 mg, 6.15 mmol) in DMF (20 mL) was stirred at 60ºC for 12 h. After the solvent was removed in vacuum, the residue was dissolved in EtOAc. The organic phase was washed with water, brine, and dried over Na_2SO_4. Upon removal of the solvent at reduced pressure, the crude produce was purified by column chromatography (CH_2Cl_2/MeOH 1:50, $R_f = 0.3$) to afford compound **6** as a yellow oil (1.25 g, 3.27 mmol, 80 %). 300 mg of **5** were recovered.

IR ($CHCl_3$): 3300 cm^{-1}, 3012, 2933, 1734, 1590, 1520, 1251, 1216, 1099, 756, 667. ^1H NMR ($CDCl_3$): δ = 1.44 ppm (s, 9 H, Boc- CH_3), 3.35 (s, 6 H, OCH_3), 3.48-3.51 (m, 4 H, CH_2), 3.57-3.63 (m, 8 H, CH_2), 3.79 (s, 4 H, CH_2), 3.86 (s, 3 H, $COOCH_3$), 6.56 (s, 1

H, Het-H), 6.70 (s, 2 H, NH). ^{13}C NMR ($CDCl_3$): δ = 28.2 ppm, 48.0, 52.6, 59.0, 69.1, 70.2, 72.0, 81.7, 92.8, 155.8, 161.4, 166.3. UV (MeCN): λ_{max} (log ε) = 336 nm (4.647) MS (ESI, MeOH + 10mmol/l NH_4Ac): *m/z* (%) = 488.4 [MH^+] (100). Anal. Calcd. for $C_{21}H_{37}N_5O_8$: C: 51.4; H: 7.7; N: 14.4; Found: C: 51.1; H: 7.3; N: 14.2.

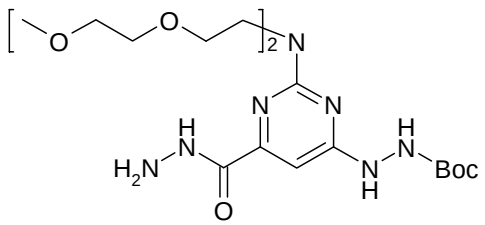

N'-(2-{Bis-[2-(2-methoxy-ethoxy)-ethyl]-amino}-6-hydrazinocarbonyl-pyrimidin-4-yl)-hydrazinecarboxylic acid tert-butyl ester (7): A solution of **6** (1.50 g, 3.07 mmol) and $NH_2NH_2{\cdot}H_2O$ (938 mg, 18.4 mmol) in methanol was refluxed for 1 h. After removal of the solvent and excess hydrazine in vacuum, the crude product **7** was isolated quantitative yields (1.49 g, 3.05 mmol) and could be used in the next step directly.

IR ($CHCl_3$): 3019 cm^{-1}, 1734, 1592, 1507, 1216, 1158, 758, 669.^{1}H NMR ($CDCl_3$): δ = 1.43 ppm (s, 9 H, Boc- CH_3), 3.34 (s, 6 H, OCH_3), 3.49-3.51 (m, 4 H, CH_2), 3.55-3.62 (m, 8 H, CH_2), 3.73-3.75 (m, 4 H, CH_2), 4.06 (s, 2 H, NH_2), 6.69 (s, 1 H, Het-H), 6.91 (s, 2 H, NH), 8.85 (s, 1 H, NH). ^{13}C NMR ($CDCl_3$): δ = 28.2 ppm, 48.4, 59.1, 69.2, 70.3, 72.0, 81.6, 90.4, 155.9, 160.4, 164.3. UV (MeCN): λ_{max} (log ε) = 328 (4.751). MS (ESI, MeOH + 10mmol/l NH_4Ac): *m/z* (%) = 488.3[MH^+] (100). Anal. Calcd. for $C_{20}H_{37}N_7O_7$: C: 49.3; H: 7.7; N: 20.1; Found: C: 48.9; H: 7.5; N: 20.1.

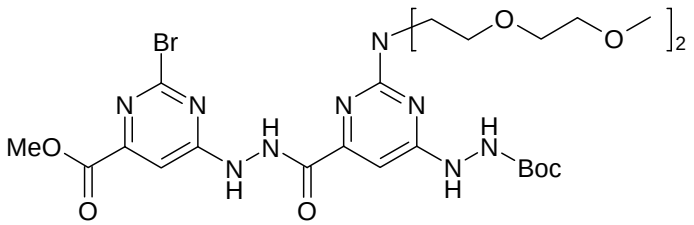

6-{N'-[2-{Bis-[2-(2-methoxy-ethoxy)-ethyl]-amino}-6-(N'-tert-butoxycarbonyl-hydrazino)-pyrimidine-4-carbonyl]-hydrazino}-2-bromo-pyrimidine-4-carboxylic acid methyl ester (9): A mixture of **7** (1.50 g, 3.07 mmol), **8** (996 mg, 3.38 mmol), and NEt_3 (372 mg, 3.68 mmol) in DMF (15 mL) was stirred at 70ºC for 14 h. After the

solvent was removed in vacuum, the residue was dissolved in EtOAc. The organic phase was washed with water, brine, and dried over sodium sulfate. Upon removal of the solvent in reduced pressure, the crude produce was purified by column chromatography (CH_2Cl_2/MeOH 1:40, $R_f = 0.25$) to afford compound **9** as a yellow oil (1.06 g, 1.69 mmol, 55 %). 150mg of **7** was recovered.

IR ($CHCl_3$): 3019 cm^{-1}, 1724, 1601, 1479, 1216, 1115, 770, 668. ^1H NMR ($CDCl_3$): $\delta = 1.43$ ppm (s, 9 H, Boc- CH_3), 3.32-3.36 (m, 6 H, OCH_3), 3.52 (m, 4 H, CH_2), 3.61-3.67 (m, 6 H, CH_2), 3.82 (s, 6 H, CH_2), 3.97 (s, 3 H, $COOCH_3$), 6.80 (s, 1 H, Het-H), 6.76 (s, 1 H, Het-H), 11.06 (s, 2 H, NH). ^{13}C NMR ($CDCl_3$): $\delta = 28.3$ ppm, 48.2, 53.6, 59.1, 61.6, 69.6, 70.2, 70.5, 72.0, 81.7, 152.5, 156.1, 158.7, 160.5, 164.4. UV (MeCN): λ_{max} (log ε) = 330 (5.163). MS (ESI, MeOH + 10mmol/l NH_4Ac): *m/z* (%) = 704.3 [MH^+] (100). Anal. Calcd. for $C_{26}H_{40}BrN_9O_9$: C: 44.5; H: 5.7; N: 17.9; Found: C: 44.2; H: 5.6; N: 18.3.

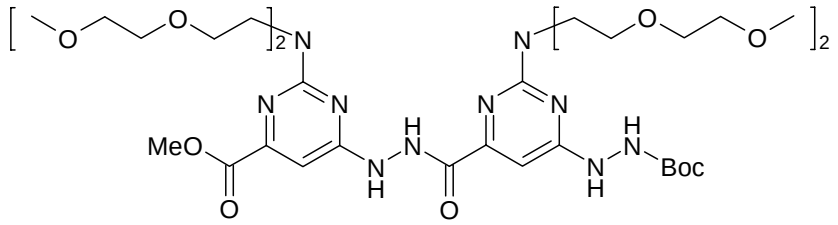

2-{Bis-[2-(2-methoxy-ethoxy)-ethyl]-amino}-6-{N'-[2-{bis-[2-(2-methoxy-ethoxy)-ethyl]-amino}-6-(N'-tert-butoxycarbonyl-hydrazino)-pyrimidine-4-carbonyl]-hydrazino}-pyrimidine-4-carboxylic acid methyl ester (10): A solution of **4** (1.00 g, 1.42 mmol), **4** (470 mg, 2.13 mmol), and NEt_3 (172 mg, 1.70 mmol) in DMF (10 mL) was stirred at 82ºC for 14 h. After the solvent was removed in vacuum, the crude product was purified by column chromatography (CH_2Cl_2/MeOH 1:35, $R_f = 0.30$) to afford compound **10** as a yellow oil (968 mg, 1.21 mmol, 85 %). 50mg of **9** was recovered.

IR ($CHCl_3$): 3288 cm^{-1}, 3018, 2892, 1734, 1576, 1521, 1249, 1216, 1099, 757, 668. ^1H NMR ($CDCl_3$): $\delta = 1.42$ ppm (s, 9 H, Boc- CH_3), 3.32-3.35 (m, 12 H, OCH_3), 3.46-3.48 (m, 10 H, CH_2), 3.56-3.63 (m, 14 H, CH_2), 3.77-3.79 (m, 8 H, CH_2), 3.83 (s, 3 H, $COOCH_3$), 6.62 (s, 1 H, Het-H), 6.74 (s, 1 H, Het-H), 7.50 (s, 2 H, NH), 9.68 (s, 1 H, NH). ^{13}C NMR ($CDCl_3$): $\delta = 28.2$ ppm, 48.1, 48.4, 52.6, 59.0, 69.1, 69.2, 70.2, 71.9,

81.5, 93.4, 155.5, 156.0, 160.5, 161.4, 166.0. UV (MeCN): λ_{max} (log ε) = 338 (5.204). MS (ESI, MeOH + 10mmol/l NH_4Ac): *m/z* (%) = 843.6 [MH^+] (100), 422.3 [$M+2H^+$] (31), 394.3 [$M+2H^+-C_4H_8$] (10).

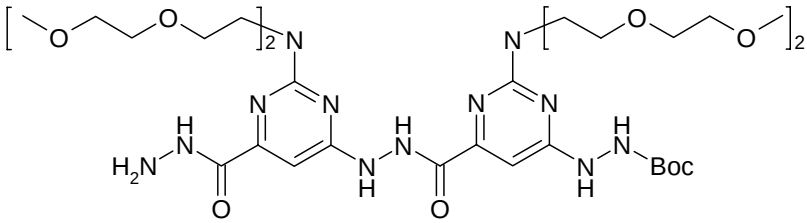

N'-{2-{Bis-[2-(2-methoxy-ethoxy)-ethyl]-amino}-6-[N'-(2-{bis-[2-(2-methoxy-ethoxy)-ethyl]-amino}-6-hydrazinocarbonyl-pyrimidin-4-yl)-hydrazinocarbonyl]-pyrimidin-4-yl}-hydrazinecarboxylic acid tert-butyl ester (11a): A solution of **10** (500 mg, 0.59 mmol) and $NH_2NH_2{\cdot}H_2O$ (180 mg, 3.54 mmol) in methanol (10 mL) was refluxed for 1 h. After removal of the solvent and excess hydrazine in vacuum, the crude product **11a** could be used in the next step directly.

IR ($CHCl_3$): 3019 cm^{-1}, 1590, 1216, 759, 669. ^1H NMR ($CDCl_3$): δ = 1.41 ppm (s, 9 H, Boc-CH_3), 3.33 (s, 12 H, OCH_3), 3.49-3.51 (m, 10 H, CH_2), 3.58-3.67 (m, 14 H, CH_2), 3.79-3.81 (m, 8 H, CH_2), 4.11 (s, 2 H, NH_2), 6.95-7.06 (m,3 H, Het-H), 8.20 (s, 1 H, NH), 8.89 (s, 1 H, NH), 10.36 (s, 2 H, NH). ^{13}C NMR ($CDCl_3$): δ = 28.2 ppm, 48.6, 59.1, 69.3, 70.4, 72.0, 90.4, 156.1, 160.2, 160.5, 164.6. UV (MeCN): λ_{max} (log ε) = 333 (5.016). MS (ESI, MeOH + 10mmol/l NH_4Ac): *m/z* (%) = 843.6 $[MH]^+$ (100). Anal. Calcd. for $C_{35}H_{62}N_{12}O_{12}$: C: 49.9; H: 7.4; N: 19.9; Found: C: 49.3; H: 7.1; N: 20.0.

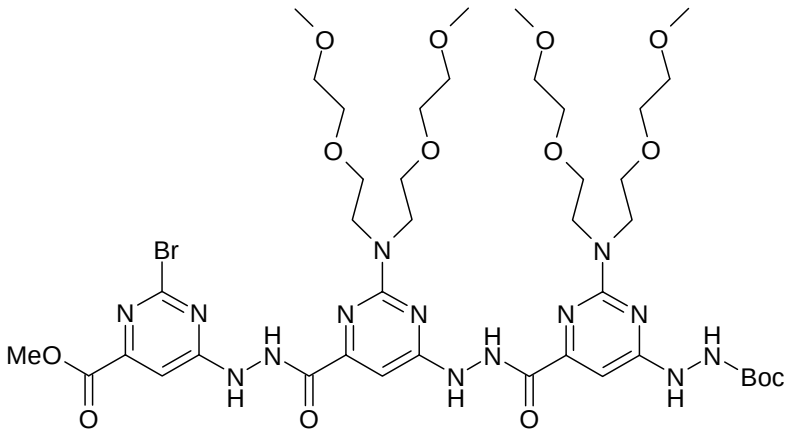

PHA compound **11b**: A mixture of **10** (1.00 g, 1.19 mmol), **8** (385 mg, 1.31 mmol), and NEt_3 (144 mg, 1.43 mmol) in DMF (15 mL) was stirred at 75-80ºC for 20 h. After the solvent was removed in vacuum, the residue was purified by column chromatography (CH_2Cl_2/MeOH 1:35, $R_f = 0.20$) to afford compound **11b** as a yellow oil (507 mg, 0.54 mmol, 45 %).100 mg of **11a** was recovered.

IR ($CHCl_3$): 3019 cm^{-1}, 1477, 1216, 758, 669. ^1H NMR ($CDCl_3$): δ = 1.39-1.44 ppm (m, 9 H, Boc-CH_3), 3.31-3.36 (m, 12 H, OCH_3), 3.51-3.58 (m, 14 H, CH_2), 3.67-3.69 (m, 8 H, CH_2), 3.83-3.93 (m, 8 H, CH_2), 4.00 (s, 3 H, CH_3), 6.94 (s, 2 H, Het-H), 7.49 (s, 1 H, NH), 7.96 (s, 1 H, NH), 10.47 (s, 1 H, NH), 10.69 (s, 1 H, NH), 11.34 (s, 1 H, NH). ^{13}C NMR ($CDCl_3$): δ = 28.2 ppm, 46.0, 48.5, 49.1, 53.7, 59.1, 69.5, 70.5, 72.0, 81.4, 94.1, 105.9, 152.6, 152.9, 156.0, 157.2, 157.7, 160.5, 164.9. UV (MeCN): λ_{max} (log ε) = 330 (5.260). MS (ESI, MeOH + 10mmol/l NH_4Ac): *m/z* (%) = 1059.6 $[MH]^+$ (100). Anal. Calcd. for $C_{41}H_{65}BrN_{14}O_{14}$: C: 46.6; H: 6.2; N: 18.5; Found: C: 46.0; H. 6.4; N. 19.2.

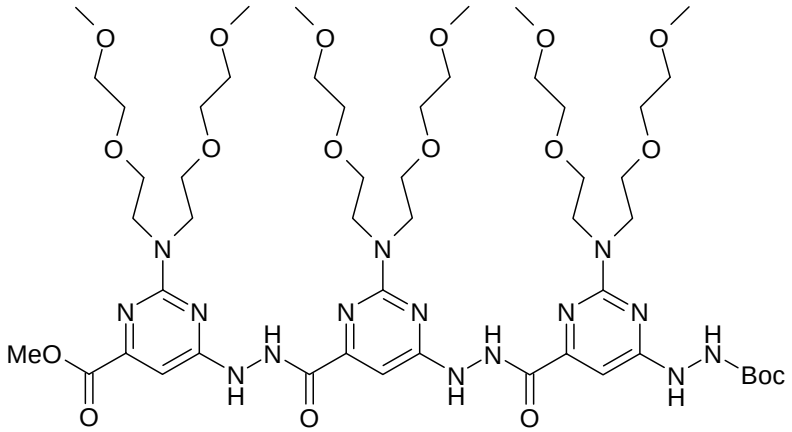

PHA compound **11**:

A solution of **11b** (500 mg, 0.47 mmol), **4** (156 mg, 0.71 mmol), and NEt_3 (57 mg, 0.56 mmol) in DMF (10 mL) was stirred at 85ºC for 18 h. After the solvent was removed in vacuum, the crude produce was purified by column chromatography (CH_2Cl_2/MeOH 1:30, $R_f = 0.20$) to afford compound **11** as a yellow oil (390 mg, 0.38 mmol, 80 %). 40 mg of **11b** was recovered.

IR ($CHCl_3$): 3019 cm^{-1}, 1577, 1474, 1216, 758, 669. ^1H NMR ($CDCl_3$): δ = 1.42 ppm (s, 9 H, Boc-CH_3), 3.32-3.34 (m, 18 H, OCH_3), 3.48-3.69 (m, 36 H, CH_2), 3.84-3.90 (m, 16 H, CH_2, CH_3), 6.98 (s, 3 H, Het-H), 7.44 (s, 1 H, NH), 10.52 (s, 5 H, NH).^{13}C NMR ($CDCl_3$): δ = 28.2 ppm, 48.2, 48.6, 52.8, 59.0, 69.5, 70.5, 72.0, 81.4, 156.1, 160.5,

161.3. UV (MeCN): λ_{max} (log ε) = 338 (6.332). MS (ESI, MeOH + 10mmol/l NH_4Ac): *m/z* (%) = 1199.0 $[MH]^+$ (100), 600$[MH_2]^{2+}$(28).

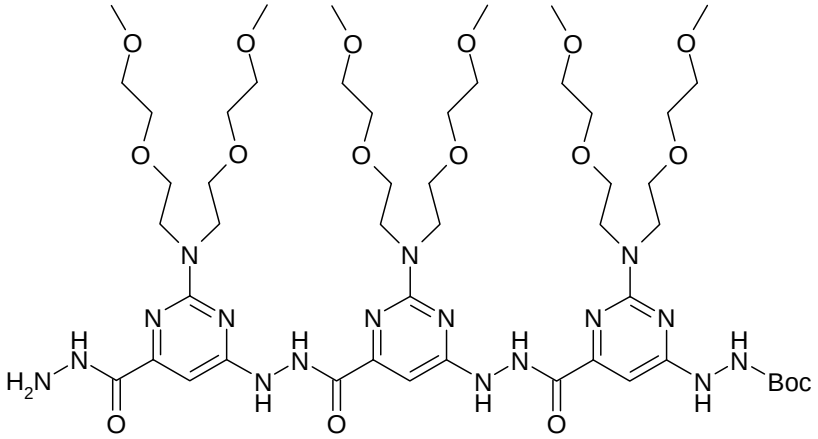

PHA compound **12a**: A solution of **11** (200 mg, 0.16 mmol) and $NH_2NH_2{\cdot}H_2O$ (50 mg, 1.01 mmol) in methanol (5 mL) was refluxed for 1 h. After removal of the solvent and excess hydrazine in vacuum, the crude product **12a** could be used in the next step directly.

IR ($CHCl_3$): 3019 cm^{-1}, 1577, 1474, 1216, 758, 669. ^1H NMR ($CDCl_3$): δ = 1.41 ppm (s, 9 H, Boc-CH_3), 3.32-3.35 (m, 18 H, OCH_3), 3.48-3.57 (m, 24 H, CH_2), 3.69-3.70 (m, 12 H, CH_2), 3.84-3.87 (m, 12 H, CH_2), 7.18 (s, 1 H, Het-H), 7.35 (s, 1 H, Het-H), 7.57 (s, 1 H, Het-H), 8.89 (s, 2 H, NH), 10.61 (s, 4 H, NH). ^{13}C NMR ($CDCl_3$): δ = 28.2, 48.5, 48.6, 59.0, 59.1, 69.5, 70.5, 72.0, 81.1, 159.2, 160.3, 160.6. UV (MeCN): λ_{max} (log ε) = 337 (5.229). MS (ESI, DCM/MeOH + 10mmol/l NH_4Ac): *m/z* (%) = 1199.0 $[MH]^+$ (33), 600.0 $[M+2H^+]$ (100). Anal. Calcd. for $C_{50}H_{87}N_{17}O_{17}$: C: 50.1; H: 7.3; N: 19.9; Found: C: 49.6; H: 7.5; N: 19.9.

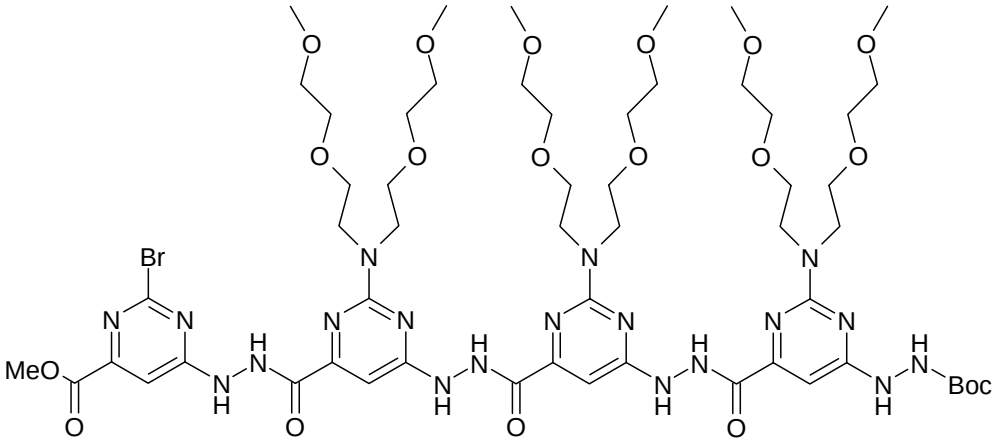

PHA compound **12b**: A mixture of **12a** (200 mg, 0.16 mmol), **8** (54 mg, 0.18 mmol), NEt_3 (25 mg, 0.25 mmol) in DMF (7 mL) was stirred at 80-83 ºC for 20 hrs. After the solvent was removed in vacuum, the residue was purified by column chromatography (CH_2Cl_2/EtOAc/MeOH 10:10:1, $R_f = 0.20$) to afford compound **12b** as a yellow solid (63 mg, 30.0%).20 mg of **12a** was recovered.

IR ($CHCl_3$): 3019 cm^{-1}, 1577, 1476, 1216, 758, 669. ^1H NMR ($CDCl_3$): δ = 1.41 (s, 9 H, Boc-CH_3), 3.33-3.35 (m, 18 H, OCH_3), 3.46-3.49 (m, 22 H, CH_2), 3.70-3.72 (m, 12 H, CH_2), 3.86-3.92 (m, 14 H, CH_2), 4.02 (s, 3H, OCH_3), 6.98 (s, 1 H, Het-H), 7.55 (s, 1 H, Het-H), 7.61 (s, 1 H, Het-H), 8.02 (s, 1 H, Het-H), 10.52 (s, 2 H, NH), 10.68 (s, 2 H, NH), 11.48 (s, 1 H, NH). ^{13}C NMR ($CDCl_3$): δ = 28.2 ppm, 48.6, 53.7, 59.0, 59.0, 69.6, 70.5, 72.0, 81.4, 94.0, 152.6, 152.8, 153.6, 160.6, 165.0. UV (MeCN): λ_{max} (log ε) = 333 (5.370). MS (ESI, DCM/MeOH + 10mmol/l NH_4Ac): *m/z* (%) = 1415.0 $[MH]^+$ (13), 708.2 $[M+2H^+]$ (100). Anal. Calcd. for $C_{56}H_{90}BrN_{19}O_{19}$: C: 47.6; H: 6.4; N: 18.8; Found: C: 47.4; H: 6.5; N: 18.9.

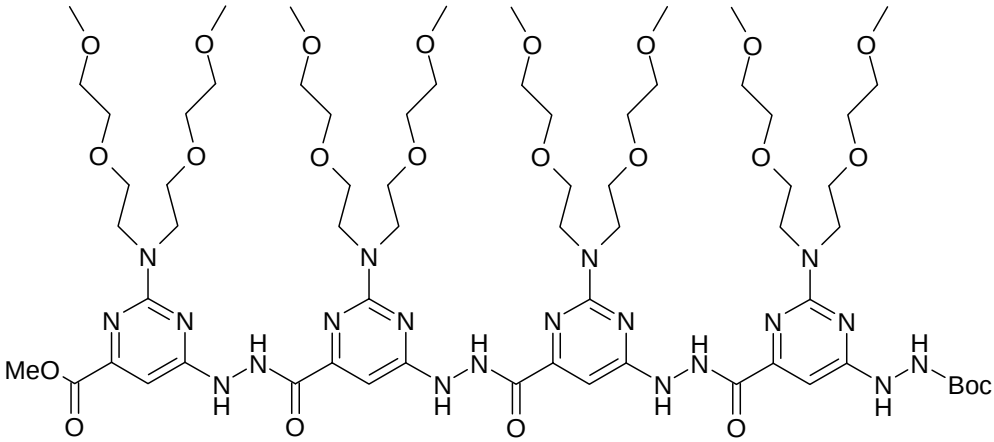

PHA compound **12**:

A solution of **12b** (63 mg, 0.044 mmol), **4** (15 mg, 0.067 mmol), NEt_3 (7 mg, 0.066 mmol) in DMF (4 mL) was stirred at 85ºC for 20 hrs. After the solvent was removed in vacuum, the crude produce was purified by column chromatography (CH_2Cl_2/EtOAc/MeOH 10:10:1, R_f = 0.25) to afford compound **12** as a yellow solid (42 mg, 70%). 8 mg of **12b** was recovered.

IR ($CHCl_3$): 3019 cm^{-1}, 1776, 1545, 1473, 1216, 1101, 758. ^1H NMR ($CDCl_3$): δ = 1.41 ppm (s, 9 H, Boc-CH_3), 3.31-3.34 (m, 24 H, CH_2, OCH_3), 3.47-3.49 (m, 16 H, CH_2), 3.57-3.58 (m, 16 H, CH_2), 3.69-3.72 (m, 16 H, CH_2), 3.87-3.91 (m, 19 H, CH_2, OCH_3), 6.68 (s, 1 H, Het-H), 7.32 (s, 1 H, Het-H), 7.59 (s, 2 H, Het-H), 10.62 (s, 4 H, NH). ^{13}C NMR ($CDCl_3$): δ = 28.2 ppm, 48.6, 59.0, 69.6, 70.5, 72.0, 81.2, 94.2, 165.6. UV (MeCN): λ_{max} (log ε) = 338 (5.336). MS (ESI, MeOH + 10mmol/l NH_4Ac): *m/z* (%) = 1554.1 $[MH]^+$ (6), 777.7 $[M+2H^+]$ (100). Calcd. for $C_{66}H_{112}N_{20}O_{23}$: C: 51.0; H: 7.3; N: 18.0; Found: C: 50.8; H: 7.6; N: 18.0.

2.8. References

[1] T. K. Sawyer, „Structure-Based Design: Diseases, Targets, Techniques and Developments“, ed. P. Veerapandian, Marcel Dekker, **1997**, 559, New York.

[2] J. H. Hartley, T. D. James, and C. J. Ward, *J. Chem. Soc., Perkin Trans. 1* **2000**, 3155.

[3] M. Kruppa, C. Mandl, S. Miltschitzky, and B. Koenig, *J. Am. Chem. Soc.* **2005**, *127*, 3362.

[4] R. Arienzo and J. D. Kilburn, *Tetrahedron* **2002**, *58*, 711; R. J. Fitzmarice, G. M. Kyne, D. Douheret, J. D. Kilburn, *J. Chem. Soc., Perkin Trans. 1* **2001**, 841; A. J. Brouwer, H. van der Linden, and R. M. J: Liskamp, *J. Org. Chem.* **2000**, *65*, 1750; E. J. Iorio and W. C. Still, *Bioorg. Med. Chem. Lett.* **1999**, *9*, 2673.

[5] S. Miltschitzky, V. Michlova, S. Stadlbauer, and B. Koenig, *Heterocycles* **2005**, in press.

[6] For other examples of peptide β-sheet mimetics, see: J. S. Nowick and D. M. Chung, *Angew. Chem. Int. Ed.* **2003**, *42*, 1765; J. S. Nowick, D. M. Chung, K. Maitra, S. Maitra, K. D. Stigers, and Y. Sun, Y., *J. Am. Chem. Soc.* **2000**, *122*, 7654; P. Rzepecki, H. Gallmeier, N. Geib, K. Cernovska, B. Konig, and T. Schrader, *J. Org. Chem.* **2004**, *69*, 5168; For a review, see: S. Miltschitzky and B. Koenig, *OPPI* **2005**, in press.

[7] J. R. Lakowicz, *Acc. Chem. Res.* **1999**, *31*, 173.

[8] J. Kim and M. Lee, *Biochem. Biophys. Res. Comm.* **2004**, *316*, 393.

[9] B. Pispisa, A. Palleschi, C. Mazzuca, L. Stella, A. Valeri, M. Venanzi, F. Formaggio, C. Toniolo, and Q. B. Broxterman, *J. Fluorescence* **2002**, *12*, 213.

[10] H. Y. Shrivastava and B. U. Nair, *Inorg, Biochem.* **2004**, *98*, 991.

[11] C. Selve, J.-C. Ravey, M.-J. Stebe, C. El Moudjahid, E. M. Moumni, and J.-J. Delpuech, *Tetrahedron* **1991**, *47*, 411.

[12] P. Brazeau, W. Vale, R. Burgus, N. Ling, M: Butcher, J. Rivier, and R. Guillemin, *Science* **1973**, *179*, 77.

[13] R. Hall, G. M. Besser, A. V. Schally, D. H. Coy, D. Evered, D. J. Goldie, A. J. Kastin, A. S. McNeilly, C. H. Mortimer, C. Phenekos, W. M. G. Tunbridge, and D.

Weightman, *Lancet* **1973**, *1*, 581; T. M. Siler, G. Vandenberg, and S. S. C. Yen, *Clin. Endocrinol. Metab.* **1973**, *37*, 632.

[14] S. S. C. Yen, T. M. Siler, and G. W: DeVane, *N. Engl. J. Med.* **1974**, *290*, 935; C. H. Mortimer, W. M. G. Tunbridge, D. Carr, L. Yeomans, T. Lind, D. H: Coy, S. R. Bloom, A. J. Kastin, C. N. Mallison, G. M: Besser, A. V. Schally, and R. Hall, *Lancet* **1974**, *1*, 697.

[15] S. Bloom, C. Mortimer, M. Thorner, G. Besser, R. Hall, A. Gomez-Pan, U. Roy, D. Coy, A. Kastin, and A. Schally, *Lancet* **1974**, *2*, 1106.

[16] M. Brown, J. Rivier, and W. Vale, *Endocrinology* **1976**, *98*, 336; J. E. Rivier, M. Brown, and W. Vale, *J. Med. Chem.* **1976**, *19*, 1010.

[17] The initial slopes of the emission titration curves at excitation at 281 nm are similar. The intensity of Trp8 emission is quenched to the same degree as the emission of PHA **14** increases resulting clearly from a FRET process. The selective excitation of **14** at 320 nm leads to a steeper slope of the emission enhancement, which indicates an additional effect of the peptide binding on the PHA emission.

[18] H. J. Schneider, R. Kramer, S. Simova, and U. Schneider, *J. Am . Chem. Soc.* **1988**, ***110***, 6442; C. S. Wilcox, *"Frontiers in Suplramolecular Chemistry and Photochemistry"* ed. by H. J. Schneider and H. Duerr, VCH, Weinheim, **1991**.

[19] J. R. Lakowicz, *"Principles of Fluorescence Spectroscopy"* **1983**, Plenum Press, New York.

[20] P. Job, *Compt. Rend* **1925**, *180*, 925; M. T. Blanda, J. H. Horner, and M. Newcomb, *J. Org. Chem.* **1989**, *54*, 4642.

[21] E. A. Burnstein, N. S. Vedenkina, and M. N. Ivkova, *Photochem. Photobiol.* **1973**, *18*, 263.

[22] We cannot calculate a binding constant, because the stoichiometry of binding and the binding motif remain presently unknown. A dynamic assembly of one SRIF and one PHA is likely.

[23] J. B. Sumner, *J. Biol. Chem.* **1919**, *37*, 137.

[24] H. Bittiger and H. P. Schuebli, *"Concanavalin A as a Tool"* **1976**, Wiley, New York.

[25] K. D. Hardman, R. C: agarwal, and M. J. Freiser, *J. Mol. Biol.* **1982**, *372*, 6388.

[26] S. Parkin, B. Rupp, and H. Hope, *Acta Crystallogr.* **1996**, *D52*, 1161.

[27] A. Chatterjee and D. K. Mandal, *Biochim. Biophys. Acta.* **2003**, *1648*, 174; M. N. Pflumm and S. Beychok, *Biochemistry* **1974**, *13*, 4982; H. E. Auer and T. Schulz, *J. Pept. Protein. Res.* **1984**, *24*, 569.

[28] M. M. Burger and K. D. Noonan, *Nature* **1970**, *228*, 512; H. B. Bosmann, *Febs Lett.* **1972**, *22*, 97.

3. Molecular Recognition of His with NTA-Ligands

3.1. Introduction

Molecular recognition is based on the reversible interactions of ions or molecules. It is thus the chemistry of non-covalent bonds such as hydrogen bonds, electrostatic or van der Waals interactions.[1] The strength of hydrogen bonds and electrostatic interactions decrease rapidly as the polarity of the surrounding solvent increases.[2] However, the recognition of substrates such as peptides, hormones, or carbohydrates under physiological conditions is of great importance for medicinal applications and the design of biosensors.

We currently investigate the interactions of synthetic receptors on peptide β-strands in organic solvents and buffered solutions.[3] Oligomers of these receptors must adopt a linear conformation to be complementary to extended β-sheets. We focused on substituted pyrrols and pyrimidines.

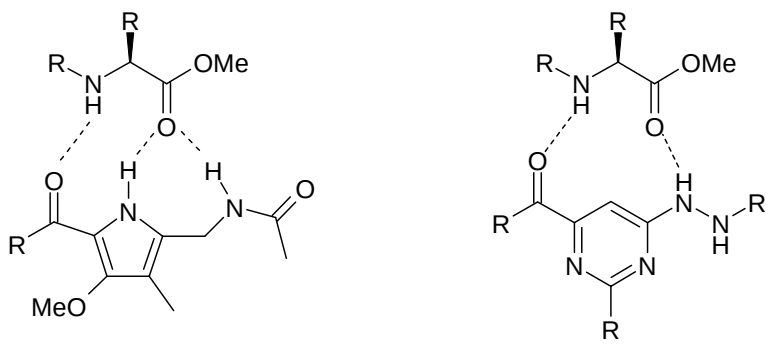

methoxypyrrole amino acid (MOPAS) pyrimidine hydrazine acid (PHA)

Figure 1: Synthetic receptors MOPAS (left) and PHA (right) and their assumed binding motif to a peptide strand

These heterocyclic peptide mimics bind peptides via hydrogen bonds. The binding of methoxypyrrole amino acid (MOPAS) and pyrimidine hydrazine acid (PHA) to peptides was investigated by ^{1}H-NMR and fluorescence titration. The chemical induced shift (CIS) of separated proton signals and the relative change of the emission maximum of the pyrimidine were measured. Binding affinities in chloroform and phosphate buffer (pH 7.2) of approx $1 \cdot 10^{3}$ M^{-1} were derived from these data assuming a 1:1 binding

motif. The binding of the heterocyclic peptide mimics is weak due to a limited number of hydrogen bonds. Self-assoziation of the peptides and mimics complicate the data evaluation and decrease efficiency. A combination of hydrogen bonding with strong ionic interaction and reversible metal to ligand coordination may allow intramolecular formation of hydrogen bonds overcoming the problem of self-association and weak binding.[4]

Various transition metal ions (e.g. Cu^{2+}, Ni^{2+}, Zn^{2+}) bind to the imidazole side chains of surface exposed histidines of proteins.[5] This coordination interaction (M^{2+}His) is used for protein purification by immobilized metal affinity chromatography (IMAC)[6] and two-dimensional protein crystallization.[7] The binding constant of amino acids with a series of divalent metal nitrilotriacetates $[M(NTA)]^-$ (M = Mn^{2+}, Co^{2+}, Ni^{2+}, Cu^{2+}, Zn^{2+}) has been intensively studied over the last decades.[8] Especially the (NTA)/histidine-tag (HT) technology has become a powerful tool in the bioscience.[9]

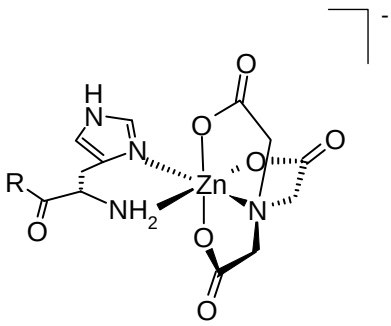

Figure 2: Coordinative interactions between terminal His and Zn(II)-NTA

Figure 2 shows the binding motif. The Zn^{2+} ion is coordinated by the lone pairs of the imidazole and the amine nitrogens forming an octahedral complex. The NH_2-residue of His is essentially for the Zn-NTA binding.

The binding affinity of NTA to peptides in organic solvents was derived from an ITC binding experiment of a Li[Ni(NTA)-Gly-Boc]-complex to NH_2-His-Leu-Leu-Val-Phe-OMe in DMSO. A binding affinity of $(5.05\pm0.33)\cdot10^5$ kcal/mole was determined. The binding is 500 fold tighter than the affinity of Zn-NTA to H-His-OH in buffered aqueous solution. This results from the higher affinity of Ni-NTA to His compared to Zn-NTA[10] but likely also from the more extended structure of Li[Ni(NTA)-Gly-Boc].

3.2. Results and Discussion

Combining rather weak hydrogen binding of PHA receptors to β-peptide strands and the rather strong interaction of M-NTA to His, a receptor with superior binding ability under physiological conditions can be synthesized. The initial binding event is the strong coordinative interactions between the metal complex and histidine. Although Ni^{2+} or Cu^{2+} NTA complexes show higher affinities to *N*-terminal His,[12] Zn^{2+} was chosen to obtain a diamagnetic compound. This allows the investigation of interactions with NMR techniques. After complex formation, the subsequent process of peptide backbone binding is intramolecular, which is more favorable than intermolecular processes.[11] Gly was chosen as the spacer to assist the receptor molecule by two additional hydrogen bond binding sites.

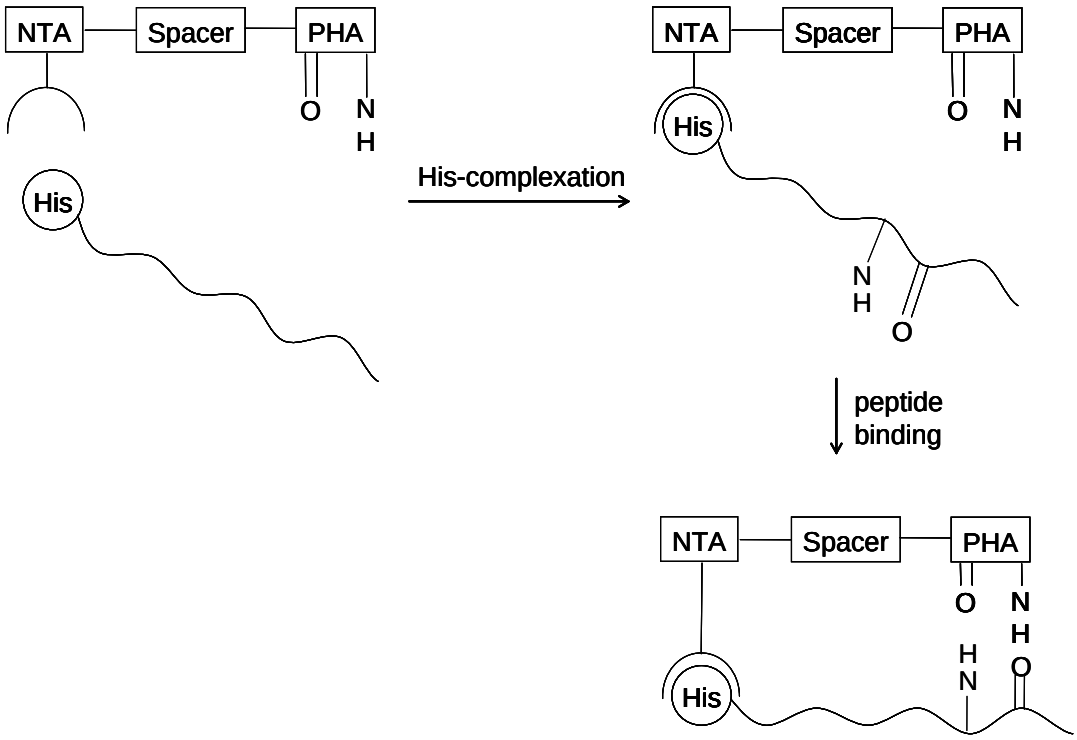

Figure 3: Assumed binding mechanism

The synthesis of the peptide-binding complex is shown in figure 4. Compound **1**,[12] obtained from lysine methyl ester, is coupled to Boc-Gly-OH. After Boc deprotection, the PHA unit **4**, which we have reported recently,[4] was introduced by standard peptide

coupling chemistry. Cleavage of the methyl ester under basic conditions generates the NTA ligand. The complexation with Zn^{2+} leads to the desired receptor **6**.

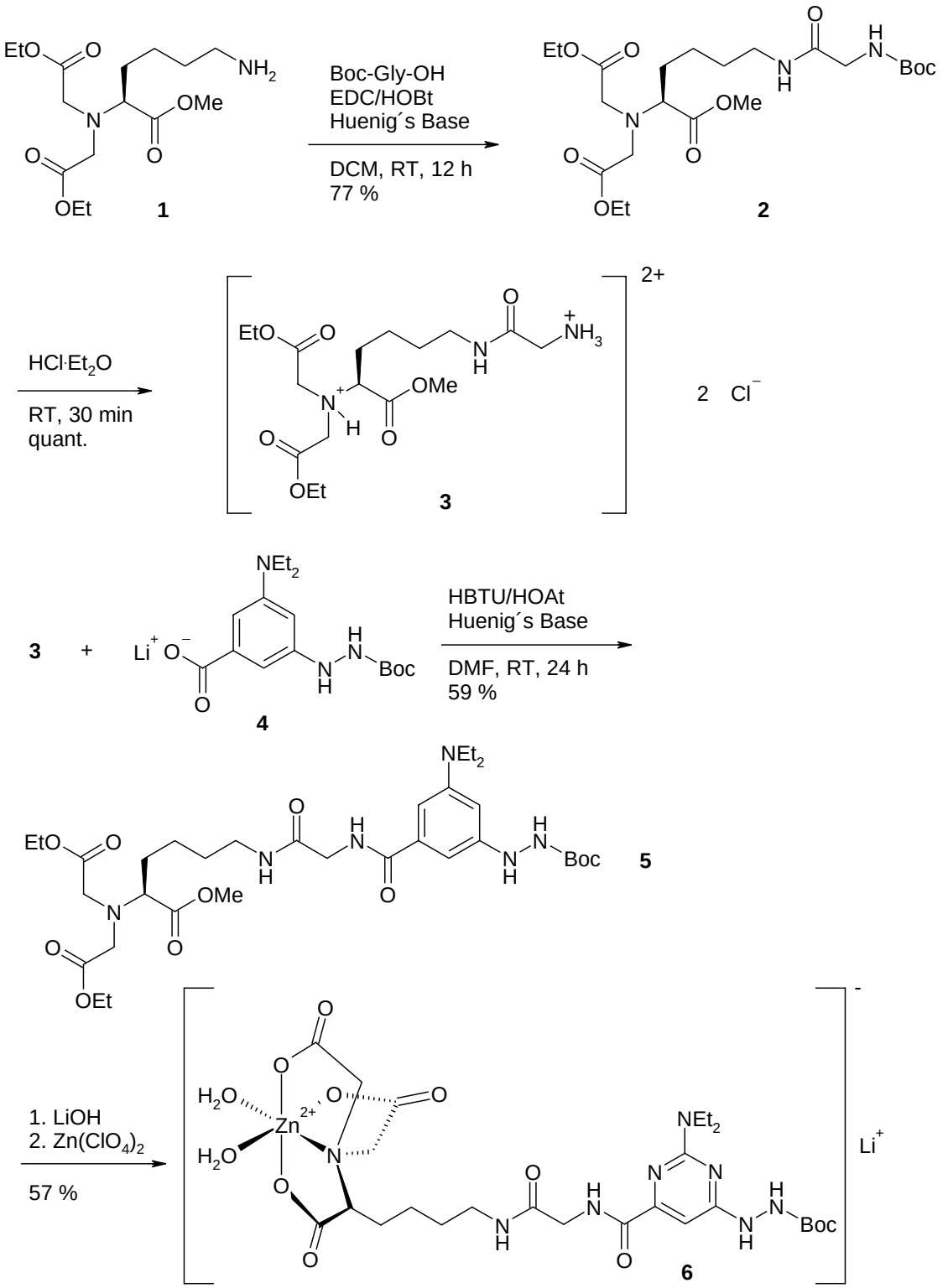

Figure 4: Synthesis of the receptor **6**

Structural information about the binding motif of **6** to the pentapeptide NH_2-His-Leu-Leu-Val-Phe-OMe was derived from 2D-NOE NMR experiments in DMSO-[D6].[13] The NMR spectra of **6**·H-His-Leu-Leu-Val-Phe-OMe ($c = 3.30 \cdot 10^{-2}$ M), obtained by dissolving equimolar amounts of **6** and the pentapeptide were analyzed allowing complete assignment of the resonance signals.

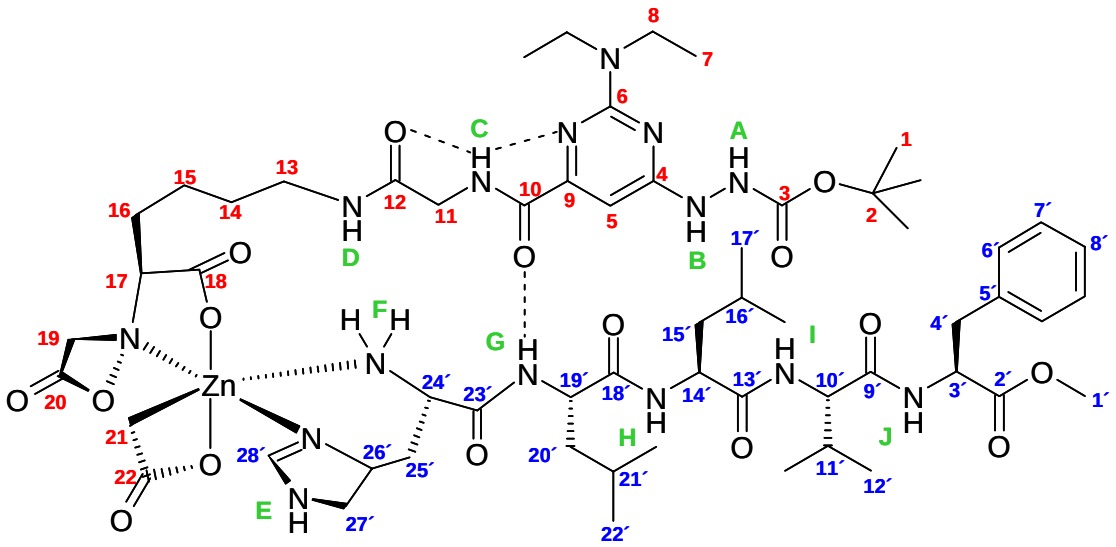

Figure 5: Structure and numbering of the proposed aggregate formed in an equimolar mixture of **6** and H-His-Leu-Leu-Val-Phe-OMe ($c = 3.30 \cdot 10^{-2}$ M) in DMSO-[D6]

The temperature-induced shift of bounded and free NH signals indicates hydrogen bonding.[14] While shifts of <-2 ppb/K indicate a strong interaction, values of >-4 ppb/K are crucial for solvent expressed atoms.[15] The smallest ppb/K value (-2.57 ppb/K) was obtained for NH C. This proton is probably hydrogen bound to both the lone pair of the oxygen atom of the amide bond and the lone pair of the nitrogen atom in the pyrimidine ring. NH G shows another weak intermolecular hydrogen bond by a temperature dependent shift of -2.95 ppb/K. All other temperature dependent shifts of **6** show values of 3 ppb/K or higher indicating no strong binding of **6** to the receptor as expected.

Further information about the binding motif was obtained from ROESY experiments. Figure 7 shows an expanded part of the spectra indicating interactions between NH signals of **6** to the pentapeptide.

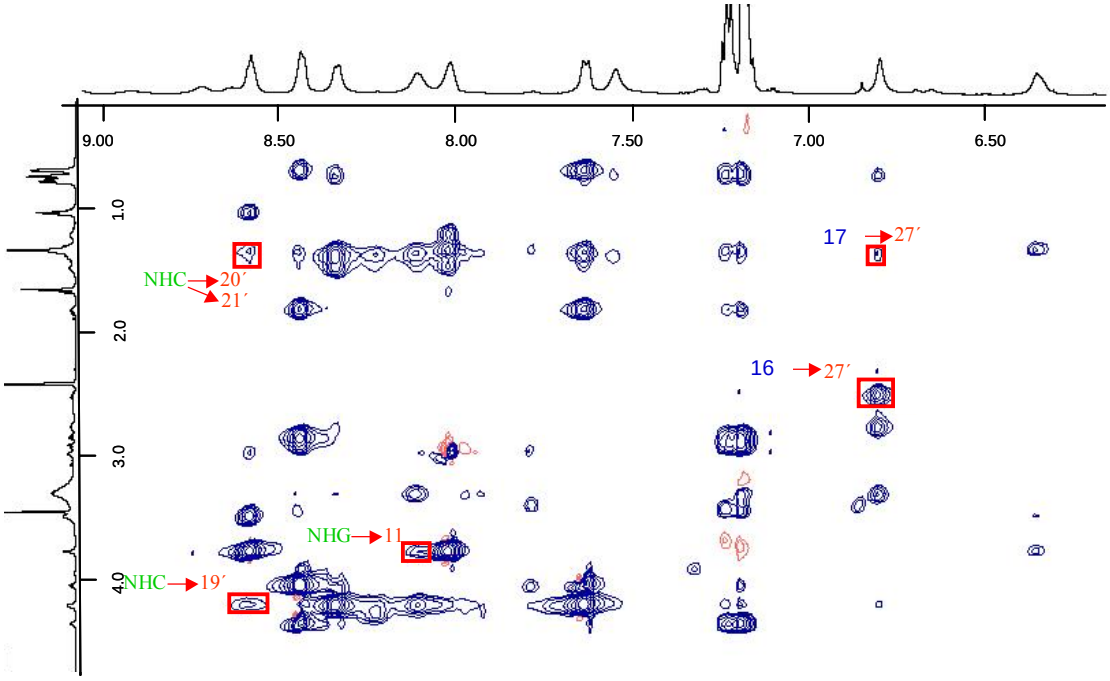

Figure 3: Part of the ROESY spectra of an equimolar mixture of **6** and H-His-Leu-Leu-Val-Phe-OMe (c = $3.30 \cdot 10^{-2}$ M) in DMSO-[D6]

In summary, 2D NOESY and ROESY[16] spectra revealed ten intrastrand contacts, which are indicated in figure 8 justifying the depicted structure in figure 4.[17]

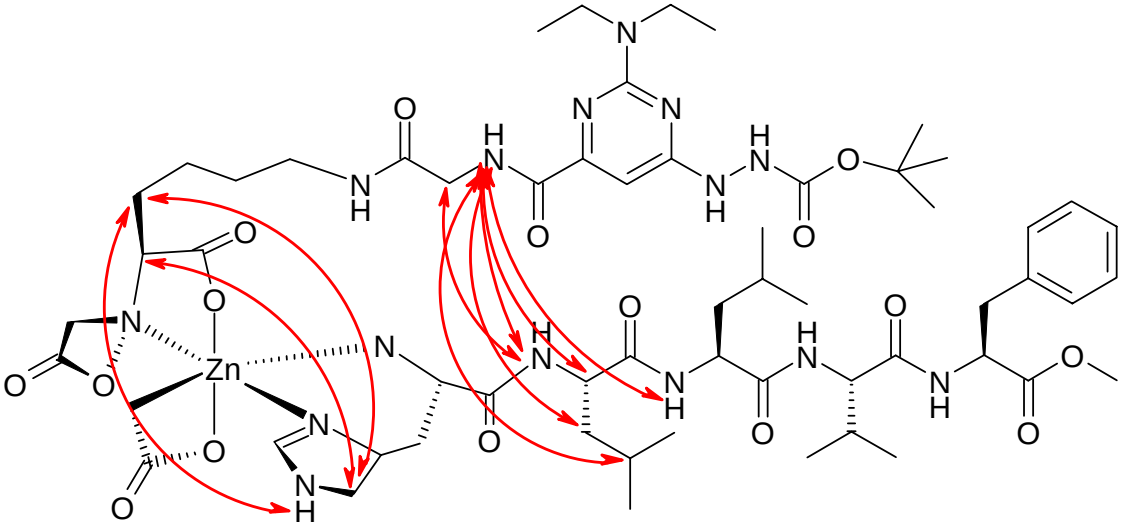

Figure 4: Spectroscopically detected NOE contacts of **6** and NH_2-His-Leu-Leu-Val-Phe-OMe in a $3.30 \cdot 10^{-2}$ M solution DMSO-[D6] (arrows)

The determination of the binding affinity between the receptor **6** and the pentapeptide was carried out in MeCN. The PHA receptor **6** emits around 320 nm when excited at

215 nm allowing a photochemical investigation of interactions to a peptide strand. The fluorescence titration of **6** to the pentapeptide H-His-Leu-Leu-Val-Phe-OMe is shown in figure 4. The emission intensities are corrected for dilution during the titration.

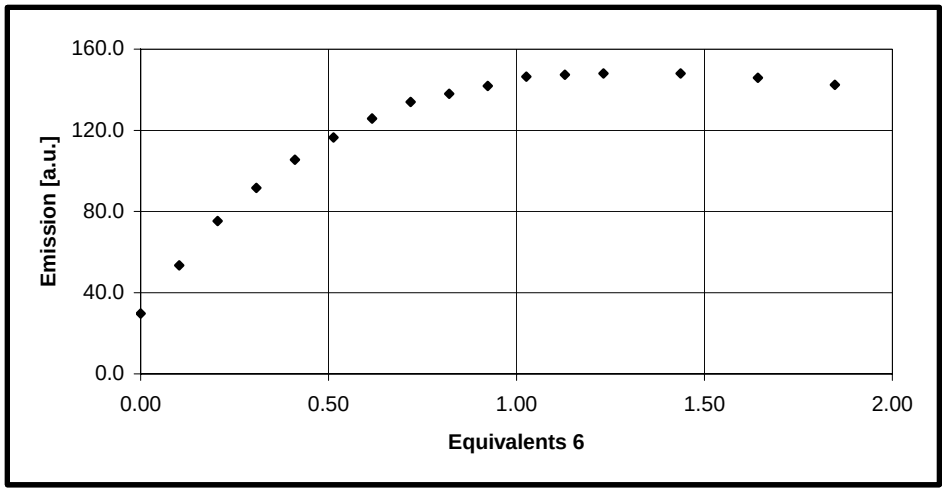

Figure 5: Fluorescence titration curve of a $2.03 \cdot 10^{-4}$ M solution of H-His-Leu-Leu-Val-Phe-OMe in MeCN with **6** (excitation at 215 nm)

The emission of **6** strongly depends on the polarity of the solvent and its microenvironment. It is decreased with increasing solvent polarity. The addition of **6** to a solution of the pentapeptide leads to an enhanced intensity. This indicates the substitution of solvating H_2O in the receptors environment by the less polar terminal His and hydrogen binding of the PHA moiety to the peptide. A plateau of the emission intensity is observed after the injection of 1 equivalent **6**. The further addition leads to a decrease of intensity due to unbound PHA receptor. A binding affinity of $1.07 \cdot 10^5$ L/mol was calculated by non-linear fitting.[18] While the PHA moiety shows poor binding affinity to oligopeptides with no clear binding motif, the synthesized receptor **6** binds well defined with a 100-fold higher affinity.

3.3. Conclusions

Divalent metal nitrilotriacetates $[M^{2+}(NTA)]^-$ (M = Mn, Co, Ni, Cu, Zn) are part of analytical applications in medicinal chemistry. The combination of an imidazole-coordinating metal complex, which binds to *N*-terminal His, with a fluorescent pyrimidine hydrazine acid (PHA) moiety leads to a luminescent biosensor. The synthesis of the receptor, containing Zn, and its binding affinity to the pentapeptide H-His-Leu-Leu-Val-Phe-OMe is reported. The binding process proceeds in two steps. Initially, a strong interaction of the NTA to the imidiazole of the His occurs. The weaker hydrogen binding process of the PHA moiety to the backbone of the peptide becomes intramolecular in the second step. The binding process is monitored by fluorescence spectroscopy showing an emission response of PHA upon peptide binding.

3.4. Experimental Part

Emission Titrations:

A solution of the PHA molecule ($c = 5.00 \cdot 10^{-3}$ mol/L) was added in portions by a microsyringe to a solution of a peptide ($c = 2.03 \cdot 10^{-4}$ mol/L). Volume and concentration changes were taken into account for the analysis of the binding event.[17]

Synthesis of new compounds:

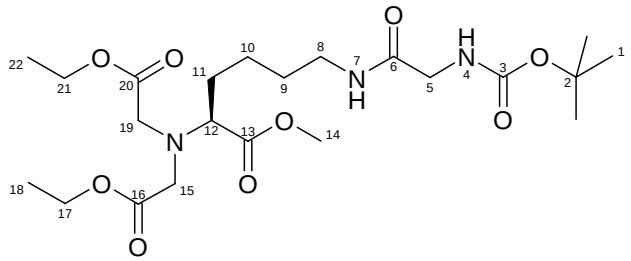

2-(Bis-ethoxycarbonylmethyl-amino)-6-(2-tert-butoxycarbonylamino-acetylamino)-hexanoic acid methyl ester: To a solution of 131 mg (0.75 mmol) Boc-Gly-OH, 122 mg (0.90 mmol) HOBt, 158 µL (140 mg, 0.90 mmol) NEt_3, and 447 µL (339 mg, 2.63 mmol) Huenig´s Base in 2 mL DMF was added a solution of 302 mg (0,75 mmol) amine **1** in 1 mL DMF at 0 °C. The reaction mixture was allowed to warm to rt and stirred for 18 h. The solution was diluted with H_2O (4 mL) and extracted with CH_2Cl_2 (2·10 mL). The organic phases were dried over Na_2SO_4, evaporated, and then concentrated under reduced pressure. The residue was purified by column chromatography (EtOAc, $R_f = 0.36$) to afford **2** as a colorless oil in 76 % (280 mg, 0.57 mmol) yield.

IR (KBr disk): 3362 cm^{-1}, 2981, 2938, 2251, 1740, 1670, 1166. ^{1}H-NMR ($CDCl_3$, 400 MHz): $\delta = 1.28$ ppm (t, $^3J = 7.1$ Hz, 6 H; COSY: $C^{18}H_3$, $C^{22}H_3$), 1.47 (s, 9 H; COSY: C^1H_3), 1.48-1.67 (m, 4 H; COSY: $C^{10}H_2$, C^9H_2), 1.70-1.74 (m, 2 H; COSY: $C^{11}H_2$), 3.28-3.31 (m, 2 H; COSY: C^8H_2), 3.45 (t, $^3J = 7.6$ Hz, 1 H; COSY: $C^{12}H$), 3.61 (s, 2 H; COSY: $C^{15}H_2$), 3.62 (s, 2 H; COSY: $C^{19}H_2$), 3.71 s, 3 H; COSY: $C^{14}H_3$), 3.81-3.85 (m, 2 H; COSY: C^5H_2), 4.17 (q, $^3J = 7.1$ Hz, 4 H; COSY: $C^{21}H_2$, $C^{17}H_2$), 5.42 (bs, 1 H; COSY: N^4H), 6.51 (bs, 1 H; COSY: N^7H). ^{13}C-NMR ($CDCl_3$, 100 MHz; HSQC): $\delta = 14.2$ ppm (+, C^{18}, C^{22}), 22.5 (-, C^{10}), 28.2 (-, C^9), 28.3 (+, C^1), 29.3 (-, C^{11}), 39.1 (-, C^8), 44.2 (-, C^5), 51.4 (+, C^{14}), 52.7 (-, C^{19}, C^{15}), 60.7 (-, C^{17}, C^{21}), 64.1 (+, C^{12}), 79.9

(C_{quat}, C^2), 156.0 (C_{quat}, C^3), 169.5 (C_{quat}, C^6), 171.5 (C_{quat}, C^{16}, C^{20}), 173.3 (C_{quat}, C^{14}). MS (ESI, DCM/MeOH + 10 mmol/l NH_4Ac): *m/z* (%) = 490.3 [$M+H^+$] (100). HRMS Calcd for $C_{22}H_{39}N_3O_9$: 489.2686; Found: 489.2680±0.0004.

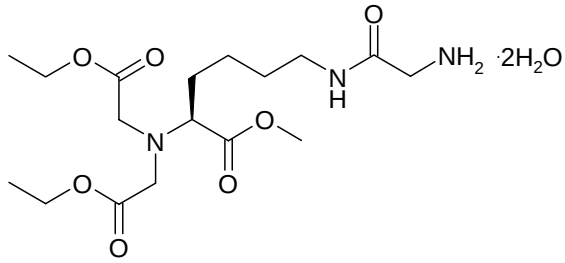

6-(2-Amino-acetylamino)-2-(bis-ethoxycarbonylmethyl-amino)-hexanoic acid methyl ester dihydrochloride: Boc protected amine **2** (259 mg, 0.53 mmol) was dissolved in 3 mL of ether saturated with HCl. The solution was allowed to warm to rt, stirred for 15. The precipitation was filtered off, washed with cold ether and dried in vacuum to afford **3** as a colorless, hygroscopic salt in almost quantitative (242 mg, 0.52 mmol, 99 %). The salt was used without further purifications.

mp: > 200 °C (decomp). IR (KBr disk): 3423 cm^{-1}, 2955, 1747, 1656, 1558, 1378, 1224, 1019, 914, 706. ^{1}H-NMR (DMSO-[D6], 300 MHz): δ = 1.17 ppm (t, ^3J = 7.1 Hz, 6 H, CH_3CH_2O), 1.30-1.48 (m, 4 H, CH_2 Lys), 1.51-1.63 (m, 2 H, CH_2 Lys), 3.01-3.14 (m, 2 H, CH_2 Lys), 3.32-3.42 (m, 1 H, CH Lys), 3.34-3.54 (m, 4 H, CH_2CO_2Et), 3.55-3.61 (m, 5 H, CH_2 Gly, OCH_3), 4.04 (q, ^3J = 7.0 Hz, 4 H, CH_3CH_2O), 8.16-8.34 (m, 3 H, NH), 8.48-8.52 (m, 1 H, NH Lys), 9.94 (bs, 1 H, NH). ^{13}C-NMR (DMSO-[D6], 150 MHz): δ = 15.1 ppm (+), 22.6 (-), 28.4 (-), 29.2 (-), 38.4 (-), 39.9 (-), 51.0 (+), 52.1 (-), 59.0 (-), 63.7 (+), 165.5 (C_{quat}), 170.7 (C_{quat}), 172.3 (C_{quat}). MS (ESI, DCM/MeOH + 10 mmol/l NH_4Ac): *m/z* (%) = 390.2 [$M+H^+$] (100).

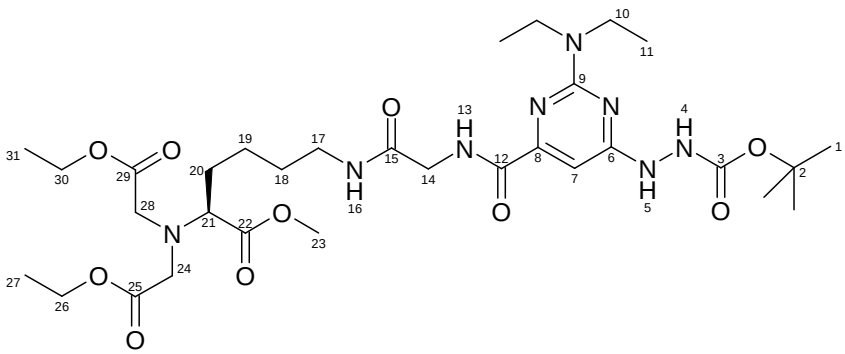

2-(Bis-ethoxycarbonylmethyl-amino)-6-(2-{[6-(N'-tert-butoxycarbonyl-hydrazino)-2-diethylamino-pyrimidine-4-carbonyl]-amino}-acetylamino)-hexanoic acid methyl ester: A solution of 120 mg (0.26 mmol) **3**, 86 mg (0.26 mmol) **4**, 70 mg (0.52 mmol) HOBt, 197 mg (0.52 mmol) HBTU and 224 µL (168 mg, 1.30 mmol) Huenig´s Base in 4 mL DMF was stirred 24 h at rt. The solution was allowed to cool to 0 °C, diluted with cold H_2O (5 ml), and extracted with CH_2Cl_2 (3·10 mL). The organic phases were dried over $MgSO_4$, evaporated, and then concentrated under reduced pressure. The residue was purified by column chromatography (EtOAc, $R_f = 0.30$) to afford **5** as a white solid in 59 % (106 mg, 0.15 mmol) yield.

mp: 144 °C; IR (KBr disk): 3325 cm^{-1}, 2989, 1735, 1649, 1532, 1380, 1187, 1093. ^{1}H-NMR ($CDCl_3$, 600 MHz): $\delta = 1.17$ ppm (t, $^3J = 6.9$ Hz, 6 H; HSQC: $C^{11}H_3$), 1.22-1.28 (m, 6 H; HSQC: $C^{27}H_3$, $C^{31}H_3$), 1.35-1.45 (m, 2 H; COSY: $C^{19}H_2$), 1.47 (s, 9 H; HSQC: C^1H_3), 1.55-1.60 (m, 2 H; COSY: $C^{18}H_2$), 1.66-1.72 (m, 2 H; COSY: $C^{20}H_2$), 3.23-3.33 (m, 2 H; COSY: $C^{17}H_2$), 3.40 (t, $^3J = 7.6$ Hz, 1 H; HSQC: $C^{21}H$), 3.58-3.62 (m, 8 H; HSQC: $C^{10}H_2$, $C^{24}H_2$, $C^{28}H_2$), 3.67 (s, 3 H; HSQC: $C^{23}H_3$), 4.07-4.16 (m, 6 H; HSQC: $C^{14}H_2$, $C^{26}H_2$, $C^{30}H_2$), 6.45-6.75 (m, 2 H; HSQC: N^4H, N^5H), 6.65 (bs, 1 H; HSQC: C^7H), 6.69 (bs, 1 H; COSY: $N^{16}H$), 8.51 (t, $^3J = 5.0$ Hz, 1 H; HSQC: $N^{13}H$). ^{13}C-NMR ($CDCl_3$, 150 MHz): $\delta = 13.2$ ppm (+; HSQC: C^{11}), 14.2 (+; HSQC: C^{27}, C^{31}), 22.9 (-; HSQC: C^{19}), 28.2 (+; HSQC: C^1), 28.4 (-; HSQC: C^{18}), 29.6 (-; HSQC: C^{20}), 39.1 (-; HSQC: C^{17}), 41.9 (-; HSQC: C^{10}), 43.2 (-; HSQC: C^{14}), 51.4 (+; HSQC: C^{23}), 52.7 (-; HSQC: C^{24}, C^{28}), 60.6 (-; HSQC: C^{26}, C^{30}), 64.6 (+; HSQC: C^{21}), 81.7 (C_{quat}; HMBC: C^2), 115.4 (+; HSQC: C^7), 155.7 (C_{quat}), 155.8 (C_{quat}; HMBC: C^3), 156.9 (C_{quat}), 160.1 (C_{quat}; HMBC: C^9), 164.8 (C_{quat}; HMBC: C^{12}), 168.7 (C_{quat}; HMBC: C^{15}), 171.5 (C_{quat}; HMBC: C^{25}, C^{29}), 173.2 (C_{quat}; HMBC: C^{22}). MS (ESI, MeOH + 10 mmol/l NH_4Ac): *m/z* (%) = 719.4 [$M+Na^+$] (22), 697.4 [MH^+] (100).

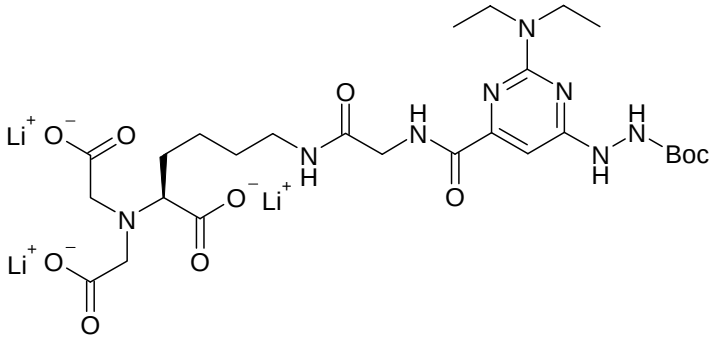

2-(Bis-carboxymethyl-amino)-6-(2-{[6-(N'-tert-butoxycarbonyl-hydrazino)-2-diethylamino-pyrimidine-4-carbonyl]-amino}-acetylamino)-hexanoic acid Li-salt:

73 mg (0.10 mmol) ester **5** and 3 mg (0.30 mmol) LiOH were dissolved in a 4:1 mixture acetone/water and stirred 1 d at 40 °C. The solvents are removed under reduced pressure to afford the hygroscopic lithium salt (61 mg, 95 %) in almost quantitative yield. The salt is used without further purification.

mp: > 250 °C (decomp). ^{1}H-NMR (D_2O, 300 MHz): δ = 0.52-0.73 ppm (m, 6 H), 0.86-1.69 (m, 15 H), 2.78-3.22 (m, 5 H), 3.34-3.63 (m, 4 H), 3.84-4.06 (m, 4 H), 6.34 (s, 1 H), 7.12-7.24 (m, 1 H), 7.34-7.45 (m, 1 H). ^{13}C-NMR (D_2O, 75 MHz): δ = 12.4 ppm (+), 13.6 (+), 23.2 (-), 27.5 (+), 28.1 (+), 28.4 (-), 30.2 (-), 39.2 (-), 41.5 (-, 2 C), 42.6 (-), 56.8 (- 2 C), 66.2 (+), 166.5 (C_{quat}), 170.8 (C_{quat}); further signals could not be labelled. MS (ESI, H_2O/MeCN/MeOH + 10 mmol/l NH_4Ac): *m/z* (%) = 391.3 [M+H$^+$] (100), 408.2 [M+NH_4^+] (22), 798.7 [2M+NH_4^+] (37), 803.6 [2M+Na$^+$] (23).

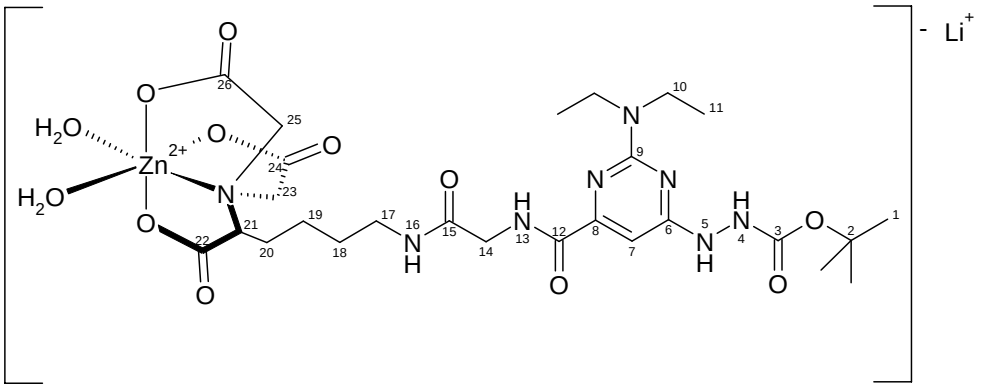

Zn-NTA-complex **6**:

64 mg (0.10 mmol) **5** is suspended in 10 mL H_2O and 13.6 mg (0.10 mmol) $ZnCl_2$ is added. The reaction mixture is stirred for 45 min at 40 °C. The mixture is filtered off

and the solvent is removed under reduced pressure. The solid is dissolved in EtOH and treated with hexanes precipitating **6** in 65 % (47 mg, 0.047 mmol) yield.

IR (KBr disk): 3412 cm^{-1}, 2987, 2944, 2880, 1931, 1605, 1537, 1418, 1264, 965, 820. ^{1}H-NMR (MeOH-[D4], 600 MHz): δ = 1.15 ppm (t, ^{3}J = 7.0 Hz; 6 H; COSY: $C^{11}H_3$), 1.29-1.68 (m, 15 H; HSQC: C^{1}; COSY: $C^{17}H_2$, $C^{18}H_2$, $C^{19}H_2$), 3.03-3.21 (m, 3 H; COSY: $C^{20}H_2$, $C^{21}H$), 3.31-3.34 (m, 4 H; HSQC: $C^{23}H_2$, $C^{25}H_2$), 3.63 (q, ^{3}J = 7.0 Hz, 4 H; COSY: C^{10}), 4.05-4.10 (m, 2 H; HSQC: $C^{14}H_2$), 6.52 (s, 1 H; HSQC: $C^{7}H$). ^{13}C-NMR (MeOH-[D4], 150 MHz): δ = 13.8 ppm (+; HSQC: C^{11}), 26.8 (-; HSQC: C^{19}), 28.3 (-; HSQC: C^{18}), 28.7 (+; HSQC: C^{1}), 30.3 (-; HSQC: C^{17}), 42.8 (-; HSQC: C^{10}), 43.6 (-; HSQC: C^{14}), 55.7 (-; HSQC: C^{23}, C^{25}), 60.3 (-; HSQC: C^{20}), 69.1 (+; HSQC: C^{21}), 81.7 (C_{quat}; HMBC: C^{2}), 91.8 (+; HSQC: C^{7}), 157.7 (C_{quat}), 158.7 (C_{quat}), 161.9 (C_{quat}; HMBC: C^{34}), 167.3 (C_{quat}), 171.1 (C_{quat}), 178.1 (C_{quat}), 178.3 (C_{quat}), 179.5 (C_{quat}), 180.5 (C_{quat}). MS (ESI, H_2O/MeOH + 10 mmol/l NH_4Ac): *m/z* (%) = 687.4 $[M-H^{+}]^{-}$ (100).

3.5. References and Notes

[1] J.-M. Lehn, *„Supramolecular Chemistry; Concepts and Perspectives“*, VCH, Weinheim, **1995**; H. Dugas, *“Bioorganic Chemistry, A Chemical Approach to Enzyme Action”*, Springer, New York, **1996**.

[2] P. Horvath, A. Gergely, and B. Noszal, *J. Chem. Soc. Perkin Trans. 1* **1996**, 1419; T. R. Kelly and M. H. Kim, *J. Am. Chem. Soc.* **1994**, *116*, 7072; K. Ariga, and E. V. Anslyn, *J. Org. Chem.* **1992**, *57*, 417.

[3] C. Bonauer, M. Zabel, and B. Koenig, *Org. Lett.* **2004**, *6*, 1349; S. Miltschitzky, V. Michlova, S. Stadlbauer, and B. Koenig, *Heterocycles* **2005**, in press.

[4] For examples see: M. Kruppa, C. Mandl, S. Miltschitzky, and B. Koenig, *J. Am. Chem. Soc.* **2005**, *127*, 3362; M. Kruppa, C. Bonauer, V. Michlova, and B. Koenig, *J. Org. Chem.* **2005**, in press.

[5] W. Bal, J. Christodolou, P. J. Sadler, and A. J. Tucker, *Inorg. Biochem.* **1998**, *70*, 33; P. J. Sadler and J. H. Viles, *Inorg. Biochem.* **1996**, *35*, 4490.

[6] M. Y. Wang, Y. Y. Kau, M. S. Lee, S. R. Doong, J. Y. Ho, and L. H. Lee, *Biotechnol. Bioeng.* **2000**, *67*, 104; G. Changa, D. E. Bochkariov, G. G. Jokdadze, J. Hopp, and P. Nelson, *J. Chromatogr., A* **1999**, *864*, 247.

[7] D. W. Pack, G. Chen, K. M. Maloney, C. T. Chen, and F. H. Arnold, *J. Am. Chem. Soc.* **1997**, *119*, 2479.

[8] D. Hopgood and R. J. Angelici, *J. Am. Chem. Soc.* **1968**, *90*, 2508; For recent examples see: A. T. Wright and E. V. Anslyn, *Org. Lett.* **2004**, *6*, 1341; N. Haddour, S. Cosnier, and C. Gondron, *J. Am. Chem. Soc.* **2005**, *127*, 5752; M. Zhou, S. Haldar, F. Franses, J.-M. Kim, and D. H. Thompson, *Supramol. Chem.* **2005**, *17*, 101.

[9] K. Terpe, *Appl. Microbiol. Biotechnol.* **2003**, *60*, 523.

[10] A. L. Beauchamp, J. Israeli, and H. Saulnier, *Can. J. Chem.* **1969**, *47*, 1269.

[11] Typical examples are cycloadditions or cyclization reactions and intramolecular folding.

[12] B. R. Hart and K. J. Shea, *J. Am. Chem. Soc.* **2001**, *123*, 2071.

[13] DMSO was favored over chloroform due to less signal overlaps and higher solution of the signals in the ^{1}NMR spectra.

[14] H. Friebolin, *"Basic One- and Two-Dimensional NMR Spectroscopy"*, VCH, Weinheim, **2004**; S. Nerger and S. Braun, *"200 and More NMR Experiments"*, VCH, Weinheim, **2004.**

[15] H. Kessler, *Angew. Chem.* **1982**, *94*, 509; Y. A. Bara, A. Friedrich, H. Kessler, and M. Molter, *Chem. Ber.* **1978**, *111*, 1045.

[16] The ROESY spectrum was recorded on a Bruker Avance 600 NMR spectrometer at 300 K with a mixing time of 500ms.

[17] Further contacts are restricted due to signal overlap.

[18] H. J. Schneider, R. Kramer, S. Simova, and U. Schneider, *J. Am . chem. Soc.*, 1988, **110**, 6442; C. S. Wilcox, 'Frontiers in Suplramolecular Chemistry and Photochemistry, ' ed. by H. J. Schneider and H. Duerr, VCH, Weinheim, 1991.

4. Synthesis of an Amino Acid with Protected Cyclen Side Chain Functionality*

4.1. Introduction

Metal ions are an important feature of protein structure and function. In many cases they are crucial for the activity of allosteric and catalytic centers.[1] During the last years, many applications and studies based on functionalized metallopeptides appeared in the literature. Burger and Still have accomplished the split/pool synthesis of encoded libraries bearing peptidic appendages attached to a cyclen core binding to Cu(II) ions in aqueous solution. The structural data indicate that specific amino acid combinations produce more effective metal binders.[2] Such ligands that display high affinity and selectivity for metal ions may find use as sensors. With the goal of developing artificial nucleases for DNA hydrolysis, metal-coordinating peptides have been tethered to a DNA intercalating Rh(III) complex to position metal ions close to the sugar-phosphate backbone. The intercalator provides DNA binding affinity, and a metal binding peptide contributes reactivity.[3] In a combinatorial approach Long reported a method to optimize the desoxyribose-based cleavage of B-DNA by Ni(II)·Xaa-Xaa-His metallopeptides. This metallotripeptid domain is based on the amino-terminal, square-planar Ni(II) chelating domain of serum albumin.[4] Scrimin *et al.* reported a dinuclear Zn(II) complex of a heptapeptide active in catalyzing the intramolecular transphosphorylation of the RNA model substrate 2-hydroxypropyl-*p*-nitrophenyl phosphate.[5] In further studies, they showed that these Zn(II) complexes in addition have a remarkable activity in the hydrolytic cleavage of plasmide DNA.[6] Although structure and application of the mentioned metallopeptides are different, a common feature are metal ion coordination sites created by artificial and natural amino acids. We report here the efficient synthesis of an artificial amino acid containing a protected cyclen unit as metal ion chelate in the side chain of glutamine. The compound may serve as a versatile building block to introduce a metal ion binding site with high affinity in peptide sequences, and in the construction of synthetic receptors.

---

* The results of this chapter have been published: S. Miltschitzky and B. Koenig, *Synth. Comm.* **2004**, *34*, 2077

4.2. Results and Discussion

Cyclen **1** was converted into the 3-fold Boc protected derivative **2** following reported procedures.[7] The protected cyclen **2** was used in a peptide coupling reaction with Cbz-Glu(OH)-OBn. Best results in amide bond formation were obtained with HOAt, HATU and collidin. The simultaneous deprotection of the benzyl ester and the Cbz nitrogen protecting group of **3** is achieved by hydrogenation on Pd/C. The clean reaction yields amino acid **4** after separation from the catalyst by simple filtration in 78%. To prepare **4** for use in peptide coupling reactions, its amino group was Fmoc protected. Treatment with Fmoc-Cl and Na_2CO_3 as base in aqueous dioxane solution gives **5**, which is isolated by precipitation after acidification. To demonstrate the ability of **5** to undergo peptide coupling a simple dipeptide with glycine was prepared. The benzyl ester of glycine hydrotosylate is coupled to **5** using HOAt, HATU and Hünig´s base in DMF solution. The resulting dipeptide **6** is precipitated with water.

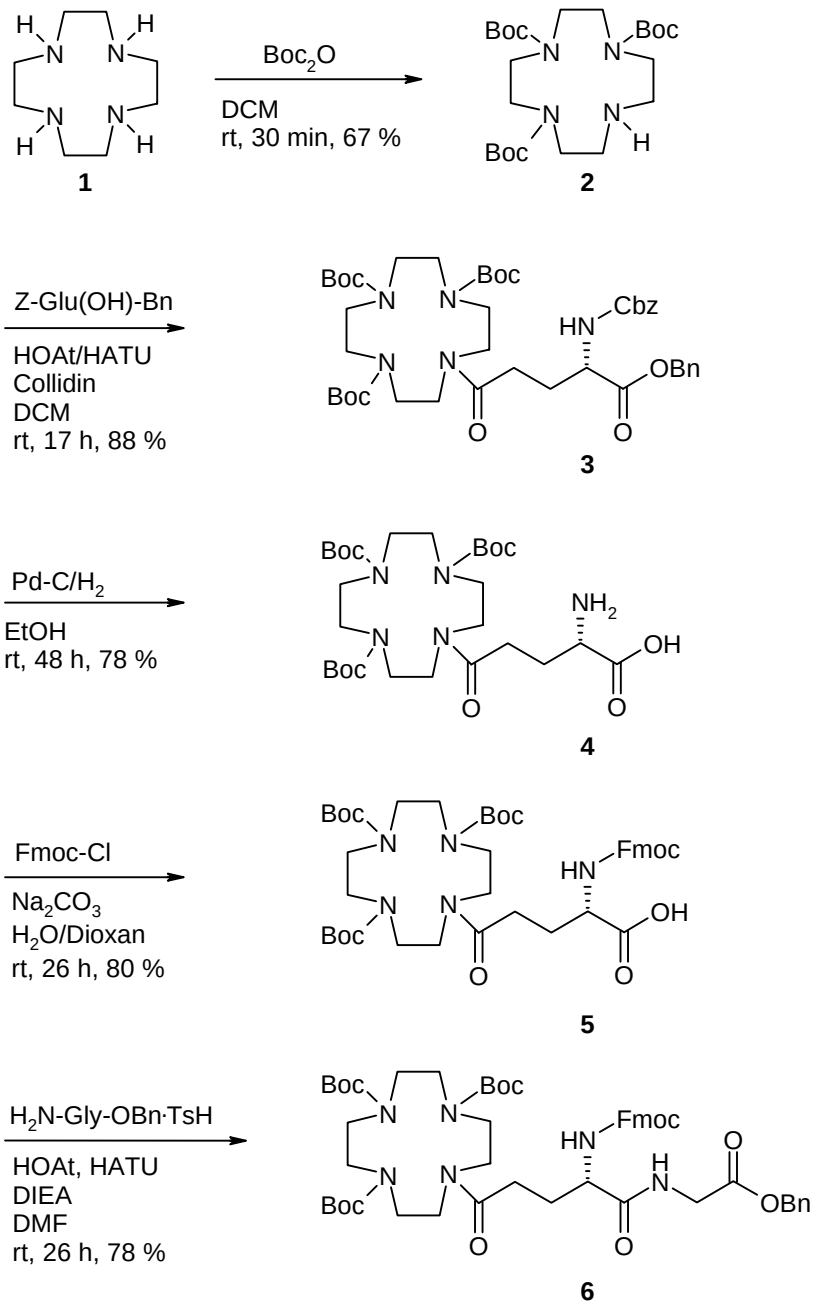

Scheme 1. Synthesis of cyclen amino acid 5 and its coupling to dipeptide **6**

4.3. Conclusions

In summary, we have reported the synthesis of a protected Glu(cyclen)-Gly dipeptide. The protected cyclen side chain moiety serves after deprotection as a high affinity ligand for many transition metal ions. The orthogonal protection allows a versatile use of the artificial cyclen amino acid in peptide synthesis, including automated solid phase synthesis and combinatorial techniques. In combination with natural or non-natural amino acids peptides with one or more metal ion coordination sites can be prepared for applications in molecular recognition and catalysis.

4.4. Experimental Part

General. Compound **2** was prepared by a known method.[7] Melting points were measured on a hot-plated microscope apparatus and are not corrected. UV/VIS spectra: Varian Cary 50 Bio. IR spectra: Bio-Rad FTS 3000 FT-IR. ^{1}H- and ^{13}C-NMR spectra: Bruker AC 250 or Bruker Avance 300; at 300 K; samples of approx. 30 mg of substance in 0.8 ml of deuterated solvents with TMS as the internal standard; s = singlet, bs = broad singlet, m = multiplet; the multiplicity of the ^{13}C signals was determined using the DEPT technique and is quoted as (+) for CH_3 or CH, (-) for CH_2 and (C_{quat}) for quaternary carbons. Elemental analysis were carried out by the microanalytical laboratory University of Regensburg. Commercially available reagents were used as received. Organic extracts were dried over anhydrous Na_2SO_4 and concentrated *in vacuo*. TLC was performed on alumina sheets (Merck KgaA, 20 x 20 cm, Silica gel 60 F_{254}).

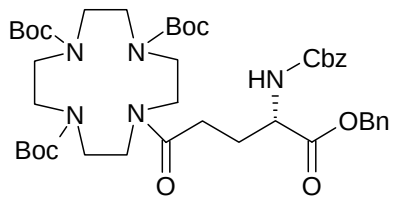

10-(4-Benzyloxycarbonyl-4-benzyloxycarbonylamino-butyryl)-1,4,7,10-tetraazacyclododecane-1,4,7-tricarboxylic acid tri-*tert*-butyl ester (3):[1] In a flame dried flask, **2** (142 mg, 0.3 mmol), Cbz-Glu(OH)-OBn (122 mg, 0.33 mmol), HOAt (49 mg, 0.36 mmol), HATU (137 mg, 0.36 mmol) and collidine (360 µl, 2.74 mmol) were dissolved in 5 ml dichlormethane (DCM) under a nitrogen atmosphere and stirred for 65 h at room temp. The crude product was purified by column chromatography (SiO_2, ethyl acetate/hexane, 3:1, R_f = 0.56) to give 198 mg (88 %) of compound **3**, as a white solid.

MP: 74 °C. ^{1}H-NMR (250 MHz, $CDCl_3$): δ = 1.45 (m, 27 H, Boc-CH_3), 2.05 (m, 1 H, *CH_2*-CON-cyclen), 2.18 (m, 1 H, *CH_2*-CON-cyclen), 2.38 (m, 2 H, *CH_2*-CH_2-CON-cyclen), 3.39 (m, 16 H, cyclen-CH_2), 4.37 (m, 1 H, *CH*-CO_2Bn), 5.08 (s, 2 H, *CH_2*-Ph), 5.17 (s, 2 H, *CH_2*-Ph), 6.00 (br s, 1 H, NH-CO), 7.33 (m, 10 H, Ph-H). ^{13}C-NMR (63 MHz, $CDCl_3$): δ = 27.1 (-, *CH_2*-CON-cyclen), 28.4 (+, CH_3-Boc), 28.5 (+, CH_3-Boc),

29.2 (-, *CH*$_2$-CH$_2$-CON-cyclen), 49.7 (-, cyclen-CH$_2$), 49.9 (-, cyclen-CH$_2$), 50.3 (-, cyclen-CH$_2$), 51.3 (-, cyclen-CH$_2$), 53.9 (+, *CH*-CO$_2$BN), 66.9 (-, *CH*$_2$-Ph), 67.1 (-, *CH*$_2$-Ph), 80.3 (C_{quat}, Boc), 80.4 (C_{quat}, Boc), 128.1 (+, Ph-H), 128.2 (+, Ph-H), 128.4 (+, Ph-H), 128.5 (+, Ph-H), 128.6 (+, Ph-H), 135.4 (C_{quat}, Ph), 136.4 (C_{quat}, Ph), 155.5 (C_{quat}, OCO-NH), 156.2 (C_{quat}, CON-Cyclen), 157.1 (C_{quat}, C=O Boc), 171.9 (C_{quat}, CO$_2$-Bn); MS (ESI, DCM/MeOH + 1 % AcOH): *m/z* (%) = 826.6 $[MH]^+$ (53), 848.6 $[M+Na]^+$ (100), 864.7 $[M+K]^+$ (5), 1674.0 $[2M+Na]^+$ (30). UV (CH$_3$CN): λ_{max} (lg ε) = 258 nm (3.780), 263 (3.785), 267 (3.708). IR (KBr disk): 3030 cm^{-1}, 2976, 2932, 1737, 1696, 1648, 1527, 753, 698. Anal. calcd. for $C_{43}H_{63}N_5O_{11}$: C: 62.52; H: 7.69; N, 8.48; Found: C: 62.22; H: 7.56; N: 8.37.

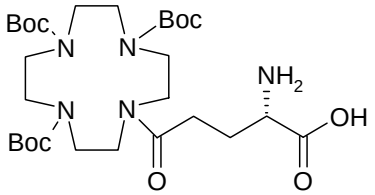

10-(4-Aminoxycarboxy-4-carboxy-butyryl)-1,4,7,10-tetraazacyclododecane-1,4,7-tricarboxylic acid tri-*tert*-butyl ester (4): A mixture of **3** (1.8 g, 2.2 mmol) in 10 ml of dry methanol and 234 mg palladium on activated charcoal was hydrogenated at 10 bar at room temp. for 48 h. The catalyst was filtered off, washed thoroughly with methanol and the combined filtrate was concentrated under reduced pressure to give **3** (1.1 g, 85 %), as a colorless solid.

MP: 147 °C. ^{1}H-NMR (250 MHz, CDCl$_3$): δ = 1.44-1.46 (m, 27 H, Boc-CH$_3$), 2.22-2.25 (m, 2 H), 2.63-2.67 (m, 2 H), 3.12-3.14 (m, 1 H, C-H), 3.25-3.50 (m, 16 H, cyclen-CH$_2$).^{13}C-NMR (DMSO-[D6], 75 MHz): δ = 26.8 (- CH$_2$-CO-cyclen), 28.0 (+, Boc-CH$_3$), 29.3 (-, CH$_2$-CH), 48.6 (-, CH$_2$-cyclen), 48.7 (-, CH$_2$-cyclen), 48.9 (-, CH$_2$-cyclen), 49.0 (-, CH$_2$-cyclen), 49.2 (-, CH$_2$-cyclen), 49.4 (-, CH$_2$-cyclen), 49.8 (-, CH$_2$-cyclen), 49.9 (-, CH$_2$-cyclen), 79.3 (C_{quat}, Boc), 79.4 (C_{quat}, Boc), 155.1 (C_{quat}, C=O Boc), 155.7 (C_{quat}, C=O Boc), 156.0 (C_{quat}, C=O Boc), 169.9 (C_{quat}, C=O amid), 172.4 (C_{quat}, C=O acid). IR (KBr disk): 3448 cm^{-1}, 2976, 2932, 2363, 1699, 1647, 1473, 1411, 1366, 1163. UV (CH$_3$CN): λ_{max} (lg ε) = 263 nm (3.691). MS (ESI, MeOH + 1 % AcOH): m/z (%) = 602.4 $[MH]^+$ (100), 624.4 $[M+Na]^+$ (40), 1203.9 $[2M+H]^+$ (1),

1225.8 $[2M+Na]^+$ (1). Anal. calcd. for $C_{28}H_{51}N_5O_9$: C: 55.9; H: 8.5; N, 11.6; Found: C: 55.6; H: 8.7; N: 11.1.

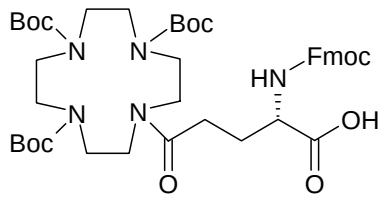

10-[4-Carboxy-(*9H*-fluoren-9-ylmethoxycarbonylamino)-butyryl]-1,4,7,10-tetraazacyclododecane-1,4,7-tricarboxylic acid tri-*tert*-butyl ester (5): Compound **4** (206 mg, 0.34 mmol) was dissolved in 21 ml of a water/dioxane mixture (5:2) and cooled to 0 °C. At this temp. Na_2CO_3 (108 mg, 1 mmol) and a solution of Fmoc-Cl (96 mg, 0.37 mmol) in 3 ml dioxane were added. The yellowish solution was stirred 30 min at 0 °C, allowed to warm up to room temp. and stirred additional 26 h. The solution was acidified with 2 N HCl and extracted three times with 25 ml of ethyl acetate. The solvent was removed to give **5** (224 mg, 80 %) , as a colorless solid.

MP.: 157 °C. ^{1}H-NMR (250 MHz, $CDCl_3$): δ = 1.43-1.49 (m, 27 H, Boc-CH_3), 2.22-2.25 (m, 2 H), 2.63-2.67 (m, 2 H), 3.12-3.67 (m, 16 H, cyclen-CH_2), 4.23-4.27 (m, 4 H), 7.30-7.34 (m, 4 H), 7.55-7.62 (m, 2 H), 7.71-7.82 (m, 2 H), 6.12 (br, 1 H, NH). ^{13}C-NMR (63 MHz, $CDCl_3$): δ = 27.41 (+, Boc-CH_3), 27.43 (+, Boc-CH_3), 27.47 (+, Boc-CH_3), 27.9 (-, CH_2CON), 29.2 (-, *CH*$_2$CH$_2$CON), 46.1 (+, Fmoc), 48.6 (-, cyclen-CH_2), 48.9 (-, cyclen-CH_2), 49.5 (-, cyclen-CH_2), 49.6 (-, cyclen-CH_2), 50.5 (-, cyclen-CH_2), 52.7 (+, C-H), 66.1 (-, CH_2 Fmoc), 79.6 (C_{quat}, Boc), 79.7 (C_{quat}, Boc), 79.8 (C_{quat}, Boc), 118.9 (+, Ar-H), 119.0 (+, Ar-H), 123.7 (+, Ar-H), 124.1 (+, Ar-H), 124.2 (+, Ar-H), 126.1 (+, Ar-H), 126.5 (+, Ar-H), 126.7 (+, Ar-H),140.2 (C_{quat}, Fmoc), 140.5 (C_{quat}, Fmoc), 142.7(C_{quat}, Fmoc), 142.9 (C_{quat}, Fmoc), 154.5 (C_{quat}, C=O Fmoc), 155.1 (C_{quat}, cyclen-C=O), 156.1 (C_{quat}, C=O Boc), 172.0 (C_{quat}, C=O acid). IR (KBr disk): 3433 cm^{-1}, 2975, 2932, 1695, 1470, 1412, 741. UV (CH_3CN): λ_{max} (lg ε) = 248 nm (4.987), 256 (5.122). MS (ESI, MeOH + 1 % AcOH): m/z (%) = 846.7 $[M+Na^+]$ (11), 824.6 $[M+H^+]$ (72), 724.5 $[MH^+$-Boc] (100), 624.4 $[MH^+$-2Boc] (24). Anal. calcd. for $C_{43}H_{61}N_5O_{11}$: C: 62.7; H: 7.5; N: 8.5; Found: C: 63.0; H: 7.3; N: 7.5.

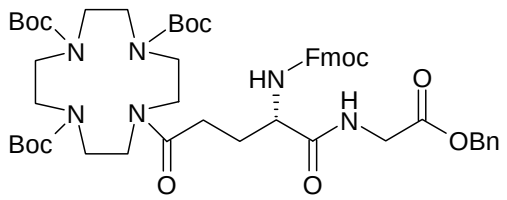

10-[4-(Benzyloxycarbonylmethyl-carbamoyl)-4-(*9H*-fluoren-9-ylmethoxycarbonylamino)-butyryl]-1,4,7,10-tetraazacyclododecane-1,4,7-tricarboxylic acid tri-*tert*-butyl ester (6): A mixture of Tos-O$^-$ ^+H_3N-Gly-OBn (101 mg, 0.30 mmol), **5** (275 mg, 0.33 mmol), HOAt (45 mg, 0.33 mmol), HOAT (125 mg, 0.33 mmol) and Hunig´s base (102 µl, 0.60 mmol) was stirred at room temp. for 26 h. The solution was cooled in a ice bath and the crude product was precipitated with water. The solid was filtered off and washed thoroughly with ice water giving **6** as a colorless solid (228 mg, 78 %). For analysis a sample was purified by column chromatography (SiO_2, ethyl acetate/hexane, 3:1, R_f = 0.24).

MP.: 147 °C. ^{1}H-NMR (600 MHz, $CDCl_3$): δ = 1.43-1.45 (m, 27 H, Boc-CH_3), 1.96-2.05 (m, 1 H), 2.12-2.19 (m, 1 H,), 2.45-2.56 (m, 1 H), 2.68-2.79 (m, 1 H), 3.18-3.74 (m, 16 H, cyclen-CH_2), 3.90-4.46 (m, 6 H, CH Fmoc, CH_2 Fmoc, CH Glu, CH_2-Gly), 6.44 (bs, 1 H, N-H Fmoc), 7.20-7.45 (m, 9 H, Ar-H), 7.54 (m, 2 H, Ar-H), 7.69-7.80 (m, 3 H, Ar-H, N-H amid). ^{13}C-NMR (63 MHz, $CDCl_3$): δ = 28.4 ppm (+, Boc-CH_3), 28.5 (+, Boc-CH_3), 29.1 (-), 29.7 (-), 41.4 (-), 47.1 (+, CH), 50.1 (-, cylclen-CH_2), 50.6 (-, cyclen-CH_2), 51.4 (-, cyclen-CH_2), 54.3 (+, CH), 67.0 (-, CH_2 ester), 67.1 (-, CH_2 Fmoc), 80.4 (C_{quat}, Boc), 80.5 (C_{quat}, Boc), 119.9 (+, Ar-H), 125.2 (+, Ar-H), 125.2 (+, Ar-H), 125.3 (+, Ar-H), 127.0 (+, Ar-H), 127.1 (+, Ar-H), 127.7 (+, Ar-H), 128.0 (+, Ar-H), 128.1 (+, Ar-H), 128.4 (+, Ar-H), 128.5 (+, Ar-H), 128.6 (+, Ar-H), 129.1 (+, Ar-H), 135.3 (C_{quat}), 141.2 (C_{quat}), 141.3 (C_{quat}), 143.8 (C_{quat}), 144.0 (C_{quat}), 155.5 (C_{quat}), 156.4 (C_{quat}), 157.1 (C_{quat}), 169.4 (C_{quat}), 172.1 (C_{quat}). IR (KBr disk): 3433 cm^{-1}, 2975, 2932, 1695, 1470, 1412, 741. UV (CH_3CN): λ_{max} (lg ε) = 266 nm (5.666). MS (ESI, MeCN): m/z (%) = 988.6 [M+NH_4^+] (28), 971.6 [M+H^+] (100).

4.5. References and Notes

[1] Licini, G.; Scrimin, P. Metal-Ion Peptides: From Catalysis to Protein Tagging. Angew. Chem. **2003**, *115* (38), 4720-4723. Angew. Chem. Int. Ed. Engl. **2003**, *42* (38), 4572-4575.

[2] Francis, M.; Jamison, T.; Jacobsen, E. Combinatorial Libraries of Transition Metal Complexes, Catalysts and Materials. Curr. Op. Chem. Biol. **1998**, *2* (3), 422-428.

[3] Copeland, K.; Fitzsimons, M.; Houser, R.; Barton, J. DNA Hydrolysis and Oxidative Cleavage by Metal-Binding Peptides Tethered to Rhodium Intercalators. Biochemistry **2002**, *41* (1), 343-356.

[4] Huang, X.; Pieczko, M.; Long E. Combinatorial Optimization of the DNA Cleaving Ni(II)·Xaa-Xaa-His Metalltripeptide Domain. Biochemistry **1999**, *38* (7), 2160-2166.

[5] Rossi, P.; Felluga, F.; Tecilla, P.; Formaggio, F.; Crisma, M.; Toniolo, C.; Scrimin, P. A Bimetallic Helical Heptapeptide as a Transphosphorylation Catalyst in Water. J. Am. Chem. Soc. **1999**, *121* (29), 6948-6949.

[6] Sissi, C.; Rossi, P.; Felluga, F.; Formaggio, F.; Palombo, M.; Tecilla, P.; Toniolo, C.; Scrimin, P. Dinuclear Zn(II) Complexes of Synthetic Heptapeptides as Artificial Nucleases. J. Am. Chem. Soc. **2001**, *123* (13), 3169-3170.

[7] Brandes, S.; Gros, C.; Denat, F.; Pullumbi, P.; Guilard, R. New Facile and Convenient Synthesis of Bispolyazamacrocycles Using Boc Protection. Determination of Geometric Parameters of Dinuclear Copper(II) Complexes Using ESR Spectroscopy and Molecular Mechanics Calculations. Bull. Soc. Chim. Fr. **1996**, *133* (1), 65-73. The major side product of the reaction, a 4-fold protected cyclen, can be recycled by deprotection with TFA and eluation from basic ion exchanger giving **1** quantitative.

C. Summary

The mimicry of peptide and protein structures has emerged as a focal point of bioorganic and medicinal chemistry. Peptidomimetic chemistry can serve as a basis for drug development and peptidomimetic model systems can provide fundamental insights into the folding and structure of proteins.

In this work, 6-hydrazinopyrimidine-4-carboxylic acids (PHA) as a building block for extended β-strand mimics were selected. Molecular modelling calculations on force field level (MMFF, program package Spartan) indicate that oligomers of substituted PHA adopt a linear conformation required to be complementary to peptide β-sheets.

In the first chapter, the synthesis of substituted PHA molecules and their inter- and intramolecular peptide binding properties in organic solvents are reported. Binding affinities were determined by NMR spectra and emission changes. The luminescence of substituted PHA receptors, which changes in non-polar solvents upon peptide binding, allows the use of PHA receptors as chemosensors and emitting probes. The incorporation of substituted PHA molecules into an amino acid sequence bearing D-Pro-Gly leads to turn structures. They allow the investigation of the possible binding motif due to intramolecular hydrogen bonds and NOE contacts between the PHA moiety and the peptide backbone.

In further studies, highly water-soluble PHA receptors were synthesized in cooperation with Dr. Li. Therefore, ethylene-glycol chains were introduced by substitution reactions. Binding affinities of these receptors to the biological active peptides Somatostatin (SRIF) and Concanavalin A (ConA) were carried out under physiological conditions. The binding affinities were determined from the PHA excitation by direct light absorption (at 382 nm) or a FRET process utilizing the Trp emission. The native or only partially denaturated protein structures of ConA, possessing extended and surface exposed β-sheet structures, show higher PHA affinity than the completely denaturated or digested protein structures of ConA and SRIF. The protein binding affinity of the

PHA changes with the proteins secondary and tertiary structure. Extended β-sheet structures, complementary to the PHA structure, lead to higher affinities.

The combination of an imidazole-coordinating metal complex, which binds to *N*-terminal His, with a fluorescent PHA moiety results in a luminescent probe. The binding affinity to the pentapeptide H-His-Leu-Leu-Val-Phe-OMe was monitored by fluorescence titration experiments. Initially, the strong interaction of Zn^{2+}(NTA) complex to the terminal His of the pentapeptide occurs, followed by intramolecular hydrogen bonds of the PHA moiety to the peptide.

In the fourth chapter, the synthesis of a protected Glu(cyclen)-Gly dipeptide is reported. The protected cyclen side chain moiety serves after deprotection as a high affinity ligand for many transition metal ions. The orthogonal protection allows a versatile use of the artificial cyclen amino acid in peptide synthesis, including automated solid phase synthesis and combinatorial techniques.

D. Abbreviations

Ala	Alanine
Ar	Aryl
Boc	*tert*-Butoxycarbonyl
c	Concentration
calcd.	calculated
Cbz	Benzyloxycarbonyl
Cs	Cesium
d	days
DCC	Dicyclohexylcarbodiimide
DCM	Dichloromethane
DCU	1,3-Dicyclohexylurea
DIEA	Ethyl diisopropyl amine (Huenig´s base)
DMF	Dimethylformamide
EE/AcOEt	Ethylacetate
EI	Electronic Ionisation
eq	equivalents
ESI	Electronic spray ionisation
ESI	Electronspray Ionisation
Et	Ethyl
FAB	Fast-Atom Bombardment
Gly	Glycine
h	hour(s)
HATU	*O*-(7-Azabenzotriazole-1-yl)-*N*,*N*,*N*,*N*-tetramethyluroniumhexafluorophosphate
His	Histidine
HOAt	1-Hydroxy-7-azabenzotriazole
HOBt	1-Hydroxybenzotriazole
HPLC	High Performance Liquid Chromatography
IR	Infrared spectroscopy
J	Coupling Constant
Leu	Leucine

MeCN	Acetonitrile
Mg_2SO_4	Magnesium sulfate
min	minutes
mp.	melting point
MS	Mass Spectroscopy
Na_2SO_4	Sodium sulfate
NaCl	Sodium chloride
NEt_3	Triethyl amine
NIR	Near Infrared
NMR	Nuclear Magnetic Resonance
NOE	Nuclear-Overhauser-Effect
NTA	Nitrilotriacetic acid
Ph	Phenyl
PHA	Pyrimidine Hydrazine Acid
Phe	Phenylalanine
$POBr_3$	Phosphorylbromide
$POCl_3$	Phosphorylchloride
R_f	Retention Factor
rt	room temperature
sh	shoulder
Tab.	Table
TFA	Trifluoroacetic acid
TLC	Thin Layer Chromatography
TMS	Tetramethyl silane
Tos	*p*-Toluene-sulfonyl
UV	Ultraviolett Spektroscopy
Val	Valine
x	Mole Fraction

E. Appendix

Publications

- *Synthesis of an Amino Acid with Protected Cyclen Side Chain Functionality*

  S. Miltschitzky and B. König, *Synth. Comm.* **2004**, *34*, 2077.

- *Strong Emission Increase of a Dicarboxyterpyridine Europium (III) Complex in the Presence of Citrate and Hydrogen Peroxide*

  V. N. Kozhevnikov, C. Mandl, S. Miltschitzky, A. Duerkop, O. S. Wolfbeis, and B. Koenig, *Inorg. Chim. Acta.* **2005**, *358*, 2445.

- A Luminescent Receptor with Affinity for N-Terminal Histidine in Peptides in Aqueous Solution.

  M. Kruppa, C. Mandl, S. Miltschitzky, and B. Koenig, *J. Am. Chem. Soc.* **2005**, *127*, 3362.

- *Synthesis of Substituted Pyrimidine Hydrazine Acids (PHA) and their Use in Peptide Recognition*

  S. Miltschitzky, V. Michlova, S. Stadlbauer, and B. Koenig, *Heterocycles* **2005**, in press.

- *Small Peptides with a β-Hairpin Structure*

  S. Miltschitzky and B. Koenig, *OPPI* **2005**, in press.

- Keynotes in Organic Chemistry

  S. Miltschitzky, B. König, *Angew. Chem.* **2004**, *116*, 2246.

- Keynotes in Organic Chemistry

  S. Miltschitzky, B. König, *Angew. Chem. Int. Ed.* **2004**, *43*, 2196.

Poster Presentations

- *Summerschool of Medicinal Chemistry* (09/2002), Regensburg, Germany
- *GdCH Jahrestagung* (10/2003), Munich, Germany
- *1st World Congress on Synthetic Receptors* (10/2003), Lisbon, Portugal
- *XII. Reaction Mechanism* (072004), Dublin, Ireland (Poster awarded)
- *2nd Summerschool of Medicinal Chemistry* (10/2004), Regensburg, Germany

Conferences

- Symposium *Green Chemistry* DBU (7/2002), Freising, Germany
- Calorimetrie-Seminar der Fa. Microcal (6/2002), Martinsried, Germany
- Seminar of Peptide Synthesis with Mikrowaves (11/2004), Munich, Germnay
- Symposium *Molecular Recognition* (6/2003), Prague, Czech Republik
- GDCh-Seminar *BWL für Chemiker* (6/2003), Leipzig, Germany
- GDCh-Seminar *Marketing für Chemiker* (2/2003), Frankfurt, Germany
- GDCh-Alpenforum (6/2004), Oberammergau, Germany
- Conference *Oberflächenanalytik* (11/1999), Karlsruhe, Germany

Curriculum Vitae

Personal Details

Name:	Stefan Harald Miltschitzky
Date of Birth:	04.06.1976
Place of Birth:	Amberg
Nationality:	German
Status:	single

Education

1982-1986	Johannes Hess Volksschule in Burghausen
1986-1995	Aventinus-Gymnasium in Burghausen
1995	Abitur at the Aventinus-Gymnasium Burghausen

Civilian Service

07/95-07/96	Kreiskrankenhaus Burghausen

Tertiary Education

11/96-09/01	Chemistry studies, University Regensburg
04/97	Elective course: Medicinal Chemistry
10/98	Intermediate Diploma
10/98	Elective course Technical Chemistry (Dechema/Frankfurt and University Regensburg)
10/98-06/99	Student assistant at the Institute of Physical Chemistry, Prof. Dr. W. Kunz
04/99	Elective course Analytical Chemistry
12/00	Diploma examination

01/01-09/01	Diploma Thesis in Organic Chemistry, University of Regensburg, Prof. Dr. B. König
11/01-06/05	PhD work in the research group of Prof. Dr. B. König
01/05-03/05	Research collaboartion with Prof. Dr. Jeff Aubé, University of Kansas, Lawrence/USA

Industrial internships

03/97-04/97	Wacker Chemie, Burghausen (quality assurance)
08/97-09/97	Wacker Chemie, Burghausen (quality assurance)
08/98-09/98	Wacker Chemie, Burghausen (quality assurance)
08/99-09/99	Wacker Chemie, Burghausen (quality assurance)
10/99	Dr. Schubach, Passau (Toxicology)
03/00-04/00	Infineon Technology, Munich (Analytics)

F. Acknowledgments

Mein besonderer Dank gilt Herrn Prof. Dr. B. König für die Überlassung des spannenden und vielseitigen Themas. Ganz besonders möchte ich mich für die gewährte Freiheit in der Forschung und das stets mit Anregung und Diskussion verbundene Interesse an meiner Arbeit bedanken.

Den Mitarbeitern der Zentralen Analytik der Fakultät für Chemie und Pharmazie danke ich für die stets schnelle und gewissenhafte Durchführung der analytischen Messungen. Insbesondere Herrn. Dr. T. Burgemeister, Herrn. F. Kastner, Frau N. Pustet, Frau A. Schramm and Frau G. Stühler für die Aufnahme der NMR-Spektren, Herrn. Dr. K. K. Mayer, Herrn. J. Kiermeier and Herrn W. Söllner für die Messungen der Massenspektren, Herrn. G. Wandinger und Herrn H. Schüller für die Durchführung der Elementaranalysen sowie Herrn. Dr. M. Zabel und Frau S. Stempfhuber für die Röntgenstrukturanalysen.

Frau E. Liebl, Herrn Dr. W. Braig, Frau Dr. C. Braig, Frau H. Leffler-Schuster, Herrn. E Lautenschlager und Frau B. Badziura und allen übrigen Festangestellten des Lehrstuhls König danke ich für ihre Unterstützung.

Herrn Dr. R. Vasold für die Durchführung von HPLC-Messungen, aber auch für seinen Kaffee, unvergessene Geburtstags-Buffets sowie informative Gespräche über den FCB.

Allen jetzigen und früheren Mitarbeitern des Lehrstuhls danke ich für das angenehme Klima während und nach der Arbeitszeit. Besonders bedanken möchte ich mich bei Dr. Wolfgang Pitsch, Dr. Michael Klein, Dr. Roland Reichenbach-Klinke, Frau Dr. Maria Fonseca-Hechavarria, Giovanni Imperato, Thorsten Graf und Michi Egger, die meine Gesangesfreuden im Labor ertragen haben.

Ein Dank an M. Kruppa, Thomas Suhs, Eva Engel, Dr. Christoph Bonauer, Dr. Christian Mandl, Dr. Radek Cibulka, Dr. Katerina. Cernovska, Stefan Ritter, Dr.

Thomas Walenzyk, Georg Discherl, Jiri Svoboda, Michael Subat und Stefan Stadlbauer für die vielen anregenden fachlichen und fachfremden Diskussionen.

Stefan Stadlbauer danke ich für seine Zusammenarbeit im Rahmen seines Praktikums, die mir eine große Hilfe und Zeitersparnis gewesen ist.

Bei Dr. Valery Kozhevnikov, Dr. Veronika Michlova, Dr. Christian Mandl, Dr. Xiaqiang Li und Michael Kruppa für die gute Zusammenarbeit in verschiedenen gemeinsamen Projekten.

Prof. Dr. Armin Geyer und Daniela Fischer für ihre stete Hilfsbereitschaft in allen NMR-technischen Fragen.

Meinen langjährigen Studienfreunden Frau Dr. Anja Kaiser, Dr. Christian Trieflinger, Frau Dr. Natascha Naarmann, Thomas Schmidt, Alexander Ebner für ihre Hilfsbereitschaft, ihre Freundschaft und unzählige kulinarische Stunden.

Den alten Schulkameraden aus Burghausen danke ich für ihre langjährige Freundschaft und den gemeinsamen Unternehmungen an den Wochenenden in meiner Heimatstadt.

Meiner lieben Liz für Ihre Fähigkeit, mich immer wieder zu aufzuheitern und mich darin erinnert, dass es auch ein Leben neben der Chemie gibt.

Meinem Bruder Hans-Peter und Claudia für die Regensburg-Besuche und für viele kulinarische Anregungen per Telefon.

Meinen beiden Omas, die immer für mich da waren und mir immer neuen Mut geschenkt haben.

Zuletzt, aber vor allem meinen Eltern für ihre langjährige Unterstützung und ihren finanziellen und privaten Rückhalt während meiner Studienzeit.